

CRANFIELD UNIVERSITY

MITESH KANTILAL PATEL

ANALYSIS OF VOLATILE ORGANIC COMPOUNDS IN BREATH AS A
POTENTIAL DIAGNOSTIC MODALITY IN DISEASE MONITORING

CRANFIELD HEALTH

PhD

Academic Year: 2011 - 2012

Supervisor: Dr Christopher Walton
December 2011

CRANFIELD UNIVERSITY

CRANFIELD HEALTH

PhD

Academic Year 2011 - 2012

MITESH KANTILAL PATEL

ANALYSIS OF VOLATILE ORGANIC COMPOUNDS IN BREATH AS A
POTENTIAL DIAGNOSTIC MODALITY IN DISEASE MONITORING

Supervisor: Dr Christopher Walton
December 2011

© Cranfield University 2011. All rights reserved. No part of this
publication may be reproduced without the written permission of the
copyright owner.

ABSTRACT

The use of breath odours in medical diagnosis dates back to classical times, though in its modern form the technique is only a few decades old. There are several breath tests in common clinical use, though all of them involve administration of a known or labelled exogenous compound. More recently, over the last twenty years, interest has focussed on analysis of endogenous metabolites in breath, but despite a large number of published studies reporting a number of disease markers, there has been little or no impact on clinical practice. Nonetheless, breath analysis offers a number of potential advantages over current biochemical methods.

One major advantage of breath analysis is its non-invasive nature, which has led to significant interest in its use at point-of care for monitoring chronic diseases such as diabetes and the chronic infections ubiquitous in cystic fibrosis. However, breath analysis classically involves the use of expensive laboratory based analytical equipment which requires extensively-trained personnel and which cannot readily be miniaturised. Systems based on simple gas sensors might offer a way of overcoming these limitations.

In recent years, Cranfield University has developed an instrument called the single metal oxide sensor gas analyser (SMOS-GA, more commonly referred to as the “Breathotron”) as a proof of concept for sensor-based breath analysis. In this project the Breathotron has been used in conjunction with selected ion flow tube mass spectrometry (SIFT-MS) and thermal desorption gas chromatography mass spectrometry (TD-GC-MS) to determine the changes in the concentrations of volatile organic compounds (VOCs) in breath in a number of experimental situations which are relevant to the diagnostic monitoring of diabetes mellitus. Studies conducted on clinically healthy volunteers were: an oral glucose tolerance test (OGTT); a six minute treadmill walking test; and a bicycle ergometer test. Additionally Breathotron and analytical data were also obtained during a hypoglycaemic clamp study carried out on hypoglycaemia-unaware Type I diabetics.

The principle breath volatiles determined analytically were: acetone, acetaldehyde, ammonia isoprene though data on a number of others was also available. In general, it proved difficult to establish any reproducible relationship between the concentration of any compound measured and blood glucose concentration any of the experimental interventions. It was notable, though, that statistically significant associations were observed occasionally in data

from individual volunteers, but even these were not reproduced in those trials which involved repeated measurements. This remained true even where spirometry data were used to derive VOC clearance rates. This may explain previous reports from smaller studies of an association between glucose and breath acetone concentration. It seems probable that any experimentally-induced changes in breath VOC concentration or clearance were of much smaller magnitude than background variability and was consequently not detectable.

These observations were mirrored in the sensor-derived results. Multivariate analysis across all trials where Breathotron data were obtained suggested clustering by individual volunteer rather than glycaemic status. This suggests that there exists a “background” breath volatile composition, dependent perhaps on such factors as long-term diet, which is independent of our experimental intervention.

The Breathotron was also used as a platform to assess the performance of three different types of mixed metal oxide sensor in vitro. Calibration curves were generated for acetone, ammonia and propanol covering the physiological range of concentrations and with a similar water content to breath. Close correlations were obtained between concentration and the amplitude of the sensor response. Sensor response reproducibility was also determined using acetone at a concentration of 10ppm with dry and humidified test gas. There were significant differences between sensor types in overall reproducibility and in response to humidity. These results suggest that had there been substantial changes in breath VOC composition as a result of our experimental interventions, any of the types of sensor used would have been capable of responding to them.

In summary, these results do not support the efficacy of breath VOC analysis as a means of non-invasive diagnostic monitoring.

Keywords:

Breathotron, diabetes, gas sensor, GC-MS, SIFT-MS

ACKNOWLEDGEMENTS

I would firstly like to thank my supervisor Chris Walton for his help, guidance and support over the past four years. Not only has he been my teacher and mentor, but a jolly good friend as well. I would also like to thank my original supervisor Claire Turner for her continued support, advice and input.

I also would like to thank my second supervisor Conrad Bessant and Michael Cauchi for help and advice, especially with data analysis techniques, and our external collaborators Dr Mark Evans, Dr Paul Castle and Prof Mark Lewis.

I owe a debt of gratitude to Dave Pitts and Dawn Fowler for their help with the design and implementation of various aspects of my experiments, and their general words of advice and encouragement when things went ‘pear shaped’. They are two of the nicest people that I have ever had the pleasure to meet, and I could not have done this without them. I would also like to thank Veronica Brown for helping with sample collection.

Thanks to the ‘Tea Group’ for fuelling me with ample cake, biscuits, caffeine, ideas, advice, inspiration, and laughs. I would like to thank my fellow research students, especially Natalie Kenny and Amit Patel, for reminding me that studying for a PhD isn’t ‘all work and no play’.

To my Mum, Dad and brother Dharmesh, thank you for all that you’ve done for me. I wouldn’t be where I am today without you.

Lastly and by no means least, I would like to thank the long list of people that I haven’t got space to thank individually for your wisdom, guidance, help, advice, encouragement, enthusiasm and support over the years. It has, and will not ever be forgotten.

“Jai Shree Krishna”

TABLE OF CONTENTS

ABSTRACT	i
ACKNOWLEDGEMENTS	iii
LIST OF FIGURES	ix
LIST OF TABLES	xviii
LIST OF EQUATIONS	xx
LIST OF ABBREVIATIONS AND NOTATION	xxi
1 Introduction and Literature Review	1
1.1 Introduction	1
1.2 Breath	3
1.2.1 Respiratory physiology	3
1.2.2 Lung function and spirometry	5
1.2.3 Spirometry	7
1.2.4 Other methods for lung function assessment	9
1.3 Existing applications of breath analysis	12
1.3.1 Determining blood alcohol content in exhaled breath	12
1.3.2 Monitoring asthma using exhaled nitric oxide	12
1.3.3 Urea breath test for detection of <i>Helicobacter pylori</i> infection	13
1.3.4 Hydrogen breath test for carbohydrate intolerance and bacterial overgrowth ...	13
1.4 A general background of diabetes mellitus	14
1.4.1 The different types of diabetes	14
1.4.2 Type 1 Diabetes Mellitus	15
1.4.3 Type 2 Diabetes Mellitus	16
1.4.4 Gestational Diabetes Mellitus	16
1.4.5 Hypoglycaemic unawareness	16
1.5 Biochemistry of Diabetes	17
1.5.1 Insulin	17
1.5.2 Glucagon	17
1.5.3 Adrenaline	18
1.5.4 Cortisol	18
1.6 Methods of glucose determination	18
1.6.1 Urine glucose	18
1.6.2 Blood glucose	18
1.6.3 Electronic blood glucose meters using mediated enzymes	20
1.6.4 Other methods of measuring blood glucose levels	20
1.7 Volatile organic compounds	22
1.7.1 VOCs as biomarkers	22
1.7.2 Lipid peroxidation and oxidative stress	25
1.7.3 Low Density Lipoprotein	26
1.7.4 Diabetes	26
1.7.5 Non Alcoholic Fatty Liver Disease, Alcoholism and Liver Failure	27
1.7.6 Nitrogen containing compounds	27

1.8	Collection and analysis of volatile samples.....	27
1.8.1	Tedlar® bags	28
1.8.2	SUMMA® canisters	29
1.8.3	Nalophan®	29
1.8.4	Solid phase micro-extraction.....	29
1.8.5	Sorbent tubes	29
1.9	Analysis methods for VOC determination	30
1.9.1	Mass spectrometry.....	30
1.9.2	Gas chromatography mass spectrometry	31
1.9.3	Fast flow tube methods for VOC quantification.....	33
1.10	Sensor based technologies for VOC profiling	34
1.10.1	Electronic Nose (eNose).....	34
1.10.2	Sensor technologies typically used in eNose devices	35
1.11	Breathotron	39
1.11.1	History of the device	40
1.11.2	Operation	40
1.12	Conclusion.....	44
2	Non-invasive monitoring of VOCs in exhaled breath of healthy adults using Breathotron, SIFT-MS and GC-MS during an oral glucose tolerance test.....	47
2.1	Introduction	47
2.2	Materials and methods.....	48
2.2.1	Modifying a Breathotron face mask.....	48
2.2.2	Blood glucose meter calibration.....	50
2.2.3	Oral glucose tolerance test.....	50
2.2.4	Breathotron	51
2.2.5	SIFT-MS.....	52
2.2.6	ATD GC-MS	53
2.3	Results.....	55
2.3.1	Modifying a Breathotron face mask.....	55
2.3.2	Calibration of blood glucose meter	56
2.3.3	Oral glucose tolerance test.....	57
2.3.4	Breathotron data analysis	59
2.3.5	SIFT-MS.....	66
2.3.6	GC-MS	82
2.4	Discussion.....	88
2.5	Conclusion.....	94
3	Analysis of VOCs in exhaled breath, blood and skin from type-1 diabetics during a hypoglycaemic clamp.....	97
3.1	Introduction	97
3.2	Materials and Methods.....	97
3.2.1	Hypoglycaemic clamp	97
3.2.2	Breathotron	98
3.2.3	Breath	98

3.2.4 Skin	100
3.2.5 Blood.....	100
3.2.6 SIFT-MS.....	100
3.2.7 ATD GC-MS	100
3.3 Results.....	101
3.3.1 Hypoglycaemic clamp.....	101
3.3.2 Breathotron	102
3.3.3 SIFT-MS.....	106
3.3.4 GC-MS.....	122
3.3.5 Comparison with Breathotron sensor data	132
3.3.6 Comparison of SIFT-MS data to GC-MS data.....	135
3.4 Discussion.....	136
3.5 Conclusion.....	143
4 Monitoring the change in VOC concentration in breath under the influence of induced respiratory complication during a 6-Minute Walk Test using SIFT- and GC-MS.....	145
4.1 Introduction	145
4.2 Methods and Materials.....	146
4.2.1 6-Minute walk test	146
4.2.2 SIFT-MS.....	148
4.2.3 ATD GC-MS	148
4.3 Results.....	149
4.3.1 6-Minute walk test	149
4.3.2 SIFT-MS.....	154
4.3.3 GC-MS.....	166
4.4 Discussion.....	173
4.5 Conclusion.....	178
5 Monitoring the effect of exercise on exhaled metabolite concentration in real time using SIFT-, GC-MS and Breathotron	179
5.1 Introduction	179
5.2 Materials and methods.....	179
5.2.1 Modifications to the Breathotron Face Mask	179
5.2.2 Calibration of the bicycle ergometer.....	182
5.2.3 Bicycle ergometer challenge	182
5.2.4 SIFT-MS.....	185
5.2.5 Breathotron	185
5.2.6 GC-MS.....	186
5.3 Results.....	186
5.3.1 Bicycle ergometer challenge	186
5.3.2 Breathotron	206
5.3.3 Principal components analysis	208
5.3.4 GC-MS.....	211
5.4 Discussion.....	215
5.5 Conclusion.....	220

6 Investigating and improving the reliability and reproducibility of the Breathotron.....	223
6.1 Introduction	223
6.2 Materials and methods.....	224
6.2.1 Breathotron maintenance	224
6.2.2 Breathotron system tests	226
6.2.3 Sine wave.....	226
6.2.4 Breathotron modifications	228
6.2.5 Response of the modified systems to dry and humid gas samples	232
6.2.6 Acetone, ammonia and propanol calibration curves	232
6.3 Results.....	233
6.3.1 Breathotron system tests	233
6.3.2 Response of Breathotron to dry and humid acetone gas samples	233
6.3.3 Principal components analysis	235
6.3.4 Breathotron modifications	237
6.3.5 Acetone, ammonia and propanol calibration curves	244
6.4 Discussion.....	249
6.5 Conclusion.....	253
7 Conclusions and future work	255
7.1 Conclusions	255
7.2 Future work.....	258
REFERENCES	260
APPENDICES (ON CD)	

LIST OF FIGURES

Figure 1.1 Alveolar capillary unit – the site of gaseous exchange. Reproduced from Pocock and Richards (1999).....	4
Figure 1.2 Subdivisions of lung volumes (Pocock and Richards, 1999).....	6
Figure 1.3 A typical digital hand held spirometer shown with disposable cardboard mouth piece	8
Figure 1.4 A wet spirometer with inverted bellows (Singh, 2010).....	8
Figure 1.5 The different types of sensor used in modern spirometers. Reproduced from Singh, (2010)	9
Figure 1.6 A typical peak flow meter	10
Figure 1.7 Fowler's method (nitrogen washout) for measuring anatomical dead space (Pocock et al., 1999).....	11
Figure 1.8 Differences between T1DM and T2DM (Whelan, 2007).....	15
Figure 1.9 The Clark oxygen electrode (Newman and Turner, 2007)	19
Figure 1.10 An example of a Perkin Elmer thermal desorption tube (Hübschmann 2009)	30
Figure 1.11 A typical GC-MS system diagram (McMaster, 2008)	32
Figure 1.12 Principles of SIFT-MS	33
Figure 1.13 MMOS operating principal (adapted from City Technology, 2002)	37
Figure 1.14 Breathotron Mk IIb shown ready for use, with face mask and TD tube in place.....	39
Figure 1.15 Breathotron Mk IIb schematic	41
Figure 1.16 An example of a raw and smoothed Breathotron signals.....	43
Figure 2.1 Line diagram (above) and photograph (below) of the modified Breathotron sampling mask that allows tandem sampling with SIFT-MS.....	49
Figure 2.2 Continuous breathing directly into the SIFT-MS using a disposable cardboard tube	56
Figure 2.3 Continuous breathing directly into the SIFT-MS using a modified Breathotron face mask	56
Figure 2.4 Therasense glucose meter calibration curve	57
Figure 2.5 Change in blood glucose concentration during the OGTT	59
Figure 2.6 The change in sensor response at each of the half hourly sampling intervals for volunteer A	60
Figure 2.7 Maximum sensor resistance at half hourly intervals during the OGTT for all volunteers.....	61
Figure 2.8 Signal segmentation method	63

Figure 2.9 Scores plot for OGTT data derived from smoothed and zeroed sensor signals (ΔR_s) with no scaling.....	65
Figure 2.10 Online, continuous SIFT-MS data from the initial pre-glucose solution breath sample from volunteer A.....	67
Figure 2.11 Mean exhaled formaldehyde concentration plotted against time and blood glucose concentration	68
Figure 2.12 Mean exhaled acetaldehyde concentration plotted against time and blood glucose concentration	69
Figure 2.13 Mean exhaled acetone concentration plotted against time and blood glucose concentration	70
Figure 2.14 Mean exhaled acetic acid concentration plotted against time and blood glucose concentration	71
Figure 2.15 Mean exhaled isoprene concentration plotted against time and blood glucose concentration	72
Figure 2.16 Mean exhaled methanol concentration plotted against time and blood glucose concentration	73
Figure 2.17 Mean exhaled ethanol concentration plotted against time and blood glucose concentration	74
Figure 2.18 Mean exhaled propanol concentration plotted against time and blood glucose concentration	75
Figure 2.19 Mean exhaled hydrogen sulphide concentration plotted against time and blood glucose concentration	76
Figure 2.20 Mean exhaled ammonia concentration plotted against time and blood glucose concentration	77
Figure 2.21 Mean exhaled β -hydroxybutyric acid concentration plotted against time and blood glucose concentration	78
Figure 2.22 Mean exhaled water concentration plotted against time and blood glucose concentration	79
Figure 2.23 Mean exhaled carbon dioxide concentration plotted against time and blood glucose concentration	80
Figure 2.24 Multiple chromatogram alignment of samples collected from volunteer A at each sampling intervals during an OGTT	83
Figure 2.25 Exhaled breath acetone concentration quantified using GC-MS plotted against time and blood glucose concentration.....	84
Figure 2.26 Exhaled breath isoprene concentration quantified using GC-MS plotted against time and blood glucose concentration.....	85

Figure 2.27 Exhaled breath cyclopentane concentration quantified using GC-MS plotted against time and blood glucose concentration.....	86
Figure 2.28 Exhaled breath propanol concentration quantified using GC-MS plotted against time and blood glucose concentration.....	87
Figure 3.1 An exploded view of a custom made Nalophan [®] bag fitting consisting of polypropylene tube and Swagelok [®] fittings.....	99
Figure 3.2 An example of a Nalophan [®] gas sampling bag filled with a gaseous sample	99
Figure 3.3 Maximum Breathotron sensor resistance (ΔR_{\max}) Vs. Measured blood glucose concentration	103
Figure 3.4 PCA scores plot for the hypoglycaemic clamp shows clustering by volunteer and not blood glucose concentration	105
Figure 3.5 Exhaled breath acetone concentration quantified using the H_3O^+ precursor ion against measured blood glucose concentration for all eight volunteers during the hypoglycaemic clamp	106
Figure 3.6 Exhaled breath acetone concentration quantified using the NO^+ precursor ion against measured blood glucose concentration for all eight volunteers during the hypoglycaemic clamp	107
Figure 3.7 Exhaled breath acetaldehyde concentration against measured blood glucose concentration for all eight volunteers during the hypoglycaemic clamp	107
Figure 3.8 Exhaled breath ammonia concentration against measured blood glucose concentration for all eight volunteers during the hypoglycaemic clamp	108
Figure 3.9 Exhaled breath methanol concentration against measured blood glucose concentration for all eight volunteers during the hypoglycaemic clamp	108
Figure 3.10 Exhaled breath ethanol concentration against measured blood glucose concentration for all eight volunteers during the hypoglycaemic clamp	109
Figure 3.11 Exhaled breath propanol concentration against measured blood glucose concentration for all eight volunteers during the hypoglycaemic clamp	109
Figure 3.12 Exhaled breath isoprene concentration against measured blood glucose concentration for all eight volunteers during the hypoglycaemic clamp	110
Figure 3.13 Skin headspace acetone concentration quantified using the H_3O^+ precursor ion against measured blood glucose concentration for all eight volunteers during the hypoglycaemic clamp	112
Figure 3.14 Skin headspace acetone concentration quantified using the NO^+ precursor ion against measured blood glucose concentration for all eight volunteers during the hypoglycaemic clamp	113
Figure 3.15 Skin headspace acetaldehyde concentration quantified against measured blood glucose concentration for all eight volunteers during the hypoglycaemic clamp	113

Figure 3.16 Skin headspace ammonia concentration quantified against measured blood glucose concentration for all eight volunteers during the hypoglycaemic clamp	114
Figure 3.17 Skin headspace methanol concentration quantified against measured blood glucose concentration for all eight volunteers during the hypoglycaemic clamp	114
Figure 3.18 Skin headspace ethanol concentration quantified against measured blood glucose concentration for all eight volunteers during the hypoglycaemic clamp	115
Figure 3.19 Skin headspace propanol concentration quantified against measured blood glucose concentration for all eight volunteers during the hypoglycaemic clamp	115
Figure 3.20 Skin headspace isoprene concentration quantified against measured blood glucose concentration for all eight volunteers during the hypoglycaemic clamp	116
Figure 3.21 Blood headspace acetone concentration quantified using the H_3O^+ precursor ion against measured blood glucose concentration for all eight volunteers during the hypoglycaemic clamp	118
Figure 3.22 Blood headspace acetone concentration quantified using the NO^+ precursor ion against measured blood glucose concentration for all eight volunteers during the hypoglycaemic clamp	118
Figure 3.23 Blood headspace formaldehyde concentration against measured blood glucose concentration for all eight volunteers during the hypoglycaemic clamp	119
Figure 3.24 Blood headspace acetaldehyde concentration against measured blood glucose concentration for all eight volunteers during the hypoglycaemic clamp	119
Figure 3.25 Blood headspace ammonia concentration against measured blood glucose concentration for all eight volunteers during the hypoglycaemic clamp	120
Figure 3.26 Blood headspace methanol concentration against measured blood glucose concentration for all eight volunteers during the hypoglycaemic clamp	120
Figure 3.27 Blood headspace ethanol concentration against measured blood glucose concentration for all eight volunteers during the hypoglycaemic clamp	121
Figure 3.28 Blood headspace propanol concentration against measured blood glucose concentration for all eight volunteers during the hypoglycaemic clamp	121
Figure 3.29 Blood headspace isoprene concentration against measured blood glucose concentration for all eight volunteers during the hypoglycaemic clamp	122
Figure 3.30 GC-MS breath acetone concentration against measured blood glucose concentration for all eight volunteers during the hypoglycaemic clamp	124
Figure 3.31 GC-MS breath acetaldehyde concentration against measured blood glucose concentration for all eight volunteers during the hypoglycaemic clamp	124
Figure 3.32 GC-MS breath acetic acid concentration against measured blood glucose concentration for all eight volunteers during the hypoglycaemic clamp	125
Figure 3.33 GC-MS breath 2-butanone concentration against measured blood glucose concentration for all eight volunteers during the hypoglycaemic clamp	125

Figure 3.34 GC-MS breath methanol concentration against measured blood glucose concentration for all eight volunteers during the hypoglycaemic clamp	126
Figure 3.35 GC-MS breath methylglyoxal concentration against measured blood glucose concentration for all eight volunteers during the hypoglycaemic clamp	126
Figure 3.36 GC-MS breath phenol concentration against measured blood glucose concentration for all eight volunteers during the hypoglycaemic clamp	127
Figure 3.37 GC-MS breath propanol concentration against measured blood glucose concentration for all eight volunteers during the hypoglycaemic clamp	127
Figure 3.38 GC-MS breath isoprene concentration against measured blood glucose concentration for all eight volunteers during the hypoglycaemic clamp	128
Figure 3.39 GC-MS blood headspace acetone concentration against measured blood glucose concentration for all eight volunteers during the hypoglycaemic clamp	129
Figure 3.40 GC-MS blood headspace acetaldehyde concentration against measured blood glucose concentration for all eight volunteers during the hypoglycaemic clamp	130
Figure 3.41 GC-MS blood headspace acetic acid concentration against measured blood glucose concentration for all eight volunteers during the hypoglycaemic clamp	130
Figure 3.42 GC-MS blood headspace 2-butanone concentration against measured blood glucose concentration for all eight volunteers during the hypoglycaemic clamp	131
Figure 3.43 GC-MS blood headspace methanol concentration against measured blood glucose concentration for all eight volunteers during the hypoglycaemic clamp	131
Figure 3.44 GC-MS blood headspace methylglyoxal concentration against measured blood glucose concentration for all eight volunteers during the hypoglycaemic clamp	132
Figure 3.45 Breathotron sensor ΔR_{\max} plotted against exhaled breath acetone quantified using the H_3O^+ precursor ion	133
Figure 3.46 Breathotron sensor ΔR_{\max} plotted against exhaled breath acetone quantified using the NO^+ precursor ion.....	134
Figure 3.47 Breathotron sensor ΔR_{\max} plotted against exhaled breath acetone quantified using GC-MS.....	135
Figure 3.48 Comparison of acetone quantified using GC-MS against the concentration of acetone quantified using SIFT-MS.....	136
Figure 4.1 Blood glucose concentration measured at the four sampling intervals	151
Figure 4.2 Perceived dyspnoea during the two walk tests	152
Figure 4.3 Blood oxygen saturation (SpO_2) during the two walk tests	153
Figure 4.4 Heart rate data in beats per minute for both walk tests	154
Figure 4.5 Exhaled breath formaldehyde concentration during the experiment quantified using SIFT-MS.....	158

Figure 4.6 Exhaled breath acetaldehyde concentration during the experiment quantified using SIFT-MS.....	159
Figure 4.7 Exhaled breath acetone concentration during the experiment quantified with the H_3O^+ precursor ion using SIFT-MS	159
Figure 4.8 Exhaled breath ammonia concentration during the experiment quantified using SIFT-MS.....	160
Figure 4.9 Exhaled breath isoprene concentration during the experiment quantified with the H_3O^+ precursor ion using SIFT-MS	160
Figure 4.10 Exhaled breath methanol concentration during the experiment quantified using SIFT-MS.....	161
Figure 4.11 Exhaled breath ethanol concentration during the experiment quantified using SIFT-MS.....	161
Figure 4.12 Exhaled breath propanol concentration during the experiment quantified using SIFT-MS.....	162
Figure 4.13 Exhaled breath β -hydroxybutyric acid concentration during the experiment quantified using SIFT-MS.....	162
Figure 4.14 Exhaled breath isoprene concentration during the experiment quantified with the NO^+ precursor ion using SIFT-MS	163
Figure 4.15 Exhaled breath acetone concentration during the experiment quantified with the NO^+ precursor ion using SIFT-MS	163
Figure 4.16 Exhaled breath nitric oxide concentration during the experiment quantified using SIFT-MS.....	164
Figure 4.17 Exhaled breath pentane concentration during the experiment quantified using SIFT-MS.....	164
Figure 4.18 Exhaled breath nitrogen dioxide concentration during the experiment quantified using SIFT-MS	165
Figure 4.19 Exhaled breath acetaldehyde concentration during the experiment quantified using GC-MS.....	168
Figure 4.20 Exhaled breath isopentane concentration during the experiment quantified using GC-MS.....	169
Figure 4.21 Exhaled breath pentane concentration during the experiment quantified using GC-MS.....	169
Figure 4.22 Exhaled breath ethanol concentration during the experiment quantified using GC-MS.....	170
Figure 4.23 Exhaled breath isoprene concentration during the experiment quantified using GC-MS.....	170

Figure 4.24 Exhaled breath acetone concentration during the experiment quantified using GC-MS.....	171
Figure 4.25 Exhaled breath propanol concentration during the experiment quantified using GC-MS.....	171
Figure 4.26 Exhaled breath 1-propanol concentration during the experiment quantified using GC-MS.....	172
Figure 4.27 Exhaled breath 2-butanone concentration during the experiment quantified using GC-MS.....	172
Figure 5.1 Line diagram (top) photograph (bottom) of the modified Breathotron face mask with secondary flow sensor in series and two sample outlets.....	181
Figure 5.2 Principle of cycle ergometry (Reproduced from Roberts et al., 1997)	182
Figure 5.3 Ergometer challenge experimental set up showing the proximity of the ergometer to the Breathotron and SIFT-MS.....	185
Figure 5.4 Physiological parameters and continuous online sampling of exhaled breath from volunteer B during the first ergometer challenge.....	192
Figure 5.5 Physiological parameters and continuous online sampling of exhaled breath from volunteer B during the second ergometer challenge.....	193
Figure 5.6 Physiological parameters and continuous online sampling of exhaled breath from volunteer K during the first ergometer challenge.....	194
Figure 5.7 Physiological parameters and continuous online sampling of exhaled breath from volunteer K during the second ergometer challenge.....	195
Figure 5.8 Physiological parameters and continuous online sampling of exhaled breath from volunteer D during the first ergometer challenge	196
Figure 5.9 Physiological parameters and continuous online sampling of exhaled breath from volunteer K during the second ergometer challenge.....	197
Figure 5.10 Physiological parameters and continuous online sampling of exhaled breath from volunteer H, the positive control, during the first ergometer challenge	198
Figure 5.11 Physiological parameters and continuous online sampling of exhaled breath from volunteer H, the positive control, during the second ergometer challenge, VOC production could not be calculated due to a problem with the flow sensor.....	199
Figure 5.12 Physiological parameters and continuous online sampling of exhaled breath from volunteer M during the first ergometer challenge	200
Figure 5.13 Physiological parameters and continuous online sampling of exhaled breath from volunteer M during the second ergometer challenge	201
Figure 5.14 Physiological parameters and continuous online sampling of exhaled breath from volunteer L during the first ergometer challenge	202

Figure 5.15 Physiological parameters and continuous online sampling of exhaled breath from volunteer M during the second ergometer challenge	203
Figure 5.16 Physiological parameters and continuous online sampling of exhaled breath from volunteer N during the first negative control experiment (did not exercise)	204
Figure 5.17 Physiological parameters and continuous online sampling of exhaled breath from volunteer N during the second negative control experiment (did not exercise)	205
Figure 5.18 Change in maximum Breathotron sensor resistance ΔR_{\max} during the first experiment	208
Figure 5.19 Scores plot from both ergometer challenges shows that samples from individual volunteers cluster together, but not by phases of the experiment with no repeatability between the first and second experiment	210
Figure 5.20 Change in exhaled breath acetone concentration quantified using GC-MS during both ergometer challenges	212
Figure 5.21 Change in exhaled breath isoprene concentration quantified using GC-MS during both ergometer challenges	213
Figure 5.22 Change in exhaled breath acetaldehyde concentration quantified using GC-MS during both ergometer challenges	214
Figure 5.23 Change in exhaled breath propanol concentration quantified using GC-MS during both ergometer challenges	215
Figure 6.1 CAP25 'piggyback' board shown with sensors in place	225
Figure 6.2 A fully assembled sensor block on a Breathotron	226
Figure 6.3 A comparison of the three different MMOS sensors that were selected to be evaluated	228
Figure 6.4 Circuit diagram for Figaro® 'piggyback' board prototype	230
Figure 6.5 Prototype Figaro® MMOS sensor 'piggyback' board connected to an Arduino	231
Figure 6.6 Modified 'piggyback' board shown with Figaro® TGS2602	232
Figure 6.7 Overlay of 1Hz injected sine waves at unity gain for each of the three systems	233
Figure 6.8 Difference in typical smoothed change in sensor resistance in response to dry 10 ppm acetone reference gas	234
Figure 6.9 Difference in typical smoothed change in sensor resistance in response to wet 10 ppm acetone reference gas	235
Figure 6.10 Difference in typical smoothed change in sensor resistance in response to zero grade air	235
Figure 6.11 PCA scores plot of dry and wet 10 ppm acetone reference gas and zero grade air	237
Figure 6.12 Raw unsmoothed Figaro® TGS 2602 sensor response to acetone in lab air	238

Figure 6.13 Comparison of CAP25, Figaro® TGS2602 and 2620 gas sensors to dry 10 ppm acetone gas from a cylinder	240
Figure 6.14 Comparison of CAP25, Figaro® TGS2602 and 2620 gas sensors to humid 10 ppm acetone gas.....	241
Figure 6.15 Comparison of CAP25, Figaro® TGS2602 and 2620 gas sensors to zero grade air	242
Figure 6.16 Scores plot for dry and wet 10 ppm acetone and zero grade air comparing CAP25, Figaro® TGS2602 and 2620 gas sensors, with zoomed inset	244
Figure 6.17 Log-log plots for the CAP25, TGS2602 and 2620 in response to acetone.....	246
Figure 6.18 Log-log plots for the CAP25, TGS2602 and 2620 in response to ammonia	247
Figure 6.19 Log-log plots for the CAP25, TGS2602 and 2620 in response to propanol	248

LIST OF TABLES

Table 1.1 Typical values for respiratory variables in healthy young adult males at rest (Pocock and Richards, 1999)	6
Table 1.2 Biochemical effects of insulin (Holt et al. 2007).....	17
Table 1.3 Physical origins of some endogenous breath molecules (Risby, 2005).....	24
Table 1.4 Examples of volatile disease biomarkers (Amann et al., 2005).....	25
Table 1.5 Common metal oxides used in sensors (Gardner and Bartlett, 1999)	38
Table 1.6 Summary of data parameters recorded in a Breathotron output file (Bishop, 2006; Patel, 2007).....	42
Table 1.7 Elements of structured array ‘Sensor’ produced by MMOSOhms100.m.....	43
Table 2.1 VOCs quantified using the H_3O^+ precursor ion on the SIFT-MS.....	53
Table 2.2 Lung function data for the volunteers that took part in the OGTT	59
Table 2.3 Calculated linear correlation coefficients for time and blood glucose concentration vs. ΔR_{max}	62
Table 2.4 Cumulative variance for different normalisation and data scaling methods with the method which captured the greatest variance in bold	64
Table 2.5 Linear correlation coefficients for exhaled VOCs quantified using SIFT-MS vs. Time. 81	
Table 2.6 Linear correlation coefficients for exhaled VOCs quantified using SIFT-MS vs. Blood glucose concentration	82
Table 2.7 Linear correlation coefficients for exhaled VOC concentration quantified using GC-MS vs. Time.....	88
Table 2.8 Linear correlation coefficients for exhaled VOC concentration quantified using GC-MS vs. Blood glucose concentration.....	88
Table 3.1 Actual blood glucose concentrations recorded during the hypoglycaemic clamp ...	102
Table 3.2 Linear correlation coefficients for Breathotron sensor resistance Vs. Measured blood glucose concentration	103
Table 3.3 Linear correlation coefficients for exhaled breath VOCs vs. Measured blood glucose concentration	110
Table 3.4 Linear correlation coefficients for skin headspace VOCs vs. Measured blood glucose concentration	116
Table 3.5 Linear correlation coefficients for blood headspace VOCs vs. Measured blood glucose concentration	122
Table 3.6 Linear correlation coefficients GC-MS breath VOCs vs. Measured blood glucose concentration	128

Table 3.7 Linear correlation coefficients GC-MS blood headspace VOCs vs. Measured blood glucose concentration	132
Table 3.8 Linear correlation coefficients Breathotron ΔR_{\max} vs. Acetone concentration quantified using SIFT-MS.....	134
Table 3.9 Linear correlation coefficients Breathotron ΔR_{\max} vs. Acetone concentration quantified using GC-MS.....	135
Table 4.1 The Borg rating of perceived exertion (RPE) dyspnoea scale (10 point) (Borg 1970)	148
Table 4.2 Height, weight and respiratory function data	149
Table 4.3 Total distance walked (6MWD) during control and with respiratory restriction walk tests	151
Table 4.4 Results of the tests within subjects ANOVA analysis on SIFT-MS data data (* = $P < 0.05$, ¹ = Greenhouse-Giessier correction applied)	166
Table 4.5 Results of the tests within subjects ANOVA analysis on GC-MS data (* = $P < 0.05$, ¹ = Greenhouse-Giessier correction applied)	173
Table 5.1 Lung function and BMI of the seven volunteers	187
Table 5.2 ANOVA analysis of online SIFT-MS and clearance data.....	206
Table 6.1 Linear correlation coefficients for the CAP25, TGS2602 and TGS2620 calibration curves	249

LIST OF EQUATIONS

(1.1) 11

(1.2) 38

(2.1) 51

(5.1) 182

LIST OF ABBREVIATIONS AND NOTATION

ΔR	Change in resistance
ΔR_s	Change in sensor resistance
$^{\circ}\text{C}$	Degrees Celsius
μg	Micrograms
$\mu\text{g mL}^{-1}$	Micrograms per millilitre
μl	Microlitre
^{13}C	Carbon 13
^{14}C	Carbon 14
6MWT	Six minute walk test
AC	Alternating current
ADC	Analogue to digital
ATP	Adenosine triphosphate
BAC	Blood alcohol content
BCAA	Branched chain amino acid
BMI	Body mass index
c s^{-1}	Counts per second
CA	California
cAMP	Cyclic adenosine monophosphate
CF	Cystic fibrosis
CGMS™	Continuous Glucose Monitoring System
CHF	Congestive heart failure
CHF	Congestive heart failure
cm	Centimetre
CO	Carbon monoxide
CO ₂	Carbon dioxide
COPD	Chronic obstructive pulmonary disorder
CRF	Clinical Research Facility
CSG	Chronic superficial gastritis
csv	Comma separated values
CUHREC	Cranfield University Research Ethics Committee
DC	Direct current
DNA	Deoxyribonucleic acid
DSUG	Dipstick urine glucose
DUI	Driving under influence
EI	Electron ionisation
eNose	Electronic nose
ERV	Inspiratory reserve volume
FDA	Federal Drug Administration
FRC	Functional residual capacity
FRV	Functional reserve volume
FS	Full scan mode
g	Grams

GC	Gas chromatography
GC-MS	Gas chromatography mass spectrometry
GDM	Gestational diabetes mellitus
GI	Gastrointestinal
GOx	Glucose oxidase
GSH	Glutathione
HBT	Hydrogen breath test
HCT	Haematocrit
HMG-CoA	Hydroxymethylglutaryl-CoA
HP®	Hewlett Packard
IBS	Irritable bowel syndrome
IL	Illinois
IMS	Ion mobility spectroscopy
IR	Infrared
K	Kelvin
K ₂ HPO ₄	Dipotassium phosphate
kb	Kilo bytes
kDa	Kilo Daltons
kg	Kilo grams
KH ₂ PO ₄	Monopotassium phosphate
kmh	Kilometres per hour
kPa	Kilo Pascal
kΩ	Kilo Ohms
L	Litre
LDH	Lactate dehydrogenase
LDL	Low density lipoprotein
LVBG	Laboratory venous glucose
m	Metres
<i>m/z</i>	Mass to charge ratio
MB	Megabytes
MDA	Malondialdehyde
mg L ⁻¹	Micro grams per litre
mg min ⁻¹	Micrograms per minute
MIM	Multi ion mode
min	Minutes
mL	Millilitres
mL min ⁻¹	Millilitres per minute
mM	Millimoles
mm	Millimetres
MMOS	Mixed metal oxide semiconductor
MN	Minnesota
MOS	Metal oxide semiconductor
mph	Miles per hour
MS	mass spectrometry

ms	Milli second
MTBE	Methyl tert-butyl ether
mW	Milli watts
N ₂	Nitrogen
NAFLD	Non-alcoholic fatty liver disease
ND	No detect
ng	Nanograms
ng μL^{-1}	Nanograms per microlitre
ng L ⁻¹	Nanograms per microlitre
NHS	National Health Service
nmol L ⁻¹	Nanomoles per litre
NO	Nitric oxide
NST	Nordic Sensor Technologies
NY	New York
O ₂	Oxygen
OGTT	Oral glucose tolerance test
PA	Pennsylvania
Pani	Polyaniline
PBS	Phosphate buffer solution
PC	Personal computer
PC	Principal component
PCA	Principal components analysis
PDA	Personal digital assistant
PEEK	Polyether ether ketone
PEF	Peak expiratory flow
PEPCK	Phosphoenolpyruvate carboxykinase
PFT	Pulmonary function test
PID	Photoionisation detector
pmol L ⁻¹	Picomoles per litre
PNC	Purine deamination cycle
ppb	Parts per billion
ppm	Parts per million
ppt	Parts per trillion
Ppy	Polypyrrole
PTFE	Polytetrafluoroethylene
PTh	Polythiophene
PTR-MS	Proton transfer mass spectrometry
PVF	Polyvinyl fluoride
R ₀	Baseline resistance
ROS	Reactive oxygen species
RV	Residual volume
s	Seconds
S2N	Signal to noise ratio
SAW	Surface acoustic wave

SD	Flash memory
SIC	Single ion chromatogram
SIFT-MS	Selected ion flow tube mass spectrometry
SMBG	Self-monitoring of blood glucose
SMOS-GA	Single metal oxide semiconductor gas analysis
SPME	Solid phase micro extraction
stp	Standard temperature and pressure
T1DM	Type 1 diabetes mellitus
T2DM	Type 2 diabetes mellitus
TB	Tuberculosis
TBARS	Thiobabituric acid reactive substance
TCA	Tricarboxylic acid
TD	Thermal desorption
TIC	Total ion chromatogram
TK	Tyrosine kinase
TSCG	Test strip capillary glucose
UK	United Kingdom
US	United States of America
USB	Universal serial bus
UV	Ultraviolet
V	Volts
VC	Vital capacity
VOC	Volatile organic compound
VT	Tidal volume
W	Watts
w/w	Weight for weight
WA	Washington
WHO	World Health Organisation
YSI	Yellow Springs Instrument
Ω	Ohms

1 Introduction and Literature Review

1.1 Introduction

Breath analysis for diagnosis and clinical monitoring is not a revolutionary new concept. The potential of using breath was first acknowledged by ancient Greek and Chinese physicians, however, during more recent times, analysis of bodily fluids, faecal matter, biopsies and a variety of imaging techniques have become commonplace in clinical settings.

The traditional method of monitoring long-term metabolic conditions, such as diabetes, is by the analysis of urine and blood samples. The collection of biological samples such as blood and urine presents a number of challenges:

- Samples have to be collected by suitably qualified individuals,
- Storage and destruction of biological samples,
- Painful and invasive nature of blood sample collection, and
- The increased risk of infection.

The attractiveness of breath analysis is the non-invasive nature of sample collection, the lack of storage and destruction issues and potentially, the reduced need for qualified medical personnel. Faster diagnostic methods may ultimately reduce diagnostic time, leading to clinical decisions being made in a timelier fashion, and subsequently reduce healthcare costs. Self-monitoring using breath may ultimately prove more comfortable, and increase compliance amongst certain patient groups.

One of the major challenges faced in developing instruments for breath analysis is developing a rapid analysis technique. Mass spectrometry (MS) can be used to analyse gaseous samples, but these are only useful in a laboratory setting, with analysis time, cost, size and complexity being the influencing factors preventing the widespread use of MS in the clinical environment.

Gas analysis instruments known as electronic nose, or eNose, devices attempt to mimic a conventional biological olfactory system and contain an array of sensors and a pattern recognition system for rapid sample classification (Gardner and Bartlett, 1999). These devices are typically large-in-size, complex and have high power consumption. They are not generally designed to be portable, and are primarily bench-top instruments. For breath gas analysis to become widely adopted, devices must be smaller, lightweight, consume little power and must be easy to use by clinicians and patients alike.

It would ultimately prove more efficient if the chemical compounds (herein referred to as 'biomarkers') associated with a particular condition were to be identified using laboratory based gas analysis techniques, such as selected ion flow tube mass spectrometry (SIFT-MS) and gas chromatography mass spectrometry (GC-MS), and then for suitable sensors to be selected for a device based on the data obtained. Biomarkers are typically low molecular weight proteins, hormones and metabolic by-products that are produced endogenously through cellular biochemical reactions.

The presence, absence or changes in concentration of these biomarkers can be monitored over time and may provide diagnostic information, or can be used to monitor long-term conditions such as metabolic disorders, cystic fibrosis (CF), respiratory disease, cancer, as well as monitoring infections, efficacy of treatments and athletic performance.

Glucose is the brain's primary energy source. In the absence of glucose, during fasting for example, the body looks for an alternative source of energy primarily from glycogen stores. After depletion of glycogen stores within the liver, ketogenesis is favoured. In ketogenesis the compounds acetoacetic acid, acetone and β -hydroxybutyric acid are produced as precursors from fatty acids stored in the liver and adipose tissue. The exhaled acetone concentration is in proportion to plasma ketone concentrations (Musa-Veloso et al., 2002) and has been shown to be an indicator of blood glucose concentration in previously published literature (Galassetti et al., 2005; Turner et al., 2008; Lee et al. 2009). Acetone, amongst other compounds, may act as a surrogate marker for glycaemic status.

The aims of this project were to establish the extent to which determination of the concentrations of volatile organic compounds (VOCs) in exhaled breath might be used as a means of monitoring chronic disease, with a particular emphasis on diabetes, and investigate the suitability of simple, commercially-available vapour sensors for carrying this out. A combination of both *in vitro* and *in vivo* studies were performed which aimed to identify and quantify potential biomarkers of glycaemic status.

Data from two complementary analytical techniques, namely SIFT-MS) GC-MS, were used in several *in vivo* experiments to establish potential links between exhaled VOCs and blood glucose concentration. Particular interest was paid to exhaled breath acetone concentration, which is known to be elevated in diabetic patients at low blood glucose concentrations.

In conjunction to the mass spectrometry data, exhaled breath was also analysed using a prototype breath gas analyser, known as the Single Metal Oxide Semiconductor Gas Analyser (SMOS-GA) or 'Breathotron'. Data collected from this device was examined to elucidate changes in exhaled VOC concentration and determine whether this was linked to glycaemic status.

1.2 Breath

The process of breathing involves the gaseous exchange via the nose and mouth of oxygen (O_2) into the body that is utilized by the mitochondria within cells to generate adenosine triphosphate (ATP), and exhalation of carbon dioxide (CO_2) (4%), oxygen (18%), nitrogen (N_2) (78%), water vapour (H_2O) and a mixture of various gases. These gases are present in the $nmol\ L^{-1}$ to $pmol\ L^{-1}$ range (Miekisch et al., 2004). Lipid degeneration products, aromatic compounds, amine compounds and hydrogenated compounds are also excreted in breath (Manolis, 1983). This exchange takes place in the alveoli of the lungs by passive diffusion.

1.2.1 Respiratory physiology

This description of respiratory physiology is derived from Pocock and Richards (1999). Air flows through the nose and mouth into the airways of the lungs, situated in the chest cavity, before meeting the respiratory surface that is the site of gaseous exchange. At rest, the normal route of air is via the nose, which traps airborne particles, moistens and warms the inhaled air. During times when there is an increased demand for oxygen, intensive exercise for example, air can be inhaled through the mouth as this pathway offers a lower resistance to air flow. Inhaled air then passes through membrane lined cavity situated immediately behind the nose and mouth, called the pharynx, that serves to connect them to the oesophagus, and into to the larynx, a hollow muscular organ that holds the vocal cords. The resistance to air flow in the larynx is high, and this is property is exploited for vocalization.

The first component of the respiratory tree linking the larynx to the lungs is the trachea; in an adult, it is approximately 1.8 centimetre (cm) in diameter and 12 cm in length. The trachea then branches into two arms, the bronchi, which again split into two smaller branches, of which there are twenty-three generations, in each lung until they reach the respiratory surface. C-shaped rings of cartilage hold open the trachea and primary bronchi. The smaller bronchi are held open by overlapping plates of cartilage. Branch generations four to sixteen

are known as bronchioles, all generations to this point are known as conducting airways, as they play no significant part in gaseous exchange.

The sixteenth generation terminates at the terminal bronchioles that form the first generation of the respiratory bronchioles branch into alveolar ducts that form the alveolar sacs consisting of two or more alveoli where gaseous exchange occurs. Bronchioles are less than 1 mm in diameter and do not contain any cartilage and collapse when the pressure outside the lungs is greater than the pressure in the airways, this happens during forced expiration. In total, the respiratory bronchioles, alveolar ducts, and alveoli that comprise the transitional and respiratory airways, provide a large surface area of approximately 60-80 m² for gaseous exchange. There are approximately 300 million alveoli in a typical adult lung, each with a rich supply of capillaries, thought to be as numerous as 1000 per each alveolus. The junction of the alveoli and capillaries is known as the alveolar-capillary unit, Figure 1.1. The pulmonary blood vessels are separated from the alveolar air by as little as 0.5 μ m.

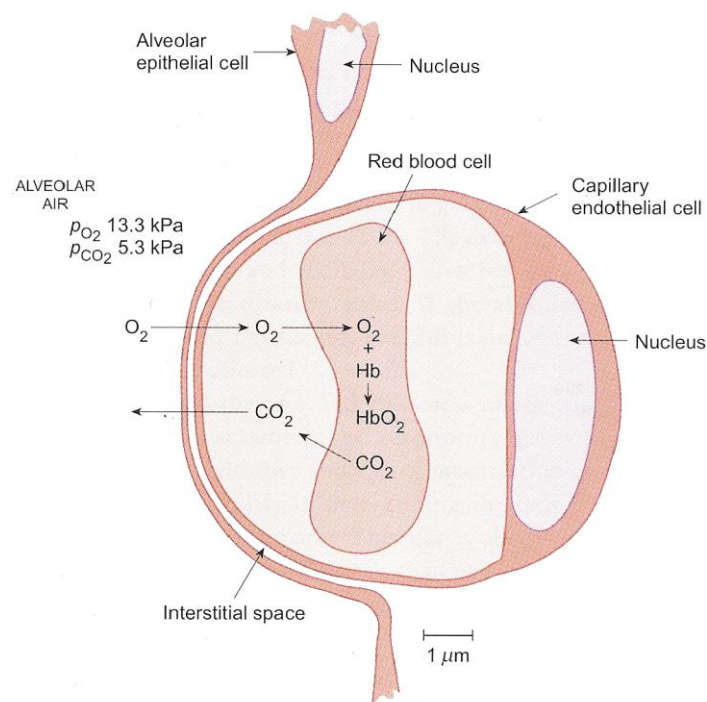


Figure 1.1 Alveolar capillary unit – the site of gaseous exchange. Reproduced from Pocock and Richards (1999).

Two different types of cell line the alveoli, these are known as the alveolar type I cells, which are squamous epithelial cells, and the type II cells that are thicker and produce the aqueous lining of the alveoli, pulmonary surfactant, a surface-active lipoprotein, is also produced and secreted by these cells. Pulmonary surfactant works by lowering the surface tension of the

aqueous lining of the alveoli, preventing their collapse (atelectasis), as much lower pressures are required to keep them open. Pulmonary surfactant also increases pulmonary (lung) compliance, the ability of the lungs to 'distend under pressure as measured by pulmonary volume change per unit pressure change'; this provides a measure of the comparative stiffness of the lungs (Best et al., 1990). A low pulmonary compliance results in extra effort to inhale a normal volume of air.

Between the capillaries in the walls of the alveoli are the connective tissues of the lung, formed from elastic and collagen fibres. The lung parenchyma, which is sponge-like in appearance, is formed from alveoli linked by connective tissue. Small passages, called the pores of Kohn, connect neighbouring alveoli.

Cholinergic fibres innervate the smooth muscle to the vagus nerves. Bronchoconstriction is caused by the activation of these nerves. Circulating adrenaline causes bronchodilation of the smooth muscle through the β -adrenergic receptors that cause smooth muscle relaxation. The drug salbutamol is used by asthmatics to overcome bronchospasm during asthmatic attacks. Though sympathetic nerves innervate the bronchiole circulation, there is no sympathetic innervation of the bronchiolar smooth muscle.

1.2.2 Lung function and spirometry

The name given to the process of inhalation and exhalation of air into and out of the lungs is ventilation. Contraction of the diaphragm and intercostal muscles causes a pressure change within the chest, the alveolar pressure is less than the atmospheric pressure, and air consequently flows into the lungs. Exhalation is largely passive, and is caused by the slow relaxation of the diaphragm and the elastic recoil of the chest wall.

The total lung capacity is the maximum volume of air that the lungs can contain when the lungs are expanded, and have inflated fully. The lungs are never completely devoid of air, they will still contain a small amount of air known as the residual volume (RV). The vital capacity (VC), is the amount of air that is breathed out following a maximal inspiration, this is approximately 5 litres. The tidal volume (V_T), refers to the air that is breathed in and out with each breath. The difference between the two is known as the inspiratory reserve volume (ERV). The air left in the lungs at the end of expiration is known as the functional residual volume (FRV). The various lungs volumes from an ideal spirogram are displayed graphically in

Figure 1.2 for comparison purposes. Typical values for these variables in healthy adult males are given in Table 1.1 (Pocock and Richards, 1999).

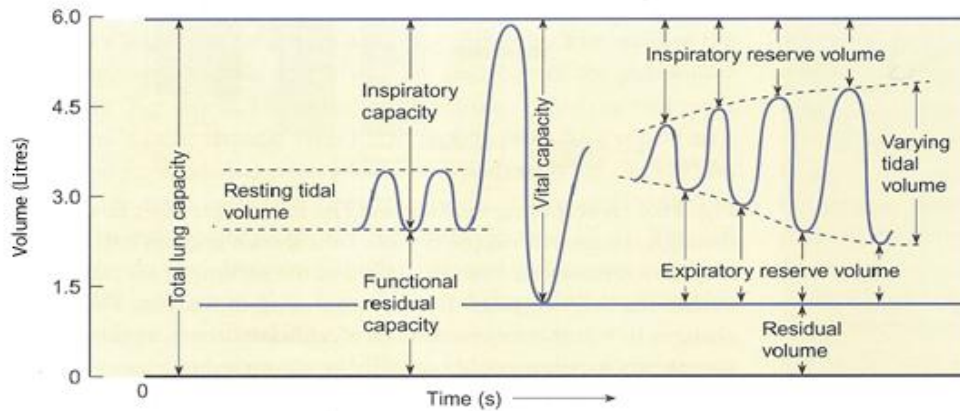


Figure 1.2 Subdivisions of lung volumes (Pocock and Richards, 1999)

Lung volume, largely, depends upon:

- Age,
- Body size,
- Gender,
- Training (state of fitness)

The tidal volume varies with the body's requirement for oxygen affecting both the inspiratory (inhalation) and expiratory (exhalation) reserve volumes. However, the vital capacity and the relative volumes remain relatively fixed. The volume of the lungs, though not the residual volume and the functional residual capacity, can be directly measured using spirometry, which will be discussed in more detail below.

Respiratory Variable	Typical value
Total lung volume (L)	6.0
Vital capacity (L)	4.8
Residual volume (L)	1.2
Tidal volume (L)	0.6
Respiratory frequency (breaths min⁻¹)	12
Minute ventilation (L min⁻¹)	7.2
Functional residual capacity (L)	2.2
Inspiratory capacity (L)	3.8
Expiratory reserve volume (L)	1.0

Table 1.1 Typical values for respiratory variables in healthy young adult males at rest (Pocock and Richards, 1999)

The function of the lungs can be measured using a lung function test, also known as a pulmonary function test (PFT). The most common methods of assessing lung function will be briefly discussed here.

1.2.3 Spirometry

Spirometry is the most common lung function test performed, the volume and the flow air exhaled breath is measured using an instrument known as a spirometer. Before the test begins, a soft nose clip is placed on the patient's nose; this is to prevent air from escaping through the nostrils. The patient is asked to make a maximal inhalation and exhale into the spirometer at maximal exhalation until their lungs are devoid of gas.

There are limitations to spirometry, as the results are highly dependent on patient cooperation. Spirometry can only be used on those that are able to comprehend the instructions, so is unsuitable for extremely young patients or those that are unconscious or sedated.

A variety of spirometers are available, and some are hand held. A typical handheld spirometer can be seen in Figure 1.3. Spirometers into one of two categories: Volume spirometers measure the amount of air inhaled, or exhaled over a period-of-time. Flow spirometers measure the velocity of airflow. A spirogram is a graph produced by a spirometer; these can show a volume-time curve or a flow-volume loop – a graph of the rate of the total volume plotted against the rate of airflow. Some spirometers provide a digital read out of the various variables they have been programmed to measure. A wet spirometer uses inverted bellows over a liquid sealant such as water, Figure 1.4, where the bellows move up and down as the patient inhales and exhales air. Data are recorded onto a rotating drum (Singh 2010).



Figure 1.3 A typical digital hand held spirometer shown with disposable cardboard mouth piece

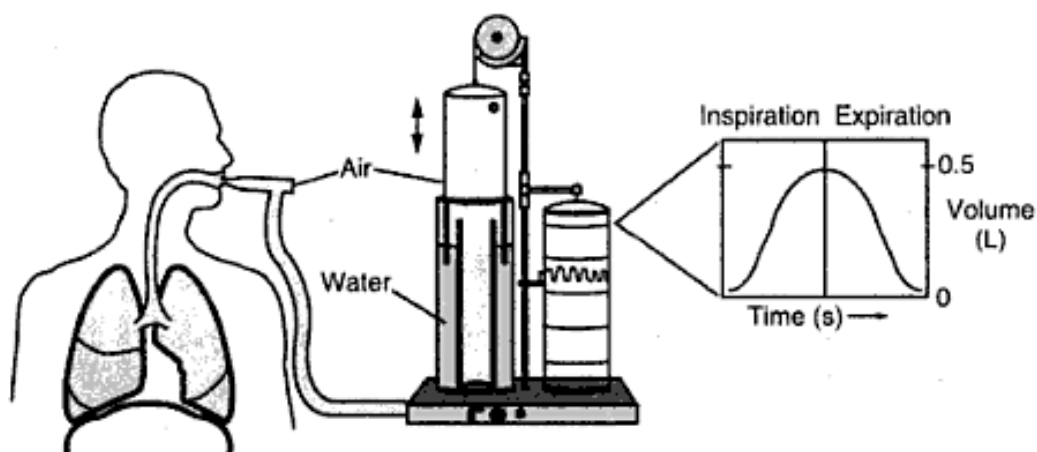


Figure 1.4 A wet spirometer with inverted bellows (Singh, 2010)

Modern spirometers use flow sensors that measure the differential pressure across a fixed resistance. The different types of sensor that are available are illustrated in Figure 1.5 (a-d), where P=Pressure, F=Flow, V=volume, R= resistance. The Fleisch type pneumotachometer (a) uses an array of capillaries that are in parallel with the flow. The Lilly type (b) is a variant of the Fleisch that uses a fine mesh to offer resistance to the airflow. Turbine sensors (c) are much simpler than the Fleisch or Lilly types. The flow of air rotates the vanes of the turbine that cuts a photocell where the flow of gas is proportional to the speed of the rotating vanes. The

advantage of the turbine is that it is unaffected by the composition of the gas, water vapour, temperature and turbulence. The disadvantage however is the poor dynamic response due to the need to use a lightweight vane. Hot wire type spirometers consist of heated platinum in the air stream. As cooler gas passes over the hot wire electrical, current is required to maintain the temperature. The disadvantage of hot wire type spirometers is that they are sensitive to the gas composition, temperature and water vapour. They also have a non-linear output and are extremely fragile.

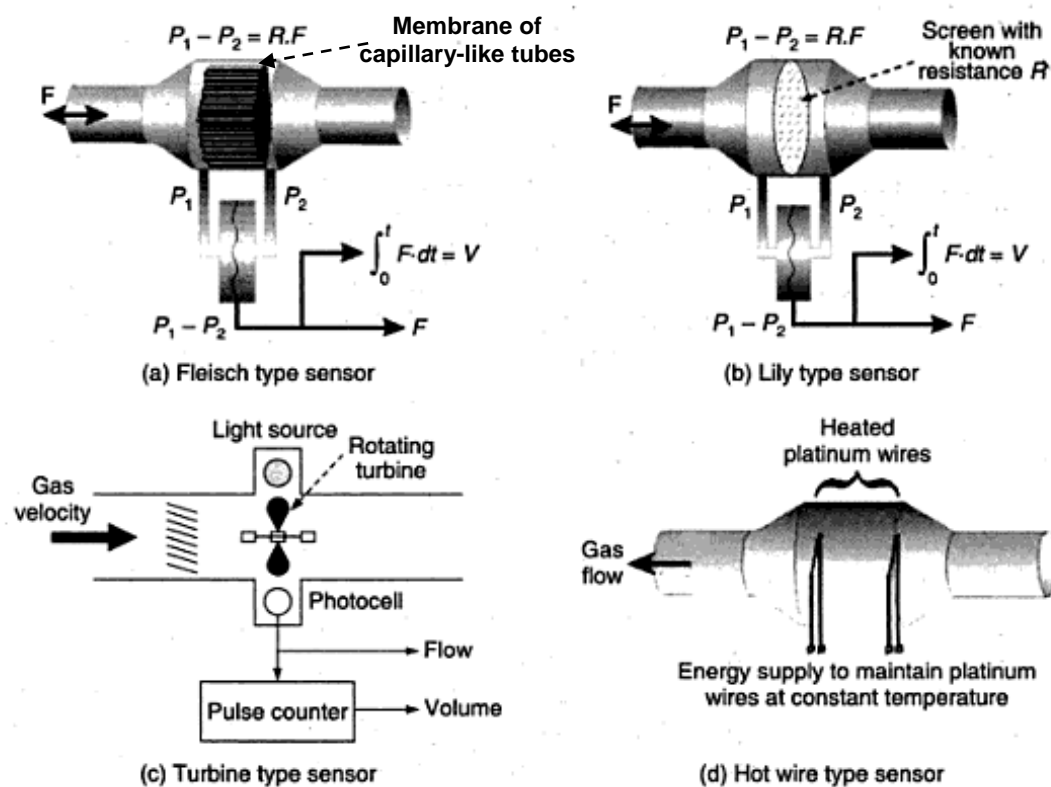


Figure 1.5 The different types of sensor used in modern spirometers. Reproduced from Singh, (2010)

1.2.4 Other methods for lung function assessment

1.2.4.1 Whole body plethysmography

Plethysmography is a very sensitive method for measuring the change in volume of an organ or the whole body by the resultant displacement of air. A pulmonary plethysmograph can be used to measure the changes in residual volume of the lungs, but as the patient is required to sit inside a sealed chamber for this to be carried out, it is more commonly known as whole body plethysmography.

The patient is required to sit in a sealed chamber, similar in size to a telephone box. They are then required to breathe into a mouthpiece. At the end of the exhalation, the mouthpiece is closed. The patient is then instructed to inhale, by doing so the lungs expand and the pressure within the lungs decreases. As the mouthpiece is closed and air within the chamber is not able to enter the lungs, the body volume has increased due to the effort of inhalation compressing the air inside the sealed chamber (Singh, 2010). A pressure transducer is used to measure the change in pressure within the chamber. Mouth and chamber pressure changes are typically measured during tidal breathing and panting manoeuvres to calculate thoracic gas volume.

1.2.4.2 Peak flow meter

A peak flow meter is a small hand held device that is used to measure velocity of exhalation, the peak expiratory flow (PEF). A typical peak flow meter can be seen in Figure 1.6. The peak flow meter is primarily used to measure the airflow through the bronchi, to determine obstruction in the airways. They are most commonly used in the treatment of patients with asthma, but not diagnosis due to the wide range of inter-individual variability, though may be used in patients with other respiratory diseases. The deviation in recorded values for a given patient can determine lung functionality, severity of asthma and possible treatment outcomes.



Figure 1.6 A typical peak flow meter

1.2.4.3 Nitrogen washout

The dead space of the respiratory system can be determined using a nitrogen washout. This is also known as Fowler's method, Figure 1.6. In respiratory physiology, there are different types of dead space, known as the anatomical dead space, which does not mix with alveolar air, and

the physiological dead space, the portion of breath that does not take part in gaseous exchange. As with other lung volumes, the anatomical and physiological dead space varies and is dependent on body size, age and gender. In a typical healthy adult, the two dead spaces are approximately of the same value. This is typically 150 mL each as per a V_T of 500 mL.

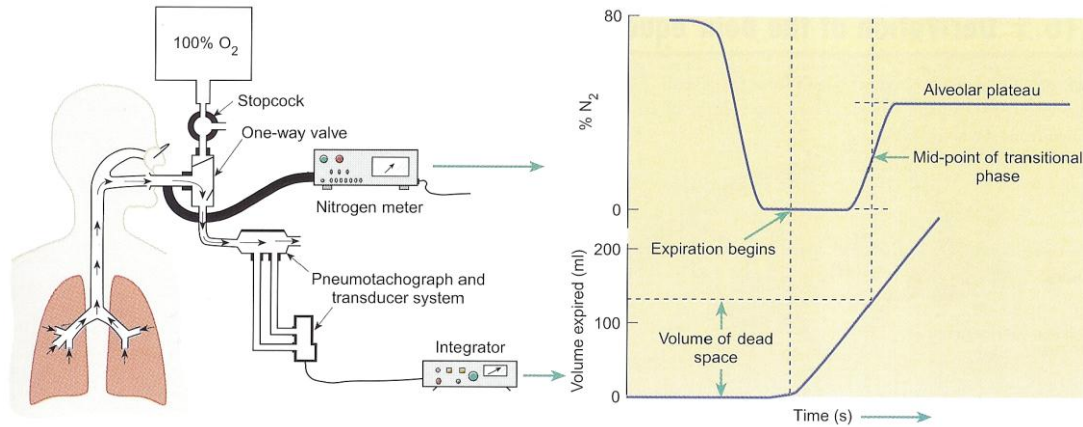


Figure 1.7 Fowler's method (nitrogen washout) for measuring anatomical dead space (Pocock et al., 1999)

The anatomical dead space can be measured by inhalation of pure O_2 by the patient. This breath is then held before exhaling. The composition of the breath in the conducting airways will be pure O_2 , however the alveoli will contain nitrogen. As the patient exhales the nitrogen concentration and volume are continuously monitored, the exhaled breath will contain an increasing concentration of nitrogen until it reaches the alveolar concentration. The alveolar dead space is the volume that is exhaled between the beginning of exhalation to the mid-point between the zero level and the plateau value. The physiological dead space is equal to the volume of the non-inspiratory airways plus the volume of air that enters alveoli that is not perfused with blood; these alveoli do not take part in gaseous exchange. The physiological dead space can be estimated by measuring the CO_2 content of exhaled alveolar breath using the Bohr equation, Equation 1.1, defined as the ratio of dead space to tidal volume (West 2008) where $P_a CO_2$ is the partial pressure of carbon dioxide in blood, and $P_e CO_2$ is the partial pressure of exhaled CO_2 .

$$\frac{V_d}{V_t} = \frac{P_a CO_2 - P_e CO_2}{P_a CO_2} \quad (1.1)$$

1.2.4.4 Helium dilution method

The functional residual capacity (FRC) and RV cannot be determined using a spirometer. The helium dilution method is used instead. The patient is required to inhale from a spirometer filled with a known concentration and volume of helium in air. As the patient inhales and exhales, the concentration of helium is diluted by the volume of air in the lungs; this can be measured to work out the FRC and RV (Pocock et al., 1999).

1.3 Existing applications of breath analysis

Breath analysis is currently used in a variety of medical applications and in law enforcement. Many of the common tests described below are specific for a particular compound. For example, a Breathalyser used to determine blood alcohol content (BAC) at the roadside cannot be used to detect NO in asthmatic patients.

1.3.1 Determining blood alcohol content in exhaled breath

In the United Kingdom, driving under influence (DUI) is a criminal charge of driving a motor vehicle under the influence of alcohol or drugs (Road Traffic Act 1988, s3A(1)). An individual suspected of 'drink driving' would be asked to provide a specimen of breath at the roadside. This involves blowing into a device known as a Breathalyser. The device approved by the Home Office for use by UK Police Forces is the Dräger 6510 (Dräger Safety AG & Co. Leubeck Germany). Fuel cell technology is commonly employed in Breathalyser devices. The fuel additive methyl tert-butyl ether (MTBE) is known to interfere with readings from older Breathalysers (Buckley et al., 2001). Newer models can detect and compensate for this interference.

The reading at the roadside is considered unreliable and therefore evidentiary equipment, based on infrared (IR) spectroscopy is used. IR spectroscopy is a form of absorbance spectroscopy that utilizes electromagnetic radiation in the infrared region. Absorption occurs when the IR wavelength is the same as the chemical bonds in ethanol, causing them to vibrate (Dasgupta, 2011). This test is conducted away from the roadside at a police station.

1.3.2 Monitoring asthma using exhaled nitric oxide

Nitric oxide (NO) is found in breath (Gustafsson et al., 1991), is a marker of inflammation and may be a potential marker for respiratory disease. Patients with asthma have a higher level of NO in their breath when compared with healthy individuals (Alving et al., 1993; Khartionov et

al., 1994; Persson et al. 1994; Yates et al., 1995). In May 2003 the US Food and Drug Administration (FDA) approved the first device for monitoring breath NO (Silkoff et al., 2004). The NIOX NO Monitoring System (Aerocrine AB, Stockholm, Sweden) works on the principal of chemiluminescence, coupled with a specific NO sensor. NO in the patient's breath reacts with ozone releasing photons that are detected by a photomultiplier tube. The device is able to detect NO down to 2 ppb.

The NIOX instrument is designed to work within a specific exhalation flow rate at which the soft palate at the back of the pharynx lifts, ensuring that the NO being analysed originates only from the lungs and not the nasal cavity (Silkoff et al., 1999). NO is not only a marker of airway inflammation, but it may also have anti- and pro-inflammatory effects (Silkoff et al., 2000).

1.3.3 Urea breath test for detection of *Helicobacter pylori* infection

Helicobacter pylori (H.Pylori) is a gram-negative bacterium that infects the stomach and duodenum causing peptic ulcers, chronic superficial gastritis (CSG) and various cancers. The bacterium is found on the inner surface of the stomach epithelial cells and occasionally inside epithelial cells (Petersen and Krogfelt, 2003). The enzyme urease is produced in large concentrations and catalyses hydrolysis of urea to CO₂, where the carbon isotope (¹³C or ¹⁴C) is incorporated into exhaled CO₂, and ammonia which is toxic to epithelial cells (Smoot, 1997).

One method of diagnosis is the urea breath test, where a fasted patient ingests non-radioactive ¹³C or radioactive ¹⁴C labelled CO₂ (Saad and Chey, 2007; Malfertheiner et al., 2007). After a period of thirty minutes, the patient's breath is tested. Two different methods must be used for the two isotopes, with ¹³C labelled CO₂ using isotope mass spectrometry, whilst ¹⁴C labelled CO₂ is measured using a scintillation counter (Shirin et al., 2001; Israeli et al., 2003).

1.3.4 Hydrogen breath test for carbohydrate intolerance and bacterial overgrowth

The hydrogen breath test (HBT) is used to diagnose gastrointestinal problems involving carbohydrate intolerance, such as irritable bowel syndrome (IBS), and bacterial overgrowth. Anaerobic bacteria in the colon produce hydrogen when they are exposed to unabsorbed carbohydrates (Yamada and Kakehi, 2011). Some of the hydrogen produced diffuses into the blood stream and is exhaled from the lungs.

The patient is required to fast for a minimum of 12 hours, after which they are required to breathe into a balloon. The hydrogen in the balloon is then analysed, and the patient is required to ingest a small amount of sugar. The sugar used is dependent on the specific test. Additional samples of breath are analysed every fifteen minutes for three to five hours. The results of the test are dependent on the specific sugar used and the pattern of exhaled hydrogen after consuming the sugar.

1.4 A general background of diabetes mellitus

Diabetes mellitus is a complex chronic metabolic disorder that is characterised by hyperglycaemia, an abnormally high blood glucose level. The existence of diabetes has been documented by physicians over many thousands of years. Ancient Vedic text describes it as a disease that causes intense thirst, increased urine output and wasting of the body (Gordon, 1960).

At the turn of the century an estimated 177 million people worldwide had diabetes, this was projected to increase to 366 million by 2030 (Wild et al. 2004). There are an estimated 2.35 million people in England alone living with diabetes; this figure is expected to rise to more than 2.5 million by the end of the decade (Roberts, 2006). In 2002, diabetes accounted for 5% (£1.3 billion) of the total National Health Service (NHS) expenditure; this is now estimated to be over 10% (Wanless, 2002; Roberts, 2006).

1.4.1 The different types of diabetes

According to the amended World Health Organisation (WHO) guidelines (2003) there are three variations of Diabetes Mellitus:

- Type 1 Diabetes Mellitus (T1DM) (formerly insulin dependent Diabetes Mellitus),
- Type 2 Diabetes Mellitus (T2DM) (formerly non-insulin dependent Diabetes Mellitus),
- Gestational Diabetes Mellitus (GDM).

The symptoms consistent with all forms of Diabetes are (Holt et al., 2007):

- Polyuria (excessive urine production),
- Polydipsia (excessive thirst),
- Weight loss,
- Difficulties with vision,
- Fatigue

The differences between T1DM and T2DM are briefly explained diagrammatically in Figure 1.8

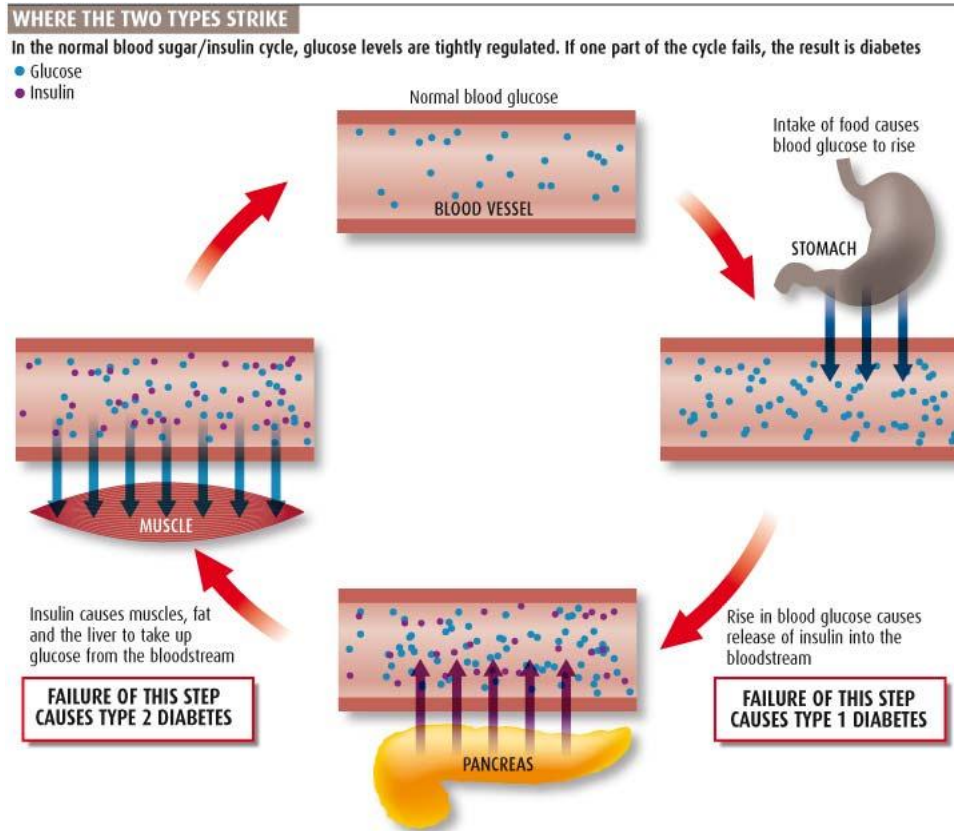


Figure 1.8 Differences between T1DM and T2DM (Whelan, 2007)

1.4.2 Type 1 Diabetes Mellitus

Approximately 15% of patients with diabetes have type 1 diabetes mellitus (T1DM), and is partly a genetic disorder. T1DM is also known as Juvenile Diabetes, as the majority of the cases are in children, though the symptoms can appear later in an individual's life.

In T1DM, the insulin producing β -cells of the islets of Langerhans in the pancreas are destroyed in a T-cell mediated autoimmune attack (Rother, 2007), decreasing the amount of insulin that is produced. When the loss of β -cells is significant the production of insulin is inadequate, this results in hyperglycaemia. The destruction is irreversible and can take place over a period of several years; this is known as the pre-diabetic phase.

The stimulus that initiates the pre-diabetic phase is not fully understood, though it is thought to be an environmental factor, either a toxin or a virus (Tuch et al., 2000). It had been proposed that a possible trigger is an antibody against the protein bovine serum albumin (BSA) that is found in cow's milk (Karjalainen et al., 1992; Hilger et al., 2001), though a subsequent study disproved this, showing that exposure to cow's milk in diabetes-prone rodents did not alter the frequency of developing diabetes (Persaud and Barranco-Mendoza, 2004). Instead,

the authors suggested that T1DM is caused as the result of oxidative stress on the β -cells of the pancreas caused by an inflammatory response that is mediated by CD and CD8 cells (Atkinson et al., 1993; Karjalainen et al., 1992; Kolb et al., 1995).

Treatment of T1DM involves exogenous injections of insulin. In common with all other proteins, insulin is degraded by proteases in the gastrointestinal tract, and therefore it cannot be taken orally. Injections first used insulin derived from animals, but it is now chemically synthesised using recombinant deoxyribonucleic acid (DNA) technology (Holt et al. 2007).

1.4.3 Type 2 Diabetes Mellitus

T2DM is the most prevalent form of diabetes, it is characterised by resistance to insulin or reduced sensitivity to insulin, which in turn elevates blood sugar levels. This is combined with reduced insulin secretion. There is a genetic predisposition towards T2DM, but it has been observed that over 50% of patients with T2DM are clinically obese (Eberhart et al., 2005). There are many proteins involved in the metabolic pathway; genetic defects in these proteins that interact with insulin could possibly cause insulin resistance. The proliferation of childhood obesity has meant that there are increasingly more children and adolescents are diagnosed with T2DM (Silverstein and Rosenbloom, 2003).

1.4.4 Gestational Diabetes Mellitus

Gestational diabetes mellitus (GDM) is similar to T2DM, reduced insulin secretion and insulin resistance, however as the name suggests, it only occurs during pregnancy. The incidence of GDM is very low, 5-10% of all pregnancies (2004a) and the symptoms recede after delivery, however 20-50% of women affected by GDM go on to develop T2DM later on in life (Kim et al., 2002). A recent study in the US found that it is increasingly common for women to go into pregnancy with pre-existing diabetes (Lawrence et al., 2008).

1.4.5 Hypoglycaemic unawareness

Hypoglycaemic unawareness is when a diabetic patient does not realise that their blood glucose concentration is falling dangerously low (Cryer, 1997). This is more common amongst patients with long-term T1DM, and usually are suffering from autonomic neuropathy, their brain may have become desensitized to hypoglycaemia, or they are taking drugs which mask the symptoms of hypoglycaemia (Cryer, 1997). In these patients, as blood glucose concentration decreases, insulin concentration does not fall. Glucagon levels do not decrease.

1.5 Biochemistry of Diabetes

1.5.1 Insulin

Insulin is a 51 amino acid peptide comprised of two polypeptide chains, and has a molecular weight of 58 kilo Daltons (kDa). The hormone is synthesised in the β -cells of the islets of Langerhans in the pancreas, alpha-cells produce glucagon, delta-cells somatostatin and pancreatic polypeptide is produced by the PP cells (also known as F cells) (Holt et al., 2007).

Insulin binds to a receptor on the surface of the target cell. The insulin receptor is a heterotetramer, comprised of two alpha chains and two beta chains linked by disulphide bonds. Insulin binds to the extracellular alpha chains resulting in a conformational change allowing adenosine triphosphate (ATP) to bind to the intracellular beta chains triggering phosphorylation of the subunit (TK activity). Table 1.2 summaries the biochemical effects of insulin.

Insulin stimulates:	Insulin inhibits:
Glucose transport in muscle and tissue	Gluconeogenesis
Glycolysis	Glyconeogenesis
Glycogen synthesis	Lipolysis
Lipid synthesis	Proteolysis
Protein synthesis	
K ⁺ entry into cells	
Na ⁺ retention by renal tubules	

Table 1.2 Biochemical effects of insulin (Holt et al. 2007)

Glucose is the main stimulus for insulin secretion, though secretion can be influenced by other macronutrients, hormonal and neuronal factors. The rate of insulin secretion from the beta cells is 0.25 to 1.5 units per hour during the fasting state, where one unit of insulin is the biological equivalent of 34.7 μ g of pure crystalline insulin (Holt et al., 2007).

1.5.2 Glucagon

Glucagon is a 29 amino acid protein that is also produced in the islets of Langerhans, however, glucagon is made by the alpha cells. The effect of glucagon is the opposite of insulin, in that it increases blood glucose levels by promoting glyconeogenesis and gluconeogenesis. Glucagon also stimulates ketoneogenesis. Glucagon works by binding to a G-protein coupled receptor linked to adenylate cyclase, increasing the intracellular concentration of cyclic adenosine monophosphate (cAMP) (Holt et al., 2007).

1.5.3 Adrenaline

Adrenaline stimulates a rapid increase in hepatic glucose by increasing the intracellular levels of cAMP, increasing glycogenesis by altering the transcription rate of the rate limiting enzyme phosphoenolpyruvate carboxykinase (PEPCK) in the gluconeogenic pathway. The uptake of glucose in insulin sensitive tissues is impaired by adrenaline, whilst the release of free fatty acids is stimulated. Glucose levels are also increased as adrenaline has an inhibitory effect on insulin secretion (Holt et al., 2007).

1.5.4 Cortisol

The role of cortisol is in maintaining the key enzymes involved in gluconeogenesis, especially PEPCK. Cortisol binds to a promoter region on the PEPCK gene (O'Brien and Granner, 1990), increasing the transcription of the cortisol in a feed-forward mechanism. The hormone is secreted by the adrenal cortex, and there is a higher level of secretion in the morning than at other periods throughout the day. Cortisol inhibits insulin-mediated suppression of hepatic glucose production and the stimulation of glucose uptake.

1.6 Methods of glucose determination

1.6.1 Urine glucose

Ancient Ayurvedic physicians discovered that when they poured the urine of a patient with diabetes on the ground this attracted ants, due to the high glucose content and thus named the condition 'madhumeha' (honey in the urine) (Gordon, 1960).

There are two main types of chemical test strips available to diabetic patients: enzymatic dipstick urine glucose (DSUG) and laboratory venous glucose (LVBG). The fingertip is usually pricked and a drop of blood taken for testing. Ludvigsson (1984) found that there was correlation between DSUG and test strip capillary glucose (TSCG) (Dextrostix) amongst patients with juvenile diabetes and concluded that patients would benefit from using this method of testing.

1.6.2 Blood glucose

1.6.2.1 The Clark oxygen electrode

Prof. Leyland Clark is considered the father of the modern biosensor. In 1956, Clark published details of his oxygen electrode, Figure 1.9, which has laid the foundations on which biosensors are still made today (Clark et al., 1956). Clark later demonstrated in 1962 that by entrapping

glucose oxidase (GOx) in his oxygen electrode, he could measure the concentration of glucose (Clark and Lyons, 1962).

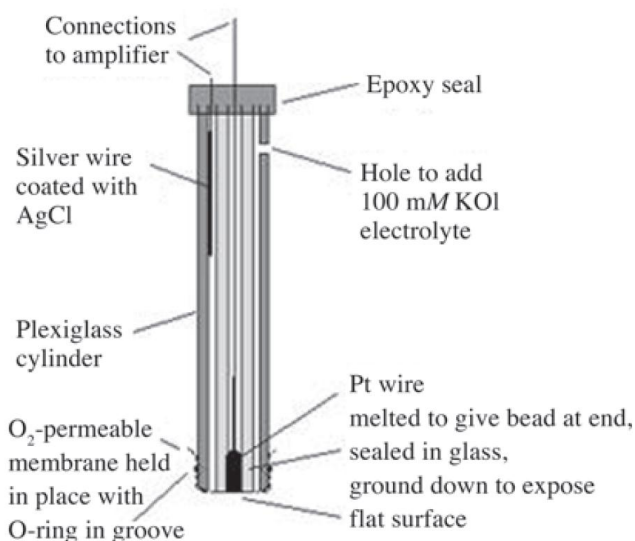


Figure 1.9 The Clark oxygen electrode (Newman and Turner, 2007)

1.6.2.2 Dextrostix and the Ames Reflectance Meter

Dextrostix, developed by Ames, were cellulose sticks impregnated with glucose oxidase peroxidase and an indicator system that promised to give approximate glucose concentration with a single drop of blood (Krynski and Logan, 1967). They worked very much in the same way as pH strips, in that the change in colour had to be compared against a colour block provided by the manufacturer. Limited use of the sticks led to poor (human) interpretability of the results, this was coupled with inaccurate readings at the extremities of the blood glucose concentration range (Kemball and Bloom 1966). However, this changed with the introduction of the Ames Reflectance Meter in 1971. The Ames Reflectance Meter is essentially a light meter designed to read the light reflected off Dextrostix, providing a more accurate and reliable strip reading method (Newman and Turner, 2007).

1.6.2.3 Yellow Springs Instrument

The Yellow Springs Instrument (YSI) Company (Ohio, US) re-launched its glucose analyser based on the amperometric detection of hydrogen peroxide in 1975 (originally launched in 1973) and quickly became established in laboratories worldwide, a legacy that still survives to this day (Newman and Turner, 2007).

The construction of the basic biosensor used in YSI glucose analysers has changed very little over the years. 'Glucose oxidase is immobilised between two membrane layers. The outer polycarbonate membrane retains the enzyme, allows glucose to pass, but prevents many larger molecules from entering, thus reducing interference. The glucose enters the enzyme layer, where it is oxidised producing hydrogen peroxide. This passes through the cellulose acetate membrane to a platinum electrode where it is measured amperometrically. The second membrane acts as a further size exclusion barrier preventing many other potentially interfering (electroactive) compounds from reaching the electrode surface' (Newman and Turner, 2005).

YSI instruments are expensive to build due to the use of platinum electrodes and require high detection voltages, which makes them prone to electrical interference. These limitations prevent the miniaturization of the device.

1.6.3 Electronic blood glucose meters using mediated enzymes

In the 1980s enzyme mediated biosensors were developed by Cranfield and Oxford universities and largely superseded the Ames Reflectance Meter. This was based on electron transfer mediator compounds, namely ferrocene and derivatives that were identified as having potential in biosensor applications (Turner et al. 1983, Ramsay and Turner, 1988; Fragkou and Turner, 2008).

1.6.4 Other methods of measuring blood glucose levels

There are several models of electronic blood glucose monitors available on the market today; these allow the self-monitoring of blood glucose (SMBG). The first continuous glucose-monitoring device to be approved by the US Food and Drug Administration (FDA) was the Continuous Glucose Monitoring System (CGMS™) (Medtronic MiniMed, Northridge, CA, USA). The device determines the concentration of glucose in the blood continuously, typically every few minutes. A disposable glucose sensor is implanted underneath the skin; the patient continues to wear this for a period of a few days before it is replaced. An electronic receiver, similar in size to an electronic pager, displays the patient's blood glucose levels continuously.

CGMSs monitor the glucose level of the interstitial fluid, as the glucose levels in interstitial fluid lags behind the levels found in blood. The level of glucose can lag by about five minutes (Steil et al., 2005; Wentholt et al., 2005; Wilhelm et al., 2006). This means that the devices cannot be used alone; they require calibration against traditional forms of blood glucose measurement.

The OneTouch® is made by Lifescan (Milpitas, CA, USA). The device relies upon using a sterile lance to draw a small drop of blood from a finger (or from the forearm that is less painful) and applying it to a test strip. The OneTouch® provides a blood glucose reading within a few seconds. However, this system also suffers similar problems to the CGMS.

There has long been concern over the quality of the results from different devices, though this has improved over time (Weitgesser et al., 1999; Chance et al., 1999). However, Chen et al., (2003) found that results from four of the bestselling blood glucose monitors had good precision, but not at the extremes of glucose concentration.

Several technical issues complicate efforts to improve the quality of SMBG devices. The most fundamental problem is attempting to measure the 'true' glucose value, as the concentration of glucose in whole blood is different to that in plasma, with the difference between the two varying with the amount of haematocrit (HCT) (Fogh-Andersen and D'Orazio, 1998; Tang et al., 2000). Other factors to take into account are that capillary glucose is again at a different concentration to that in venous blood (Larsson-Cohn, 1976; Poirier et al., 1998) and that blood cells metabolise glucose, therefore samples need to be analysed as quickly as possible (Tamada et al., 1999; ISO, 2003).

The invasive and painful nature of SMBG is often acknowledged, there have been many studies to find an alternative to using blood. Other bodily fluids such as saliva, urine, sweat and tears can contain glucose or other biomarkers that are linked to glucose concentration (Srinivasan et al., 2003; Choi et al., 2005).

Iontophoresis can be used to deliver charged drug compounds through the skin using an electrical current (Ferrante do Ammaral and Wolf, 2008). Reverse iontophoresis can supposedly be used to monitor the transport in the opposite direction, out of the skin (Sieg et al., 2004). The GlucoWatch (Animas Technologies, West Chester, PA, US) takes advantage of this technique, neutral molecules such as glucose are extracted by the electro-osmotic flow to the iontophoretic cathode together with Na⁺ ions using two independent potentiostat circuits (Potts et al., 2002). The performance of this method is questionable as glucose is not a charged molecule and therefore would not be drawn towards the skin.

Devices that use infrared technology can be used to quantify glucose levels non-invasively in skin. The majority of skin glucose is found in the free-water interstitial fluid compartment of the dermis (Pearce and Grimmer, 1972; von Zglinicki et al., 1993). Such devices rely on the

correlation between interstitial and intravascular blood glucose to be closely related (Kayashima et al., 1992; Jensen et al., 1995; Bantle and Thomas, 1997; Service et al., 1997). During rapid glucose flux this relationship breaks down however, there is a lag between blood glucose concentration and interstitial glucose concentration (Tamanda et al., 1995; Schmidtke et al., 1998; Rohrscheib et al., 2003).

Glucose levels in tears reflect blood glucose concentration (Khalil, 2004), this knowledge has been exploited to develop a fluorescent method of monitoring blood glucose concentration (Pickup et al., 2005). The sensor is in the form of a disposable contact lens. Photonic sensing is achieved by diffracting visible light through polymerised crystalline colloidal arrays that respond to different concentrations. The system has an approximate lag time of 30 minutes, and it does not suffer from interference in light intensity of the ambient surroundings. The effect of long-term use, i.e. comfort and toxicity, has still to be determined (March et al., 2006).

These alternative methods can be just as invasive as collecting blood samples, as they still require the collection of some sort of bodily fluid or require a painful procedure to be carried out. Many of these methods also require training of the operator before they can test samples.

1.7 Volatile organic compounds

1.7.1 VOCs as biomarkers

A volatile organic compound (VOC) is an organic chemical compound that has a vapour pressure of 0.01 kPa or more at 293,15K (Council Directive 1999/13/EC). Many carbon containing molecules and light chain hydrocarbons are classified as VOCs. Many VOCs within the body originate from exogenous sources, whilst a smaller number are produced endogenously (Manolis, 1983).

Many of these compounds are naturally occurring in the environment. Most people encounter VOCs in their day-to-day lives in the form of solvents, constituents of petroleum fuels (Lindstrom and Pleil, 2002), formaldehyde for example, is present in furniture. Tobacco smoke, for instance, contains various VOCs such as acetonitrile, and in consequence this is found in the breath of smokers along with furans and associated aromatic compounds (Ligor et al., 2008). Such compounds may be inhaled and pass into the body via that route.

Many VOCs are produced biogenically within the body, such as acetone and isoprene. These compounds are produced in various metabolic pathways, some of which remain unknown (Zolotov, 2005). Human breath typically contains a mixture of unsaturated hydrocarbons, ketones, alcohols and saturated hydrocarbons, the breath of smokers will contain other compounds such as acetonitrile, furans and assorted aromatic hydrocarbons (Ligor et al., 2008). The origin of some of these compounds is summarised in Table 1.3.

The normal range of VOC concentrations largely depends on several factors, such as age, gender and diet (Turner et al., 2006a). Some VOCs, such as NO, are produced in the lungs or the nasal cavity, whilst other VOCs are produced elsewhere in the body, before diffusing from the blood in the alveoli (Abbott et al., 2003; Di Francesco et al., 2005).

There are five groups of metabolites excreted in human breath. These are lipid degradation products, aromatic compounds, thio compounds, ammonia and amine compounds and hydrogenated compounds (Manolis, 1983). Many compounds in breath are present in the parts per trillion (ppt) range (Robinson and Pauling, 1974).

Compound	Physiological basis
Acetaldehyde	Ethanol metabolism
Acetone	Decarboxylation of acetoacetate
Ammonia	Protein metabolism
Carbon disulphide	Gut bacteria
Ethane	Lipid peroxidation
Ethanol	Gut bacteria
Ethylene	Lipid peroxidation
Hydrocarbons	Lipid peroxidation/metabolism
Hydrogen	Gut bacteria
Isoprene	Cholesterol biosynthesis
Methane	Gut bacteria
Methanethiol	Methionine metabolism
Methanol	Metabolism of fruit
Methylamine	Protein metabolism
Nitric oxide	Production catalysed by nitric oxide synthase
Pentane	Lipid peroxidation

Table 1.3 Physical origins of some endogenous breath molecules (Risby, 2005)

Studying the VOC content in the breath of healthy and diseased individuals can provide insight into various biochemical pathways. Indeed, elevated breath levels of certain gases are associated with several metabolic and pathogenic conditions, Table 1.4. Recent studies have attempted to find the range of normal VOC concentration in healthy individuals using SIFT-MS (Turner et al., 2006a-d; Španěl et al., 2006).

VOCs	Disease
Hydrocarbons (especially ethane and pentane)	Oxidative stress
Methylated hydrocarbons	Lung or breast cancer
Isoprene	Cholesterol metabolism
Acetone	Diabetes mellitus, ketonemia
Sulphur-containing compounds (dimethylsulphide, methyl mercaptane, ethyl mercaptane)	Liver impairment
Nitrogen-containing compounds (ammonia, dimethylamine, trimethylamine)	Uraemia, kidney impairment

Table 1.4 Examples of volatile disease biomarkers (Amann et al., 2005)

There are however, disadvantages to using exhaled breath to aid in diagnosis of disease. The most significant being, VOCs are released in the gut and oral cavity by bacteria that inevitably will add noise to the breath profile. VOCs are also released by the action of dental cleansers on soft lining materials that are used for dentures (Brozek et al., 2008). These unwanted compounds introduce a cross sensitivity problem as they can mask the true endogenous concentration.

1.7.2 Lipid peroxidation and oxidative stress

The oxidative degeneration of lipids is known as lipid peroxidation. Lipid peroxidation is triggered by a reactive oxygen species, removing an allylic hydrogen atom, and generating a free radical that then undergoes further reactions (Miekisch et al., 2004). Cell cultures that are exposed to reactive oxygen species (ROS) produce ethane and pentane from the breakdown of the cellular membrane omega-3 and 6 fatty acids and malondialdehyde (MDA). Four times more pentane is produced than ethane by lipid peroxidation, this is due to the physiological ratio of omega-3 to 6 fatty acids. Ethane concentration is lower as pentane can be metabolised by cytochrome P450 (Allerheilgen et al., 1987).

There is a link between high peroxidase activity and the exhalation of ethane and pentane (Aghdassi et al., 2003). There is correlation between the lipid degradation products, such as MDA and thiobarbituric acid reactive substance (TBARS) (also known as GSH), and the levels of ethane and pentane. MDA and TBARS are both serum markers of oxidative stress and have been found to be less sensitive than breath markers (Scholpp et al., 2002).

There is no interference from protein oxidation and colonic bacterial metabolism in the breath test for ethane and pentane (Kneepkens et al., 1994). The stable products of lipid peroxidation have low solubility in blood and are exhaled within a few minutes of their formation in tissues. Exhaled concentrations of ethane and pentane can be used to monitor oxidative stress within the body (Risby and Sehnert, 1999).

1.7.3 Low Density Lipoprotein

The concentration of isoprene in the blood stream is related to the concentrations of cholesterol and low-density lipoprotein (LDL). This could be potentially useful in diagnosing monitoring of dyslipidemias (Amann and Smith, 2005). Isoprene (2-methylbutadiene-1, 3) is believed to form in the mevalonic pathway of cholesterol synthesis (Stone et al., 1993). It is produced from dimethyl allyl pyrophosphate, which is an intermediate produced in the cholesterol pathway. The formation of mevalonate from acetic acid is the rate limiting step of sterol synthesis, and is catalyzed by hydroxymethylglutaryl-CoA (HMG-CoA). Haemodialysis patients have increased levels of endogenous isoprene (Capodicasa et al., 1999).

1.7.4 Diabetes

The most abundant VOC in exhaled human breath is acetone (propanone) (Turner et al., 2006a). Hepatocytes convert excess Acetyl-CoA, which comes from fatty acid β -oxidation, into acetone via decarboxylation (Miekisch et al., 2004). Patients with uncontrolled diabetes mellitus have elevated levels of breath acetone compared to that of healthy individuals (Lebovitz, 1995). Acetone passes from blood to breath by simple diffusion (Widmark, 1920; Briggs and Shaffer, 1921).

Several ketones are produced as by-products of fat breakdown during diabetic ketoacidosis (DKA) (Laffel, 1999). These can be used to feed the Krebs's cycle (tricarboxylic acid (TCA) cycle) when there is no glucose available. Butanoic acid (β -hydroxybutyrate) is the major ketoacid that is produced (Schade and Eaton, 1982). In patients where ketoacidosis is frequently observed, such as children, it is recommended to estimate the urinary ketone bodies or butanoic acid in blood (Schwab et al. 1999; Laffel, 2000; Casteels and Mathieu, 2003). The blood concentration of butanoic acid has been linked to skin acetone concentration, and is higher in diabetic patients compared to healthy individuals (Naitoh et al., 2002; Yamane et al., 2006).

1.7.5 Non Alcoholic Fatty Liver Disease, Alcoholism and Liver Failure

The breath of patients with liver disease was found to have elevated levels of acetone, 2-butanone, 2-pentanone and dimethyl sulphide compared to healthy patients (Van den Velde et al., 2008). The majority of endogenous breath ethanol is produced by bacterial fermentation in the oral cavity (Smith et al., 2008). The concentration of ethanol produced due to bacterial action is considerably lower than that when alcohol has been consumed. Acetaldehyde commonly found in breath is assumed to be produced by the oxidation of ethanol. Due to this, the concentration of acetaldehyde in breath is always lower than the concentration of ethanol.

1.7.6 Nitrogen containing compounds

Breath ammonia originates from the breakdown of proteins in the body (Burton and Turner 2003). This is usually excreted in urine as part of the urea cycle. The mean concentration of ammonia in the breath of healthy patients is 833 ppb, though this varies with age (Turner et al., 2006a). Impairment in the ability of the liver to convert ammonia into urea will increase the level of free ammonia in the blood stream (Miekisch et al., 2004). A high concentration of ammonia in breath is indicative of kidney or liver failure (Davies et al., 1997).

1.8 Collection and analysis of volatile samples

A variety of methods of collecting and storing breath gas samples exist, the most common use either some sort of gas sampling bag, syringes or sorbent tubes (Abbott et al., 2003). In spite of the fact that there are many instruments designed to analyse breath, there are several technical aspects preventing the widespread use of breath in a clinical setting. These problems are sampling, pre-concentration and data analysis (Miekisch et al., 2004).

There are two basic methods of breath sampling (Miekisch et al., 2004), the first being mixed expiratory sampling, in which the total breath including dead space air is collected. This is the most common method as it is easier to perform in spontaneously breathing subjects, as it also does not require any additional equipment.

The second method is alveolar sampling, where only pure alveolar gas is collected. Alveolar gas samples have a lower concentration of contaminants and a higher concentration of endogenous VOCs as there is no dilution by the dead space gas (Schubert et al., 1999; Schubert et al., 2001).

Background samples are needed to help distinguish between endogenous VOCs and exogenous contaminants. There are several ways to achieve this, the simplest being to subtract inspiratory from expiratory concentrations or by calculating 'alveolar gradients' (Phillips, 1997). These methods do not take into account pulmonary adsorption and exhalation of VOCs. Another method is to have volunteers breathe pure uncontaminated air for a period of time before taking samples (Risby and Sehnert, 1999). Whilst this method is effective, it is not practical.

Sampling may be conducted with a single expiration, or a certain period of time. If a single sample of breath is taken, it must be representative of subsequent breaths (Miekisch et al., 2004).

There is some evidence to suggest that nasal cavity breath sampling is more desirable to oral cavity breath for the analysis of trace compounds (Smith et al. 2008). This is especially true for ammonia.

In most studies breath samples are collected from volunteers and patients at the bedside. These are usually collected using Tedlar® bags, inert electropolished SUMMA® gas canisters (Pleil and Lindstrom, 1997), special adsorption materials (Philips and Greenberg, 1992; Mueller et al., 1998), or a method called cryofocussation (Knutson and Viteri, 1996). These methods are different to preconcentration methods discussed later.

1.8.1 Tedlar® bags

Tedlar® sampling bags are made from polyvinyl fluoride (PVF) and are available in a range of sizes. The bags are chemically inert and are resistant to gas permeation and adsorption. One of the disadvantages of using these bags is their high cost. Tedlar® also market the bags as single use, though they can be reused following extensive washing with pure nitrogen three times before reusing, with no detrimental effect on results. Tedlar® bags have been used to collect breath samples for gas analysis. Samples kept in Tedlar® bags are stable for up to four hours, but cannot be stored more than six hours (Deng et al., 2004). The half-lives of methanol, acetaldehyde, acetone, isoprene, benzene, toluene and styrene can be between five and thirteen days inside Tedlar® bags (Steeghs, et al., 2007).

1.8.2 SUMMA® canisters

The canisters are essentially stainless steel vessels where the internal surface has been electropolished, to give a mirror like appearance, and chemically deactivated. The result is that the internal surface of the canisters is chemically inert. The canisters are extremely robust and samples can be kept in the canisters for a considerable length of time without degradation (Lindstrom and Pleil, 2002). The canisters are also extremely durable, and can be easily transported. The downside is that the canisters are very expensive.

1.8.3 Nalophan®

Bags made from the plastic Nalophan® are a cheaper, disposable alternative to Tedlar® bags. A Tedlar® bag or SUMMA® gas canister can cost several pounds; in comparison Nalophan® bags only cost a few pence. However the samples have a relatively short lifespan of a few hours as Nalophan® is slightly porous and volatiles are gradually lost over time (van Harreveld, 2003). In a recent study into the suitability of different polymer bags for breath analysis it was found that bags made from Nalophan® were just as good as Tedlar® bags for storing samples up to five hours (Mochalski et al., 2009). The advantage of using Nalophan® is that it does not emit VOCs that are detectable using SIFT-MS (Turner et al., 2008).

1.8.4 Solid phase micro-extraction

Breath contains a large proportion of water vapour and trace amounts of VOCs. Any system designed to concentrate VOCs must not concentrate water vapour, as this can interfere with results. Preconcentration of VOCs is required because they are present in the ppb-ppt range in breath. There are a variety of methods available to do this, the most popular being sorbent traps and solid phase micro extraction (SPME) fibres (Grote and Pawliszyn, 1997; Miekish et al., 2001). Care must be taken when selecting sorbent traps to avoid breakthrough and memory effects as the VOCs have different boiling points. Volatiles contained within the traps can be released by heating them with microwave energy. Solid phase microextraction (SPME) fibres can also be used to preconcentrate volatile species found within breath (Grote and Pawliszyn 1997), though the number of volatiles that can be absorbed is limited.

1.8.5 Sorbent tubes

Any system designed to concentrate VOCs must not concentrate water vapour. This particular problem can be overcome by using steel thermal desorption (TD) tubes packed with a porous material for capturing volatile species (Bellar et al., 1979; Zlatkis et al. 1977), Figure 1.10.

Materials that are suitable for use as the packing inside the tubes must include a low contaminant background, high thermal stability and must have sufficient absorptive strength in order to capture volatile compounds and release them when heat is applied. A variety of different sorbents are available that are dependent on the compounds of interest. Typical packing materials for breath analysis include carbon (graphite) and TENAX® (Bellar et al., 1974; Zlatkis et al., 1977).

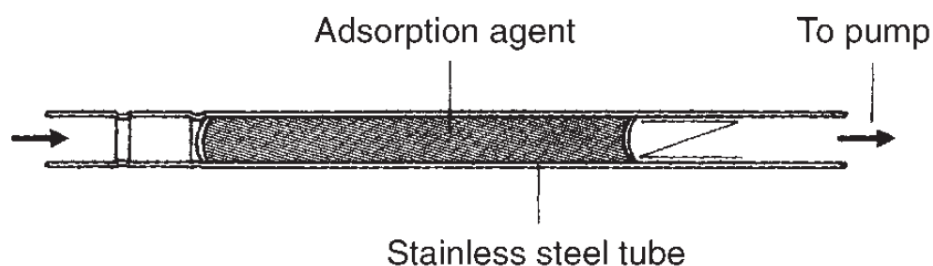


Figure 1.10 An example of a Perkin Elmer thermal desorption tube (Hübschmann 2009)

1.9 Analysis methods for VOC determination

The analysis of VOCs can be achieved using a variety of different methods, each with their own advantages, disadvantages and technical limitations. Breath samples, for example, are typically analysed using MS; the headspace of blood and urine samples can be analysed using this method.

1.9.1 Mass spectrometry

Mass spectrometry (MS) is a technique that can be used to analyse organic compounds; it provides information on the molecular weight, presence of specific elements and functional groups. A spectrum of mass/charge ratio (m/z) is produced. The molecules of the sample have to be ionised to produce the mass spectrum, there are several methods available to do this, the most common being electron ionisation (EI). In EI the sample is bombarded with electrons, molecules in the sample lose an electron to form molecular ions. These fragmented ions are then accelerated through a magnetic field towards a detector; the magnetic field causes the ions to be deflected. The extent of deviation is related to the m/z ratio of the ion (Hoffmann and Stroobant, 2007).

In addition to the molecular ion other ion fragments, known as daughter ions, are also detected which are characteristic of particular functional groups.

Mass spectra often contain many peaks of varying intensities due to fragmentation. The most intense peak is known as the base peak, and is usually a relatively stable fragment rather than a molecular ion.

1.9.2 Gas chromatography mass spectrometry

Gas chromatography mass spectrometry (GC-MS) is an analytical technique that is used for separating compounds within a complex mixture. A diagram of a typical GC-MS system can be seen in Figure 1.11. This description of GC-MS is derived from McMaster (2008) and Hübschmann (2009).

The system essentially consists of two separate parts, the gas chromatograph (GC) and the mass spectrometer (MS). A GC essentially consists of an oven which is designed to heat the GC column. The GC is comprised of two phases, the mobile or carrier phase which is an inert gas such as helium and a column, inside a temperature controlled oven, which is the stationary phase, is where the separation of the sample takes place. Sample is transferred from the GC to the MS via a heated transfer line which delivers the sample to the ion source of the MS. There are three constituents of the MS, an ionization source, mass analyser and an ion detector. The sample is bombarded with electrons in the evacuated ion chamber to produce ionized fragment molecules. These fragments are then swept into the high vacuum analyser where they are selected in the quadrupole rods.

'The direct current (DC) signal charging apposing poles of the quadrupole rods creates a standing magnetic field in which ions are aligned. Individual masses are selected from this field by sweeping it with a radio frequency (RF) signal. As different DC/RF frequencies are reached, different mass/charge ratio (m/z) ions are able to escape the analyser and reach the ion detector, producing a mass spectrum.

On entering the ion detector, the ions are deflected onto a cascade plate where the signal is multiplied and then sent to the data system as an ion current versus m/z time. The summed raw signal can then be plotted against time as a total-ion chromatogram (TIC) or a single-ion m/z can be plotted against time as a single-ion chromatogram (SIC) '(McMaster, 2008).

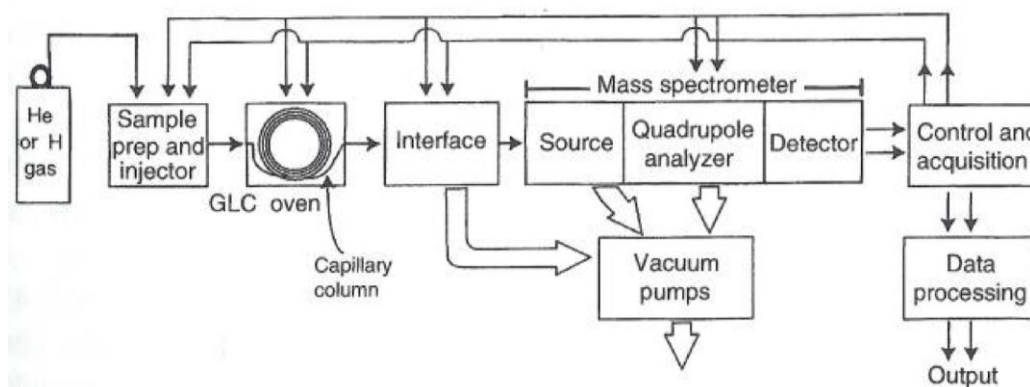


Figure 1.11 A typical GC-MS system diagram (McMaster, 2008)

Lower boiling point molecules vaporise before molecules with a higher boiling point. More volatile molecules continuously increase their lead over less volatile ones and thus separation is achieved. Both column temperature and the nature of the stationary phase influence solvent volatility and the separation. Solute separation is dependent on differences in solute volatility; this in turn influences the rate of solute vaporisation (Venn, 2008).

GC-MS is used in breath gas analysis because of its ability to identify compounds in complex mixtures. Breath was first analysed using GC-MS during the 1960s (Eriksen and Kulkarni, 1963; Stewart and Boettner 1964; Walther and Paerisch 1964; Brechner and Bethune 1965, Tassopoulos et al., 1969). The identity of compounds is determined by the elution times from the GC column and from the fragment size from the mass spectrometer. One of the problems of GC-MS is that it is not a real time solution; samples have to be collected using one of the methods described in section 1.8, before they can be introduced into the instrument.

Despite the disadvantages of GC-MS recent research suggests that GC-MS data can be used to produce a 'VOC profile', that looks at all of the volatile biomarkers in breath rather than one specifically, that can be used to aid diagnosis of diseases such as lung cancer (Basanta et al., 2007). Compared to other methods of preconcentration, such as sorbent traps, further preconcentration of samples, by using a higher volume for example is not possible (Ligor et al., 2008).

1.9.3 Fast flow tube methods for VOC quantification

1.9.3.1 Selected ion flow tube mass spectrometry

Selected ion flow mass spectrometry (SIFT-MS) allows for the real time analysis of trace gases. SIFT-MS is a quantitative mass spectrometric method that exploits Ion-molecule interactions are allowed to proceed within a defined time period, providing greater accuracy.

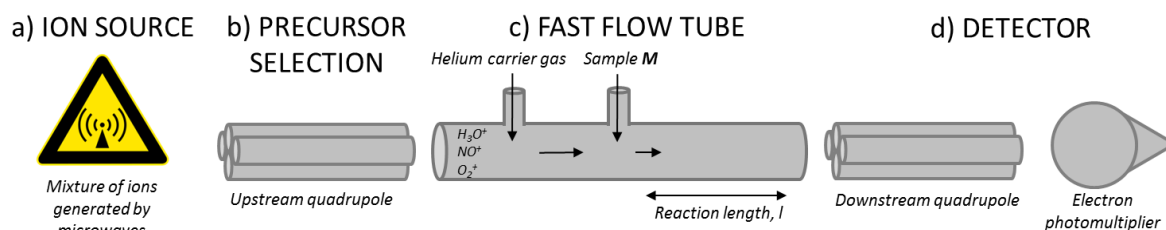


Figure 1.12 Principles of SIFT-MS

There are essentially four sections of a SIFT-MS. a) A mixture of ions is generated from a microwave source. b) Precursor ions, H_3O^+ , NO^+ and O_2^+ are selected by the upstream quadrupole and are carried into the fast flow tube by helium. c) The user-selected precursor ion then reacts with sample-forming ion clusters. d) Clusters of a certain m/z are selected by the downstream quadrupole before they are detected by an electron photomultiplier.

SIFT-MS uses a fast flow tube technique that was first developed in the 1970's (Adams and Smith, 1976). Unlike GC-MS, SIFT can be used to analyse samples in real time, this is due to the fast response time of SIFT-MS which is largely determined by the rate of flow of the carrier gas along the tube and the sample gases along the inlet tube. There is also no sample separation required. GC-MS is not suited for the analysis of compounds with a low molecular weight, such as ammonia and formaldehyde (Spangler et al., et al. 1985; Phillips and Greenberg 1992). It has been recommended that SIFT-MS studies should be supported in parallel with GC-MS because of the limited SIFT-MS library (Smith et al. 2008).

There are two modes of analysis, the full scan mode (FS) that produces a complete mass spectrum, and a multiple ion mode (MIM) that monitors the count rates of the selected precursor ion and selected product ions. There are three precursor ions available, H_3O^+ , O_2^+ and NO^+ that can be seen in the schematic, Figure 1.12. The three precursor ions are formed in a microwave discharge source and are then selected according to their mass-to-charge ratio by a mass filter and injected into the flow tube in helium carrier gas. The sample is introduced to the instrument at a known flow rate into the carrier gas and the precursor ions. The

interactions between the precursor and product ions are detected by a downstream mass spectrometer.

In the FS mode the mass spectrum is produced by sweeping the detection quadrupole over a selected mass to charge ratio (m/z) range for a chosen period of time. The count rates of the ions are calculated from the number of counts and the total sampling time for each ion. The mass spectra produced can be interpreted by relating the product ion peaks to the gases in the sample using a combination of knowledge of ion chemistry and the built-in database. In the MIM mode the downstream mass spectrometer is rapidly switched between the masses of all of the primary ions and the selected ion products, briefly pausing on each of these masses for a short time period (Smith and Španěl, 2005). In this mode more accurate quantification of the selected trace compounds can be achieved.

1.9.3.2 Proton transfer reaction mass spectrometry

Proton transfer mass spectrometry (PTR-MS) is similar technique to SIFT-MS, but does not have a mass filter, consisting of an ion source and a fast flow tube only (Hansel et al., 1995). This means that only one pre cursor ion is available for analysis (H_3O^+) in comparison to SIFT-MS.

1.9.3.3 Ion mobility spectroscopy

One of the emerging techniques is ion mobility spectroscopy (IMS). This method is used to identify the characteristic phase gas ions in a buffer gas by using their mobility and drift velocity (Ruzsanyi et al., 2005). This method was originally developed for the detection of trace compounds in air. Operation is at ambient pressure and does not require a vacuum system. It has a high sensitivity and short data acquisition time, typically 10-50 ms. IMS is not an ideal solution for identifying unknown compounds due to complex ion-molecule interaction and relatively poor mass resolution. Combining this method with GC helps with sample analysis, but this makes it unsuitable for breath analysis.

1.10 Sensor based technologies for VOC profiling

1.10.1 Electronic Nose (eNose)

An electronic nose, or e-Nose for short, is a device that can be used to identify and classify compounds. Gardner and Bartlett (1994) first defined the term electronic nose: 'An e-Nose must comprise of an array of electronic chemical sensors and a pattern recognition system'.

Hence an e-Nose is a device containing a sample handling system, sensor array, pre-processing centre and data analysis software. Exposure to an odour produces a characteristic “fingerprint” which may then be compared with another sample to compare whether the odours are of the same type. The idea of using electronic devices to measure odours was first demonstrated by Zwaaremaker and Hogewind, (1920) when they measured the change in resistance generated from a mist of an odorant in solution.

Early devices were primitive in that they lacked the ability to distinguish between different compounds. Advancements in electronics and computing meant that eNose devices began to gain the ability to classify characteristics of compounds (Persaud and Dodd, 1982; Ikegami et al., 1985; Kaneyasu et al., 1987). Many different types of sensor arrays may be found in electronic nose devices. The sensor type used depends on the application. The principles of operation of several common types are outlined below, including mixed metal oxide semiconductor (MMOS), conducting polymers, surface acoustic wave and photoionisation detectors (PID), though a wide range of other modalities is available (e.g. microarrays, optical fibres, holographic and carbon nanotubes).

Weber et al., (2010) demonstrated that a Nordic Sensor Technologies (NST) 3200 lab emissions analyser was 70% effective as a rapid analysis technique for diagnosing patients with bladder cancer from the headspace of urine samples. It was felt that as a diagnostic method this would be insufficient. This method required urine samples to be collected and incubated, which adds a considerable amount of time to the sample analysis. It was postulated by the authors that SIFT-MS would allow for faster analysis and comprehensive chemical data.

1.10.2 Sensor technologies typically used in eNose devices

1.10.2.1 Surface acoustic wave

The principle of surface acoustic wave gas (SAW) sensors is based on acoustic waves generating resonance in a piezoelectric material, typically quartz. Adsorption of a compound at the surface of the sensor produces a shift in the oscillation frequency related to mass of the compound adsorbed (Gardner and Bartlett 1999). Selectivity can be introduced by applying different coatings to the surface of the sensor.

1.10.2.2 Conducting polymer

Conducting polymers are organic polymers with semiconductor properties. Gas sensors based on this technology using polypyrrole (PPy), polyaniline (Pani) and polythiophene (PTh) polymers have been available since the early 1980s (Nyland et al., 1983).

A change in electrical resistance is seen in polymer in response to analyte gas. They are susceptible to changes in humidity which affects the baseline structure (Gardner and Bartlett, 1994; Gardner and Bartlett, 1999).

1.10.2.3 Mixed metal oxide semiconductor technology

Mixed metal oxide semiconductor (MMOS) sensors are commonly used in electronic noses or may be used singly for specific applications. A semiconductor is a material that acts as both a conductor and an insulator. The behaviour of a semiconductor can be manipulated by adding impurities. This is known as 'doping'. MMOS sensor technology has been successfully used in the automotive industry to monitor combustible and hazardous gases and vapours (Schild 1990). MMOS sensors are ideally suited to this application because of their robust nature and they are relatively inexpensive. Analyte gas is adsorbed at the surface of the semiconductor, resulting in a change in electrical resistance, Figure 1.13.

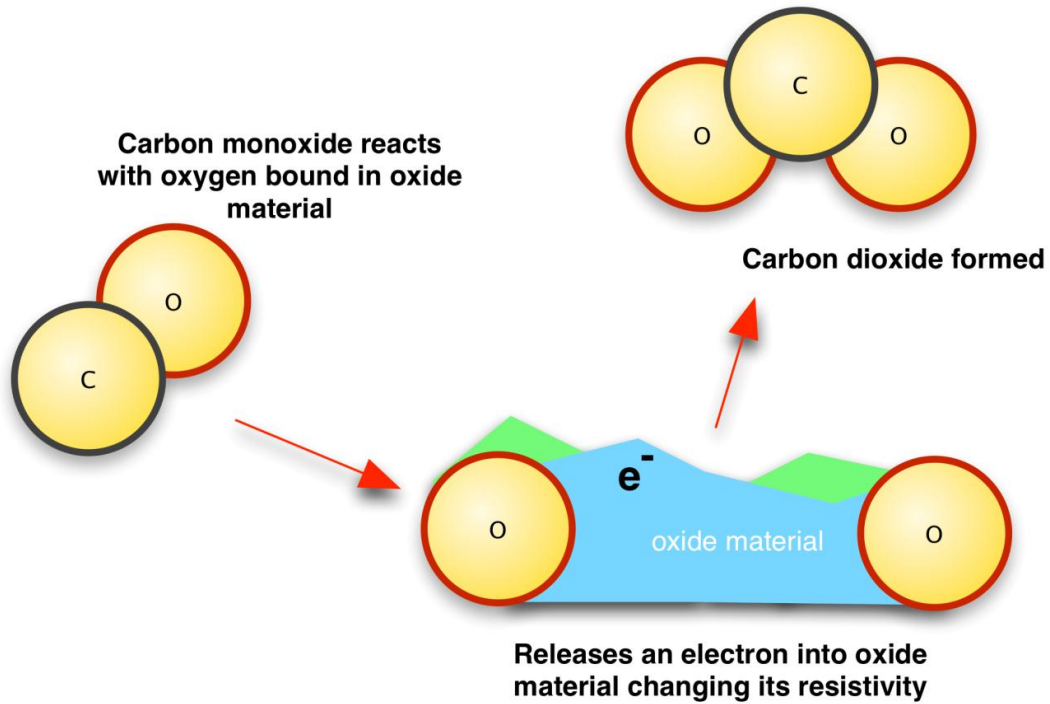


Figure 1.13 MMOS operating principal (adapted from City Technology, 2002)

Thick film gas sensors are made in a screen-printing process (Williams et al., 1998) where the semiconducting particles are printed onto a substrate, such as an alumina tile, with an integrated heater on the back. The heater is controlled to compensate for changes in flow rate, that can cause cooling, and changes in the ambient temperature that may increase or decrease the operating temperature of the sensor. The printed substrate is then fired at controlled temperatures to prevent the sensor from shrinking and or cracking. The sensitivity of thick film gas sensors fabricated with nanosized semiconductor particles is greatly enhanced (Williams et al., 1998; Baraton et al., 2001).

Sensor	Material	Comments
G	Chromium Titanium	Broadband response to reducing gases. Sensitivity can be adjusted by varying temperature.
LG	Tungsten oxide	
W	Tin oxide	Most commonly used in e-nose applications

Table 1.5 Common metal oxides used in sensors (Gardner and Bartlett, 1999)

Only a select few metal oxides are suitable to be used for MMOS sensors, this is due to a combination of resistivity, sensitivity, resistance change and humidity. MMOS sensors typically have an operating range of between 100-600°C. Some examples of common metal oxides are given in Table 1.5.

There are two different types of semiconductor, n-type and p-type. Electrons are donated in n-type semiconductors, increasing the resistance. The opposite is true for p-type semiconductors.

The variation observed in the presence of a gas is dependent on the gas sensing layer and the concentration of the target gas. The resistance of a G sensor will increase with increasing gas concentration; the sensor obeys a squared law, Equation (1.2). Where C is the concentration of the gas, R_0 is the baseline resistance and R_g is the resistance in the presence of gas.

$$C = K \left(\left(\frac{R_g}{R_0} \right) - 1 \right)^2 \quad (1.2)$$

1.10.2.4 Photo-ionisation detector

A photo-ionisation detector (PID) is a type of ion detector that uses ultraviolet light (UV) to produce ions. They can be found in GC-MS systems, though hand held instruments employing this technology are also available, which can provide instantaneous readings of analyte concentration, and are widely used for environmental monitoring, especially in confined spaces such as aircraft cabins (Crump et al., 2011).

High energy photons ionise molecules of gas which produce an electrical current in the detector. The greater the concentration of gas, the greater the current that is generated in the detector.

One of the disadvantages of hand held PIDs is the broadband response; they are not selective as they can ionise gaseous components with an ionisation energy less than or equal to the lamp output. Signal quenching can occur in high humidity environments (Smith et al. 2007).

1.11 Breathotron

The Single Metal Oxide Semiconductor Gas Analyser (SMOS-GA), also more commonly known as the Breathotron, is a novel proof of concept prototype breath analysing device designed and built by Cranfield Health (Cranfield University, Cranfield, Bedfordshire, MK43 0AL, UK) intended to be used for monitoring long term conditions such as diabetes and cystic fibrosis, though there is potential for monitoring other conditions such as chronic obstructive pulmonary disorder (COPD), congestive heart failure (CHF), cancer, tuberculosis (TB) and gastrointestinal (GI) disease (Bishop, 2006; Parker, 2006; Patel, 2007).

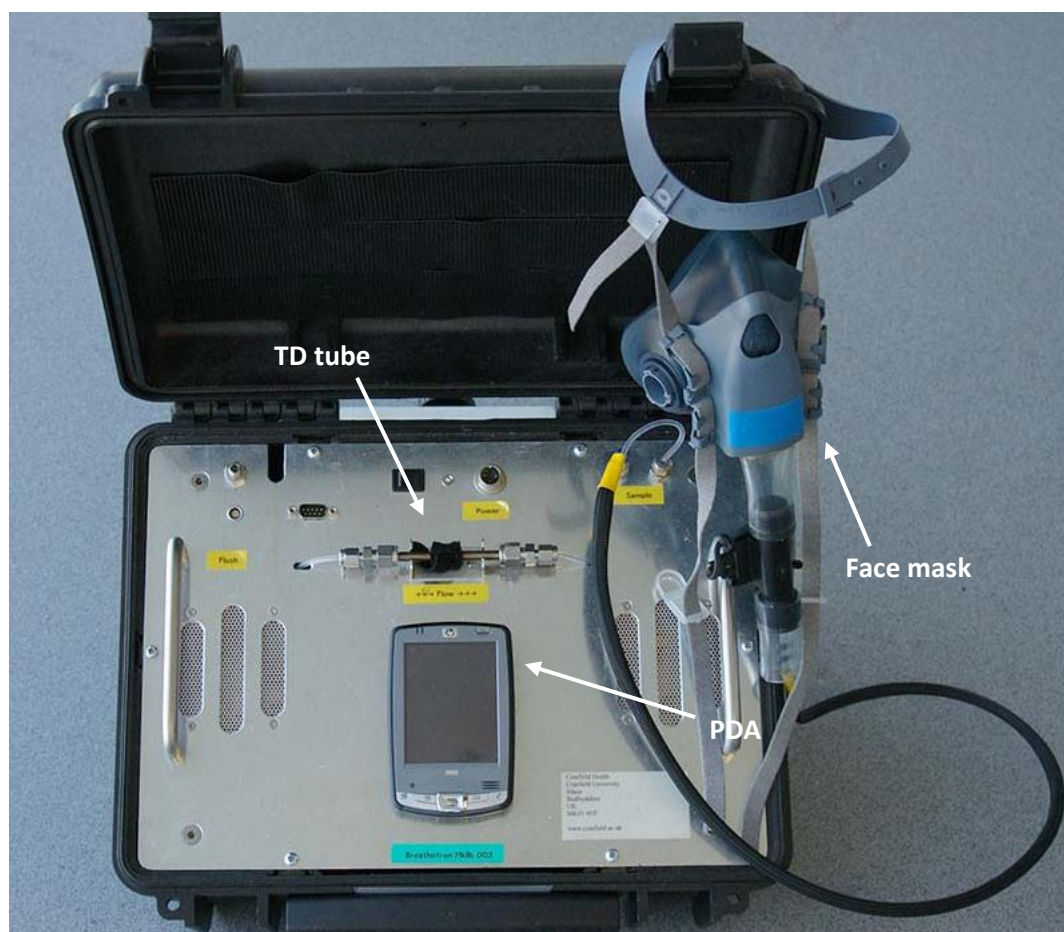


Figure 1.14 Breathotron Mk IIb shown ready for use, with face mask and TD tube in place.

1.11.1 History of the device

The eNostril, developed by Lee-Davey (2004) was designed to analyse the headspace of transformer oil and petroleum. Though it is similar to other e-nose devices, it only has one metal oxide sensor rather than an array. There are several advantages to using only a single sensor, namely power consumption, size/portability and cost, however, it will as a result, be much less broadly sensitive to specific compounds. The eNostril was developed to be a low cost, portable device, something that is particularly advantageous in medical applications. The Breathotron is an evolutionary version of this device, but it has been re-engineered to be more suitable for analysing breath samples.

The Breathotron is a stand-alone, mains powered device. It can be controlled using either a Hewlett Packard® (HP®) iPaq™ (Palo Alto, CA, US) personal digital assistant (PDA) running Microsoft® Windows Mobile 5™ (Microsoft Inc. Redmond, WA, US), or a personal computer (PC) running Microsoft® Windows XP™ connected via a USB cable. Full instructions on how to use the Breathotron, PDA and PC software can be found in Appendix 1 of Patel (2007). A Breathotron ready for use is shown in Figure 1.14.

1.11.2 Operation

The Breathotron incorporates two breath analysis components. In the first component, breath is passed through a thermal desorption (TD) tube containing an appropriate sorbent which may later be analysed using gas chromatography mass spectrometry (GC-MS) in the laboratory. The second component is the mixed metal oxide semiconductor (MMOS sensor).

To sample breath, the volunteer must wear a specially adapted facemask and must breathe normally into the device. No special breathing techniques are required. Non-return valves in the mask ensure that the volunteer breathes in ambient air and exhales through a wide bore tube that contains a flow rate sensor. This sensor monitors the flow rate during exhalation and is used to control the sampling process. A small proportion of each breath is drawn off into the instrument via a narrow bore sampling line.

The Breathotron uses a sampling loop with a known fixed volume in order to present a defined sample to the MMOS sensor. Sample is passed across the sensor by switching into the sampling position so that it becomes charged with breath drawn into the sampling port via the sampling line. Once fully charged the loop is switched to the flush position in which the contents are passed across the sensor or using reference gas at a fixed flow rate. Reference

gas is obtained via a hydrocarbon trap. The advantage of using a fixed volume sample loop means that sampling can be aborted if enough breath is not collected. A constant flow rate is maintained across the sensor whilst the device is in operation. A schematic of the device is shown in Figure 1.15.

The MMOS sensor in the Breathotron is a single Capteur CAP25 MMOS (City Technology Ltd, Portsmouth, UK), which was chosen due to its low cost and broadband response. The original application of the CAP25 is in general air quality sensing in aeronautical and automotive applications (McGeehin, 2000).

There are two Breathotron Mk IIb systems (001 and 003), and one system mechanically the same but lacking TD sampling capability which is known as the VapourGuard.

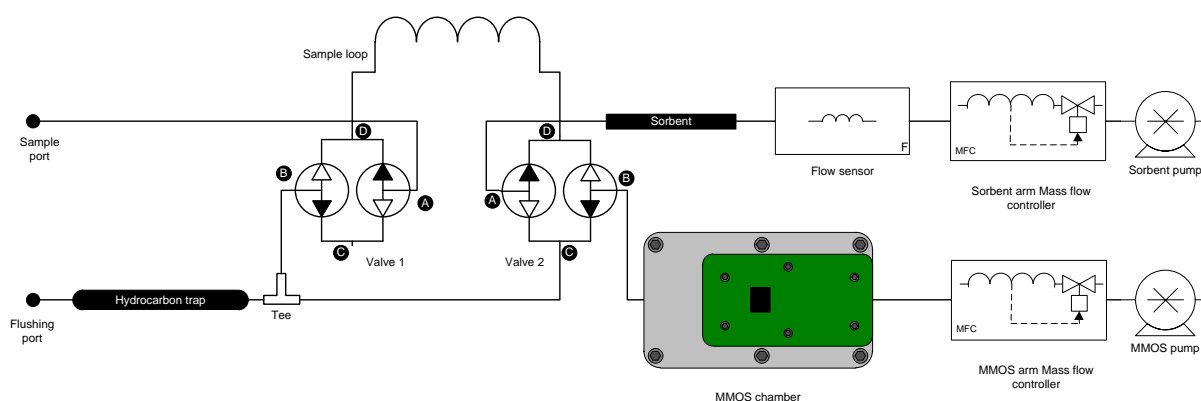


Figure 1.15 Breathotron Mk IIb schematic

The two valve arrangement allows rapid switching from metered air to sample. Breath is collected in a sample loop before it is passed over the sensor.

When used with the eNostril software on the PDA, data is saved onto a removable flash memory (SD) card inserted into the PDA. The SD card can be removed and the data downloaded onto a PC for analysis. Data from the Breathotron is saved in plain text format and is readable by eye in most text editors (e.g. Notepad, vi, TextEdit). A typical data file that is produced by the Breathotron is provided as an example in Appendix 3 of Patel (2007). The files contain basic information, such as the date and time that the sample was analysed, as well as the operating parameters of the device. These parameters have been described previously (Bishop 2006; Patel 2007), and are reproduced in Table 1.6. The rest of the file is made up of unprocessed experimental data in the form of comma separated values (csv). The output files

can range from several hundred kilo bytes (kb) to several megabytes (MB) in size, as this is dependent on sampling time.

Parameter	Description
Date	Date that the sample was analysed
Time	Time that the sample was analysed
Volume	Volume of breath analysed
MMOS Peltier	The peltier device controls the sensor block temperature.
MMOS Offset	Offset of the signal amplifier (y axis)
MMOS Gain	Gain of the MMOS sensor signal amplifier. The gain is the measure of the ability to increase the amplitude of a signal
MMOS Temp	Sensor heater temperature
Operator	Optional field for operator's name
Site	Optional field for site description
Comments	Optional field for user comments. Typically used to record TD tube numbers
ADC data	Variables recorded every 10 ms: MMOS sensor signal. Variables recorded (in addition to variables recorded every 10 ms) every 100 ms: Breath flow, sorbent MFC, MMOS MFC, block temperature, MMOS resistance, block RH, sorbent flow (block flow rate). The variables are separated by commas (,)

Table 1.6 Summary of data parameters recorded in a Breathotron output file (Bishop, 2006; Patel, 2007)

It is possible to analyse the data in a spread sheet program, such as Microsoft Excel, but more powerful analysis can be performed using a dedicated statistics package. The raw data was read into the statistical software package MATLAB® 7.9.0 (2009b) for Windows (32 bit) (Mathworks, Natick, MA, US) using the script MMOSOhms100.m (Appendix B.1.1). The script can convert a single file, or a batch of files for analysis. The script processes raw data and rearranges it into structured arrays that can then be further analysed in MATLAB. The structured array, 'Sensor', contains the elements summarised in Table 1.7.

Element	Description
Admin	Contains administrative data (e.g. date, time comments).
Channel	
Instr	Fixed instrument values.
Scalar	Peltier, gain and offset information.
Sensor	Sensor data smoothed using Savitzky Golay algorithm.

Table 1.7 Elements of structured array 'Sensor' produced by MMOSOhms100.m

MMOSOhms100.m firstly determines whether the data is from a Breathotron Mk IIa, Mk IIb, or a VapourGuard (essentially a Breathotron without TD capability) and sets up fixed offset and analogue to digital (ADC) rail voltage variables according to the type of instrument, the Mk IIb and VapourGuard use a fixed offset of 5.0 and an ADC rail voltage of 4.096 whilst the Mk IIa uses a fixed offset of 2.5 and an ADC rail voltage of 5.0. The script then strips out the parameters defined in Table 2.3 before processing the raw data in the file. The raw data is then smoothed using a Savitzky Golay smoothing algorithm, included in the Signal Conditioning Toolbox in MATLAB, with a span of 399 (which equates to 3.99 seconds) and polynomial degree of 3. Unsmoothed and smoothed signals from the same sample are overlaid for comparison in Figure 1.16. The different phases of the signal are described in Patel (2007).

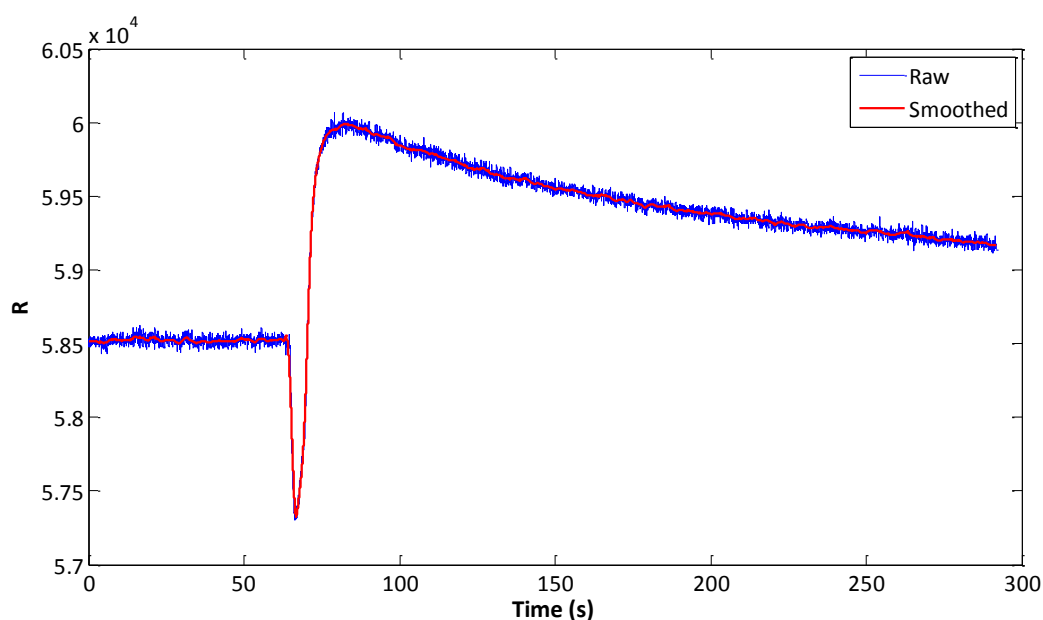


Figure 1.16 An example of a raw and smoothed Breathotron signals

The mean baseline resistance between the first element and the index where the valves are switched to pass sample over the sensor is calculated and subtracted from each point in the signal to give the change in sensor resistance relative to zero. As the valve switch times are not recorded by the Breathotron, these need to be manually set using the script `swTime.m` (Appendix B.1.2) that provides a graphical user interface to visually set the valve switch time that has a characteristic down dip. The signals cannot be aligned to the time point at which the maximum resistance is achieved, as this is influenced by the composition of the gas (Patel, 2007).

1.12 Conclusion

Analysis of endogenously produced VOCs in exhaled Breath is not commonplace, though the analysis of other non-permanent gases, for example O_2 and CO_2 , and exogenous compounds, such as ethanol are analysed routinely by various methods.

The lungs are complex organs with a rich blood supply and a large surface area to facilitate gaseous exchange. VOCs readily diffuse from the blood into the alveolar space and are exhaled. Laboratory based equipment can be used to monitor VOCs in exhaled breath, such as GC-MS, SIFT-MS, PTR-MS, IMS, and IR spectroscopy provide accurate, quantifiable results, but are costly, complex and bulky with complex data analysis also being required. These instruments are not designed for use by clinicians at the bedside or patients within their homes.

There is a large market for small, portable, hand held devices for measuring various physiological parameters such as lung function and blood glucose concentration. These devices are designed to be used by clinicians and patients alike.

Type 1 diabetes mellitus is a chronic metabolic disorder in which the pancreas produces an insufficient amount of the hormone insulin, which reduces blood glucose concentration when it is high. The cause of T1DM is thought to be a virus, or genetic pre-disposition. The current method of glucose monitoring is the 'pin prick' method. Patients are required to draw a small amount of blood from their fingertips and apply it to a glucose biosensor strip. A blood glucose meter is required to interpret the results. The number of diabetic patients is ever increasing, and the majority of the Health Service's budget is spent on the monitoring and treatment of diabetic patients and complications that occur due to the disease.

The blood glucose meter is the most popular method for self-monitoring blood glucose concentration, with many patients failing to self-monitor due to their lifestyle risking further damage to their personal health. Several non-invasive glucose monitoring techniques have been proposed, though none have made it to market to challenge the traditional blood glucose meter.

When blood glucose concentration within the body is low, the body can synthesise the necessary precursor molecules which can be used to produce energy. These precursors come from the lipolysis of fat stored within the liver and adipose tissue, and the breakdown of protein within muscles. These metabolic processes can be affected by various factors, such as hormone secretion rate and physical exercise. These compounds are thought to be indicators of glycaemic status. The by-products of these reactions are acetone and ammonia, which diffuse into the blood stream and are exhaled and may be markers of glycaemic status.

Electronic nose technology has been employed in the past to determine and monitor composition of complex gas mixtures, mostly in the aeronautic, automotive and food security sectors. A variety of sensors options are available for these devices, though many are susceptible to humidity and are therefore unsuitable for monitoring breath. The most suitable sensors are mixed metal oxide semiconductor based gas sensors. These sensors compose of a metal oxide sensing layer sandwiched with a heater due to the high operating temperatures required. There is therefore interest in their potential to monitor endogenous metabolites in exhaled breath as a method for non-invasively monitoring. There is therefore interest in their potential to be used in medical diagnostic applications for the analysis of exhaled breath.

2 Non-invasive monitoring of VOCs in exhaled breath of healthy adults using Breathotron, SIFT-MS and GC-MS during an oral glucose tolerance test

2.1 Introduction

It is advised that patients with type 1 diabetes regularly self-monitor their blood glucose concentration. This is usually achieved by taking 'pin prick' capillary blood glucose readings and applying to a test strip which and the results read by a blood glucose meter (Newman and Turner, 2005). However, many patients fail to do this for various reasons, allowing their blood sugar levels to fall either dangerously high or low. Neglectful self-monitoring over time can lead to developing long term medical complications such as retinopathy, neuropathy and renal failure caused by micro- and macro vascular damage (Tuch et al., 2000; Holt et al., 2007). In extreme cases, low blood glucose concentration can potentially lead to death.

One of the main reasons that diabetic patients cite for a failure to self-monitor blood glucose is the painful nature of the pin-prick sample collection method of the blood glucose meter. The reluctance to self-monitor in children and adolescents is further enhanced by the fear of social stigma from their peers, or through their generally more active lifestyle. Though continuous blood-glucose monitors, with sensors implanted under the skin, are available they need to be recalibrated using conventional test strips. They are also very expensive devices.

An alternative, non-invasive method which may prove to be more acceptable to diabetic patients would be to monitor a patient's breath for biomarkers that may report glycaemic status. Certain compounds, such as acetone – which gives a diabetic patient's breath a distinctive 'fruity' scent, may be possible markers of blood glucose concentration (Manolis, 1983; Phillips, 1992; Kalapos, 2003). These compounds may be detected by a handheld device that may ultimately be able to replace blood glucose meters. In this chapter three different instruments, Breathotron, SIFT- and GC-MS, were used to analyse exhaled breath of several healthy volunteers during a 120 minute oral glucose tolerance test (OGTT) to investigate relationships, if any, between VOC and blood glucose concentrations.

2.2 Materials and methods

2.2.1 Modifying a Breathotron face mask

To allow simultaneous “online” sampling of exhaled breath using both SIFT-MS and the Breathotron a suitable modification needed to be made to the face mask. There were two advantages to making this modification, firstly that the same sample would effectively be analysed using three different methods (including TD GC-MS) and secondly that breathing patterns during the experiment could be recorded and analysed in conjunction with real time SIFT-MS data.

A Breathotron face mask, a pre-modified 3M face mask (3M, Bracknell, Berkshire, RG12 8HT), was taken and a secondary PTFE sampling tube (Cole Parmer, Hanwell, London, W7 2QA), of the same bore as the pre-existing sampling tube in the Breathotron face mask, was attached downstream to the AWM 720P flow sensor (Honeywell, Bracknell, Berkshire, RG12 1EB), in the same position as the sampling line that leads to the Breathotron. This modification can be seen in Figure 2.1, where the secondary sampling line that leads to the SIFT-MS is shown coiled up. The secondary tubing was later incorporated into the braiding after adjusting to an appropriate length to reduce the internal dead space. An 1/8” to a 1/4” Swagelok® adapter fitting and a length of 800 mm polypropylene tube with 1/4” Swagelok® fittings at either end allowed the second sampling line to be connected to the sampling head on the SIFT-MS. In this way both the SIFT-MS and Breathotron can be used to sample the same gaseous sample at the same time. This eliminates the need for Nalophan® bag samples, though this means that all sampling must be conducted in the vicinity of the SIFT-MS.

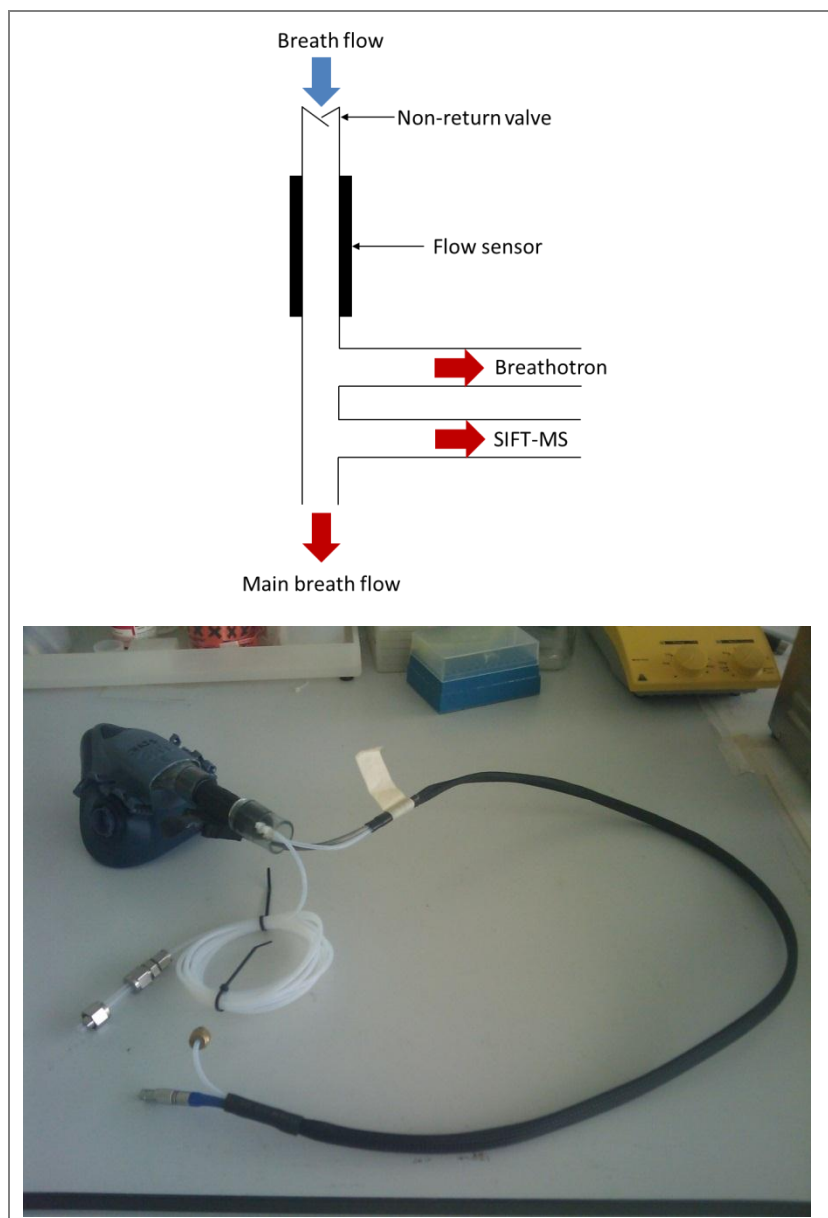


Figure 2.1 Line diagram (above) and photograph (below) of the modified Breathotron sampling mask that allows tandem sampling with SIFT-MS

A secondary length of PTFE tubing was attached downstream to the flow sensor, shown coiled up in this photograph, it was later incorporated into the braiding after cutting to remove dead space. This secondary sampling line was fed into the SIFT-MS. This ensured that the sample of breath analysed by the Breathotron and SIFT-MS were the same.

The modification was tested against the traditional method of “online” sampling of using a disposable cardboard tube. To test the effect of high ventilatory flow rates on the modification, a subject exercised on a bicycle ergometer (BodyGuard, Ergometer 990, Jonas

Øglænd, Aksjeslskap, Norway) first with the disposable cardboard tube and then with the modified Breathotron face mask.

2.2.2 Blood glucose meter calibration

Prior to starting the experiment, the blood glucose meter that was to be used for this experiment, an Abbott Therasense (Abbott Diabetes Care, Alameda, CA, US) which uses Abbott FreeStyle test strips (Abbott Diabetes Care, Alameda, CA, US), was tested with glucose solution to ensure normal operation. This was performed by making a 'meter testing' solution of glucose in phosphate buffer solution (PBS). This was made by weighing 0.2704g of glucose (Sigma-Aldrich, Gillingham, Dorset, SP8 4XT) and mixing in 250 mL of 0.1 M dipotassium phosphate (K_2HPO_4) (Sigma-Aldrich, Gillingham, Dorset, SP8 4XT) and 250 ml 0.1 M monopotassium phosphate (KH_2PO_4) (Sigma-Aldrich, Gillingham, Dorset, SP8 4XT) solution to give a stock concentration of 15 mM of glucose in solution at pH 7.0. The meter was then tested at a several concentrations between 0 and 15 mM by serial dilution of the stock solution.

2.2.3 Oral glucose tolerance test

With ethical approval from the Cranfield University Health Research Ethics Committee (CUHREC), the relevant paperwork is reproduced in Appendix D.1, volunteers from within Cranfield Health were recruited by mass email. The volunteers were asked to fast for a period of 8-14 hours before the experiment. During the fasting period they were permitted to drink water and discouraged from brushing their teeth with toothpaste.

Ethical approval was required for this study because there was a small but finite chance that the overnight fasting blood glucose measurement would have an abnormal value indicative of a stage of diabetes or insulin resistance, a research nurse was present at each OGTT study to interpret and discuss the implications of this and provide counselling with the affected volunteer, which the researcher would have been unqualified to provide. The research nurse also assisted volunteers in taking blood samples if they are unable to do so themselves.

Prior to the experiment each volunteer was assigned a random letter drawn by the volunteer 'from a hat'. The random letter assigned was known only to the volunteer and the researcher; no other identifying data were collected. Two of these letters were assigned as positive (did not fast) and negative controls (did not drink glucose solution). Upon arrival in the SIFT-MS laboratory their weight (kg) and height (m) were measured and recorded using a set of

bathroom scales and a tape measure. These were then used to calculate body mass index (BMI) using equation (2.1) (Eknoyan, 2007). Any volunteer that had a BMI less than 18 (medically considered to be underweight) or greater than 25 (overweight) was not permitted to enter the study as per the recruitment criteria. Lung function was evaluated using a hand held spirometer (MicroMedical) three times (each 30 seconds apart), averaged and recorded.

$$\text{BMI} = \frac{\text{Mass (kg)}}{(\text{Height (m)})^2} \quad (2.1)$$

After being instructed to wash their hands with soap and water to remove any residual sugar on the surface of their skin, the volunteers were then shown how to draw blood by the research nurse, approximately 25 μL , from the tip of their finger using a sterile diabetes lance kit (Abbott Diabetes Care, Alameda, CA, US). Fasted blood glucose level were analysed using the blood glucose meter and recorded prior to starting the experiment.

Fasted (baseline) breath samples were then analysed using the Breathotron and SIFT-MS (see sections 2.2.4 and 2.2.5 for more detail on methodology). When giving breath samples, volunteers were asked to breathe 'normally', as though they were not wearing the face mask. Following this the volunteers were then asked to drink a 75g solution of glucose (dextrose monohydrate 99.95%, Vitamin C 0.05%) (Boots UK Limited, Nottingham, NG2 3AA) dissolved in drinking water over a period of 10 minutes according to World Health Organisation guidelines (2003). During the experiment, volunteers were permitted to drink an unlimited quantity of water, including the control. After drinking the solution the volunteer provided finger prick blood samples and breath samples at regular 30 minute intervals for two hours.

For the comfort of the volunteers, they were asked to lie on a medical crash cart during the experiment. Though the sampling mask was removed in between the sampling intervals, they were not allowed to leave the confines of the SIFT-MS laboratory. The whole process took approximately 2 ½ hours per volunteer, after which they were allowed to eat and drink as per normal.

2.2.4 Breathotron

Breathotron 003 was randomly selected to be used. Prior to starting the experiment the instrument was serviced according to the servicing protocol. The hydrocarbon trap was removed, adsorbent emptied and then refilled with new Supelco Supelcarb™ adsorbent (Sigma-Aldrich, Gillingham, Dorset, SP8 4XT) and refitted. The MMOS sensor block was

removed and a new CAP25 sensor was fitted along with new gaskets (see Chapter 6.2.1 for in depth details of sensor block assembly and leak testing).

Prior to the start of the experiment the Breathotron was switched on and the baseline resistance left to equilibrate for a period of fifteen minutes before any samples were taken. An ambient reading of laboratory air was taken prior to any breath sampling. Face masks used in the experiment were cleaned and sterilised according to the protocol in Appendix A2.

On each of the occasions at which capillary blood samples are taken, the volunteers were asked to breathe into the Breathotron breath sampling device with a regular breathing pattern until a representative sample had been obtained. Whilst breath samples were being analysed, volunteers were advised to refrain from talking as this has an adverse effect on the data from the flow sensor.

2.2.5 SIFT-MS

The SIFT-MS instrument is a prototype, designed and developed by Trans Spectra Ltd. (Crewe, UK) and manufactured by Instrument Science Ltd. (Crewe, UK). The principles of SIFT-MS are explained in detail in Chapter 1.9.3.1.

The SIFT-MS was switched on and left to pump down for 300 seconds before the helium supply was turned on and the source ignited. The instrument was then continuously run in full scan (FS) mode whilst the source pressure was adjusted to optimise the number of counts seen by the detector, approximately 1 million counts per second (c s^{-1}) is satisfactory for the analysis of trace compounds typically found in breath. For “online” sampling of breath directly into the SIFT-MS the multi ion mode (MIM) must be used. Due to the nature of the experiment, where breath samples were being analysed by three different methods in tandem, the H_3O^+ precursor ion was exclusively used. Other precursor ions were not used, as the objective of the experiment was to effectively analyse the same breath sample with three different instruments. The selected ion products that were quantified in exhaled breath are given in Table 2.1.

Acetaldehyde
Acetic acid
Acetone
Ammonia
β -hydroxybutyric acid
Carbon dioxide
Ethanol
Formaldehyde
Hydrogen sulphide
Isoprene
Methanol
Propanol
Water

Table 2.1 VOCs quantified using the H_3O^+ precursor ion on the SIFT-MS

A background reading of laboratory air was then taken to ensure that it was free from environmental contaminants. Following this, the modified Breathotron face mask was attached to the sampling head of the SIFT-MS. On each occasion that breath samples were analysed using the Breathotron, breath was simultaneously analysed using the SIFT-MS for the same length of time as required by the Breathotron, which is dependent on ventilator rate but is typically between 5-10 minutes.

2.2.6 ATD GC-MS

The standard stainless-steel TD sorbent tubes containing dual packing, comprising of 50% Tenax[®] TA and 50% Carbotrap (Markes International Limited, Llantrisant, UK), were used following conditioning. Conditioning was carried out by purging with helium carrier gas for 2 minutes at ambient temperature (approximately 25°C) followed by 30 minutes at 335°C. Conditioned cartridges were sealed with brass locking caps and stored at 4°C until required for use.

2.2.6.1 Internal standard

To quantify the VOCs in the samples an internal standard, d8-toluene in methanol (Sigma-Aldrich, Gillingham, Dorset, SP8 4XT), was used. This was supplied as 1mL vial of 1000 $\mu\text{g mL}^{-1}$ d8-toluene in methanol which was subsequently diluted to a final concentration of 100 $\text{ng } \mu\text{L}^{-1}$.

100 μL aliquots were then dispensed into crimp top vials and stored at -80°C until required for use. The vials of the internal standard are designed for single use following which they are disposed of.

The permanent brass caps were removed from each end of the TD tube using a Caplok[®] tool (Markes International Limited, Llantrisant, UK) and a 10mm plug of salinized glass wool (Sigma-Aldrich, Gillingham, Dorset, SP8 4XT) was placed into the notched end of each tube using tweezers, and temporary PTFE caps (Perkin Elmer, Wellesley, MA) placed on each end. Standard was then applied to each of the tubes using a calibration solution loading rig (CSLR) (Markes International Limited, Llantrisant, UK). The temporary caps were removed from the TD tubes and the notched end secured into the CSLR. Using a Hamilton gas syringe, which had been cleaned three times by drawing and expelling standard solution three times to eliminate contaminants, 0.5 μL (50 ng) d8-toluene in methanol was deposited onto each tube. The gas supply was then opened at a flow rate of 500 mL min^{-1} for 20 seconds to give a final volume of 100 ng L^{-1} on each tube. Tubes were then removed from the CSLR and refitted with temporary caps, ready to be analysed.

2.2.6.2 GC-MS method

Preconcentrated volatile species were subsequently analysed using an AutoSystem XL gas chromatograph equipped with an ATD 400 thermal desorption system and TurboMass MS (Perkin; Elmer, Wellesley, MA). The carrier gas used throughout was CP grade helium (BOC Gases, Guilford, Surrey, UK) and further purified using a Mat-Sen inline filter (Sigma-Aldrich, Gillingham, Dorset, SP8 4XT). Tubes were desorbed by purging for 2 minutes at ambient temperature then for 5 min at 300°C . Volatiles purged from the tubes were captured on a cold trap which was initially maintained at 30°C . Once desorption of the tube was complete, the trap was heated to 320°C using the fastest possible heating rate and maintained at that temperature for 5 minutes whilst the effluent was transferred to the GC via a heated transfer line at 180°C coupled directly to the GC column.

A Zebron ZB624 chromatographic column was used (Phenomexex, Torrance, CA, USA). This is a wall coated open tubular column ($30\text{m} \times 0.4\text{mm} \times 0.25\text{mm}$), the liquid phase comprising a $0.25\text{ }\mu\text{m}$ layer of 6% cyanopropylphenyl and 94% methylpolysiloxane. The gas chromatograph oven was maintained at 50°C for 4 minutes following injection and was then raised at $10^{\circ}\text{C min}^{-1}$ to 220°C for 9 minutes. Separated products were transferred by a heated line to the mass spectrometer and ionised by electron bombardment. The spectrometer was set to carry out a

full scan from m/z ratios 33 to 350 using a scan time of 0.3s with a 0.1s scan delay. The resulting mass spectra were combined to form a total ion chromatogram (TIC) by the GC-MS integral software (TurboMass 4.1).

2.3 Results

2.3.1 Modifying a Breathotron face mask

The modifications made to the face mask were tested against the conventional method of on-line sampling using a disposable cardboard tube. To test the modification at high breath flow rate, a volunteer breathed into the SIFT-MS first using the conventional method using a disposable cardboard and then using the modified mask. After initial testing it was found that the nut on the back of the sampling head which prevents damage at high flow rates whilst “online” sampling using disposable cardboard tubes did not have to be removed whilst sampling using the modified Breathotron mask.

Online breath SIFT-MS data from approximately 8 minutes of breathing whilst cycling without and then with the modifications described previously in 2.2.1 can be seen in Figure 2.2 and Figure 2.3 respectively. This includes an initial rest period of approximately 1 minute. The selected ion products quantified are acetone and isoprene on the ppb scale, whilst water is plotted on the secondary axis with a percentage scale (equivalent to 1,000,000,000 ppb). Appreciably less noise can be seen when compared to breathing through a disposable cardboard tube. There is a decrease in acetone concentration of 291 ppb, isoprene 38 ppb and water by 1.9%. The noise is due to air in the tube being re-inhaled through the sampling head whilst using the disposable cardboard tube. The Breathotron mask incorporates non-return (one-way) valves which prevent exhaled breath from being drawn back into the sampling head resulting in an appreciably less noisy signal. The advantages of this method is that the same breath is analysed using all three analytical methods.

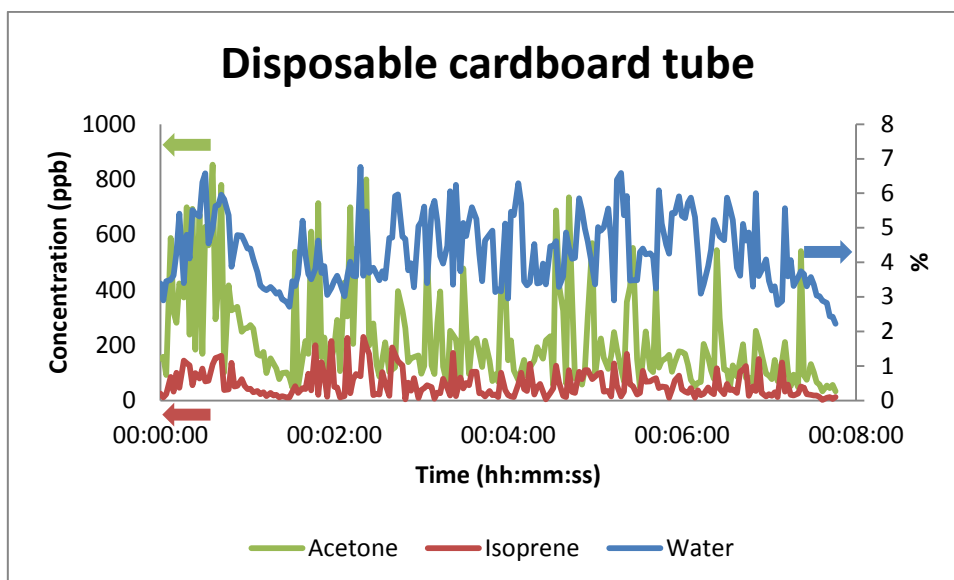


Figure 2.2 Continuous breathing directly into the SIFT-MS using a disposable cardboard tube

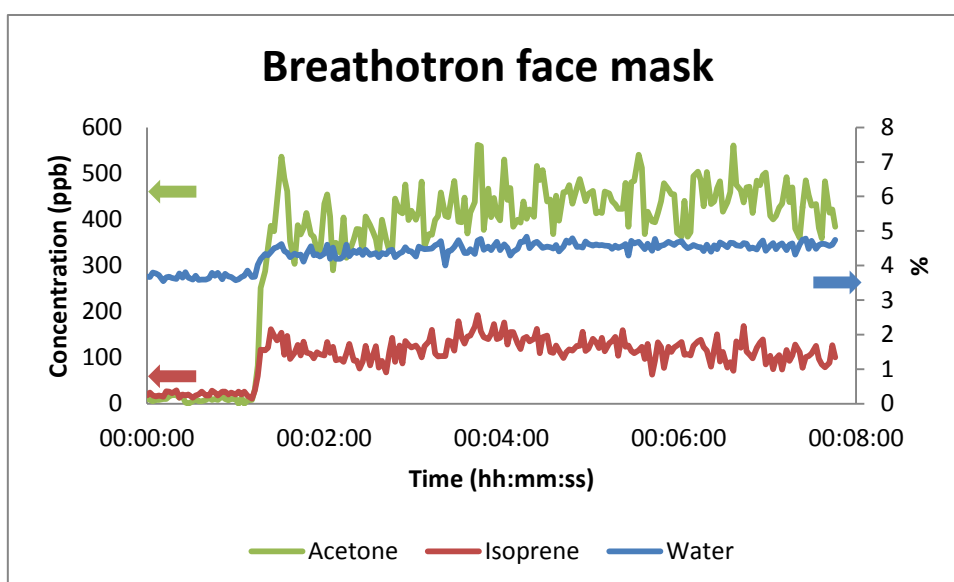


Figure 2.3 Continuous breathing directly into the SIFT-MS using a modified Breathotron face mask

2.3.2 Calibration of blood glucose meter

The Therasense blood glucose meter was tested in a concentration range from 0 mM to 15 mM, Figure 2.4. For each point a new glucose strip was used, with each concentration being tested three times. The response to glucose was linear, though the readings were approximately 10% higher than the nominal value, the error bars are too small to be reproduced. This was deemed to be within the manufacturer's specification.

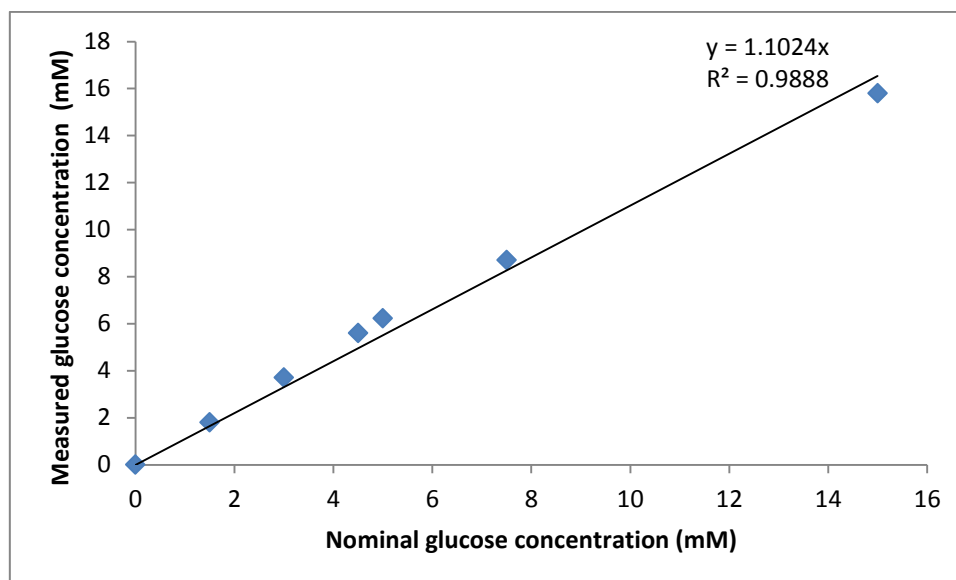


Figure 2.4 Therasense glucose meter calibration curve

2.3.3 Oral glucose tolerance test

In total eight volunteers were recruited to take part in the study, though one, the positive control, dropped out prior to the experiment. Due to scheduling and financial constraints it was not possible to recruit another volunteer to take their place. Of the seven volunteers that completed the experiment none displayed diabetic characteristics following the overnight fast and all fell within the BMI criteria. Volunteers passed the time by reading, listening to music or talking with researchers in between sampling i.e. these were not particularly stressful activities. All completed the OGTT without complication, though volunteer A complained of slight sickness (felt like vomiting) after drinking the glucose solution they elected to continue with the experiment. None of the volunteers expressed concern about the fit of the face masks; however a smaller mask was substituted by the researcher during the experiment with volunteer G due to an imperceptible breath flow. Initially it was thought that there was a problem with the flow sensor, but this was remedied by using the smaller sized face mask. The low flow rate was probably due to an ill-fitting mask allowing air to escape from the sides. Most volunteers said that they had fasted for approximately 8-10 hours prior to the experiment, however, volunteer H stated during the experiment that they had fasted for 2 hours longer than of the advised maximum 14 hours; this was double the minimum fasting time required by the protocol. Spirometry, pin prick blood glucose concentration and BMI data is reproduced in Table 2.2. The data is shown in the order that the volunteers completed the experiment. Though the sample size is small, the volunteers are normally distributed, mean

and median are approximately the same, and all values fall within 1.5 standard deviations from the mean. All of the volunteers drank 75 g glucose solution (± 0.02) with the exception of volunteer D (Control) whom was allowed to drink water during the experiment. There is a small to moderate increase in blood glucose concentration in all of the volunteers except for volunteers G and D (Control). The reason for a lack of an increase in volunteer G is unknown, and may just be due to the metabolism of this particular individual.

Volunteer	Age (years)	Gender	FEV ₁ (L)	FVC (L)	FER (L)	PEF (L)	BMI (kg m ⁻²)
A	28	F	2.48	2.82	88	382	22.0
E	29	F	2.34	3.69	63	162	21.5
G	28	M	3.75	4.22	89	491	22.9
H	22	M	3.12	4.40	70	475	20.1
C	47	F	2.86	3.36	85	260	21.3
F	46	F	2.16	2.35	92	297	24.2
D (Control)	27	M	3.83	4.20	90	421	23.9
Mean	32	-	2.94	3.58	82	355	22.3
Standard deviation	9.9	-	0.67	0.78	11	121	1.5
Median	28	-	2.86	3.69	88	382	22.0
Range	25	-	1.67	2.1	29	329	4.0

Table 2.2 Lung function data for the volunteers that took part in the OGTT

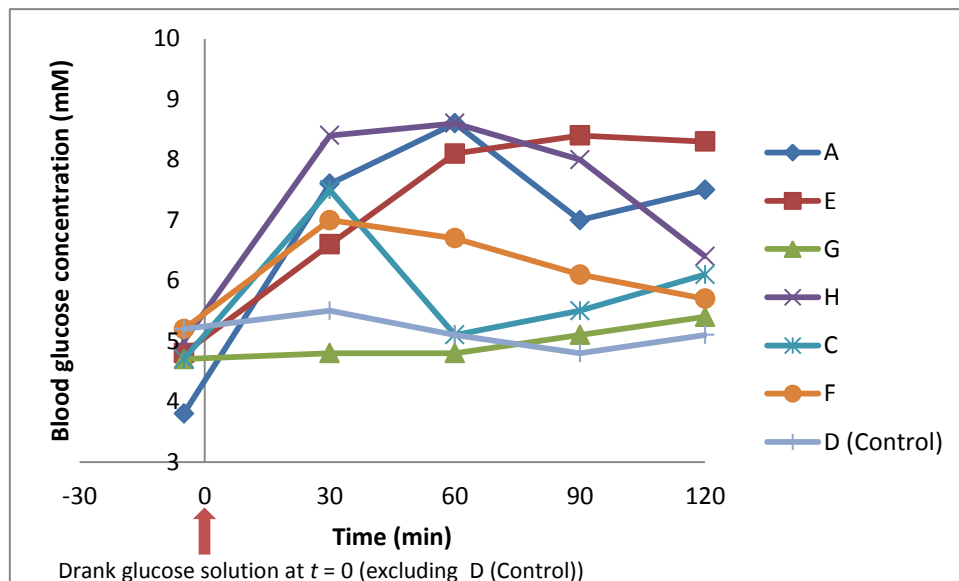


Figure 2.5 Change in blood glucose concentration during the OGTT

2.3.4 Breathotron data analysis

2.3.4.1 Analysis of sensor response

An example of the data obtained from the experiment following post processing in MATLAB® R2009b (Mathworks, Natick, MA, US) using the script MMOSOhms100.m, Appendix B.1.1, can

be seen in Figure 2.6 for volunteer A. For this volunteer, there is a decrease in the change in sensor resistance with the exception of the sample analysed at the 90 minute interval. The maximum change in sensor resistance (ΔR_{\max}) was then determined at each stage of the OGTT for each of the signals. The ΔR_{\max} plotted against time and measured blood glucose concentration for the entire cohort can be seen in Figure 2.7, where the initial reading was taken at -5 minutes prior to drinking the glucose solution. Some volunteers show display an increase in ΔR_{\max} with time, whilst the true is opposite for the others. The linear correlation coefficients of ΔR_{\max} against time and measured blood glucose concentration can be seen in Table 2.3 using the Data Analysis Toolpak included with Microsoft® Office Excel™ 2010 (Microsoft, Redmond, WA, US) with the null hypothesis that there was no relationship between the change in sensor response and time or blood glucose concentration. The null hypothesis was rejected if the probability (P) was less than 5% ($P < 0.05$). There is no significant correlation between ΔR_{\max} and time or blood glucose concentration for any of the volunteers.

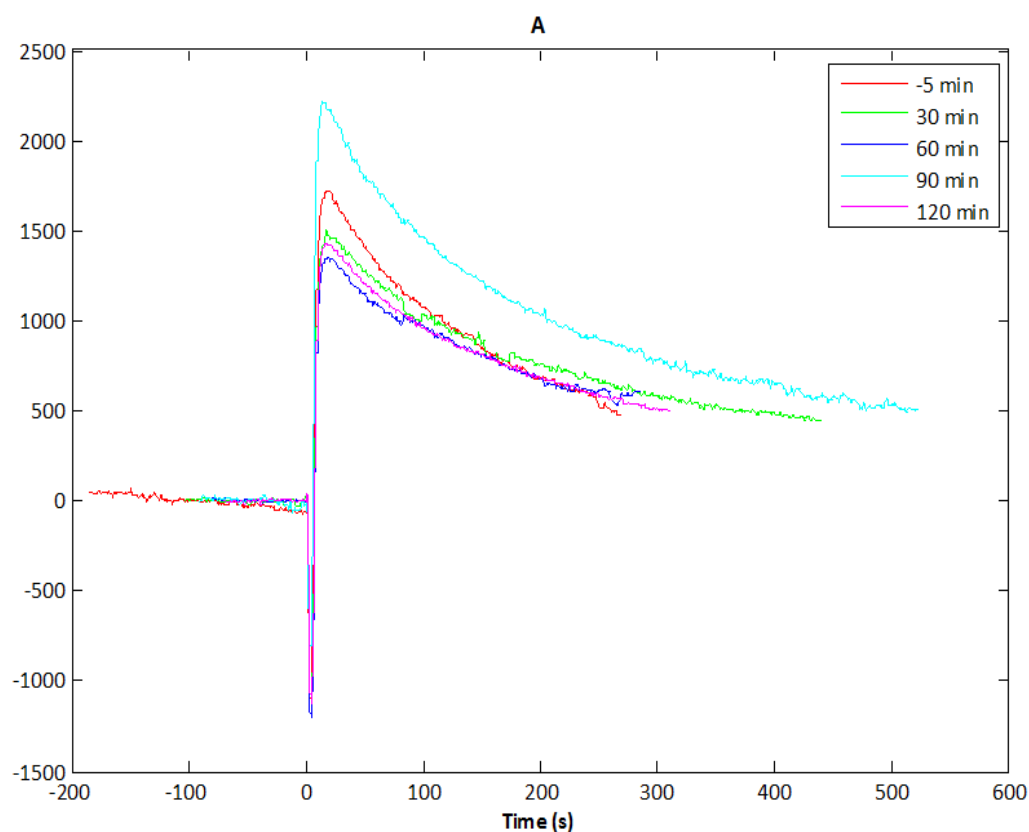


Figure 2.6 The change in sensor response at each of the half hourly sampling intervals for volunteer A

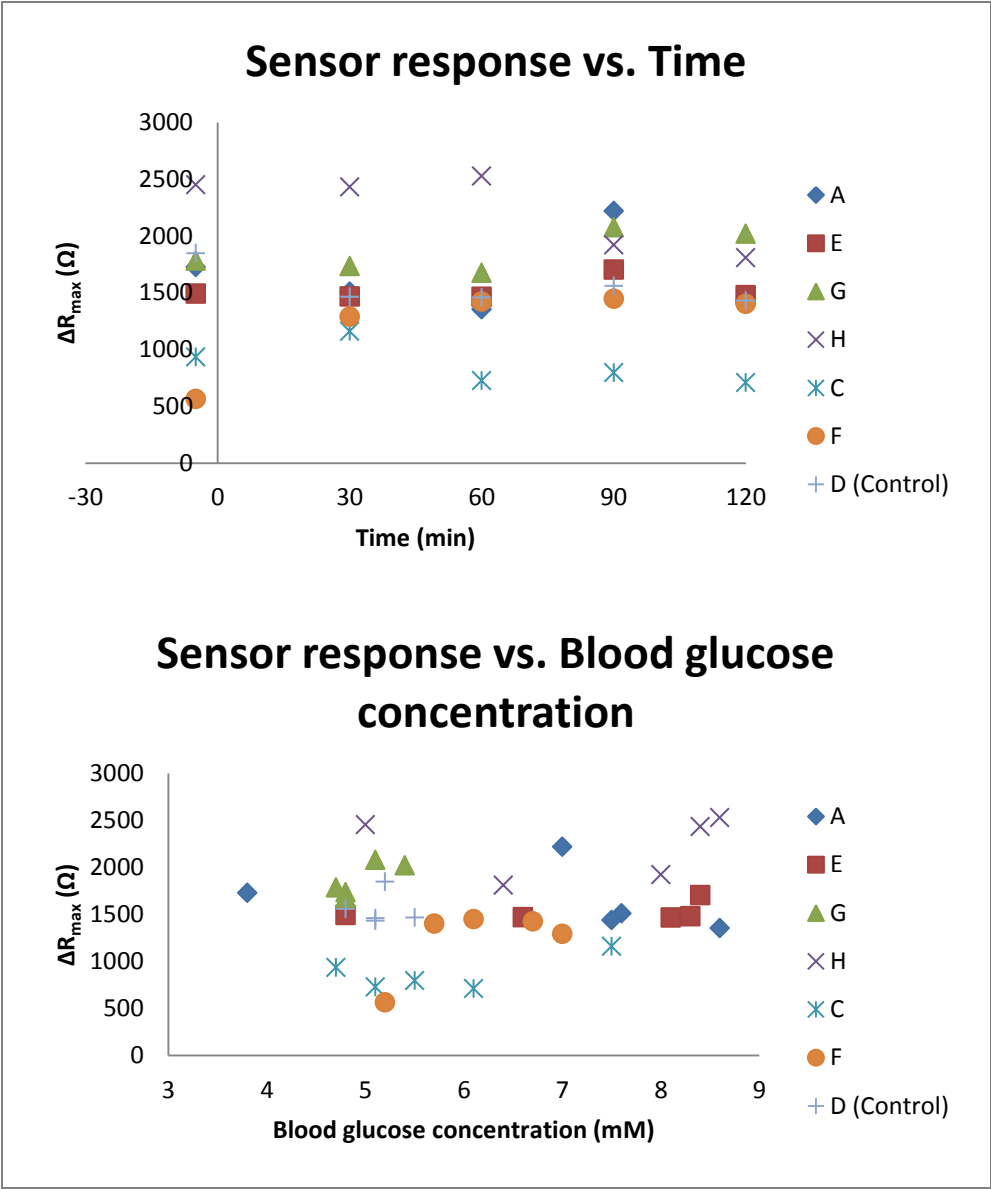


Figure 2.7 Maximum sensor resistance at half hourly intervals during the OGTT for all volunteers

Volunteer	Time vs. ΔR_{\max}	Blood concentration vs. ΔR_{\max}
A	0.06	-0.36
E	0.32	0.35
G	0.71	0.82
H	-0.84	0.13
C	-0.68	0.61
F	0.79	0.64
D (Control)	-0.70	-0.04

Table 2.3 Calculated linear correlation coefficients for time and blood glucose concentration vs. ΔR_{\max}

2.3.4.2 Principal components analysis

Variables for principal components analysis (PCA) were generated by dividing the first 20 seconds of the sensor signals, starting from the valve switching time, into equal segments each 1 second (100 data points) in width, a visual representation of this is shown in Figure 2.8, using the script segments.m (Appendix B.1.4) in conjunction with the GUI Buildmat200.m (Appendix x) to automate this process for each of the signals in turn. The gradients of the resulting segments were calculated using the polyfit function by the script segments.m for each of the 35 samples generating 40 variables for PCA, 20 amplitudes and 20 slopes. This was chosen as it was shown to be the optimal segment number and width combination in other studies (unpublished data) (Walton 2008 personal communication).

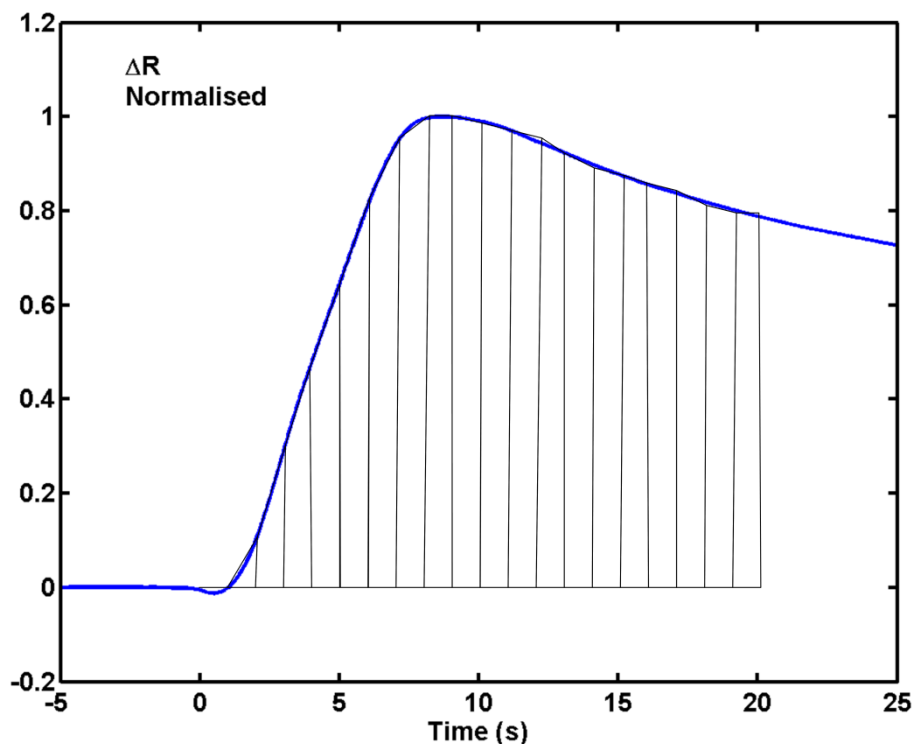


Figure 2.8 Signal segmentation method

PCA was performed firstly on smoothed zeroed change in resistance (ΔR_s) signals using the pcagui function found in the PLSToolbox 2.0.1a (Eigenvector Research Inc. Wenatchee, WA, USA) for MATLAB. The data matrix generated by Buildmat200.m was loaded into memory and analysed. Three different scaling options are available in pcagui, autoscaling (default scaling method), mean centred and no scaling and all were evaluated together with two different normalisation methods for the data.

PCA analysis, Figure 2.19, showed that breath samples did not cluster by blood glucose concentration regardless of normalisation or scaling method, Table 2.4. Instead, samples from each individual volunteer clustered together. Though similar concentrations do not cluster together, higher concentrations tend to shift toward the left of the plot in most volunteers with autoscaling and mean centred scaling methods, and towards the bottom of the plot with no scaling. Plotting the different PCs against each other does not change the clustering pattern. Regardless of the scaling method, the majority of the variance is captured by the first two principal components (PCs) with negligible variance captured by the other PCs. The greatest variance is captured by the first two PCs when no scaling method is used regardless of the normalisation method. The cluster separation improves as the variance captured by the

first two PCs increases. This method was chosen as it had been previously shown to be useful in differentiating simulated breath samples under controlled conditions (Le Davey 2003; Bishop 2006; Parker 2006; Patel 2007). In these studies a non-systematic approach was used to select suitable features for extraction from the signal. These features were typically static points on the graph, ratios between two values and gradients. Splitting the signals into 20 equal segments with width of 1 second and applying no scaling to the data proved to be most successful at clustering approximate blood glucose concentrations. This clustering pattern is probably due to the fact that VOC concentration in exhaled breath differs from individual to individual, and changes little during OGTT. The PCA plots for ΔR_s and $\Delta R_s/R_0$ are similar (not reproduced here), visually in appearance, and variance captured by the first two PCs because there was little or no drift in the baseline resistance for all of the samples (i.e. the samples have the same or similar baseline resistance prior to sampling) proving that the shape of the signal is more important than static points.

Normalisation method	Scaling method	Variance PC1 (%)	Variance PC2 (%)	Cumulative Variance
None (ΔR_s)	Autoscaling	51.10	18.68	69.78
	Mean centred	81.59	10.15	91.74
	No scaling	87.07	11.34	98.41
$\Delta R_s/R_0$	Autoscaling	51.05	18.29	69.34
	Mean centred	81.68	9.95	91.63
	No scaling	87.13	11.28	98.41
$\Delta R_s/\Delta R_{\max}$	Autoscaling	47.91	28.09	76.00
	Mean centred	75.52	17.48	93.00
	No scaling	84.08	14.10	98.18

Table 2.4 Cumulative variance for different normalisation and data scaling methods with the method which captured the greatest variance in bold

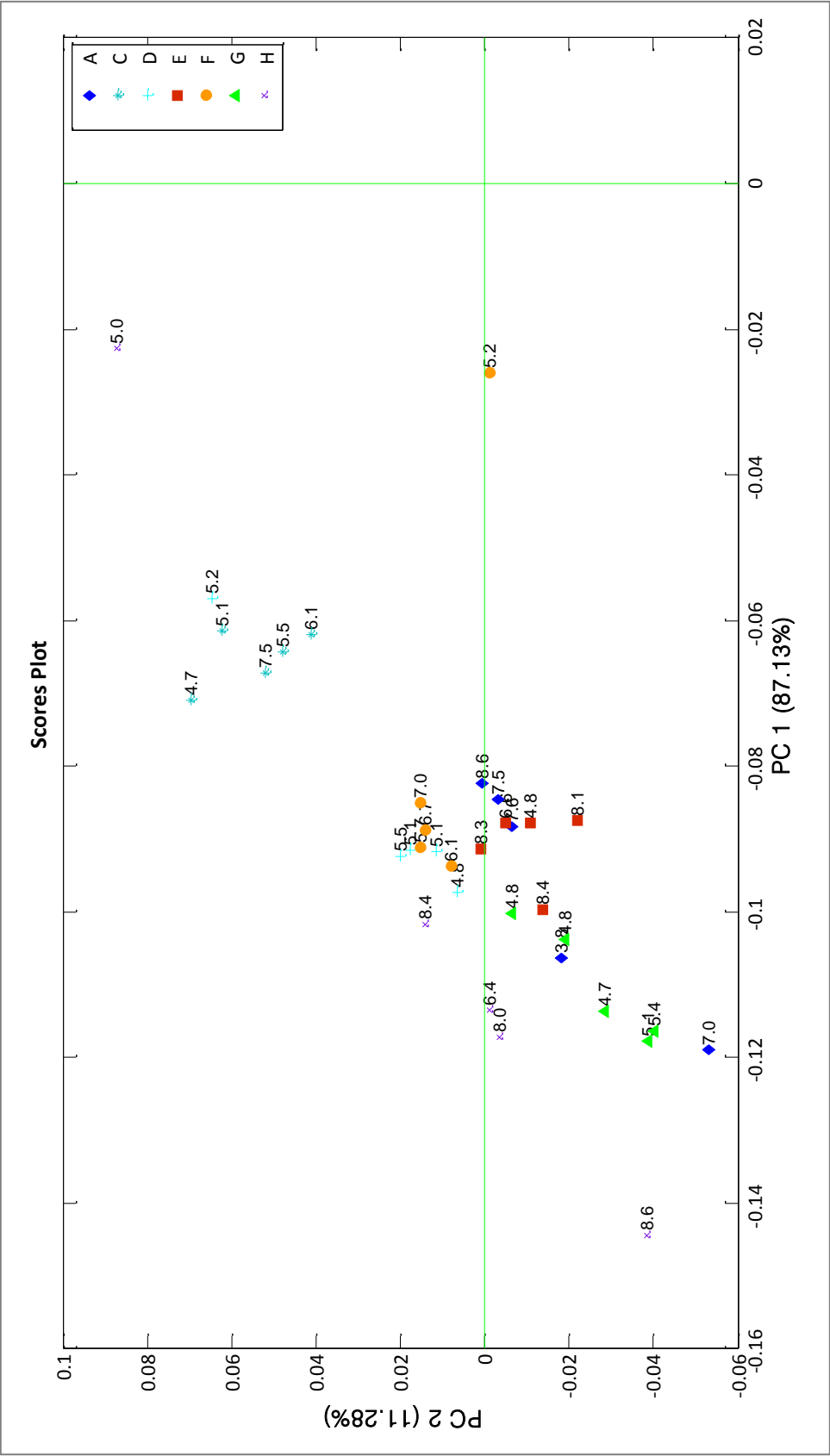


Figure 2.9 Scores plot for OGTT data derived from smoothed and zeroed sensor signals (ΔR_s) with no scaling

2.3.5 SIFT-MS

Online SIFT-MS was used to analyse breath samples simultaneously with the Breathotron. Though SIFT-MS data was collected for volunteer E, it is not reproduced here due to technical fault with the instrument. An example of the data from volunteer A prior to drinking the glucose solution can be seen in Figure 2.10. The mean concentrations of each of the samples that were collected at the 30 minute sampling intervals were determined for each volunteer, the data for mean exhaled breath formaldehyde in Figure 2.11, acetaldehyde in Figure 2.12, acetone in Figure 2.13, acetic acid in Figure 2.14, isoprene in Figure 2.15, methanol in Figure 2.16, ethanol in Figure 2.17, propanol in Figure 2.18, hydrogen sulphide in Figure 2.19, ammonia in Figure 2.20, β -hydroxybutyric acid in Figure 2.21, water in Figure 2.22 and carbon dioxide in Figure 2.23 .

The concentration of VOCs in exhaled breath varies from individual to individual, though all volunteers showed negligible concentrations of formaldehyde, propanol, hydrogen sulphide and β -hydroxybutyric acid in exhaled breath. There is little or no change in exhaled acetaldehyde, acetic acid, methanol, ethanol, propanol concentration, which remain stable though some show a decrease with concentration over time. Some of the volunteers show a small decrease in exhaled acetone concentration, but not enough to be significant, typically less than 20 ppb. The exhaled VOC concentration varies considerably between individuals, with the highest concentrations of acetone and ammonia being observed in volunteer H, whom fasted long than the other volunteers at 16 hours. There is generally a decrease in exhaled VOC concentration, both with increasing time and increasing blood glucose concentration.

Acetic acid and propanol concentration in exhaled breath is highest in the majority of volunteers and tends to be followed by acetone, acetaldehyde and ammonia. Hydrogen sulphide, propanol and β -hydroxybutyric acid are the lowest in concentration in all of the volunteers.

The oldest members of the cohort, C and F exhibit the highest concentrations of exhaled breath ammonia. In all of the volunteers, barring G and F, the concentration of exhaled ammonia increases after drinking the glucose solution at the first 30 minute sampling interval.

Though there is a decrease in acetone concentration between drinking the glucose at 0 minutes and the first 30 minute sampling interval for volunteers A, G and H, the other

volunteers either show a small increase or no change in exhaled acetone concentration, volunteer D exhibited an increase in exhaled breath acetone.

Linear regression analysis against both time, Table 2.5, and measured blood glucose concentration, Table 2.6, suggested that there were significant ($P < 0.05$) (not due to chance) correlations, where the null hypothesis was that there was no significant correlation between exhaled VOC concentration and blood glucose, between exhaled breath acetone, acetic acid, isoprene, methanol, ethanol, propanol and ammonia for at least one volunteer and are marked with an asterisk (*). However, on the whole this is not significant and could be due to chance.

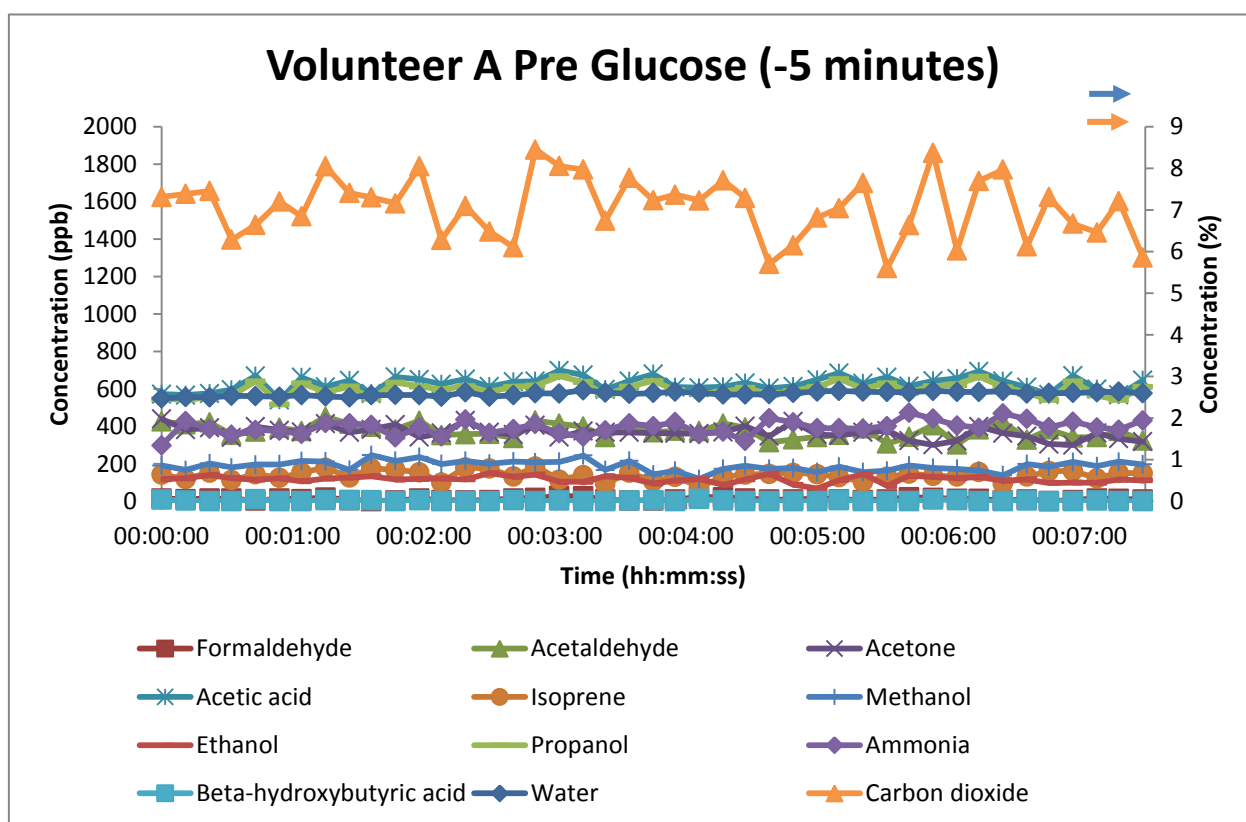


Figure 2.10 Online, continuous SIFT-MS data from the initial pre-glucose solution breath sample from volunteer A

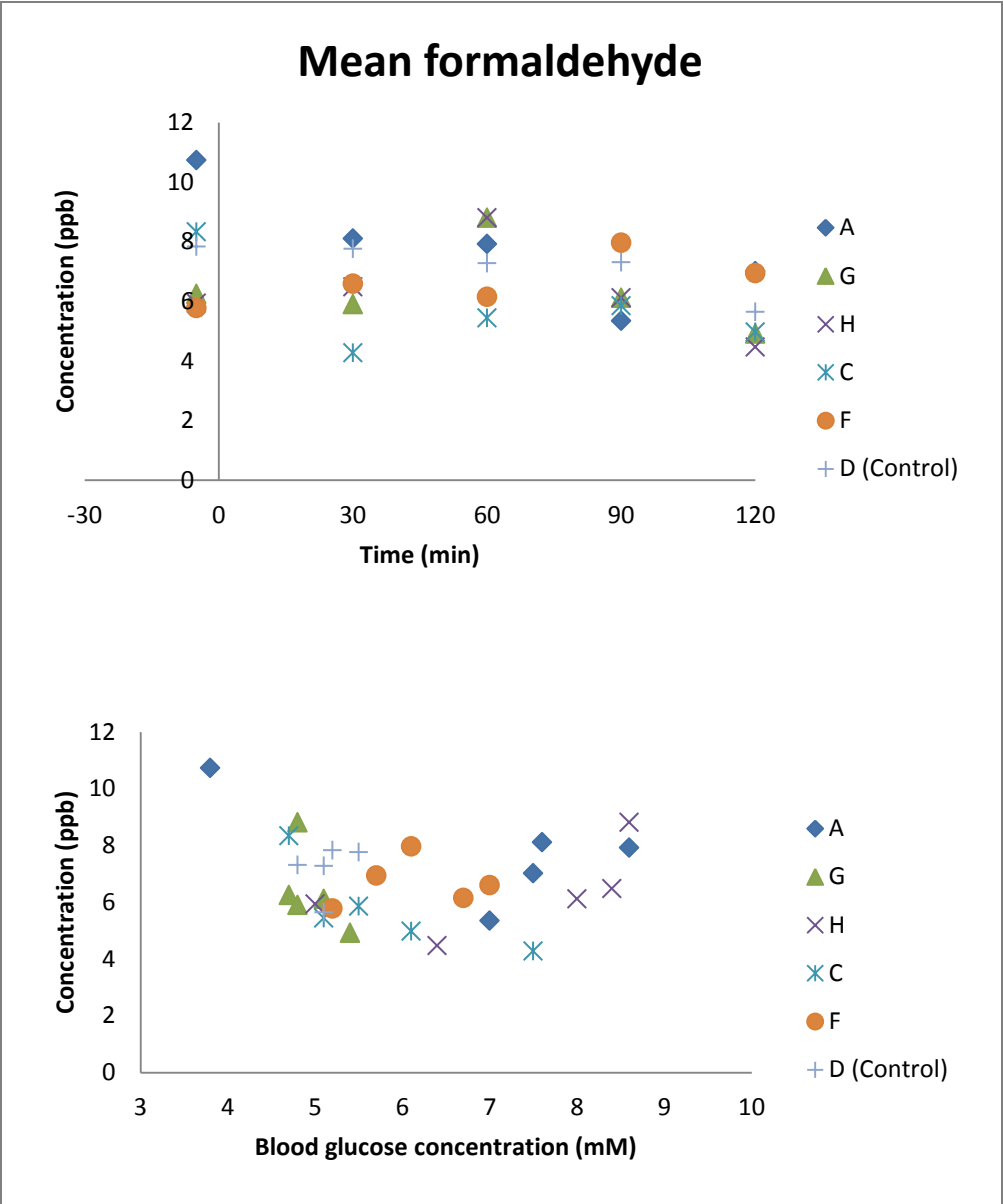


Figure 2.11 Mean exhaled formaldehyde concentration plotted against time and blood glucose concentration

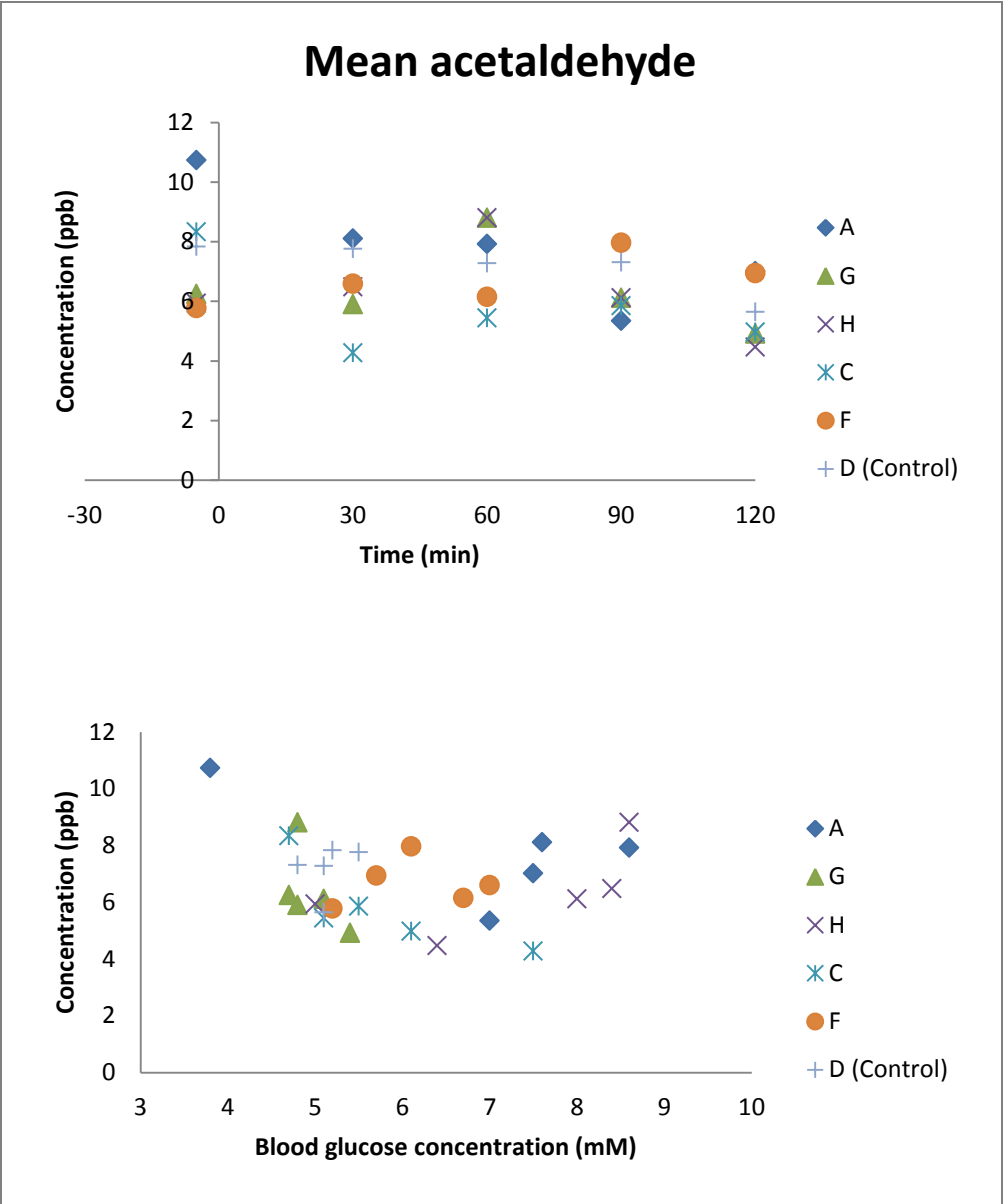


Figure 2.12 Mean exhaled acetaldehyde concentration plotted against time and blood glucose concentration

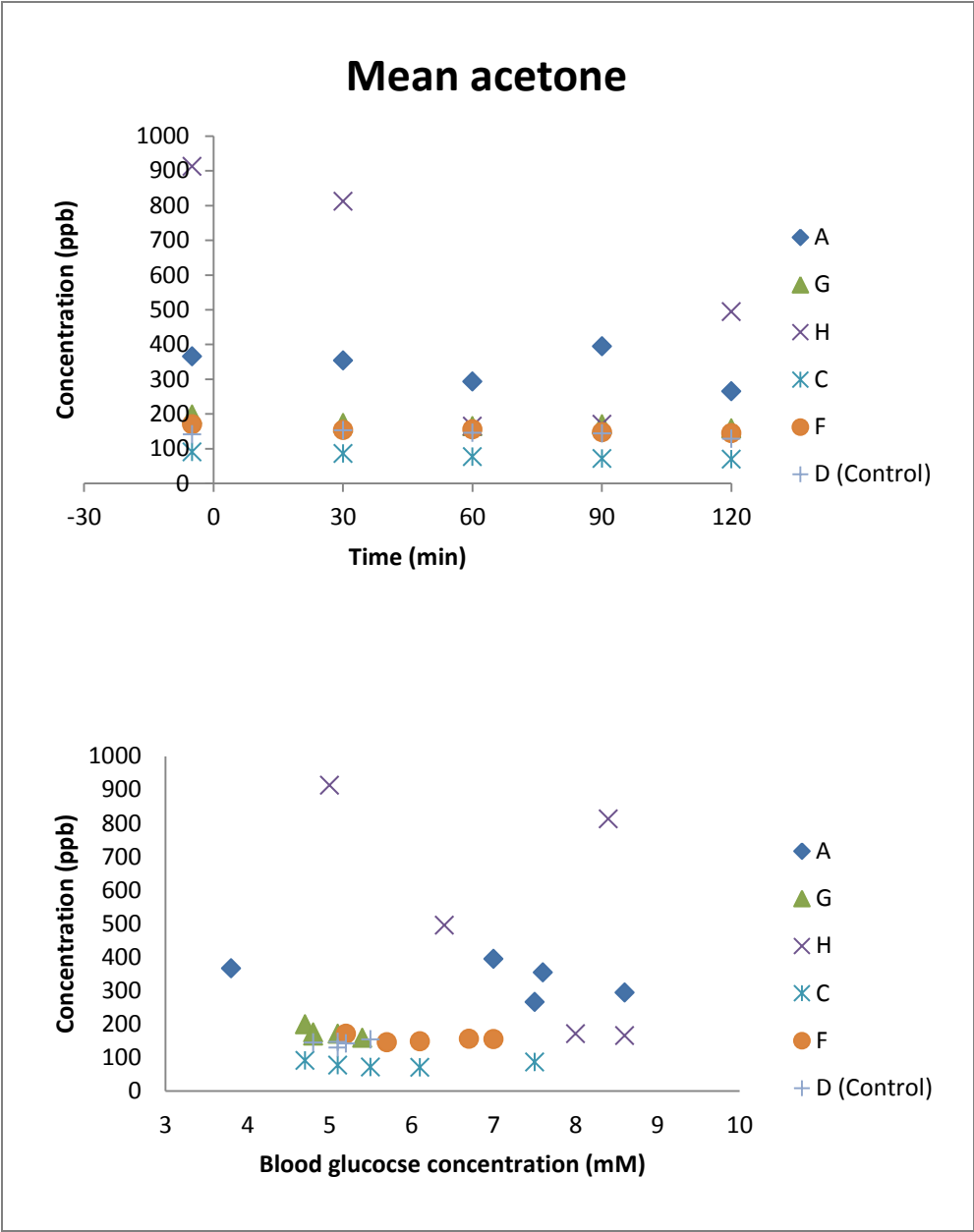


Figure 2.13 Mean exhaled acetone concentration plotted against time and blood glucose concentration

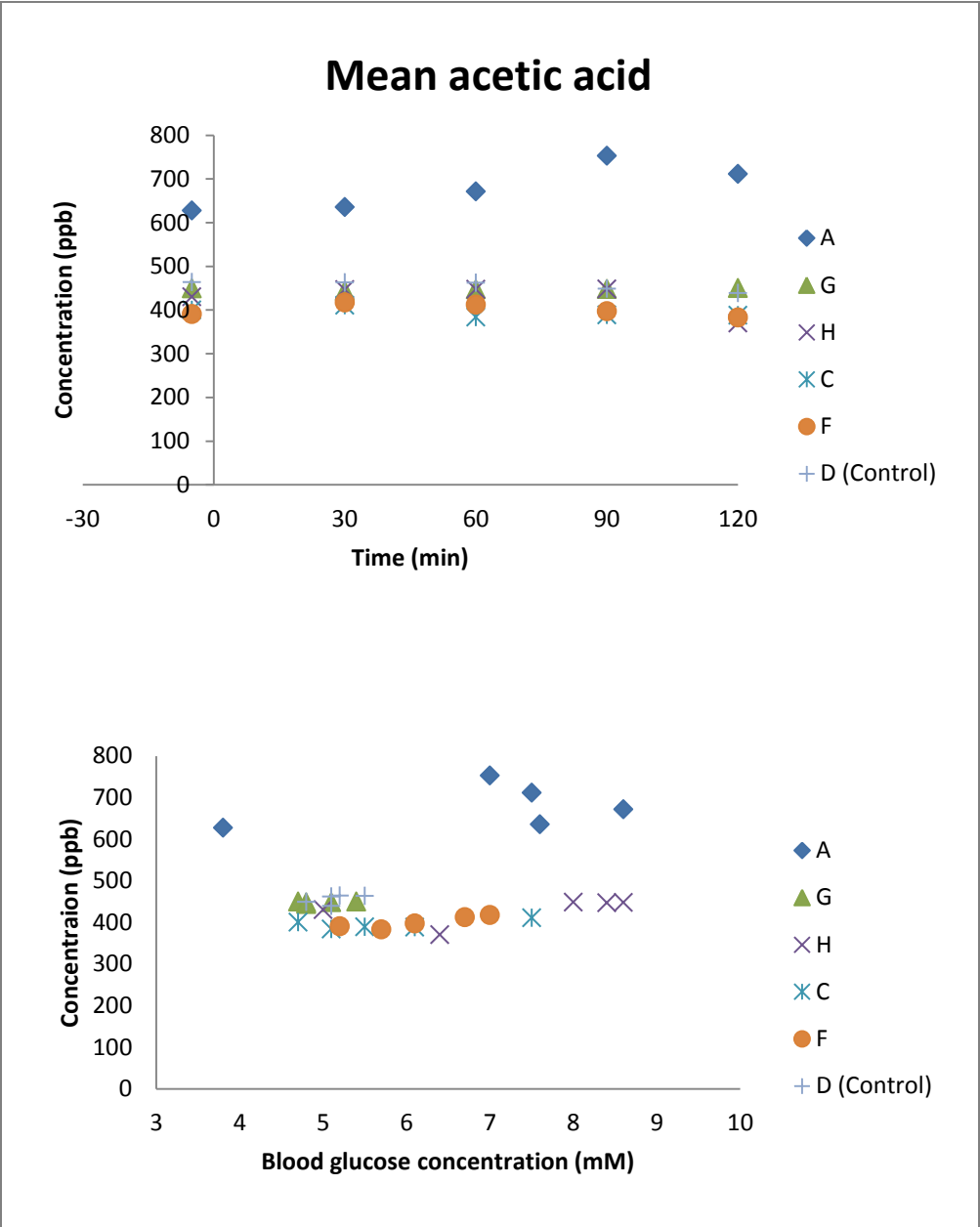


Figure 2.14 Mean exhaled acetic acid concentration plotted against time and blood glucose concentration

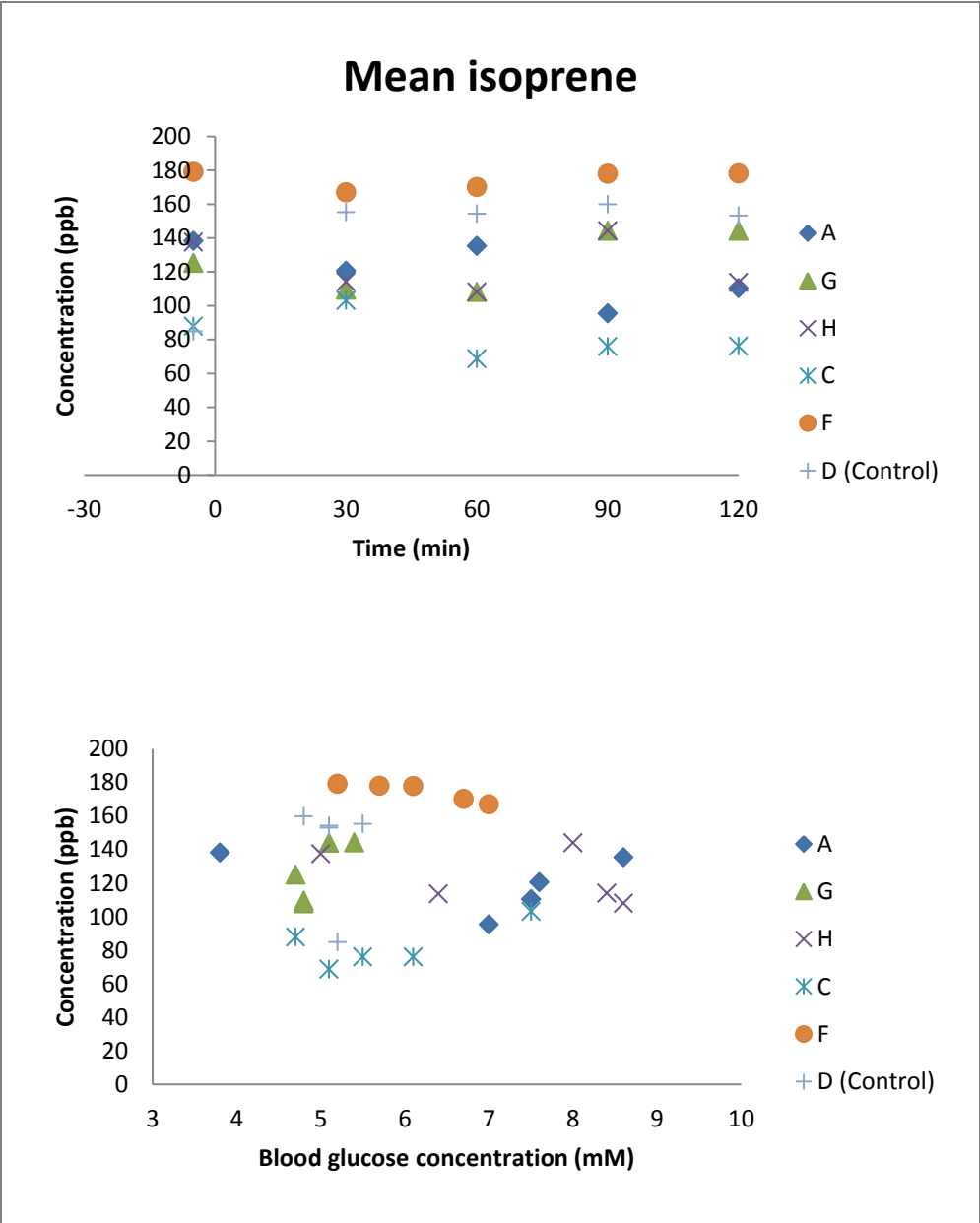


Figure 2.15 Mean exhaled isoprene concentration plotted against time and blood glucose concentration

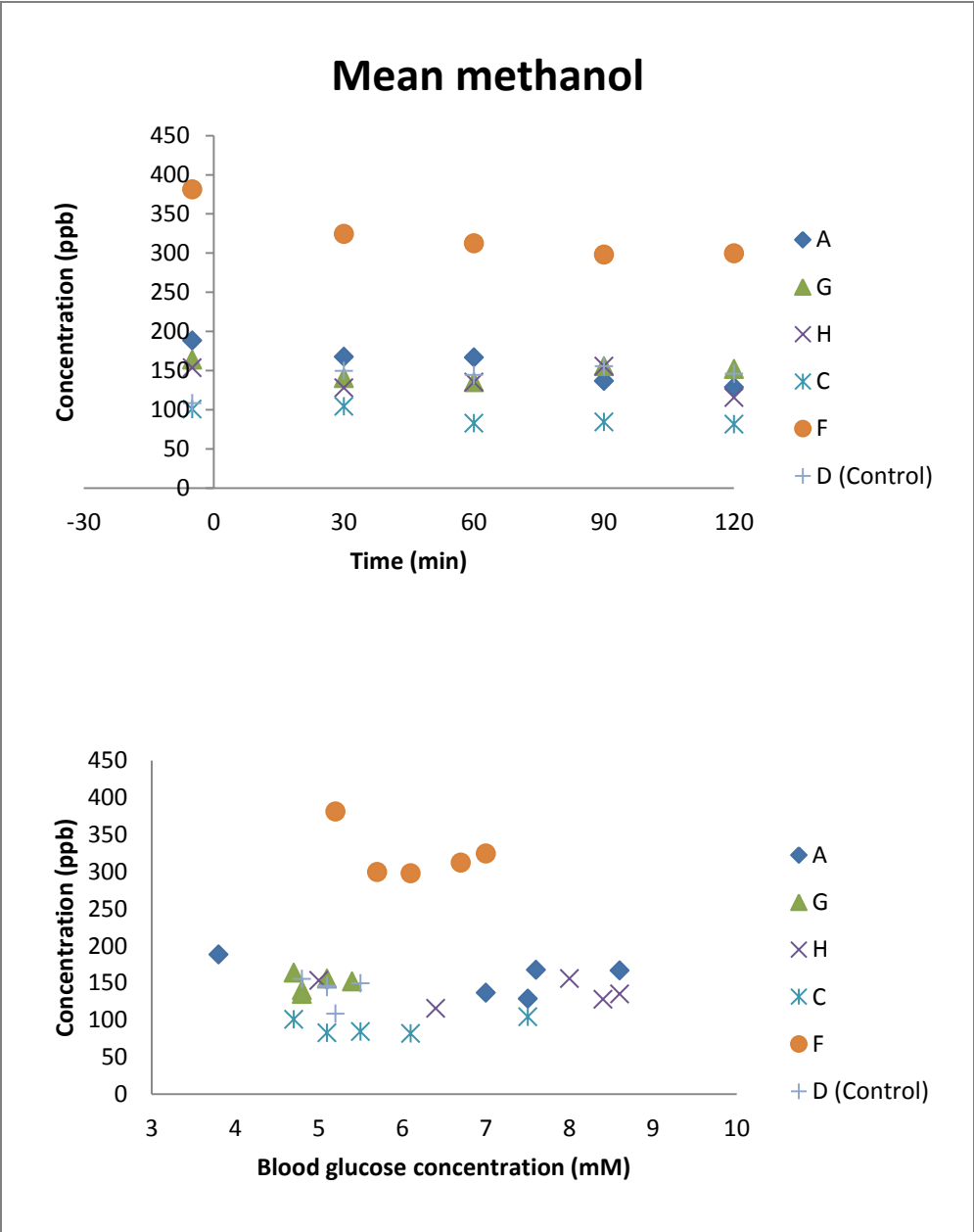


Figure 2.16 Mean exhaled methanol concentration plotted against time and blood glucose concentration

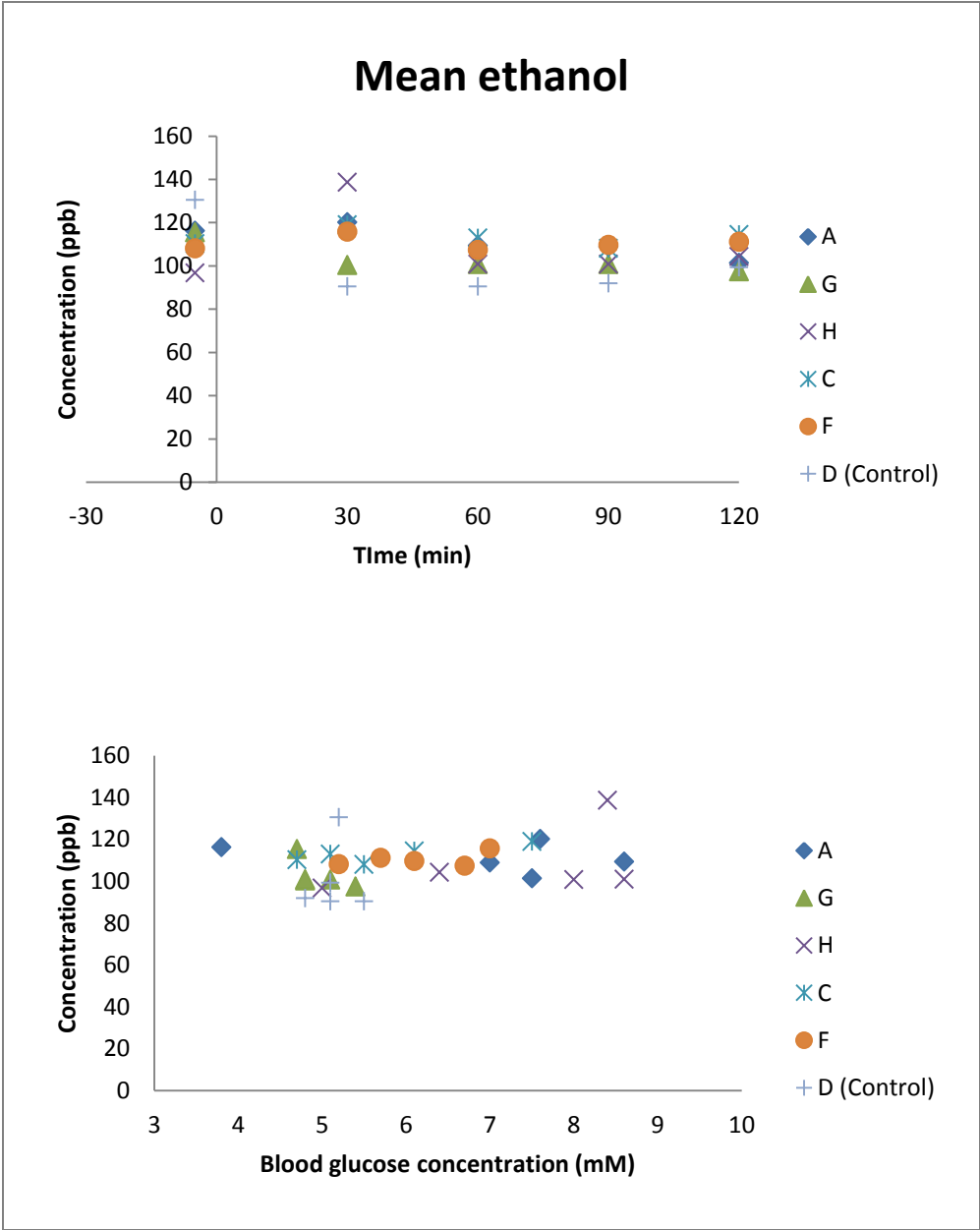


Figure 2.17 Mean exhaled ethanol concentration plotted against time and blood glucose concentration

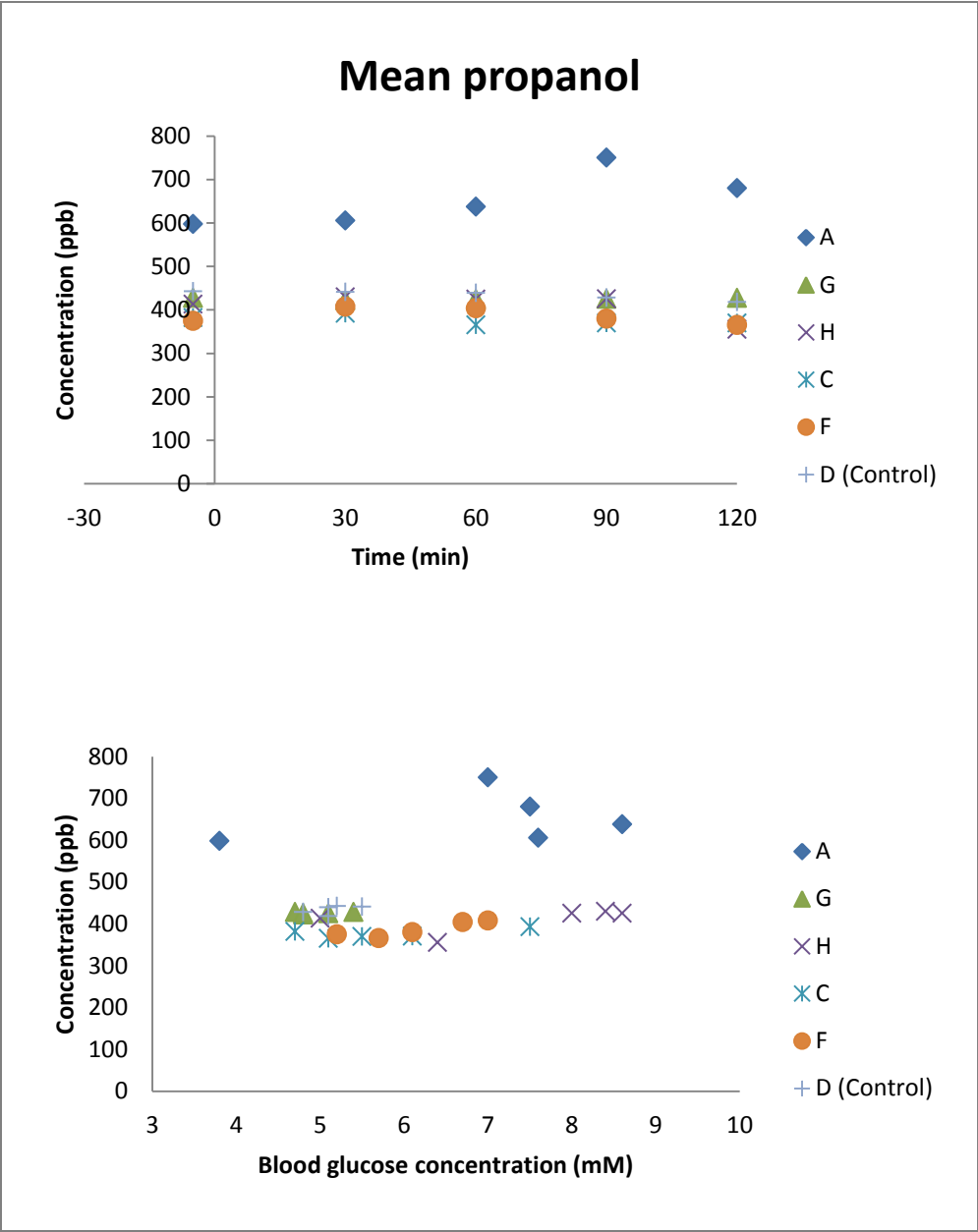


Figure 2.18 Mean exhaled propanol concentration plotted against time and blood glucose concentration

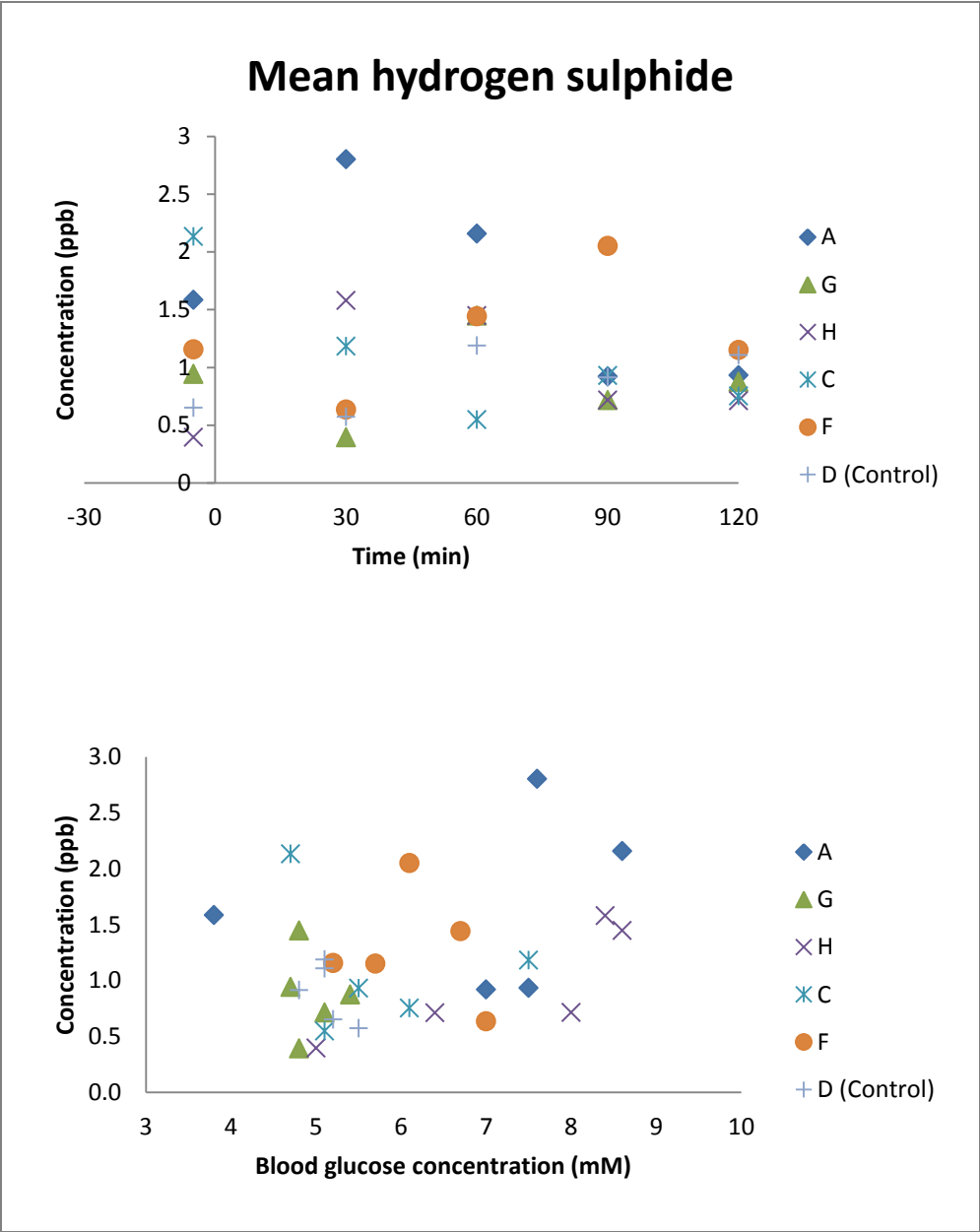


Figure 2.19 Mean exhaled hydrogen sulphide concentration plotted against time and blood glucose concentration

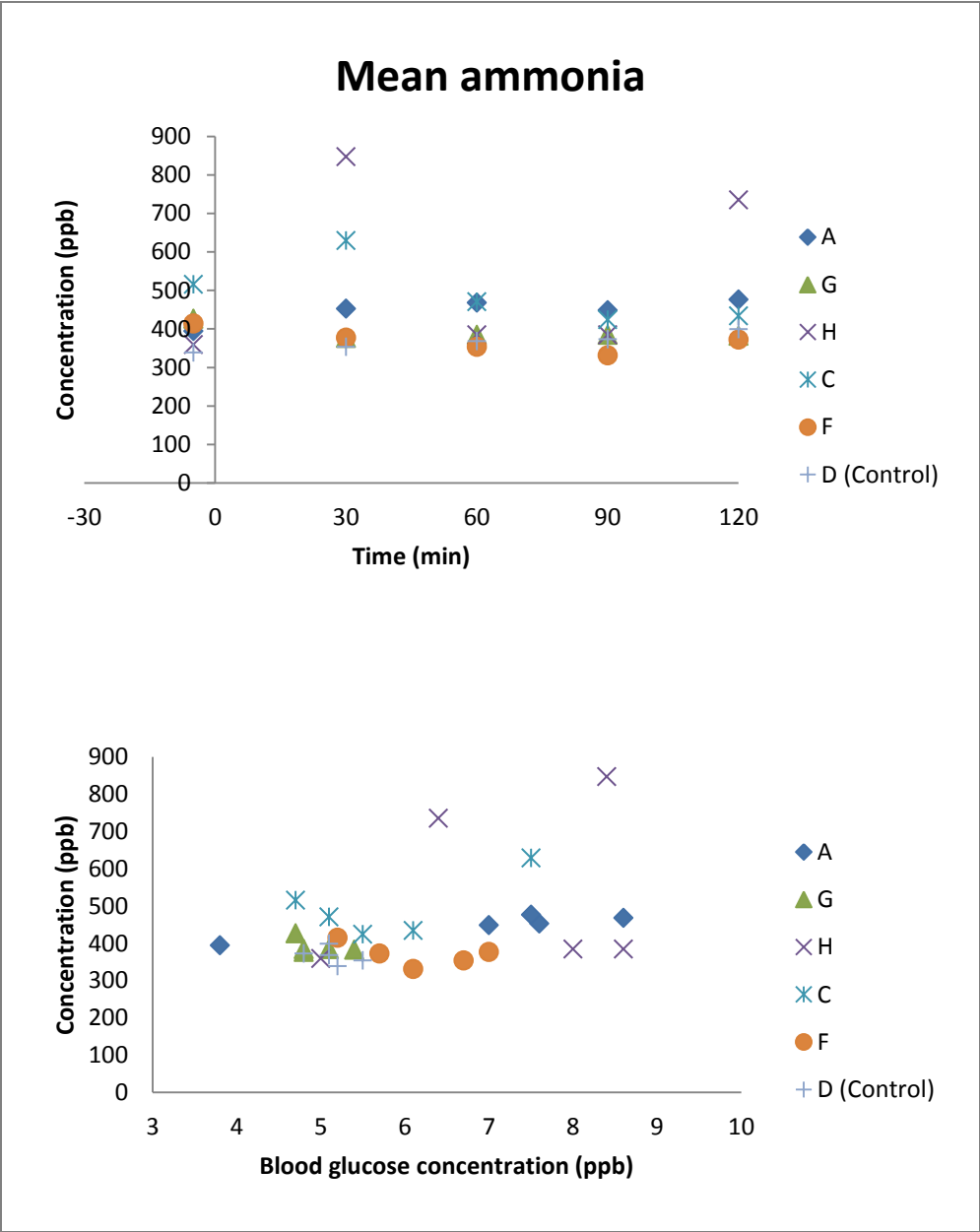


Figure 2.20 Mean exhaled ammonia concentration plotted against time and blood glucose concentration

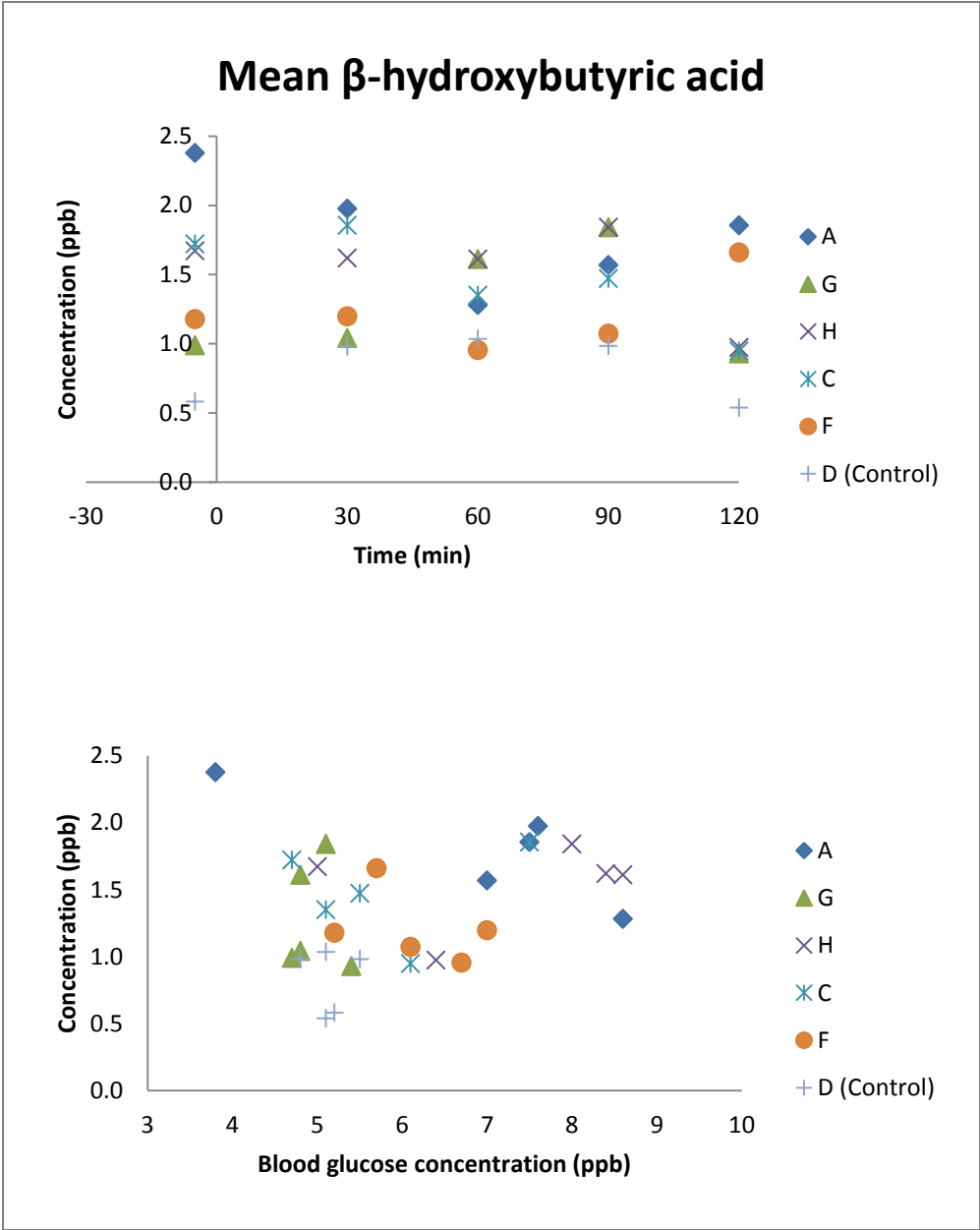


Figure 2.21 Mean exhaled β -hydroxybutyric acid concentration plotted against time and blood glucose concentration

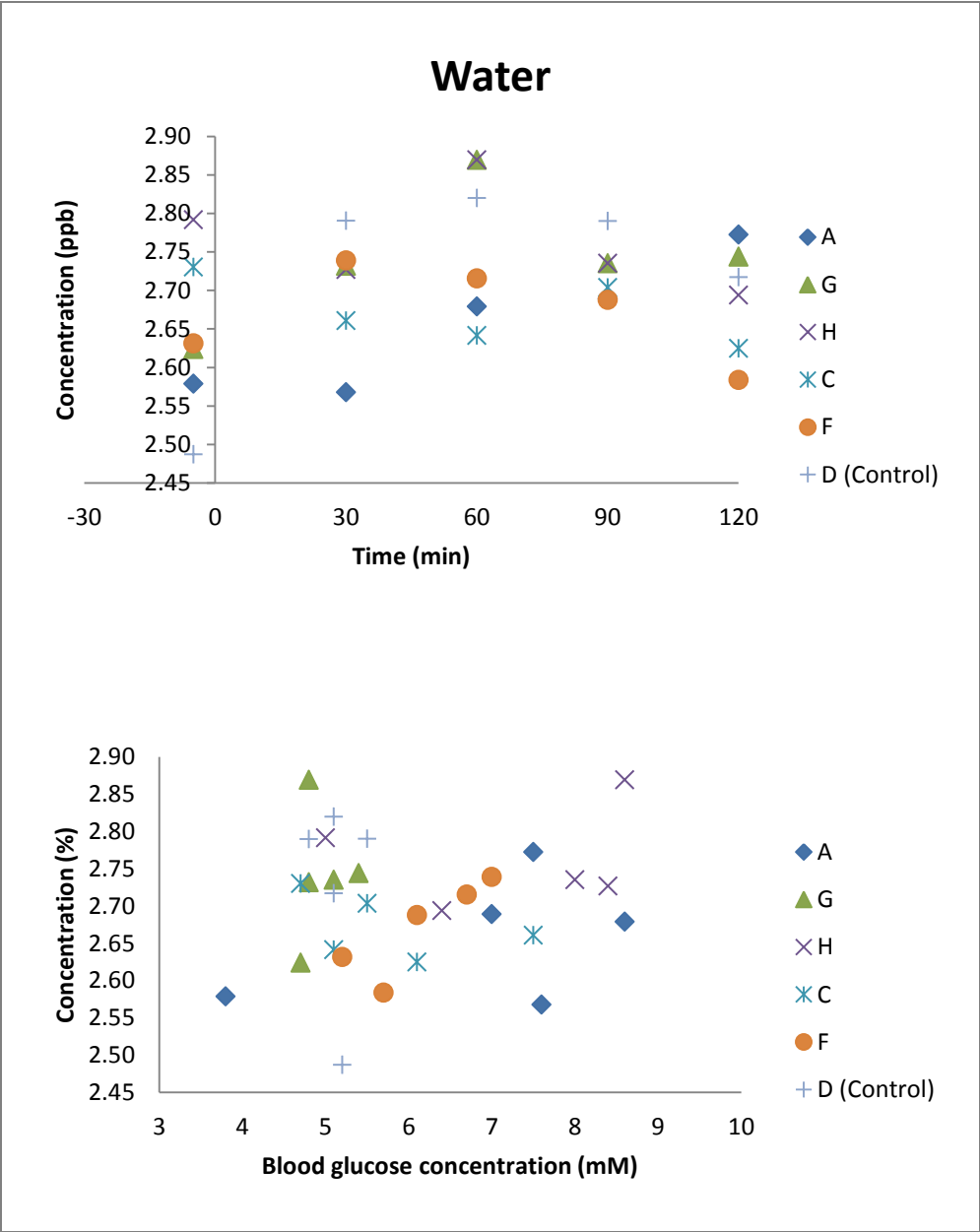


Figure 2.22 Mean exhaled water concentration plotted against time and blood glucose concentration

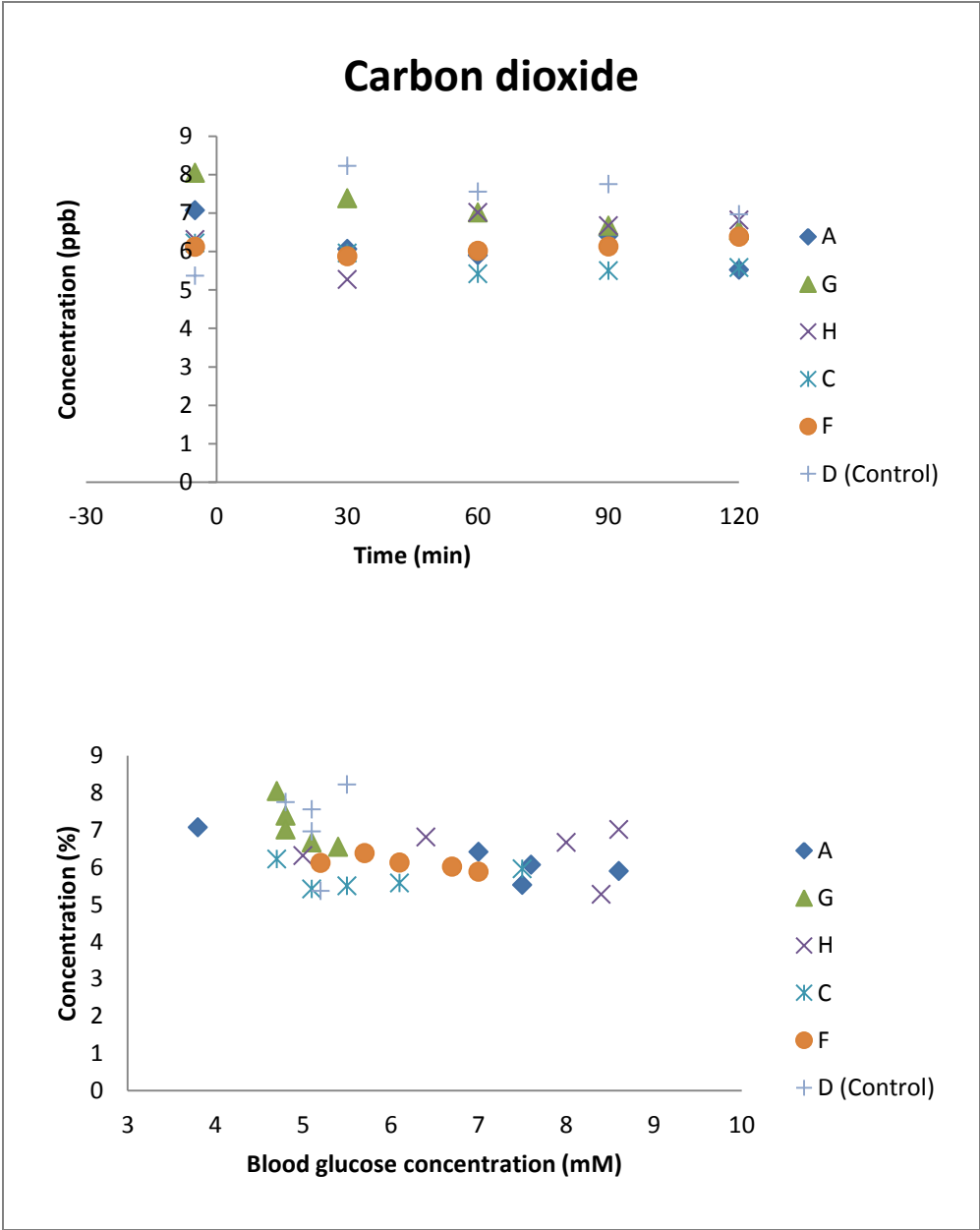


Figure 2.23 Mean exhaled carbon dioxide concentration plotted against time and blood glucose concentration

Compound	Linear correlation coefficient (R)					
	A	G	H	C	F	D (Control)
Formaldehyde	-0.83	-0.26	-0.32	-0.55	0.70	-0.85
Acetaldehyde	-0.83	-0.26	-0.32	-0.55	0.70	-0.85
Acetone	-0.48	0.88*	-0.68	-0.98 *	-0.92	-0.59
Acetic acid	0.85	0.30	-0.54	-0.65	-0.36	-0.90 *
Isoprene	-0.72	0.63	-0.19	-0.58	0.22	0.73
Methanol	-0.97 *	-0.14	-0.45	-0.84	-0.89 *	0.71
Ethanol	-0.88 *	-0.81	-0.19	-0.08	0.02	-0.59
Propanol	0.78	0.18	0.60	0.65	0.37	-0.93 *
Hydrogen Sulphide	-0.60	0.07	-0.04	-0.79	0.42	0.73
Ammonia	0.81	-0.65	0.21	-0.68	-0.68	0.98 *
β-hydroxybutyric acid	0.57	0.27	0.55	0.86	0.48	0.03
Water	0.94 *	0.46	-0.43	-0.62	-0.34	0.56
Carbon dioxide	-0.76	-0.98 *	0.54	-0.82	0.64	0.42

Table 2.5 Linear correlation coefficients for exhaled VOCs quantified using SIFT-MS vs. Time

Compound	Linear correlation coefficient (R)					
	A	G	H	C	F	D (Control)
Formaldehyde	-0.66	-0.58	0.60	-0.80	0.13	0.29
Acetaldehyde	-0.66	-0.58	0.60	-0.80	0.13	0.29
Acetone	-0.49	-0.70	-0.59	0.00	-0.36	0.41
Acetic acid	0.37	0.44	0.52	0.60	0.90 *	-0.53
Isoprene	-0.29	0.80	-0.39	0.66	-0.93 *	-0.18
Methanol	-0.52	0.15	-0.17	0.36	-0.48	-0.22
Ethanol	0.30	-0.64	0.46	0.83	0.49	0.09
Propanol	0.23	0.36	0.49	0.60	0.90	0.53
Hydrogen Sulphide	0.94 *	-0.12	0.84	-0.24	-0.21	-0.58
Ammonia	0.94 *	-0.45	0.19	0.62	-0.49	-0.43
β-hydroxybutyric acid	-0.84 *	-0.03	0.29	0.20	-0.40	-0.04
Water	0.47	0.12	0.18	-0.45	0.86	-0.12
Carbon dioxide	-0.86	-0.83	-0.10	0.06	-0.70	0.06

Table 2.6 Linear correlation coefficients for exhaled VOCs quantified using SIFT-MS vs. Blood glucose concentration

2.3.6 GC-MS

Chromatograms were converted from their native Perkin Elmer RAW files into network common data form (netCDF) (version 2.3.3) using the conversion software package Databridge, part of the Turbomass software suite (Perkin Elmer®). These were then imported into MATLAB R2009b (32-bit) using the `mzcdread` function, part of the Bioinformatics Toolbox (3.4). Chromatograms from the individual OGTT sampling intervals were then overlaid and aligned to the internal standard by padding the matrices with 'zeros' as appropriate (Weber 2009). An example of an alignment can be seen for volunteer A in Figure 2.24, where the inset shows the chromatograms aligned to the internal standard. The peak heights were normalised to the height of the internal standard peak for each chromatogram, this was achieved by dividing all of the points in the chromatogram by the intensity of the internal standard peak, so that the internal standard peak was of the same height in each of the chromatograms. As the concentration of the internal standard is known, 50 ng mL⁻¹, it is possible to determine the concentration of the other components in the chromatogram.

The chromatograms were then manually inspected to determine potential candidate compounds. Due to a technical fault where the splits on the GC-MS were set incorrectly, there are not many identifiable peaks on the chromatograms. These compounds were identified as being isoprene, acetone, propanol and cyclopentane.

Mean exhaled breath acetone concentration against time and blood glucose concentration is summarised for all of the volunteers in Figure 2.25, isoprene in Figure 2.26, cyclopentane in Figure 2.27 and propanol in Figure 2.28. The linear correlation coefficients for exhaled breath concentration against time and blood glucose concentration are summarized in Table 2.7 and Table 2.8 respectively. Peaks that were not detected in a particular sample are represented by the letters ND, significant correlations ($P < 0.05$) are marked with an asterisk (*).

The results show that there is no significant relationship between the compounds identified in exhaled breath and time or blood glucose concentration; though there is a significant increase in isoprene concentration observed with volunteer G, this is not true for the rest of the volunteers.

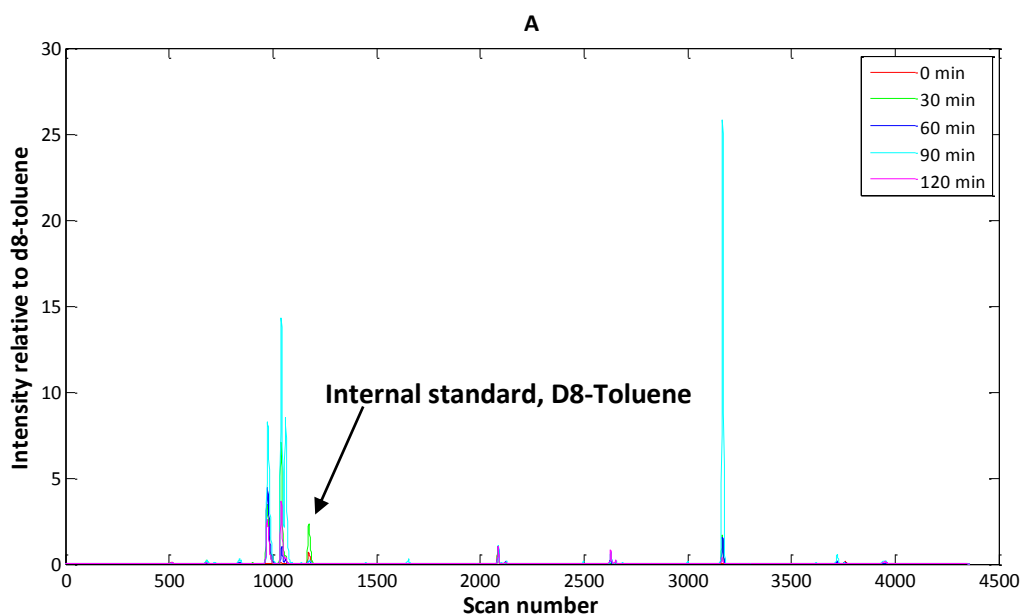


Figure 2.24 Multiple chromatogram alignment of samples collected from volunteer A at each sampling intervals during an OGTT

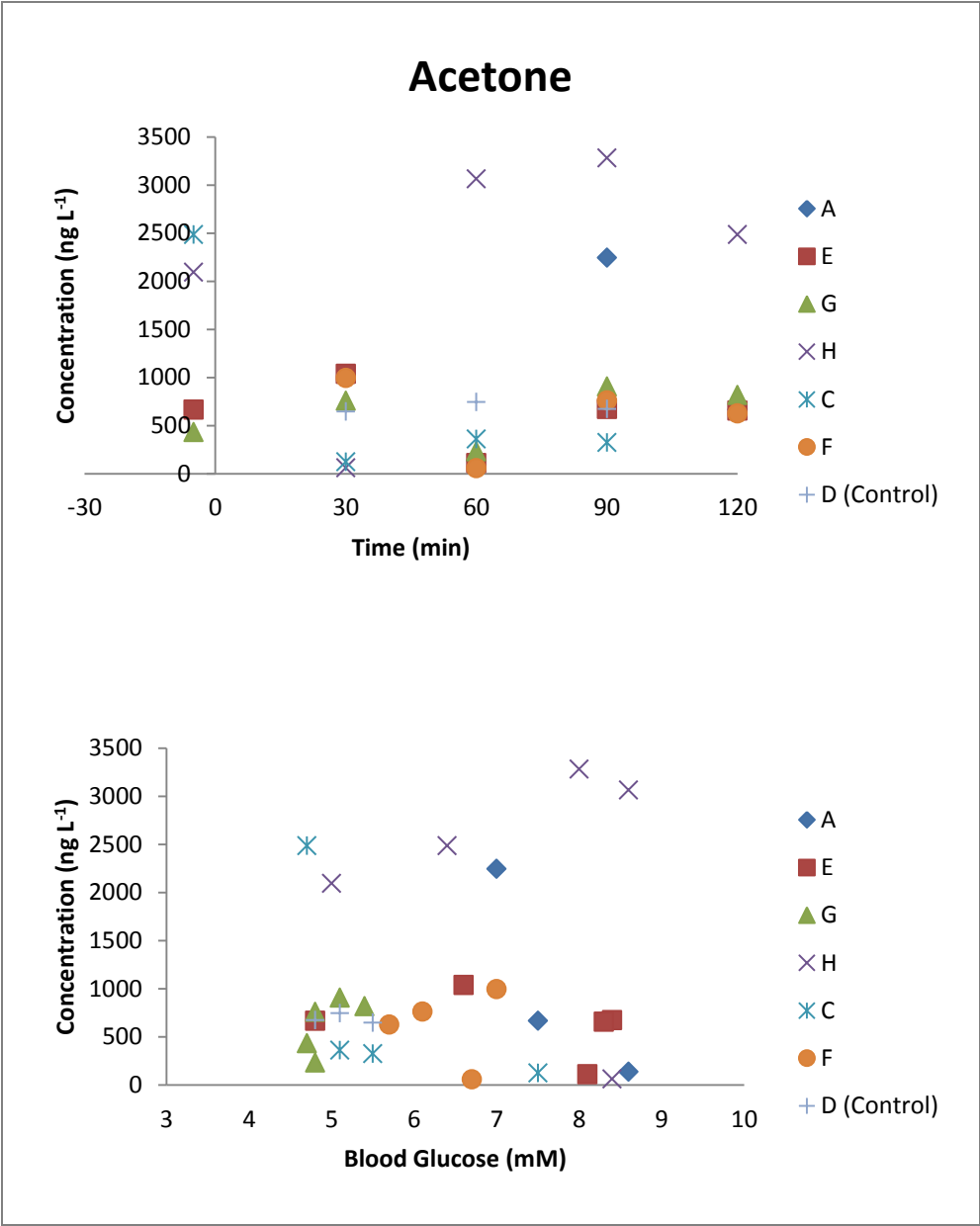


Figure 2.25 Exhaled breath acetone concentration quantified using GC-MS plotted against time and blood glucose concentration

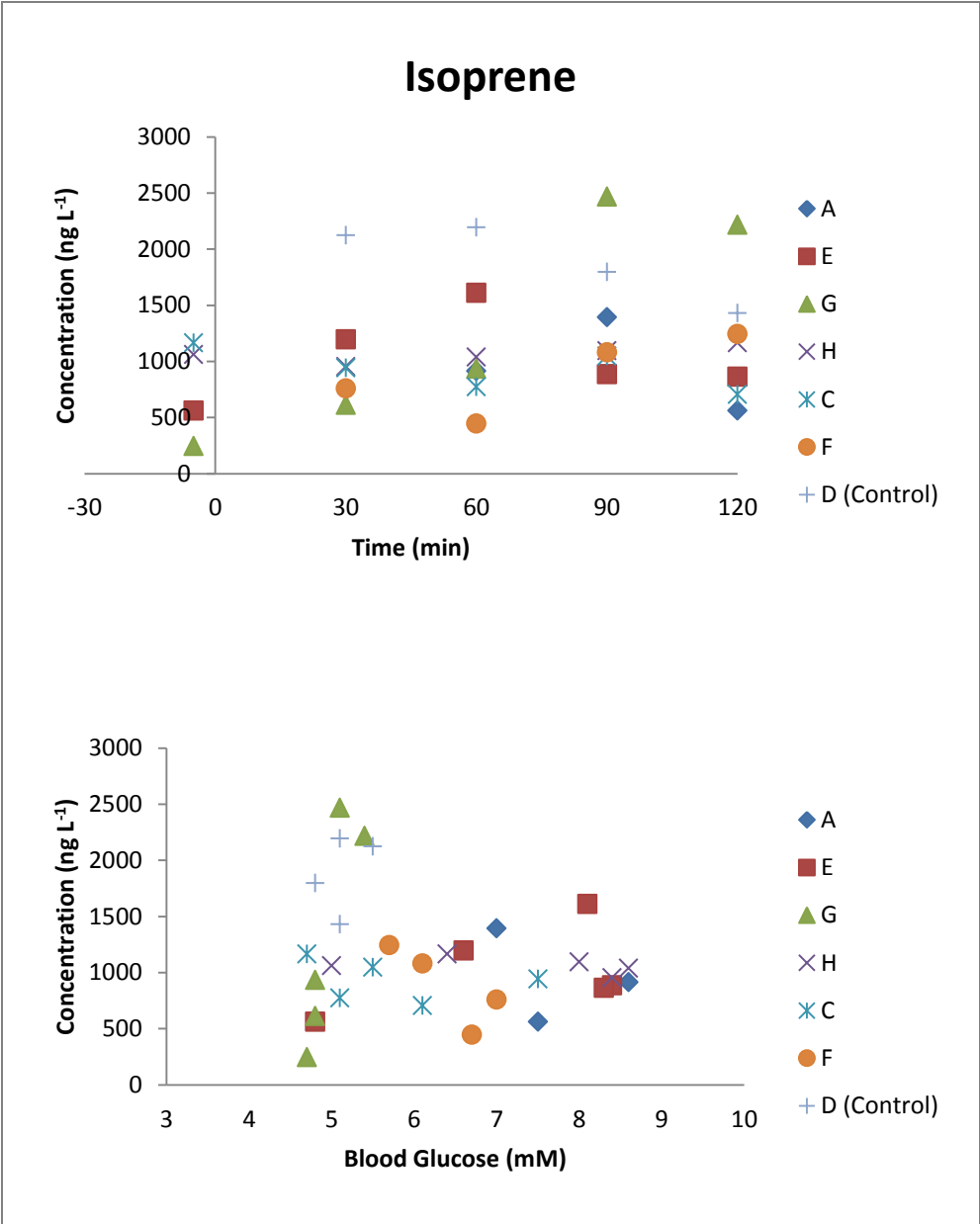


Figure 2.26 Exhaled breath isoprene concentration quantified using GC-MS plotted against time and blood glucose concentration

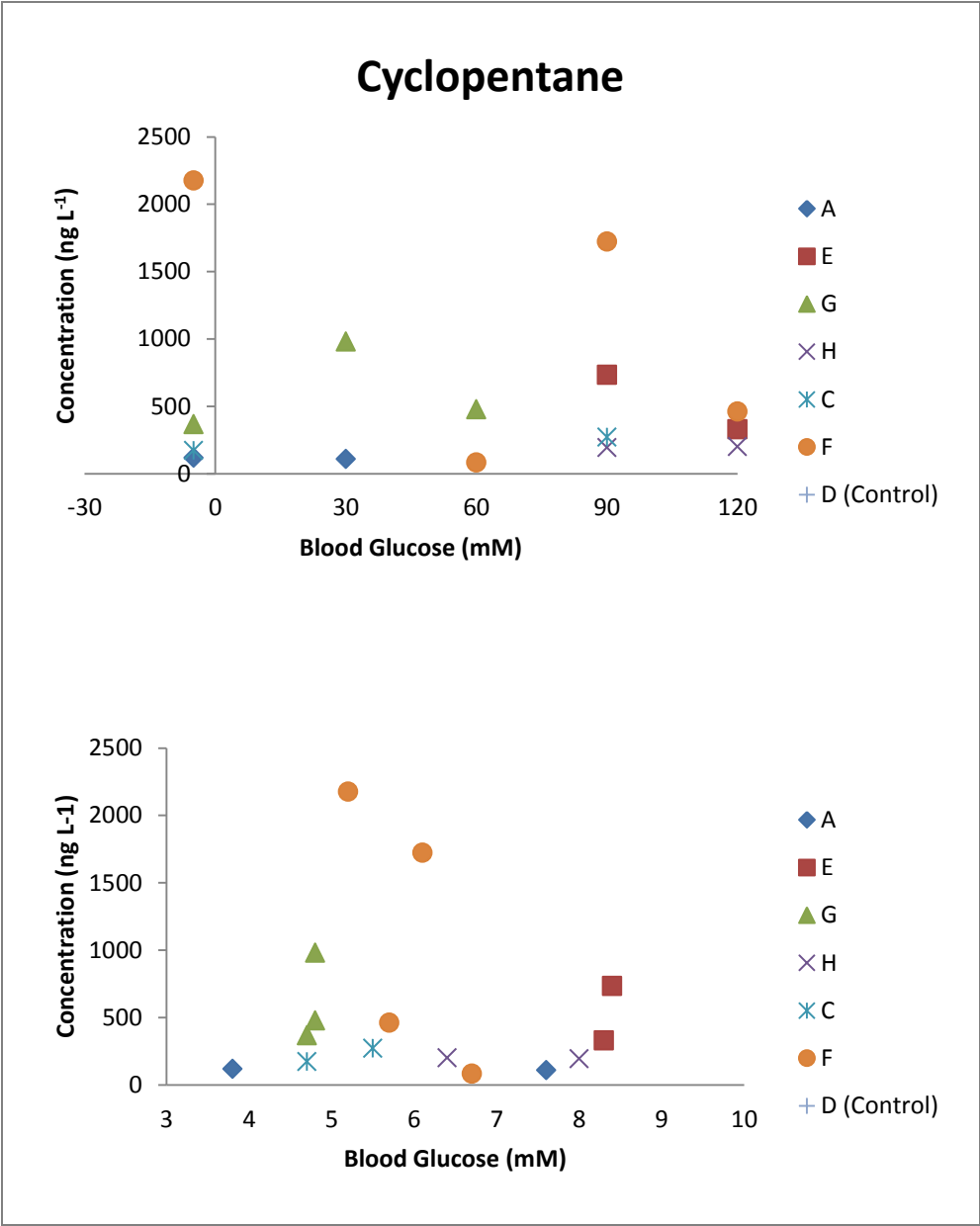


Figure 2.27 Exhaled breath cyclopentane concentration quantified using GC-MS plotted against time and blood glucose concentration

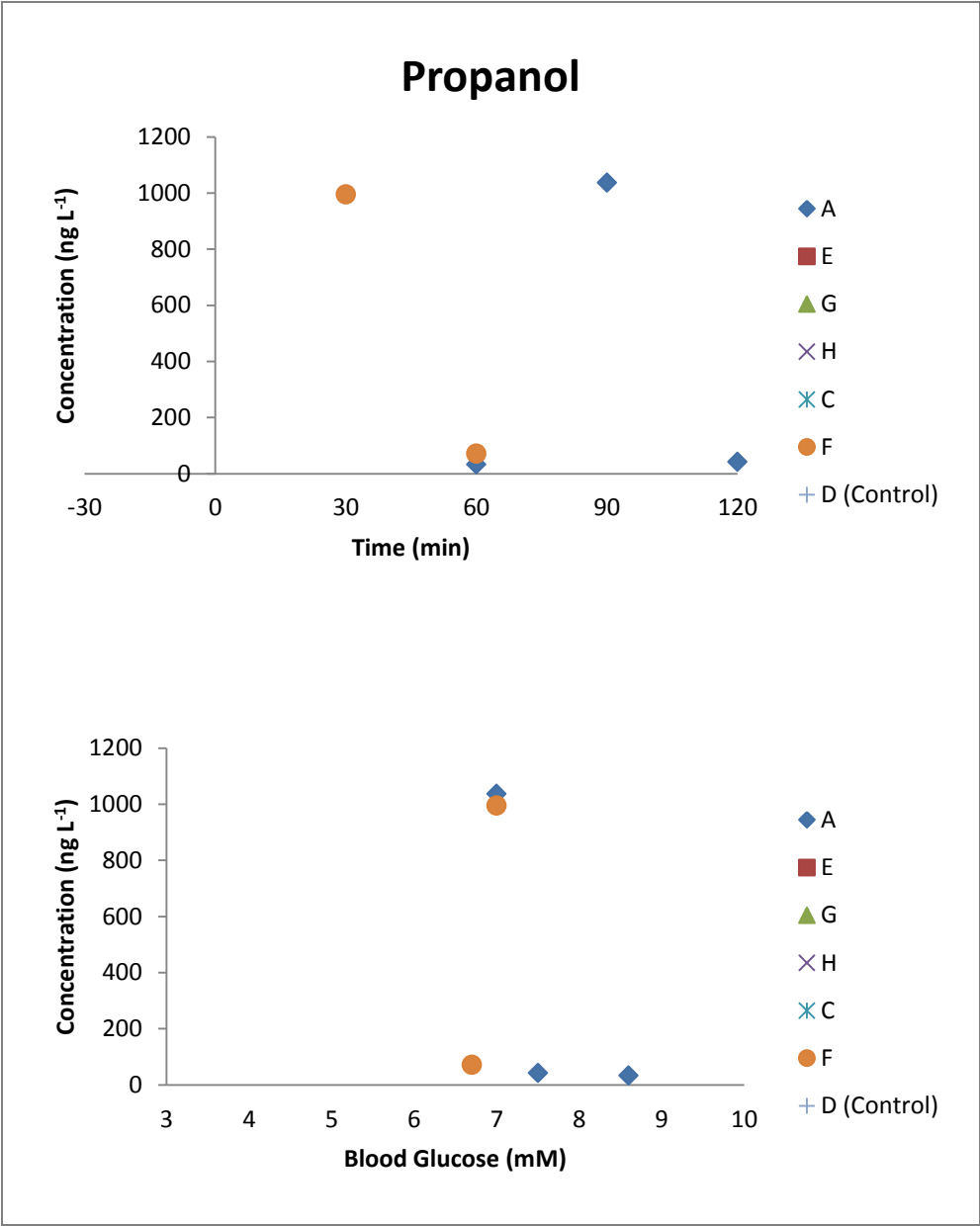


Figure 2.28 Exhaled breath propanol concentration quantified using GC-MS plotted against time and blood glucose concentration

Compound	Linear correlation coefficient (R)						
	A	E	G	H	C	F	D (Control)
Acetone	0.24	-0.35	0.5	-0.49	-0.72	-0.13	0.26
Isoprene	-0.42	0.12	0.93 *	0.71	-0.67	ND	ND
Cyclopentane	-1	-1	-0.17	1	ND	ND	ND
Propanol	0	ND	ND	ND	ND	ND	ND

Table 2.7 Linear correlation coefficients for exhaled VOC concentration quantified using GC-MS vs. Time

Compound	Linear correlation coefficient (R)						
	A	E	G	H	C	F	D (Control)
Acetone	-0.88	-0.35	0.65	-0.06	-0.61	0.01	-0.34
Isoprene	-0.38	0.49	0.88 *	-0.45	-0.3	ND	ND
Cyclopentane	-1	-1	-0.17	1	ND	ND	ND
Propanol	-0.74	ND	ND	ND	ND	ND	ND

Table 2.8 Linear correlation coefficients for exhaled VOC concentration quantified using GC-MS vs. Blood glucose concentration

2.4 Discussion

In this experiment, VOC concentration in exhaled breath was monitored in seven healthy adults during an OGTT using three different analytical methods Breathotron, SIFT-MS and GC-MS as a method for non-invasively monitoring blood glucose concentration. This is the first experiment where exhaled breath VOCs have been monitored using three different methods, a sensor based system, online SIFT-MS and GC-MS. No distinct, statistically significant relationship was established between sensor resistance or exhaled VOC and blood glucose concentration. This outcome suggests that there was no change in VOC concentration in response to the oral glucose tolerance test.

The lack of consistent, statistically significant change in exhaled VOC concentration during the experiment may be explained by a several factors, such as deficiencies in methodology or limitations of the instrumentation. However, it is likely that there was no biological change in VOC concentration in response to the OGTT.

There was little change in blood glucose concentration following consumption of the glucose solution however this is consistent with previously published studies (Galasetti et al., 2005, Turner et al., 2006a-b). All experiments were conducted according to WHO guidelines. It may have been possible that the vitamin C present in the glucose powder used may have competitively inhibited the absorption of glucose in the gastrointestinal tract as both vitamin C and glucose are absorbed by the glucose transporters GLUT1 and 3 leading to a smaller increase in glucose than would have been expected (Fraser Reid et al., 2001). However, this is unlikely due to the small concentration (0.05% w/w) of vitamin C in the glucose powder. It may have been possible that the concentration of glucose was insufficient to alter the insulin secretion rate enough to affect lipolysis.

There may have been a greater effect on VOC concentration if a higher concentration of glucose was used, or instead of consuming a large amount of glucose at the beginning of the experiment, it may prove more valuable to increment glucose consumption in a series of steps over the two hours to determine the threshold required to inhibit lipolysis and or proteolysis. A change in blood glucose concentration could also be achieved by using clamp procedure where an infusion of insulin, to decrease blood glucose concentration, or glucagon, is used to increase blood glucose concentration. Though there are ethical implications in administering an insulin infusion to healthy volunteers.

Blood glucose concentration was measured using an Abbott Therasense meter and Abbott FreeStyle test strips which during calibration was shown to be over reading by approximately 10%. According to the manufacturer, test strips can show a 5.6% discrepancy when compared with a YSI 2300 glucose analyser, though arm data (capillary) from the test strips was compared against pin prick (capillary) data using the YSI (Abbott 2007 ART12285 Rev B. 02/07). The test strips used were within their use by date, and this is unlikely to have influenced the outcome and meter function verified using a calibration solution.

Ambient temperatures within the SIFT-MS laboratory are lower than elsewhere within the laboratory due to the increased ceiling ventilation required for the instrument; there are four complete air changes per hour. This means that ambient temperatures within the SIFT-MS lab are, on average, 19°C compared to elsewhere in the main laboratory with an average of 21°C. The crash cart on which the volunteers were asked to lie was sited directly below one of the major vents. As many of the volunteers said that they felt cold during the experiment, it can be assumed that the cooling effect may have reduced blood flow to the surface of their fingertips.

It has been shown that blood glucose readings can be dependent on skin temperature, Haupt et al. (2005) showed that glucose readings between a warm fingertip and cold fingertip reading were significantly lower (0.95 mM).

To the author's knowledge, this is the first experiment where online SIFT-MS has been used to quantify exhaled breath VOCs during an OGTT using a Profile 3 (third generation) instrument. Previous studies (Turner et al., 2006a-d; Turner et al., 2008) have used a second generation instrument with single breath exhalations or bag sampling method. Where previous versions of the instrument have a short sample transfer line, the Profile 3 has a much longer, sampling line made from polyether ether ketone (PEEK) tubing which is heated using PTFE coated nichrome wire and sampling head. Some volatile species may condense within the sampling line, resulting in lower concentrations. Due to the longer path length, changes in concentration are less dynamic, with a short lag between the outbreath and the instrument responding. The use of an adapted sampling mask would increase the dead space, but would not significantly detrimental to the results. Breath-by-breath sampling would be achievable by considerable reengineering of the sample inlet system to reduce the path length, but is not within the scope of this project.

Whilst there were advantages in using online SIFT-MS in this experiment, such as the lack of contamination from mouth bacteria through nostril breathing (Smith et al., 2008), and simultaneous sampling of the same sample using all three analytical methods, there were also several disadvantages. It has been observed in other studies that very shallow breathing, or very high flows, caused by hyperventilation, can lead to discrepancies in SIFT-MS quantification, particularly exhaled acetaldehyde, acetone, isoprene, methanol, ethanol, and ammonia concentration. Anderson et al. (2006), using a quadrupole mass spectrometer, and Boshier et al., (2011), using PTR-MS, found that exhaled VOC concentration was influenced by flow rate. Whilst this information is collected by the Breathotron, due to the linear interpolation of the flow sensor signal, the maximum flow rate which can be recorded is 52 L min⁻¹.

VOC concentrations may have been underreported as out breaths are shallower whilst breathing directly into the instrument. This may be remedied by using collecting samples of breath for analysis in sampling bags as used in other studies. These are usually made from Nalopahn®, (polyethyleneterephthalate (PET)), Tedlar® (polyvinylidene fluoride (PVDF)), or the use of Douglas bags made from poly vinyl chloride (PVC) (Reichard et al., 1979; Turner et al.,

2006a-d). The use of online SIFT-MS also means that only one precursor ion can be used at a time. This limits the compounds that can be analysed at any one time. It is possible to use both the NO^+ and O_2^+ precursor ions for the quantification of acetone for example (Španěl and Smith, 2001).

There have been several MOS gas sensor based breath gas analysers mentioned in the literature (Hanada et al., 2003; Chou et al., 2006; Yu et al., 2011), but this is the first time that such an analyser has been used to attempt to non-invasively measure blood glucose concentration. Though the data shows that there is a generally a decrease in sensor resistance with an increase in blood glucose concentration following the ingestion of the glucose solution which would be consistent with the increased rate of insulin secretion which would inhibit lipolysis and proteolysis (Holt et al., 2007), though this relationship is statistically insignificant.

There was considerable variation in peak sensor resistance (ΔR_{max}) between the volunteers. Though ΔR_{max} was observed to change during the course of the experiment, there was no consistent relationship established between ΔR_{max} and blood glucose concentration. In some volunteers ΔR_{max} increased with increasing blood glucose concentration, whilst in others there was a decrease (typically 0.5-1.0 k Ω) or no change between initial and 30 minute readings. The sensor is unlikely to have been affected by drift within a 30 minute period, as in a previous study the CAP25 sensor was found to drop only 0.5 k Ω after several hours of continuous use (Patel, 2007). It is unlikely that the sensor failed to detect compounds within the exhaled breath samples as there was little change in VOC concentration seen with the SIFT- and GC-MS, which are consistent and confirm the results seen with the Breathotron. The CAP25 was shown to have a lower limit of detection of 100 ppb for acetone and isopropanol (Patel, 2007); most of the volunteers exhibit initial concentrations higher than this lower threshold. As permanent gases, such as oxygen, nitrogen and nitric oxide, were not quantified there is no way to tell if the concentration of these gases had a detrimental effect on sensor performance. This is unlikely due to the lack of change in exhaled CO_2 measured using the SIFT-MS, and would only be affected by a change in the respiratory quotient. Previous Breathotron experiments have been performed on pure gas and simulated breath samples in the laboratory, or have involved a small number of volunteers (Bishop, 2006; Patel, 2007). This is the first experiment where the Breathotron has been used to analyse samples with the SIFT-MS concurrently to determine which compounds contribute to the signal. The Breathotron uses a single MMOS sensor which was intended to be used a general air quality sensor

(McGeehin, 2000), though has been used in an electronic nose system for monitoring meat spoilage (Panigrahi et al., 2004). Various devices for the analysis of exhaled breath gas exist (Gardner et al., 2000), some of these devices promise, but none have demonstrated the ability to monitor glycaemic status. Many of these devices use an array of electrochemical sensors, whereas the Breathotron attempts to capture as much data as possible from a single sensor.

There is no evidence from the SIFT-MS, or GC-MS data to suggest that endogenously produced compounds negatively influenced the sensor. Hydrogen sulphide is known to poison the sensing layer of the sensors of this type (Gardner and Bartlett, 1999) the concentration of hydrogen sulphide quantified in exhaled breath using SIFT-MS was insufficient to have a detrimental effect on sensor performance. The concentration of ethanol was very low; whilst carbon dioxide was at the concentration that would be expected in exhaled breath. Makisimovich et al, (1996) describe the use of an adsorption semiconductor sensor specific to acetone with a sensing layer made from tin oxide doped with stibium being used for ketoacidosis diagnosis. They report a linear relationship between breath acetone concentration and conductivity, although on the data as presented this seems questionable. They report that 8% CO₂ has a negative effect on sensor performance, but 112 mg L⁻¹ of ethanol in exhaled attenuates the signal, giving a signal comparable to a higher concentration of acetone (170 mg L⁻¹). Smoking apparently also has a detrimental effect on the sensor; this is probably attributable to acetonitrile or other compounds that are typically found within tobacco smoke (Ligor et al., 2008). In addition they suggested that acetone quantification is impossible immediately after smoking, but only provide anecdotal evidence for this observation. It is unlikely that any quenching of signals occurred in this study as none of the volunteers had particularly high levels of ethanol, whilst it is also unlikely that smoking tobacco negatively affected the results as the recruitment criteria did not allow current smokers to be admitted into the study, though no data was collected on the possibility of passive smoking.

There was no statistically significant change in exhaled acetone concentration with respect to blood glucose concentration using any analytical method. The greatest concentration of acetone was not seen in the lowest blood glucose concentration, but in the volunteer that had fasted the longest; though the volunteer with the lowest blood glucose concentration exhibited the highest concentration of acetic acid. Fasted acetone concentration has been found to be higher in individuals that have fasted for longer period of time (Riechard et al., 1979). Glycogen stores may not have been sufficiently depleted for ketogenesis to occur (Holt et al., 2007). The

difference in acetone concentration between the individuals may be attributed to differences in the way that fat is stored within the body, adipose tissue and liver, and may depend on the rate of insulin secretion. The amount of fat stored in these tissues may also depend on dietary fat intake. Insulin concentration can be determined by radioimmunoassay (Negi Chandra, 2005), but would require the analysis of whole blood samples which would require further ethical approval. It may also be possible that diabetic individuals react in a different way to non-diabetic individuals and only produce excess ketones at very low blood glucose concentration (Manolis, 1983).

A relationship between exhaled breath acetone concentration and blood glucose is reported in two separate studies, one using online SIFT-MS (Turner et al. 2008), and the other using GC-MS where breath samples were collected in electro-polished gas canisters (Galasetti et al., 2005). Galasetti et al., (2005) also reports a relationship with exhaled breath ethanol concentration. In both of the previous studies 75 g of glucose solution was given following fasting and exhaled breath gas analysed over 120 minutes. Turner et al., (2008) analysed exhaled breath and capillary blood glucose at 30 minute intervals in five volunteers whilst breath was sampled using the disposable cardboard tube method. A decrease in exhaled breath acetone was not seen in all volunteers. However, the instrument used in the Turner et al., (2008) experiment is a Profile 2, whilst our experiment uses a Profile 3 with a different photomultiplier tube which is less susceptible to a drop in count rate due to overheating, increasing the signal to noise (S2N) ratio reducing accuracy. Galasetti et al., (2005) analysed breath samples every five minutes following ingestion of the glucose solution for the first 30 minutes of the experiment, and then at 30 minute intervals. Whole blood samples were collected for the analysis of serum glucose, insulin, β -hydroxybutyric acid and ethanol for 10 volunteers. Galasetti et al. (2005) reported correlation coefficients of between 0.60 and -0.70 between exhaled breath acetone and blood glucose concentration.

The pattern in exhaled methanol, ethanol and propanol is consistent with previous findings (Turner et al., 2008), where ethanol concentration increases slightly, and a small decrease is seen in these compounds over time), though the mean concentration is lower than previously reported (Turner et al., 2006a-d). This is probably due to the small sample size and age range of the volunteers. The exhaled ethanol concentration is probably lower than the study mentioned as prior to the OGTT volunteers were advised to brush their teeth using water only

and encouraged to breathe through their nostrils rather than their mouth reducing potential contamination by bacterial ethanol produced in the oral cavity.

Galasetti et al., (2005) reported an increase in exhaled breath ethanol concentration during OGTT, and suggested that the increase in endogenously produced ethanol is due to 'auto brewery syndrome', where microbial activity, specifically *Candida*, in the digestive system is stimulated by excessive intake of carbohydrate. The same increase was seen in a study by Turner et al., (2008), but only at the start of the OGTT and quickly fall to a constant level, suggesting that endogenous production does not change with glycaemic status. The source of the initial increases in ethanol is attributable to action by mouth flora when glucose is ingested. As mentioned previously, Smith et al., (2008) suggest that breath obtained from the nasal cavity is more accurate for quantification of ethanol, due to the lack of bacterial action. Furthermore the R^2 values reported for ethanol concentration and acetone concentration vs. glucose concentration in the Galasetti study were statistically insignificant, 0.55 and 0.40 respectively. However, they report seeing no ethanol in the blood samples that were taken. Their results are therefore consistent with the microbial production of ethanol as a result of carbohydrate loading, but at a site other than the digestive system. The small increase in ethanol concentration is probably due to mouth bacteria metabolising residual sugar in the mouth from drinking the glucose solution (Turner et al., 2006c; Španěl et al., 2006).

Exhaled isoprene shows a decrease with increasing blood glucose concentration in most of the volunteers. The rate of production increases with increasing blood glucose concentration. Most of the volunteers in their early to late 20s exhibit isoprene concentration within the 100-160 ppb range, with the highest concentrations in this subset being seen in male volunteers. However the two female volunteers in their 40s are completely opposite, whilst one has the highest isoprene concentration of the cohort, the other has the lowest. Isoprene is generated in several pathways, including the mevalonic acid pathway of cholesterol synthesis (Hallikainen et al., 2006) and has in the past been linked with glycaemic status, though this relationship is not clear in our results.

2.5 Conclusion

The results of this experiment suggest that there is no statistically significant relationship between exhaled VOC concentration and blood glucose concentration in healthy, non-diabetic individuals after drinking a 75g glucose solution following a 8 hour fast. Furthermore, there

were significant differences in exhaled VOC concentration between the individuals. Though a relationship between exhaled breath acetone and ethanol against blood glucose concentrations was reported in the literature, further scrutiny proved that the significance of the relationships was similar to the results that the author collected.

Whilst it is more than likely that there was no biological change in exhaled VOC concentration during the OGTT due to differences between diabetics and non-diabetics in response to dietary glucose. There are methodological limitations that may have negatively affected the outcome of the experiment.

There was only a moderate increase in blood glucose concentration during the OGTT experiment. The outcome of the experiment may have been different if pure glucose was administered to the volunteers during the OGTT, if this experiment were to be repeated it would be favourable to proceed in this way. An alternative would be to use a glucose clamp, though there are ethical implications of doing this on non-diabetic individuals.

There was large variation in exhaled VOC concentration between the individuals. Though this may partly explained by age and gender, some variation is still seen between volunteers of a similar age and the same gender. This was evidenced by the clustering pattern seen with the PCA analysis from the Breathotron data where the samples from each individual volunteer clustered together not by blood glucose concentration.

The SIFT-MS methodology used in this experiment may have prevented further relationships between exhaled VOC concentration and blood glucose being established. Though the online, continuous breath sampling method is advantageous due to the fact that the same sample of breath is analysed using the complimentary methods, this means that the number of VOC compounds that can be analysed is reduced. It may be better to collect breath samples in sampling bags to enable sampling using the other precursor ions. Collection of breath samples using bags would however introduce contamination from bacteria in the oral cavity.

3 Analysis of VOCs in exhaled breath, blood and skin from type-1 diabetics during a hypoglycaemic clamp

3.1 Introduction

In the previous chapter the change in exhaled VOC concentration and a relationship with blood glucose concentration during an OGTT in non-diabetic individuals was not established. This may have been due to the fact that blood glucose concentration did not change dramatically during the experiment. Additionally, VOC concentrations were only determined using one precursor ion using the SIFT-MS, due to the use of online sampling. There may have been significant relationships between the other compounds that can be quantified using the other precursor ions that may correlate with blood glucose concentration, and these may be seen by collecting and analysing samples from bags..

Hypoglycaemia is when blood glucose concentration falls dangerously low. The painful and invasive nature of taking pin prick blood glucose measurements is often cited as the primary reason why many diabetic patients fail to self-monitor their own blood glucose concentration (Cryer, 1997; Tuch et al., 2000; Holt et al., 2007).

A breath-based glycaemic monitoring system may be more acceptable to diabetic patients, many of which fail to self-monitor their glycaemic regularly. The consequences of a failing to self-monitor blood glucose concentration on a regular basis for patients with T1DM can be potentially very serious. Allowing blood glucose concentration to fall to dangerously low levels can result in acute hypoglycaemic episodes, with other long term complications arising due to micro- and macrovascular damage (Tuch et al., 2000; Holt et al., 2007).

The purpose of this experiment is to detect and quantify potential volatile biomarkers in exhaled breath, skin and blood headspace that may be indicative of glycaemic status using Breathotron, SIFT- and GC-MS during a hypoglycaemic clamp where an infusion of insulin was used to lower blood glucose concentration. A decrease in acetone concentration with a decrease in blood glucose concentration was expected due to the inhibition of lipolysis.

3.2 Materials and Methods

3.2.1 Hypoglycaemic clamp

Volunteers over the age of 18 years old with pre-existing type 1 diabetes mellitus (T1DM) with some degree of hypoglycaemia unawareness were recruited. Samples were collected at in the Clinical

Research Facility (CRF) at Addenbrooke's Hospital (Cambridge University Hospitals NHS Foundation Trust, Cambridge, CB2 0QQ, UK) with approval from the NHS Research Ethics Committee. Each of the volunteers had their blood glucose levels held at a series of target concentrations using a hypoglycaemic glucose clamp (DeFronzo et al., 1979). Blood glucose levels were gradually decreased from initial, un-fasted (baseline) concentration to nominal targets in stages using an infusion of insulin from approximately 5.00 mM to 3.80, 3.40, 2.80 and eventually to 2.40 mM. Volunteers were held at the given concentrations for forty minutes, except the lowest concentrations where it was only twenty minutes. At each stage of the hypoglycaemic clamp 5ml blood samples were taken through a venous cannula. These samples were divided into two 2.5 mL aliquots, one of which was analysed at the hospital for blood glucose concentration, and one of which was transported back to the laboratory and stored at -80°C.

3.2.2 Breathotron

Breathotron 001 was selected at random to be used in this study. The Breathotron was switched on and the baseline resistance of the sensor resistance was left to equilibrate for a minimum period of fifteen minutes before any samples were taken. Prior to starting the hypoglycaemic clamp, the ambient laboratory air was analysed. Volunteers were asked to breathe normally into the face mask of the Breathotron for approximately five minutes. A baseline reading was taken before the start of the clamp. Further breath samples were then analysed at each stage of insulin infusion.

3.2.3 Breath

Breath sampling bags were made from 500 mm long lengths of Nalophan® NA (polyethylene terephthalate) plastic tubing (Khale, Germany) incorporating a 70 mm length of polypropylene tube and a Swagelok® SS-400-C closure fitted into the apical opening, a fitting is shown in Figure 3.1. The Nalophan NA was carefully fan folded to wrap around the tube and then tied with two tie-wraps to secure the tubing; the basal end was also fan folded and then approximately 2 cm was folded over and secured with two tie-wraps (HellermanTyton, Wythenshawe, Manchester, M22 4TY, UK), this made an adequately air tight container (Fowler 2010). An example of a Nalophan® sampling bag filled with a gaseous sample is shown in Figure 3.2.



Figure 3.1 An exploded view of a custom made Nalophan[®] bag fitting consisting of polypropylene tube and Swagelok[®] fittings



Figure 3.2 An example of a Nalophan[®] gas sampling bag filled with a gaseous sample

3.2.4 Skin

Volatiles excreted from skin were collected by placing a suitably sized Nalophan® bag over one of the volunteer's arms to create a microenvironment (Turner et al., 2008). The construction of these bags is essentially the same as the bags described in 3.2.3, though the apical opening was not fan folded to allow the bags to be placed over an arm. The bag was then filled with zero grade air and secured in place using a plastic tie wrap. Volatiles were allowed to equilibrate in the bag for a period of ten minutes before the bags were removed, sealed using another plastic tie wrap and sent to the lab for analysis using SIFT-MS.

3.2.5 Blood

Blood samples were removed from storage at -80°C and thawed at room temperature. 2.5 ml of blood was then pipetted into 50 cm long Nalophan® sampling bags. The bags were then sealed using a plastic tie wrap, filled with CP-grade zero grade air (BOC Gases, Guilford, Surrey) making the samples suitable for analysis using SIFT- and TD GC-MS.

3.2.6 SIFT-MS

The offline SIFT-MS method was used to analyse all three types of sample, breath, skin and blood headspace, collected during the hypoglycaemic clamp. The analysis of the samples was performed in two separate stages. Gaseous samples of exhaled breath and skin headspace were analysed immediately upon arrival in the SIFT-MS laboratory, whilst blood samples were analysed at a later date.

Prior to sample transfer, the bags were placed in an incubator at 40°C (Carl Stuart, Cambridge) for 10 minutes to allow VOCs to diffuse into the headspace. Following this incubation period samples were introduced to the sampling head of the SIFT-MS using the bag fitting which incorporated a ¼" Swagelok® fitting as previously mentioned. In the multi ion mode (MIM) the methanol, ethanol, propanol, formaldehyde, acetaldehyde, acetone and ammonia product ions were specifically selected to be quantified.

3.2.7 ATD GC-MS

Following analysis by SIFT-MS, volatile species from the headspace of skin and blood samples were concentrated onto TD tubes (Markes International Limited, Llantrisant, UK) packed with TENAX®/Carbotrap by connecting the bag to a FLEC® pump. The flow rate of the FLEC® pump was set to 100 mL min⁻¹ for a period of 5 minutes to provide a total volume of 500 mL in each of

the tubes. This was done within the confines of the incubator, the bags were not removed until samples had been analysed using SIFT-MS and VOCs concentrated onto TD tubes. The tubes were then stored at 4°C with their brass permanent caps on until they were ready to be analysed.

The TD tubes containing breath, skin and blood headspace were then analysed according to the GC-MS method previously described in 2.2.6.2.

3.3 Results

3.3.1 Hypoglycaemic clamp

Eight volunteers, both male and female took part in the experiment. Each was assigned a random volunteer ID consisting of a random number and letter by the hospital. There were no controls. No other data was collected, or made available to the researchers about the volunteers. The actual blood glucose concentration from each of the volunteers is shown in Table 3.1 against the nominal target concentrations, where baseline is the un-fasted blood glucose concentration of each of the volunteers before the start of the hypoglycaemic clamp. Volunteer 1B showed the highest baseline blood glucose concentration of the cohort, and the insulin infusion was altered slightly to take this into account. There is good agreement in mean baseline blood glucose concentration amongst the volunteers ($6.86 \text{ mM} \pm 3.06$); indeed this is skewed by the high baseline blood glucose concentration of volunteer 1B. Without volunteer 1B, the mean baseline blood glucose concentration would be $5.85 \text{ mM} \pm 1.22$. With the first infusion of insulin a decrease in blood glucose concentration can be seen in all of the volunteers except for 5A where there was an increase of 1.0 mM over the baseline concentration. Blood glucose concentration continues to fall with subsequent infusions of insulin.

Target (mM)	Actual blood glucose concentration (mM)									SD
	4A	5A	1B	8A	7B	6B	10A	11A	Mean	
Baseline	8.00	4.80	13.90	5.69	6.96	4.77	5.75	5.00	6.86	3.06
10.00	-	-	12.40	-	-	-	-	-	12.40	-
8.50	-	-	7.76	-	-	-	-	-	7.76	-
5.00	5.30	5.80	4.53	5.61	5.38	5.15	5.42	4.24	5.18	0.53
3.80	4.30	4.00	-	3.37	3.47	3.48	4.05	3.73	3.77	0.35
3.30	3.20	3.40	-	3.17	3.29	3.25	3.12	3.54	3.28	0.15
2.80	2.70	2.80	3.29	2.71	2.39	2.84	2.76	2.75	2.78	0.25
2.40	2.30	2.20		2.36	2.08	2.37	2.26	2.15	2.25	0.11
2.20	-	-	2.17	-	-	-	-	-	2.17	-

Table 3.1 Actual blood glucose concentrations recorded during the hypoglycaemic clamp

3.3.2 Breathotron

3.3.2.1 Analysis of sensor signal response

Breathotron signals were processed using the same method described in Chapter 2. The data files for the baseline and nominal 5.0 signals for volunteer 8A were corrupted and hence could not be included in the analysis. Most of the signals from volunteer 7B show a problem with the sensor heater temperature, apart from the sample taken at a blood glucose concentration of 2.39 mM; the data is included here for completeness. The linear correlation coefficient (R) between ΔR_{\max} and measured blood glucose concentration was calculated using the Data Analysis Toolpak included in Microsoft® Office Excel 2010™ (Redmond, WA, US), Table 3.2. The Data Analysis Toolpak also calculates the significance of the correlation using ANOVA. The null hypothesis, that there is no significant relationship between ΔR_{\max} and blood glucose concentration was rejected if $P < 0.05$. Significant relationships between ΔR_{\max} and blood glucose concentration are indicated in the table by an asterisk (*).

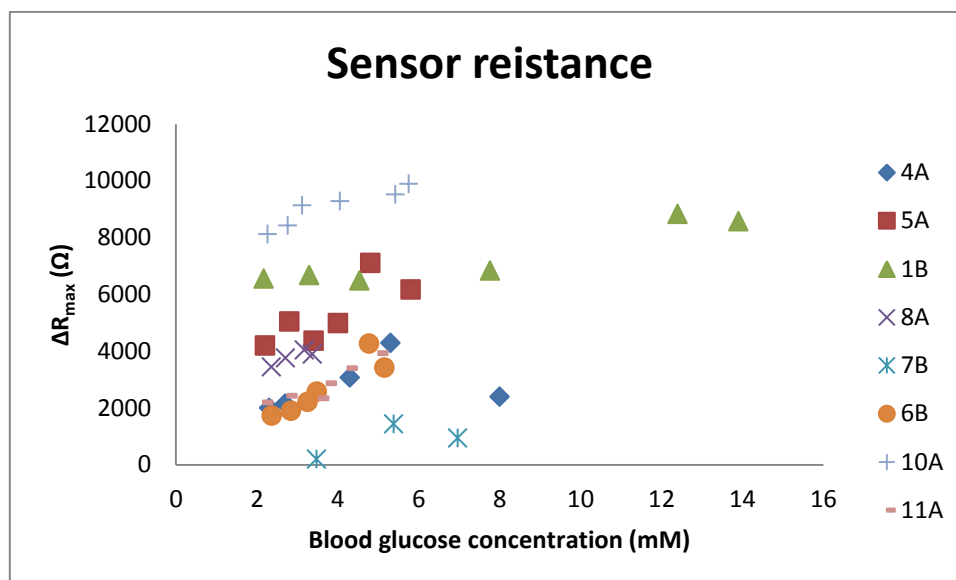


Figure 3.3 Maximum Breathatron sensor resistance (ΔR_{\max}) Vs. Measured blood glucose concentration

Volunteer	Linear Correlation Coefficient (R)
4A	0.34
5A	0.79
1B	0.93 *
8A	0.89
7B	-0.73
6B	0.92 *
10A	0.93 *
11A	0.91 *

Table 3.2 Linear correlation coefficients for Breathatron sensor resistance Vs. Measured blood glucose concentration

The highest blood glucose concentrations were observed in Volunteer 1B, but not the greatest change in resistance, or ΔR_{\max} . There is a small increase in ΔR_{\max} following the first infusion, the reason of this is unknown and is likely to be within the instrument error, though there is a decrease in sensor resistance with subsequent infusions. Signals from the nominal 5.0 and 3.8 mM steps of the infusion are not included in the analysis due to data file corruption.

3.3.2.2 Principal components analysis

In the previous experiment, Chapter 2, it was shown that variables generated by using the change in resistance of the baseline resistance of the MMOS sensor ($\Delta R_s/R_0$) and no scaling

method on signals which had been separated into 20 segments each 1 second in width for PCA captured the greatest variance and produced the best clustering. In this experiment the same method was used for PCA analysis, the result of which can be seen in Figure 3.4. Signals that were clipped or showed the sensor heater temperature problems were excluded from the analysis. As in the experiment in Chapter 2, the samples from individual volunteers cluster together, though there is some clustering of samples by measured blood glucose concentration unlike in the previous experiment.

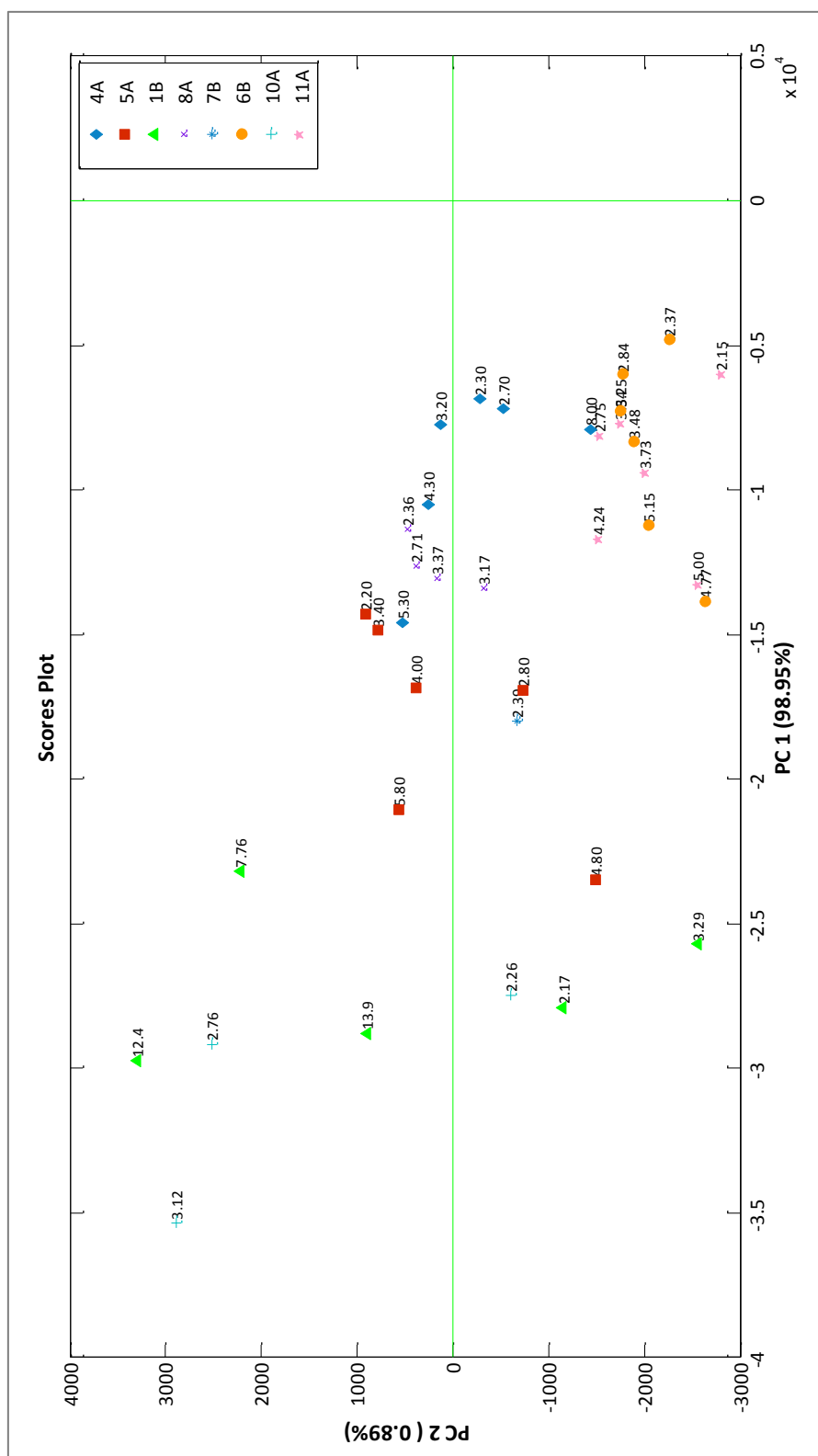


Figure 3.4 PCA scores plot for the hypoglycaemic clamp shows clustering by volunteer and not blood glucose concentration

3.3.3 SIFT-MS

3.3.3.1 Breath

Exhaled breath VOC concentrations were plotted against measured blood glucose concentration and can be seen for acetone (H_3O^+), Figure 3.5, acetone (NO^+), Figure 3.6, acetaldehyde, Figure 3.7, ammonia, Figure 3.8, methanol, Figure 3.9, ethanol, Figure 3.10, propanol, Figure 3.11, and isoprene, Figure 3.12. Each volunteer is plotted separately but on the same graph, with the calculated linear correlation coefficients in Table 3.3, again using the method previously described in Chapter 2. Significant correlations ($P < 0.05$) are marked with an asterisk (*), with the null hypothesis that there was no significant correlation between exhaled VOC and blood glucose concentration. No formaldehyde was detected in any of the breath samples and hence was not plotted.

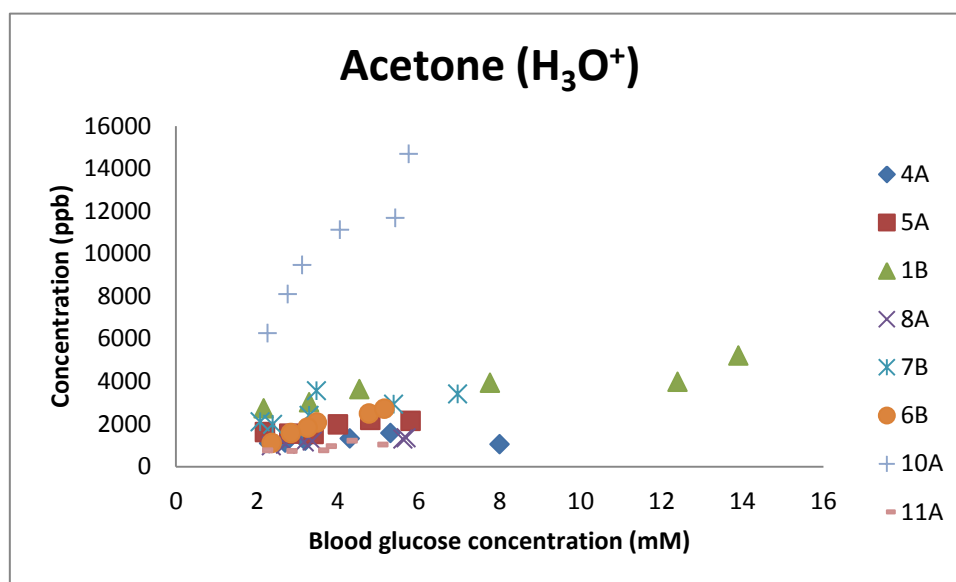


Figure 3.5 Exhaled breath acetone concentration quantified using the H_3O^+ precursor ion against measured blood glucose concentration for all eight volunteers during the hypoglycaemic clamp

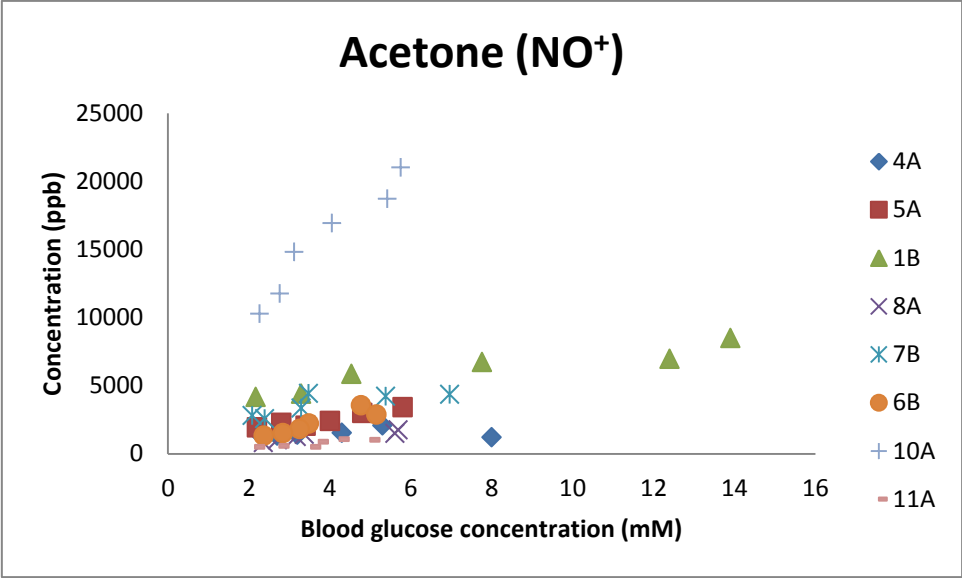


Figure 3.6 Exhaled breath acetone concentration quantified using the NO⁺ precursor ion against measured blood glucose concentration for all eight volunteers during the hypoglycaemic clamp

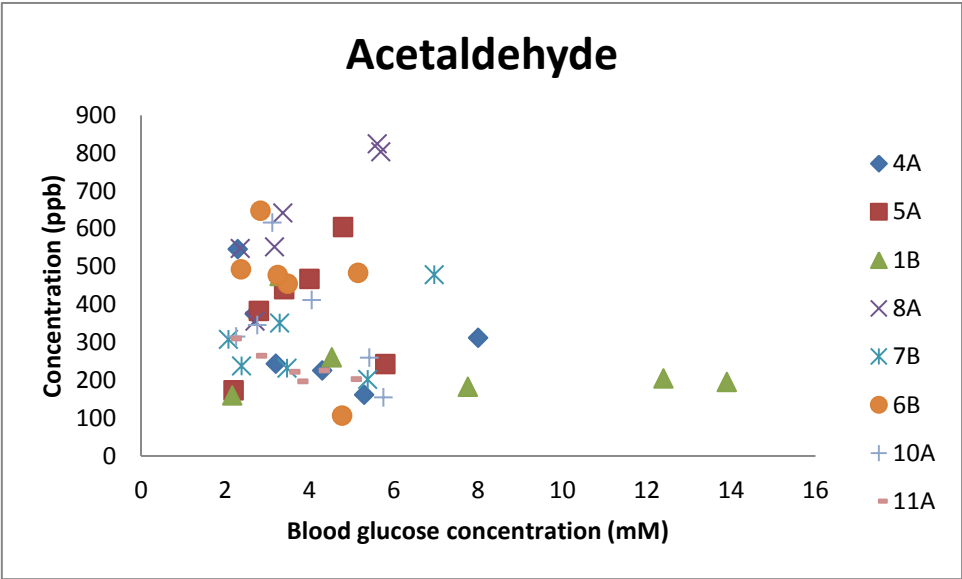


Figure 3.7 Exhaled breath acetaldehyde concentration against measured blood glucose concentration for all eight volunteers during the hypoglycaemic clamp

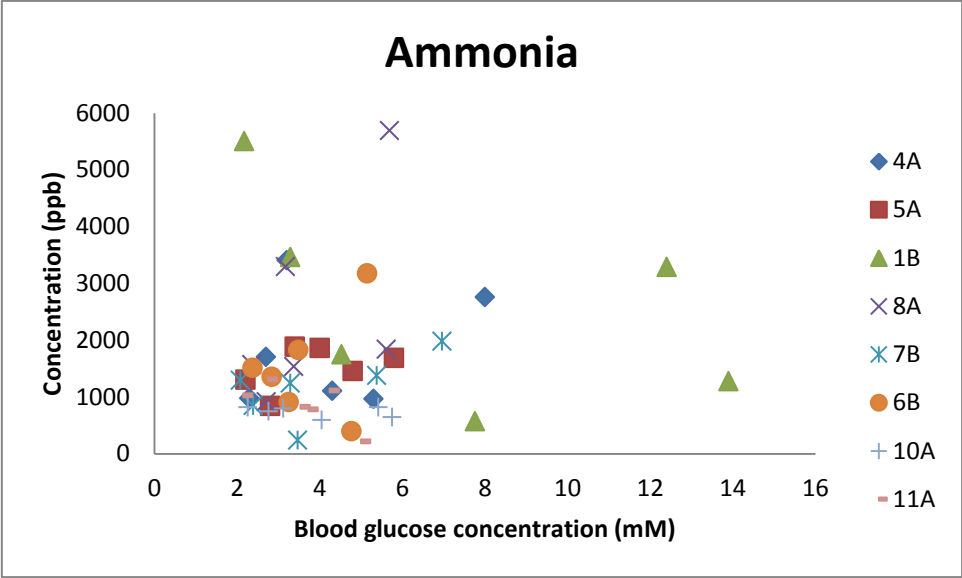


Figure 3.8 Exhaled breath ammonia concentration against measured blood glucose concentration for all eight volunteers during the hypoglycaemic clamp

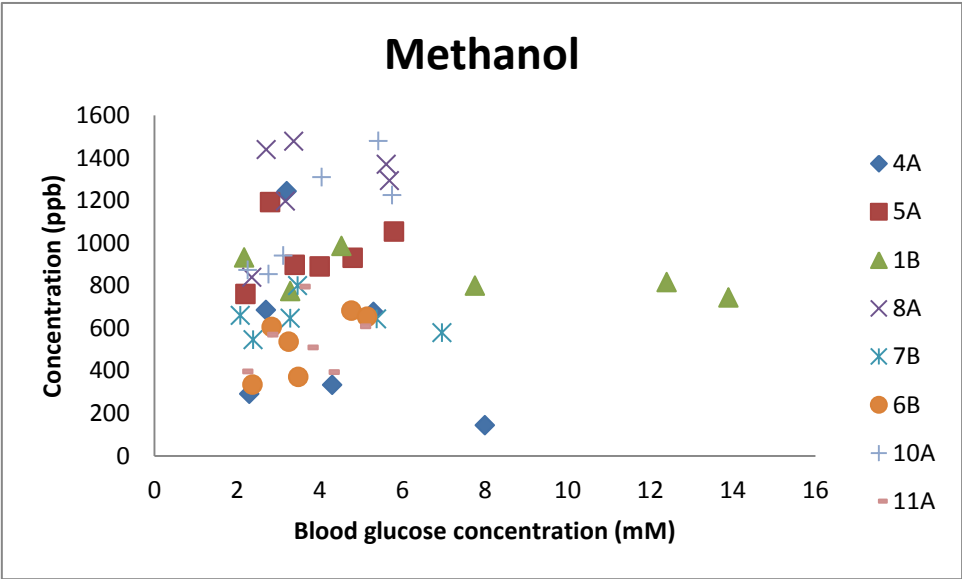


Figure 3.9 Exhaled breath methanol concentration against measured blood glucose concentration for all eight volunteers during the hypoglycaemic clamp

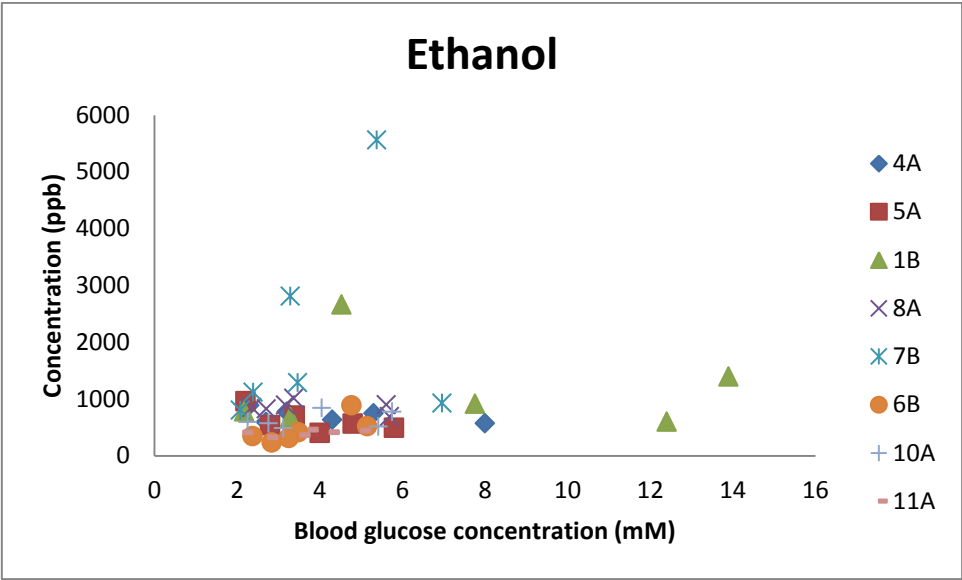


Figure 3.10 Exhaled breath ethanol concentration against measured blood glucose concentration for all eight volunteers during the hypoglycaemic clamp

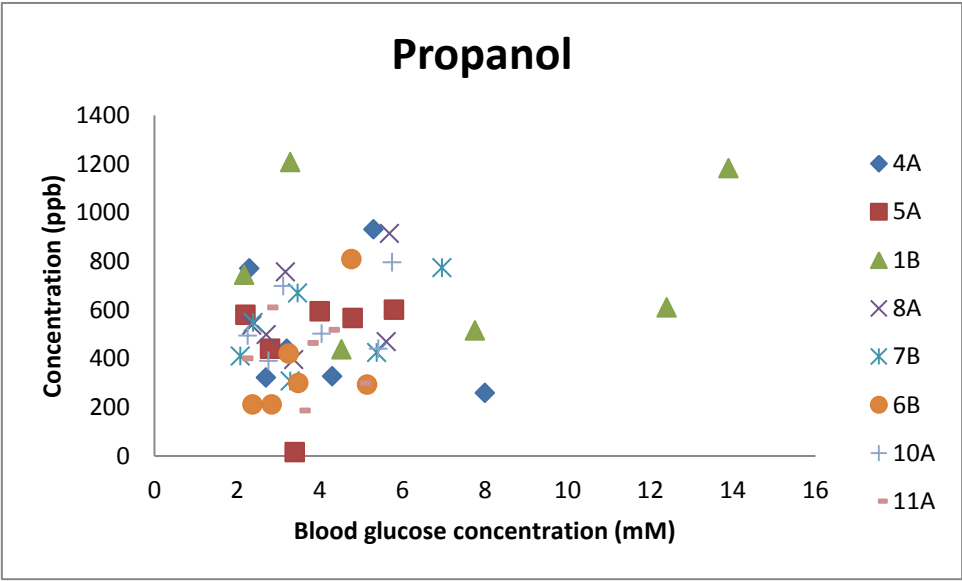


Figure 3.11 Exhaled breath propanol concentration against measured blood glucose concentration for all eight volunteers during the hypoglycaemic clamp

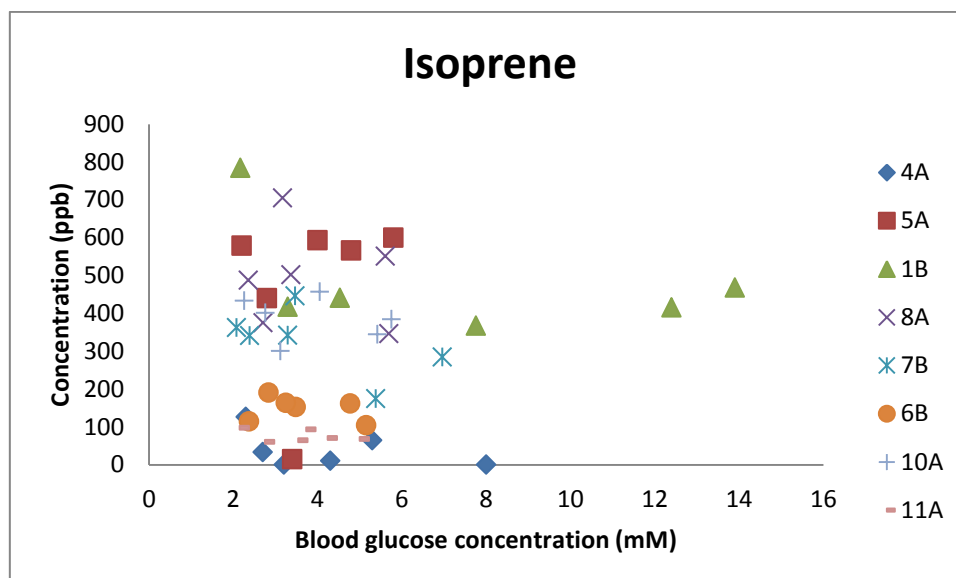


Figure 3.12 Exhaled breath isoprene concentration against measured blood glucose concentration for all eight volunteers during the hypoglycaemic clamp

Volunteer	Linear Correlation Coefficient (R)							
	Acetone H_3O^+	Acetone NO^+	Acetaldehyde	Ammonia	Methanol	Ethanol	Propanol	Isoprene
4A	0.08	0.08	-0.45	0.25	-0.44	-0.55	-0.22	-0.46
5A	0.87 *	0.95 *	0.25	0.45	0.26	-0.64	0.28	0.06
1B	0.91 *	0.94 *	-0.38	-0.50	-0.59	-0.09	0.13	-0.45
8A	0.93 *	0.88 *	0.86	0.61	0.36	-0.38	0.38	-0.18
7B	0.71	0.77	0.50	0.62	-0.18	0.30	0.52	-0.59
6B	0.98 *	0.93	-0.57	0.33	0.71	0.75	0.27	-0.27
10A	0.95 *	0.97 *	-0.57	-0.37	0.86 *	0.35	0.38	-0.20
11A	0.58	0.76	-0.86 *	-0.71	0.22	0.49	-0.29	-0.36

Table 3.3 Linear correlation coefficients for exhaled breath VOCs vs. Measured blood glucose concentration

All of the volunteers show a decrease in exhaled breath acetone quantified using the H_3O^+ precursor ion as the hypoglycaemic clamp progressed, apart from volunteer 4A that showed an increase in exhaled acetone concentration after the first infusion. The highest concentrations of acetone are seen in volunteer 10A, and the lowest in 11A. The strongest correlation is seen in volunteer 6B ($R=0.98$), with the weakest in volunteer 4A ($R=0.07$).

As seen using the H_3O^+ precursor ion, a decrease in exhaled acetone concentration is seen as blood glucose decreases during the hypoglycaemic clamp, except in volunteer 4A, where there

is an increase in concentration after the initial infusion of insulin, though this decreases with further infusions. Higher exhaled breath acetone concentrations are seen with the NO^+ precursor ion compared to the H_3O^+ . The linear correlation coefficients are greater for all of the volunteers, the greatest being 10A ($R=0.97$), except 4A ($R=0.08$).

Exhaled breath acetaldehyde concentration decreases with blood glucose concentration in most of the volunteers though there is weak correlation between the two except for volunteer 11A who shows an significant increase in exhaled acetaldehyde concentration with decreasing blood glucose ($R=-0.84$). The highest concentration of exhaled breath acetaldehyde can be seen in volunteer 8A and the lowest in volunteer 1B. No distinct relationship can be established between exhaled breath ammonia and blood glucose concentration. The highest concentration of exhaled ammonia can be seen in volunteer 8A whilst the lowest can be found in 7B.

Some of the volunteers displayed a decrease in exhaled methanol concentration with decreasing blood glucose concentration. The strongest correlation between exhaled methanol and blood glucose is seen in volunteer 10A ($R=0.86$). The highest concentrations of methanol are seen in volunteers 8A and 10A, whilst the lowest is seen in volunteer 4A.

3.3.3.2 Skin

Skin headspace VOC concentrations were plotted against measured blood glucose concentration for acetone H_3O^+ , Figure 3.13, acetone NO^+ , Figure 3.14, acetaldehyde, Figure 3.15, ammonia, Figure 3.16, methanol, Figure 3.17, ethanol, Figure 3.18, propanol, Figure 3.19, and isoprene, Figure 3.20. No formaldehyde was detected in the skin headspace samples as with the breath samples. The linear correlation coefficient was calculated for each volunteer individually and is presented in Table 3.4, and any significant relationships between VOC concentration and blood glucose were identified with an asterisk as before.

Only volunteer 4A shows significant correlation between skin headspace acetone (NO^+) and blood glucose concentration, whilst 11A shows significant correlation with skin headspace ethanol and blood glucose concentration. There is little correlation between skin headspace acetone concentrations using the H_3O^+ precursor ion, and is positive in all apart from volunteer 5A. There is weak correlation between the other quantified VOCs and blood glucose concentration.

Figure 3.28 Skin headspace acetone concentration quantified using the H_3O^+ precursor ion against measured blood glucose concentration for all eight volunteers during the hypoglycaemic clamp

Volunteer 5A shows negative correlation between skin headspace acetone and blood glucose concentration. All of the other volunteers show a positive correlation, though this is significant in none.

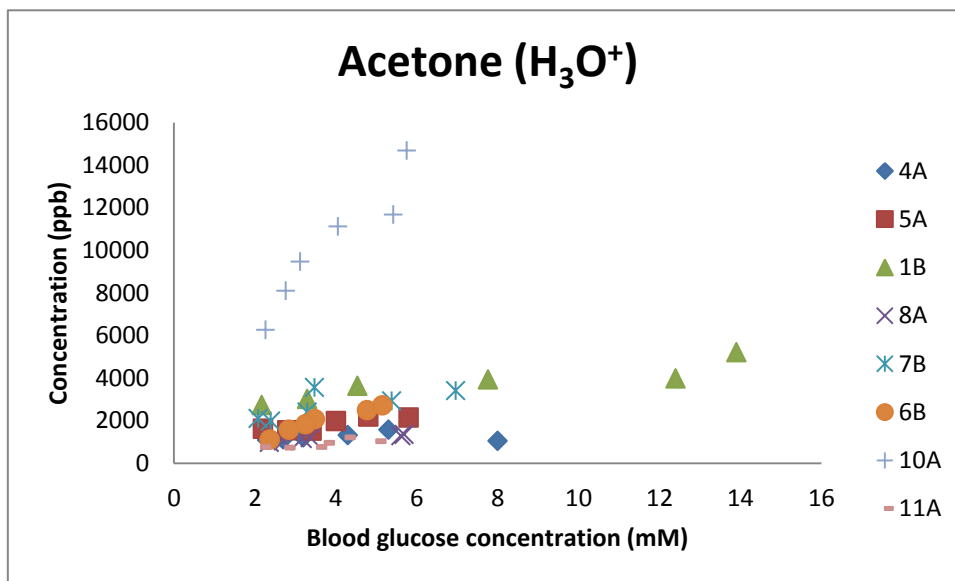


Figure 3.13 Skin headspace acetone concentration quantified using the H_3O^+ precursor ion against measured blood glucose concentration for all eight volunteers during the hypoglycaemic clamp

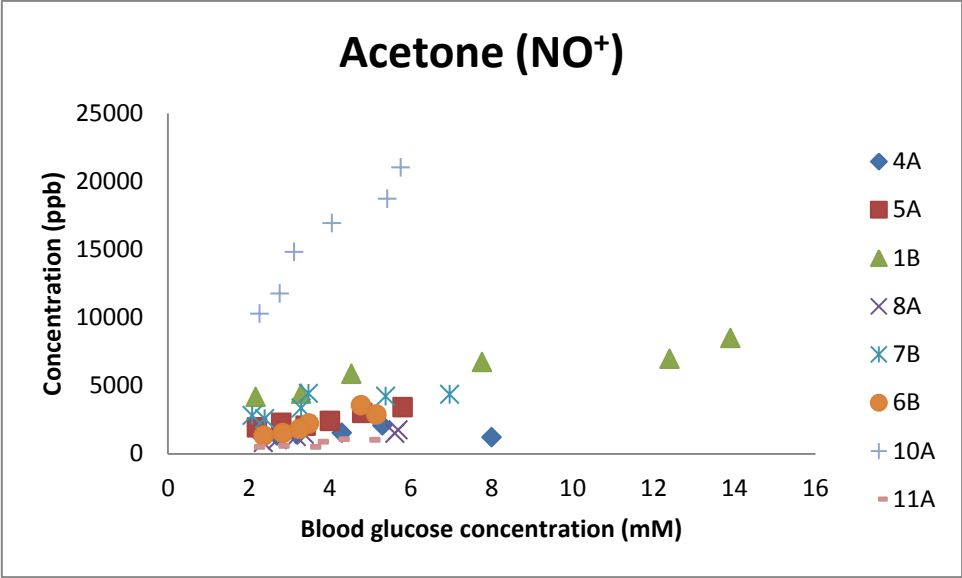


Figure 3.14 Skin headspace acetone concentration quantified using the NO⁺ precursor ion against measured blood glucose concentration for all eight volunteers during the hypoglycaemic clamp

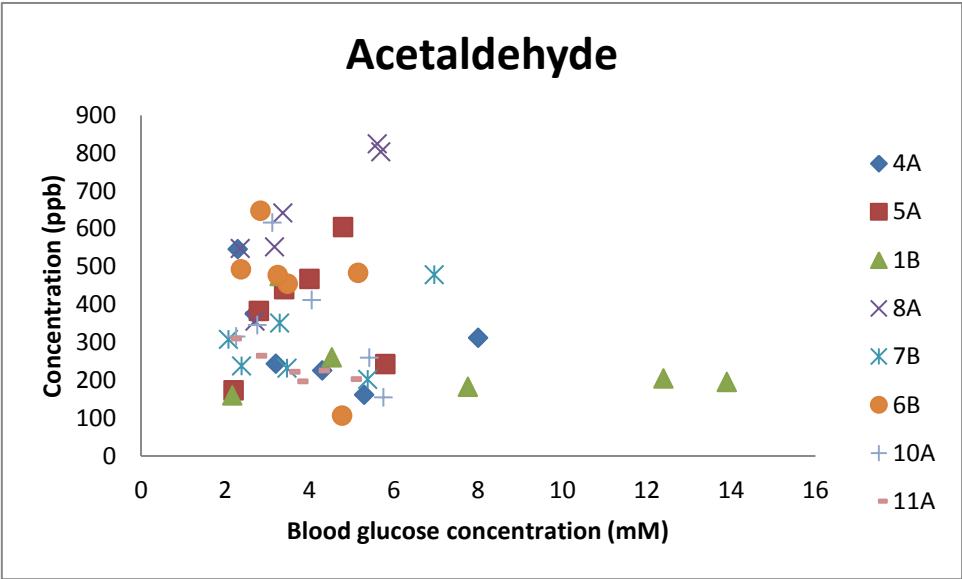


Figure 3.15 Skin headspace acetaldehyde concentration quantified against measured blood glucose concentration for all eight volunteers during the hypoglycaemic clamp

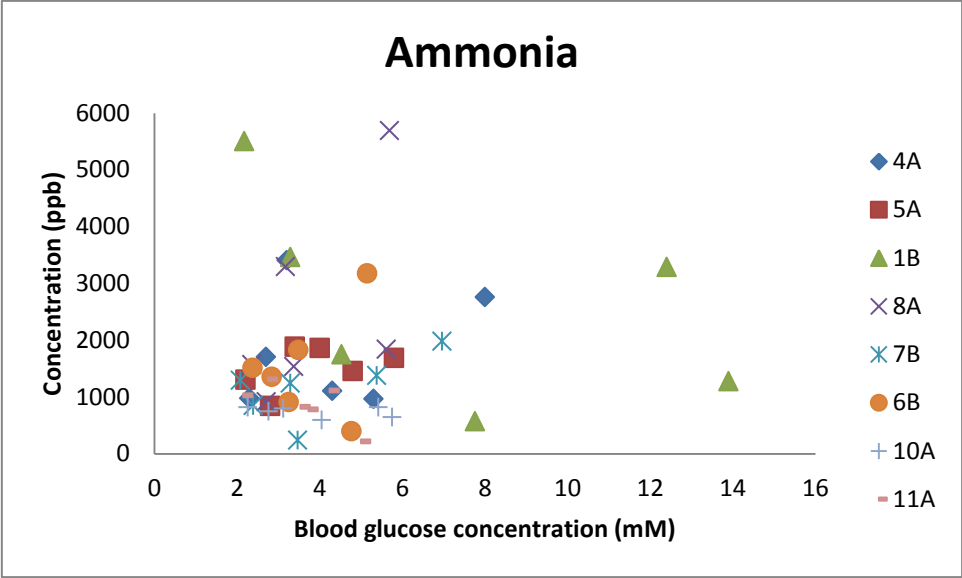


Figure 3.16 Skin headspace ammonia concentration quantified against measured blood glucose concentration for all eight volunteers during the hypoglycaemic clamp

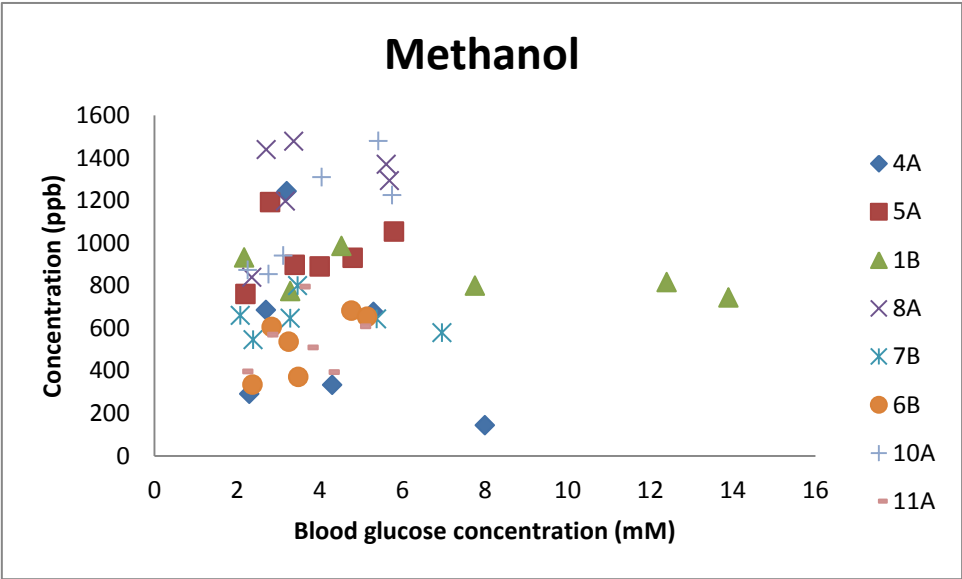


Figure 3.17 Skin headspace methanol concentration quantified against measured blood glucose concentration for all eight volunteers during the hypoglycaemic clamp

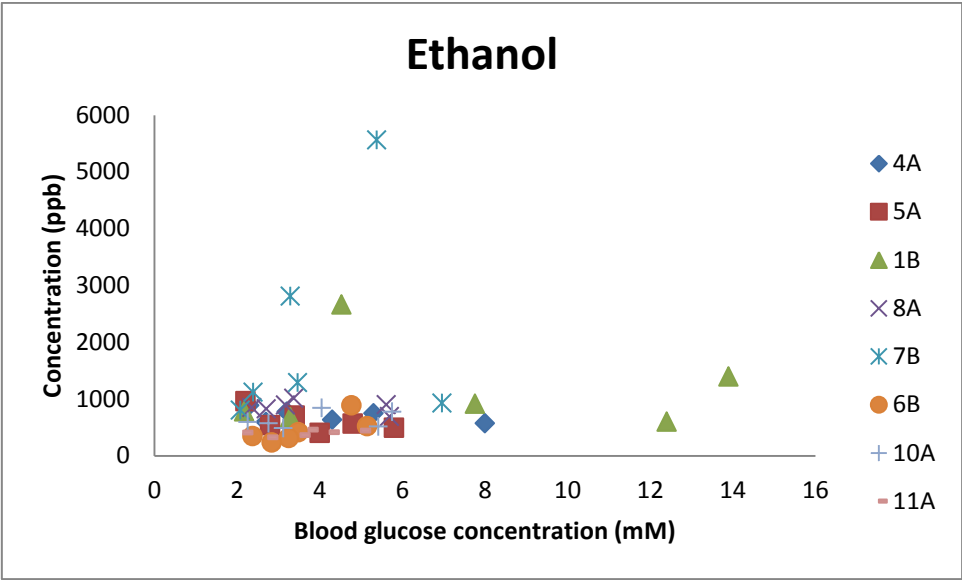


Figure 3.18 Skin headspace ethanol concentration quantified against measured blood glucose concentration for all eight volunteers during the hypoglycaemic clamp

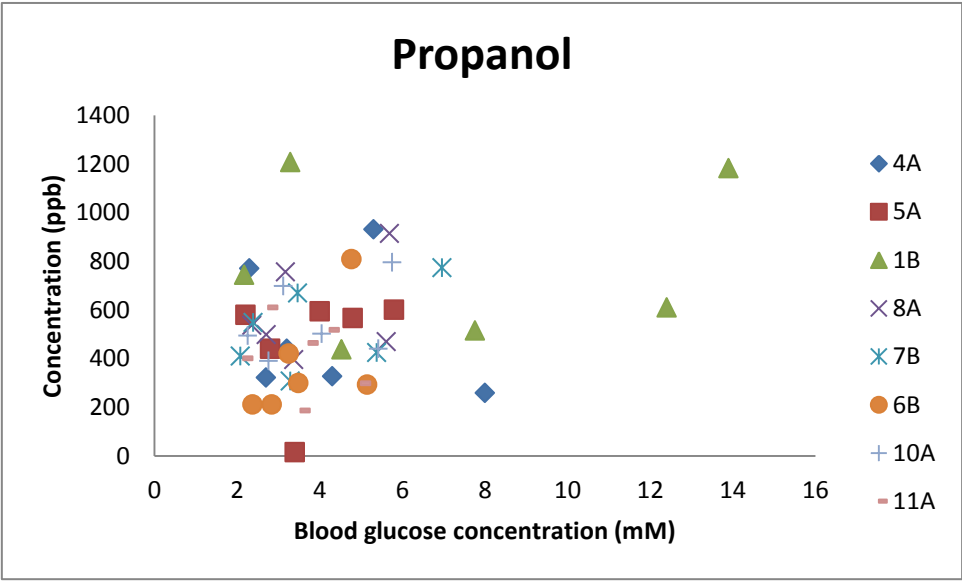


Figure 3.19 Skin headspace propanol concentration quantified against measured blood glucose concentration for all eight volunteers during the hypoglycaemic clamp

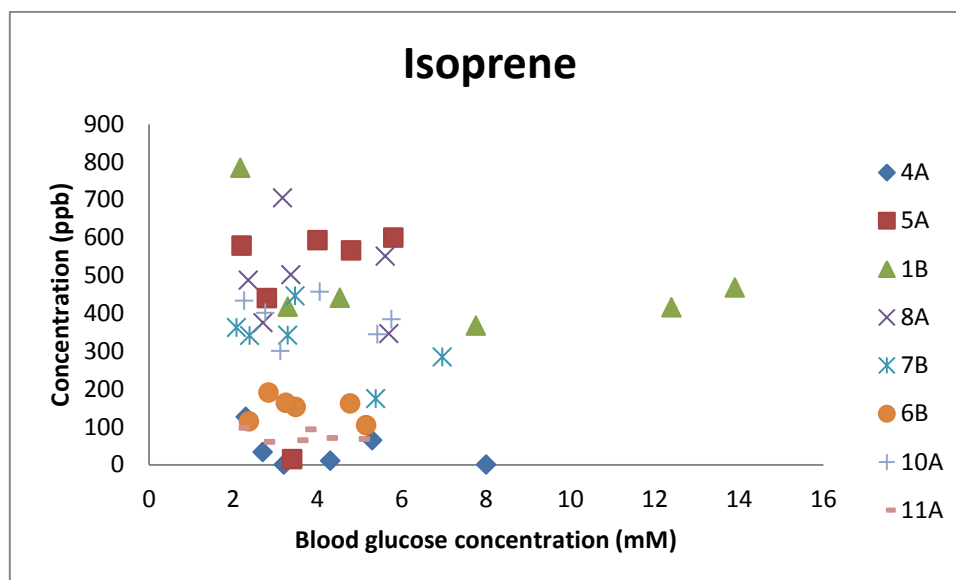


Figure 3.20 Skin headspace isoprene concentration quantified against measured blood glucose concentration for all eight volunteers during the hypoglycaemic clamp

Volunteer	Linear Correlation Coefficient (R)							
	Acetone H_3O^+	Acetone NO^+	Acetaldehyde	Ammonia	Methanol	Ethanol	Propanol	Isoprene
4A	0.51	0.87 *	-0.05	0.77	0.64	-0.06	0.18	0.33
5A	-0.69	-0.45	0.55	-0.17	-0.16	0.42	0.61	-0.73
1B	0.50	0.67	0.69	-0.24	0.89 *	0.06	0.36	-0.69
8A	0.77	0.52	0.12	0.06	0.00	-0.39	-0.12	0.28
7B	0.75	-0.57	0.22	0.45	0.78	-0.20	0.05	0.76
6B	0.34	-0.29	-0.23	0.22	-0.72	0.72	-0.34	0.51
10A	0.55	0.46	0.08	0.74	0.46	0.17	0.51	0.43
11A	0.18	0.65	0.08	-0.31	0.80	0.84*	0.75	-0.51

Table 3.4 Linear correlation coefficients for skin headspace VOCs vs. Measured blood glucose concentration

3.3.3.3 Blood

The change in blood VOC concentration were plotted against the measured blood glucose concentration for acetone H_3O^+ , Figure 3.21, acetone NO^+ , Figure 3.22, formaldehyde, Figure 3.23, acetaldehyde, Figure 3.24, ammonia, Figure 3.25, methanol, Figure 3.26, ethanol, Figure 3.27, propanol, Figure 3.28, and isoprene, Figure 3.29. Due to a blocked capillary in the SIFT-

MS sampling head, blood samples from volunteers 1B and 11A could not be analysed. The linear correlation coefficient was calculated for each volunteer individually, Table 3.5. Again, significant correlations between VOCs found in blood headspace and blood glucose concentration are identified in the table by an asterisk.

Though all volunteers show positive correlation between blood headspace acetone concentration, this is only significant in volunteers 4A, using both precursor ions (H_3O^+ $R=0.93$) (NO^+ $R=0.91$), and 11A, using the NO^+ precursor ion only ($R=0.96$).

Unlike the breath and skin headspace samples formaldehyde was detectable in blood headspace samples, with volunteer 7B showing a significant positive correlation with blood glucose concentration. The other volunteers show no correlation whilst volunteers 4A and 10A show a negative correlation.

There is weak correlation between blood headspace acetaldehyde and blood glucose concentration, this positive in volunteers 4A, 5A and 7B, and negative in volunteers 8A, 6B and 10A.

All of the volunteers show negative correlation between blood headspace ammonia and blood glucose concentration, apart from volunteer 6B. There is only significant correlation in one volunteer, 4A ($R=-0.90$).

There is little correlation between blood headspace methanol and blood glucose concentration. Volunteer 4A shows good positive correlation ($R=1.00$), but this is not significant due to the lack of data points, similarly volunteer 8A ($R=-0.79$) shows good negative correlation but it also insignificant due to the lack of data.

There is also little correlation between blood headspace ethanol and blood glucose concentration. Volunteer 4A shows good positive correlation and volunteer 8A ($R=-0.88$) shows good negative correlation but is insignificant due to the lack of data for these two volunteers.

Volunteers 4A ($R=1.00$), 5A ($R=0.92$) and 7B ($R=0.99$) show good significant correlation between blood headspace propanol and blood glucose concentration. The relationship is insignificant in volunteer 4A however due to a lack of data.

There is no clear relationship between blood headspace isoprene and blood glucose concentration, with volunteers 4A, 8A and 6B showing weak positive correlations and volunteers 5A, 7B and 10A displaying weak negative correlations.

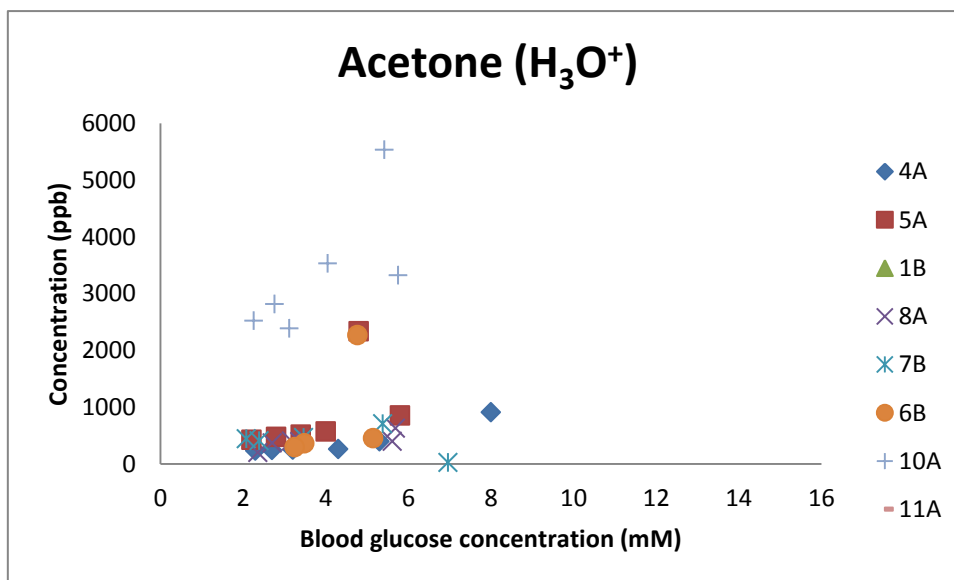


Figure 3.21 Blood headspace acetone concentration quantified using the H_3O^+ precursor ion against measured blood glucose concentration for all eight volunteers during the hypoglycaemic clamp

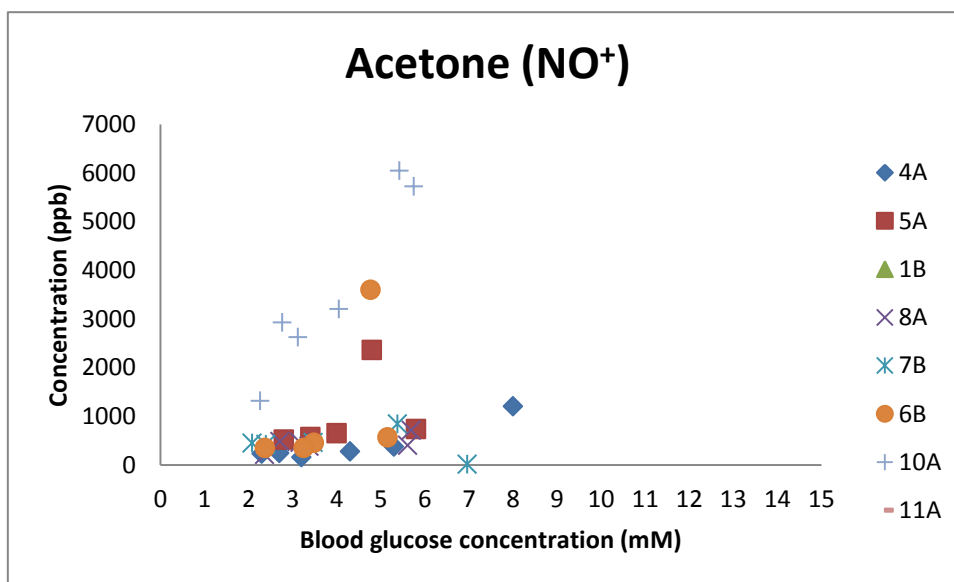


Figure 3.22 Blood headspace acetone concentration quantified using the NO^+ precursor ion against measured blood glucose concentration for all eight volunteers during the hypoglycaemic clamp

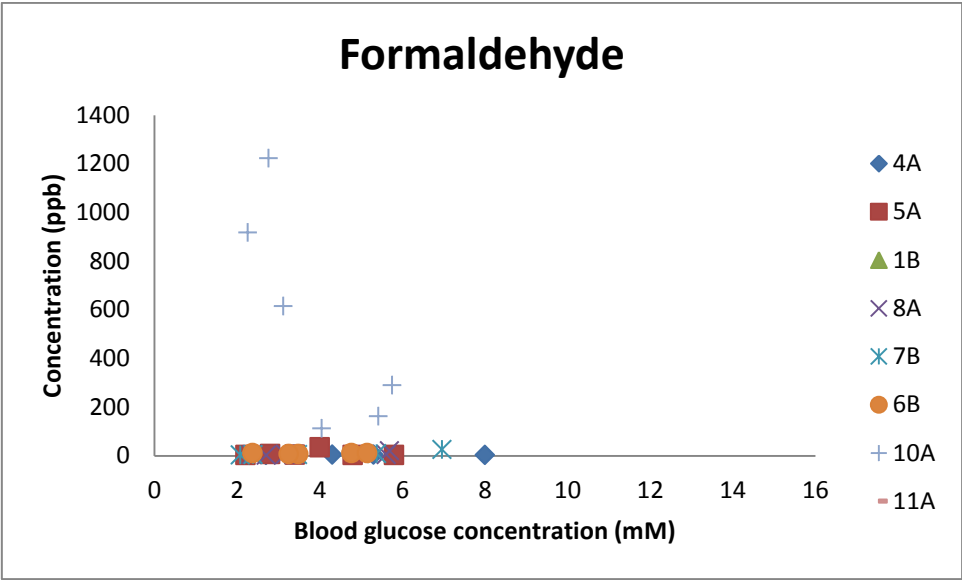


Figure 3.23 Blood headspace formaldehyde concentration against measured blood glucose concentration for all eight volunteers during the hypoglycaemic clamp

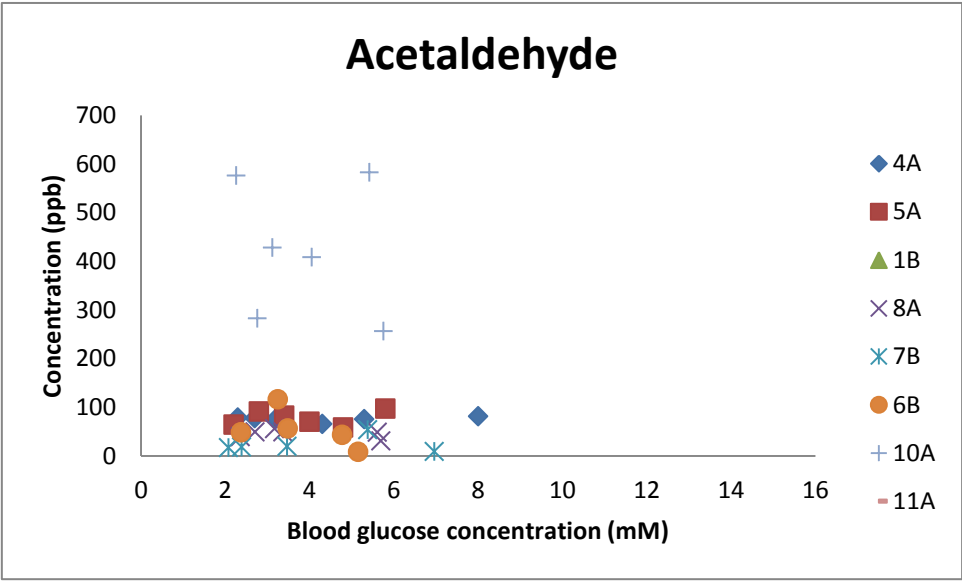


Figure 3.24 Blood headspace acetaldehyde concentration against measured blood glucose concentration for all eight volunteers during the hypoglycaemic clamp

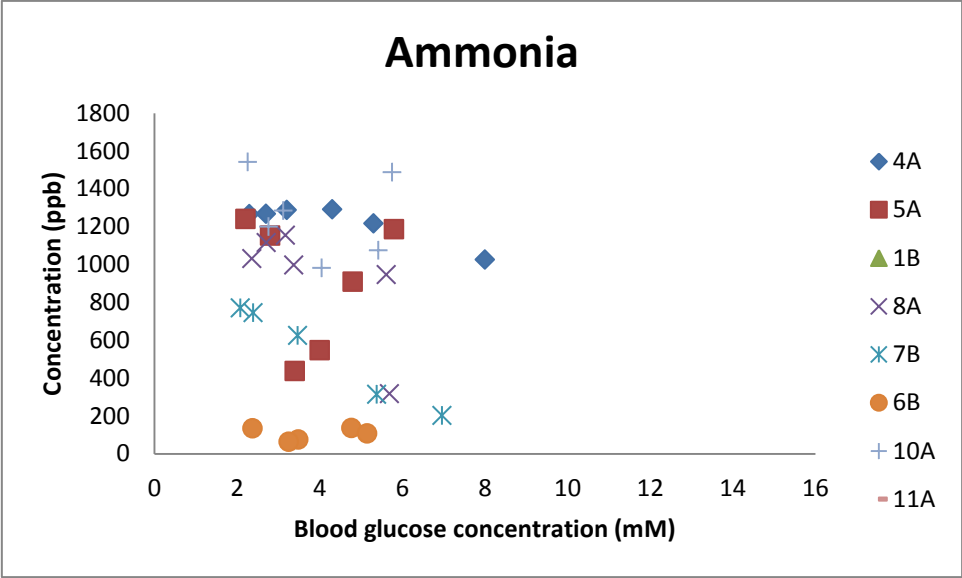


Figure 3.25 Blood headspace ammonia concentration against measured blood glucose concentration for all eight volunteers during the hypoglycaemic clamp

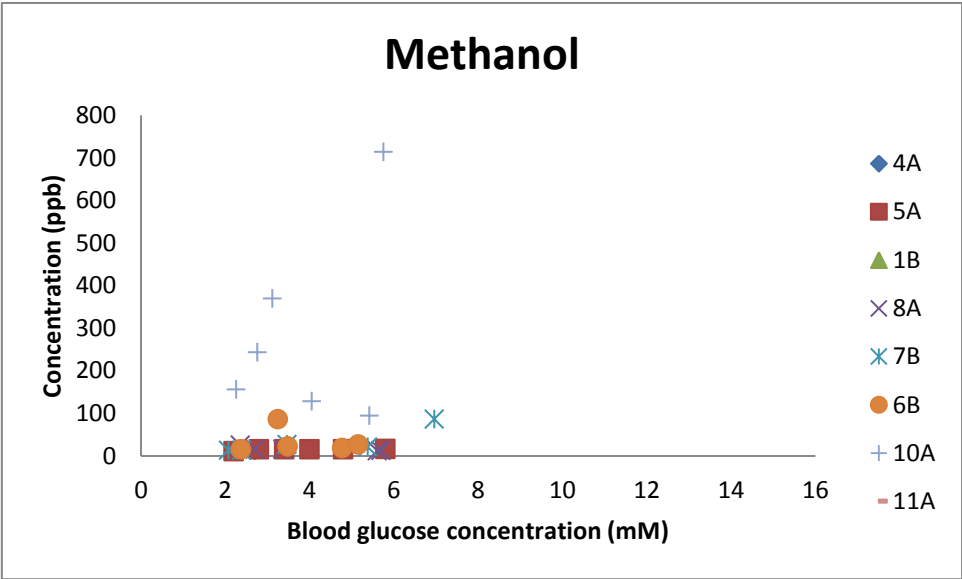


Figure 3.26 Blood headspace methanol concentration against measured blood glucose concentration for all eight volunteers during the hypoglycaemic clamp

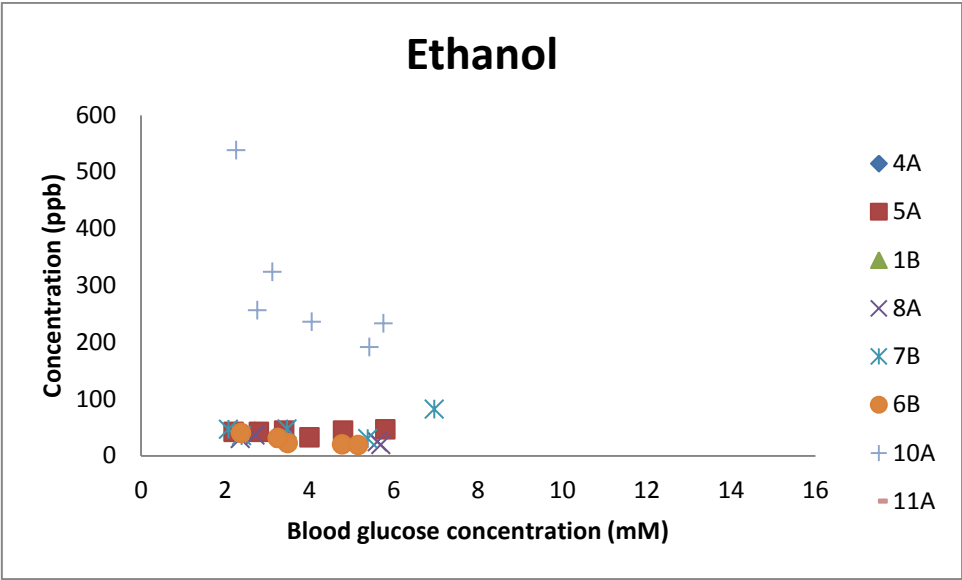


Figure 3.27 Blood headspace ethanol concentration against measured blood glucose concentration for all eight volunteers during the hypoglycaemic clamp

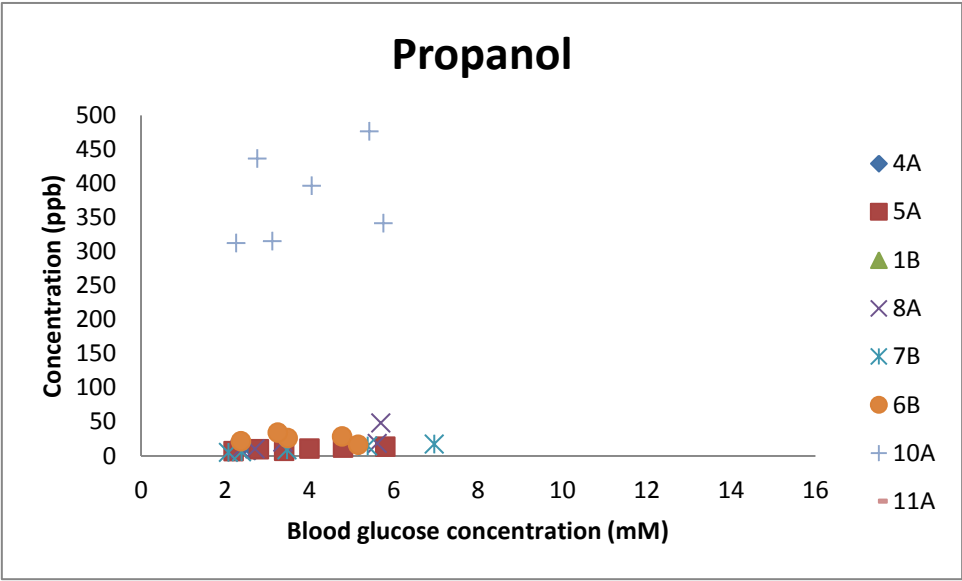


Figure 3.28 Blood headspace propanol concentration against measured blood glucose concentration for all eight volunteers during the hypoglycaemic clamp

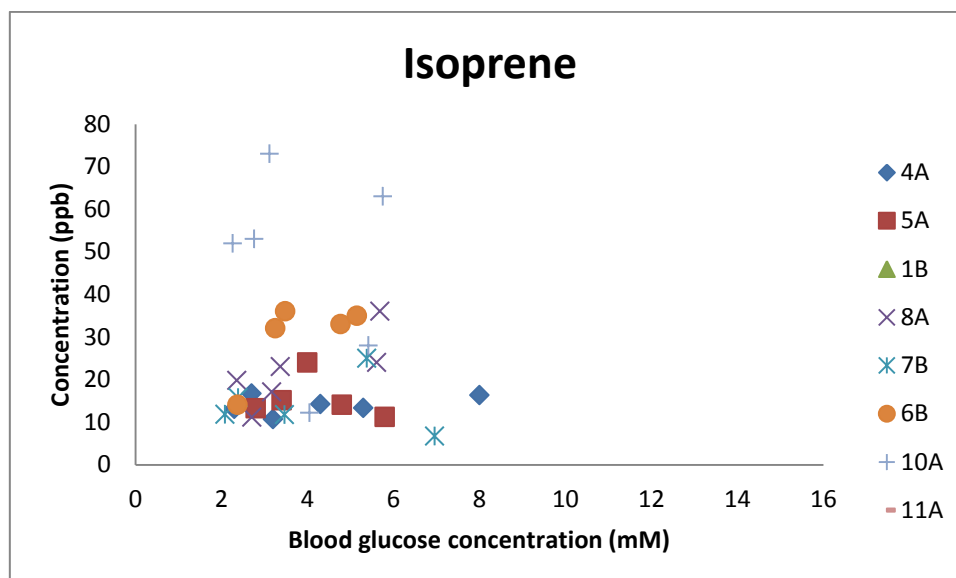


Figure 3.29 Blood headspace isoprene concentration against measured blood glucose concentration for all eight volunteers during the hypoglycaemic clamp

Volunteer	Linear Correlation Coefficient (R)							
	Acetone (H ₃ O ⁺)	Acetone (NO ⁺)	Acetaldehyde	Ammonia	Methanol	Ethanol	Propanol	Isoprene
4A	0.93 *	0.91 *	-0.42	0.21	-0.90 *	1.00	1.00	1.00
5A	0.54	0.40	0.02	0.24	-0.04	0.64	0.22	0.92 *
8A	0.75	0.61	0.63	-0.40	-0.73	-0.79	-0.88	-0.74
7B	-0.40	-0.29	0.90 *	0.16	-0.99	0.83	0.60	0.99 *
6B	0.52	0.52	0.28	-0.55	0.15	-0.17	0.90*	-0.28
10A	0.72	0.96 *	-0.79	-0.16	-0.20	0.40	-0.73	0.36

Table 3.5 Linear correlation coefficients for blood headspace VOCs vs. Measured blood glucose concentration

3.3.4 GC-MS

3.3.4.1 Breath

The mass spectra were analysed, converted and aligned according to the method mentioned in 2.3.6. GC-MS data for volunteer 5A was not available due to a technical fault with the instrument.

Metabolites that were visually identified were then quantified using the method previously mentioned in 2.3.6 were plotted against measured blood glucose concentration. The exhaled breath concentrations of acetone, Figure 3.30, acetaldehyde, Figure 3.31, acetic acid, Figure

3.32, 2-butanone, Figure 3.33, methanol, Figure 3.34, methylglyoxal, Figure 3.35, phenol, Figure 3.36, propanol, Figure 3.37, and isoprene, Figure 3.38, were plotted against measured blood glucose concentration. There was no 2-butanone detected in any of the samples collected from volunteer 11A, whilst methylglyoxal was not detected in volunteers 7B and 11 and isoprene was not detected in volunteers 4A and 11A. The linear correlation coefficients for each of these VOCs were also calculated, Table 3.6.

Acetone was the most abundant metabolite quantified in the samples. High concentrations of acetone were seen in volunteers 10A and 11A, whilst all volunteers displayed a positive correlation between exhaled breath acetone and blood glucose concentration, though this was only significant in volunteers 5A, 8A and 6B.

Volunteer 7B exhibited higher concentrations of acetaldehyde in the 5.38 and 6.96 mM samples than the other volunteers. Only volunteer 5A shows a significant positive correlation between exhaled breath acetaldehyde and blood glucose concentration. Volunteers 1B, 8A, 6B and 10A show negative correlation, whilst this is only significant in volunteer 10A.

Volunteers 7B and 6B show positive correlation between exhaled breath acetic acid and blood glucose concentration. The rest of the volunteers show negative correlation. The relationship is not significant in any of the volunteers.

Only one volunteer, 8A, shows a significant positive correlation between exhaled breath 2-butanone and blood glucose concentration. The correlation seen in volunteer 7B is insignificant due to a lack of data points.

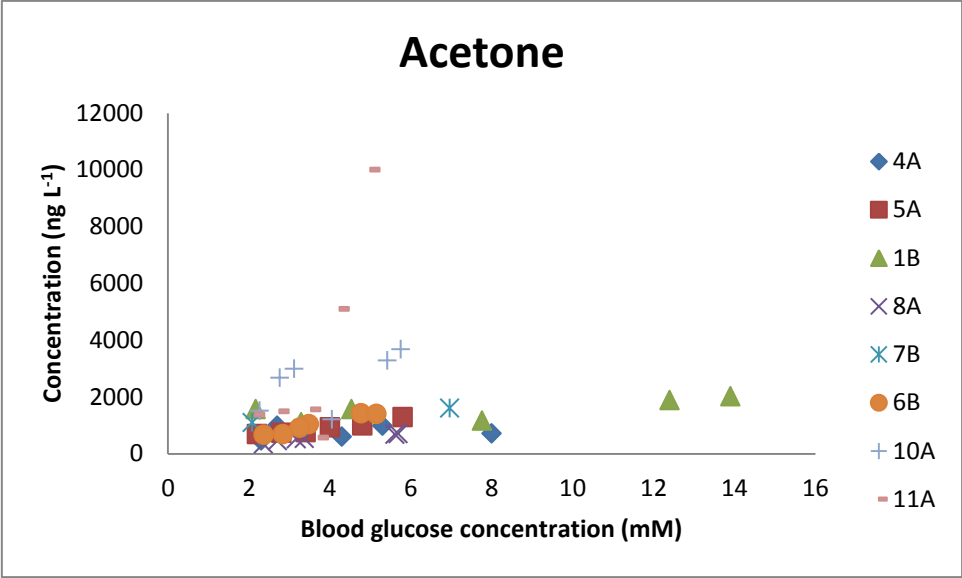


Figure 3.30 GC-MS breath acetone concentration against measured blood glucose concentration for all eight volunteers during the hypoglycaemic clamp

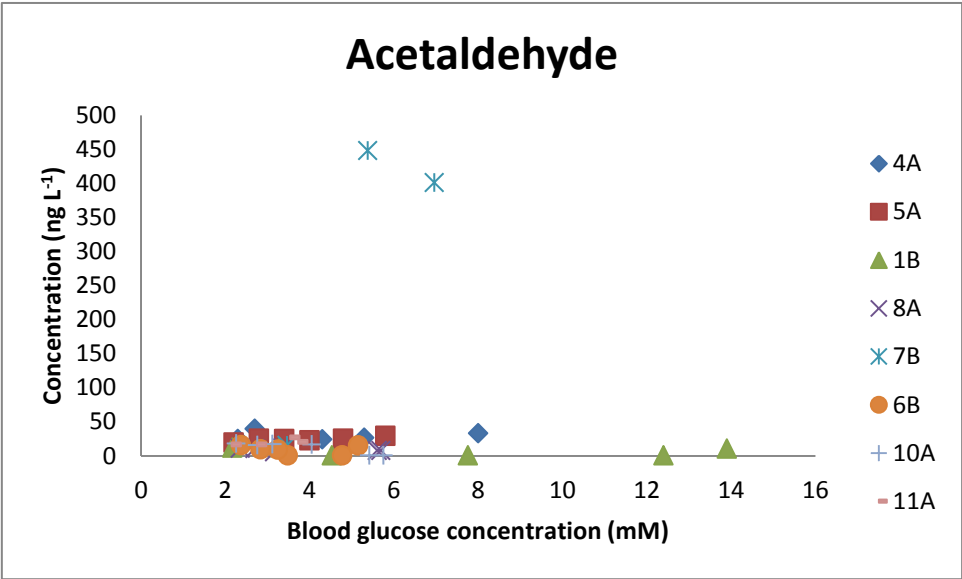


Figure 3.31 GC-MS breath acetaldehyde concentration against measured blood glucose concentration for all eight volunteers during the hypoglycaemic clamp

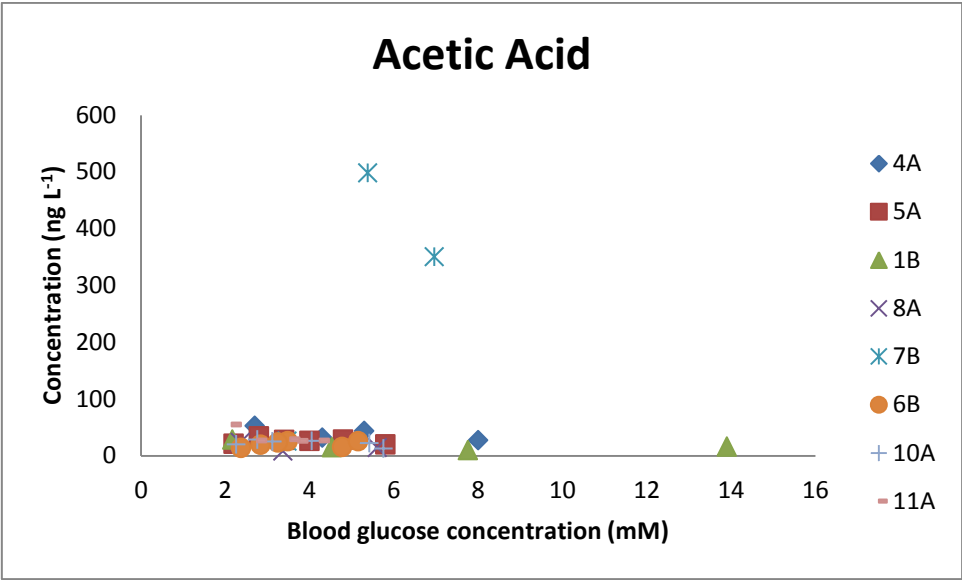


Figure 3.32 GC-MS breath acetic acid concentration against measured blood glucose concentration for all eight volunteers during the hypoglycaemic clamp

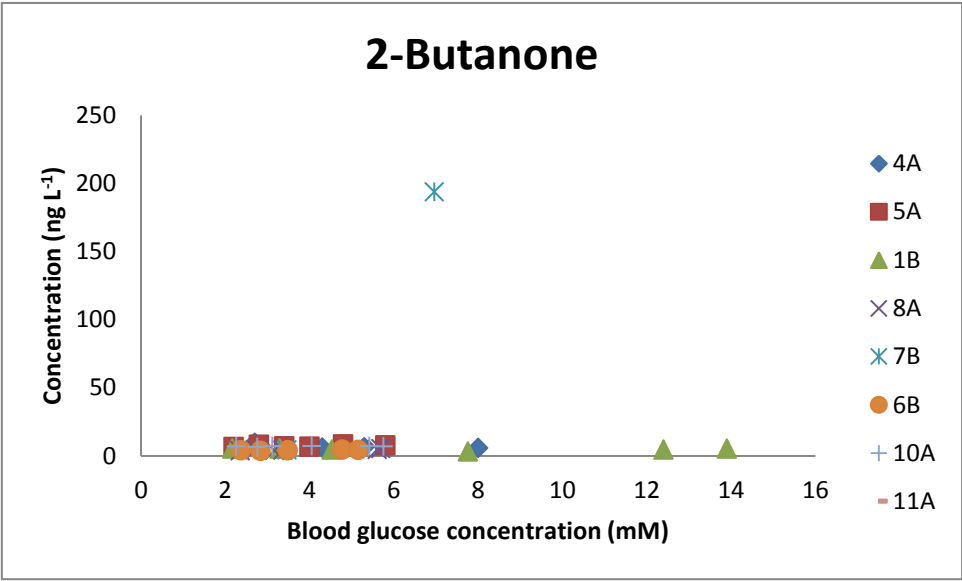


Figure 3.33 GC-MS breath 2-butanone concentration against measured blood glucose concentration for all eight volunteers during the hypoglycaemic clamp

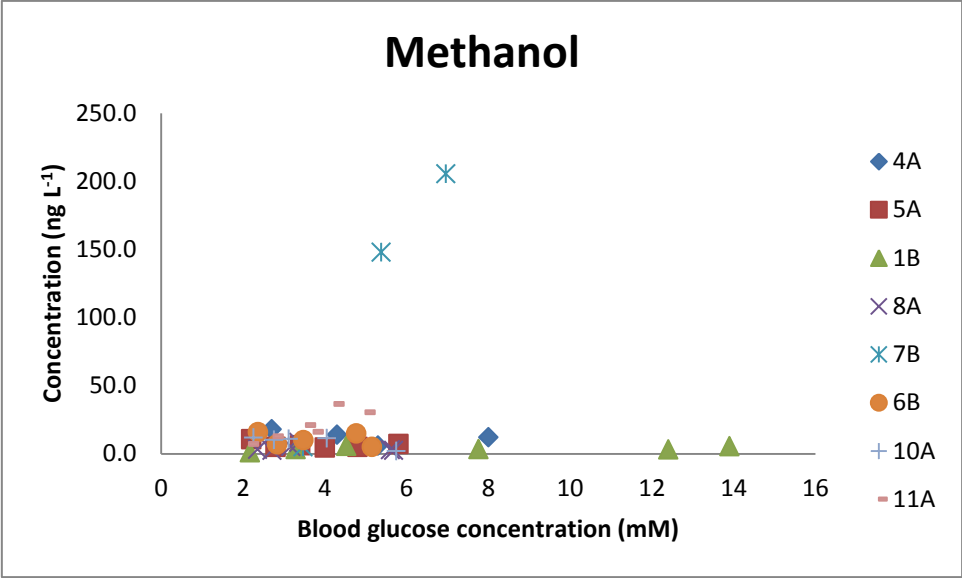


Figure 3.34 GC-MS breath methanol concentration against measured blood glucose concentration for all eight volunteers during the hypoglycaemic clamp

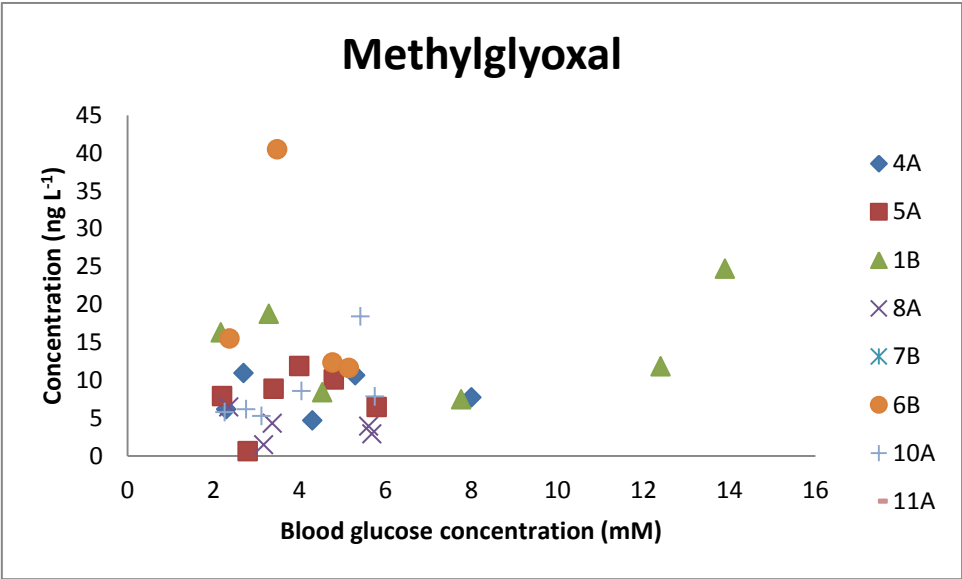


Figure 3.35 GC-MS breath methylglyoxal concentration against measured blood glucose concentration for all eight volunteers during the hypoglycaemic clamp

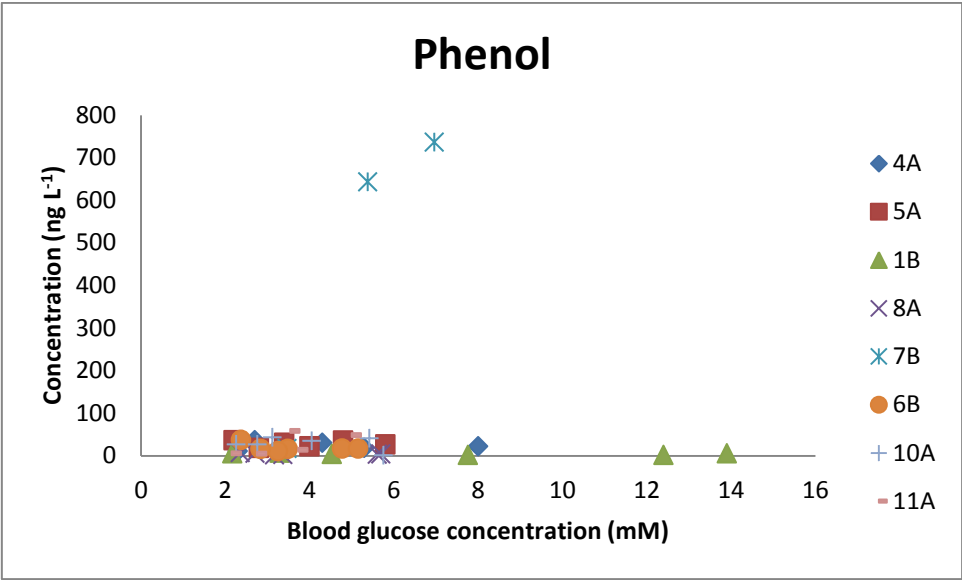


Figure 3.36 GC-MS breath phenol concentration against measured blood glucose concentration for all eight volunteers during the hypoglycaemic clamp

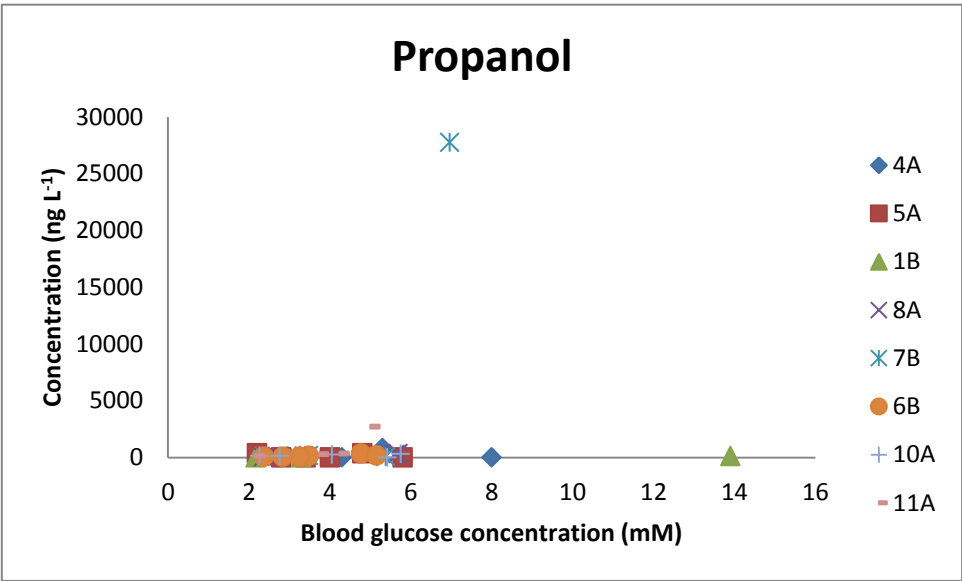


Figure 3.37 GC-MS breath propanol concentration against measured blood glucose concentration for all eight volunteers during the hypoglycaemic clamp

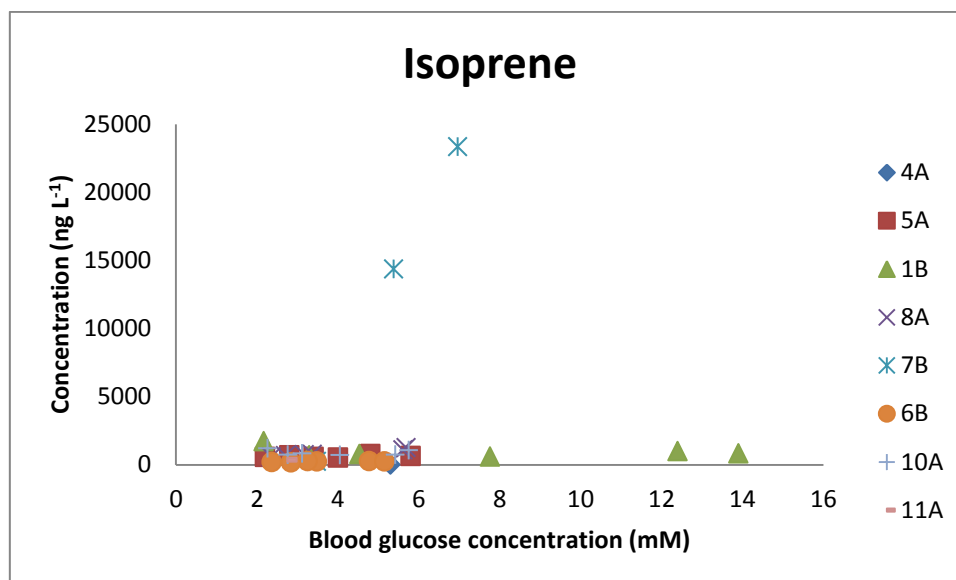


Figure 3.38 GC-MS breath isoprene concentration against measured blood glucose concentration for all eight volunteers during the hypoglycaemic clamp

Volunteer	Linear Correlation Coefficient (R)								
	Acetone	Acetaldehyde	Acetic acid	2-Butanone	Methanol	Methylglyoxal	Phenol	Propanol	Isoprene
4A	0.13	0.05	-0.12	-0.24	-0.50	0.03	-0.07	0.20	ND
5A	0.96 *	0.81 *	-0.33	0.43	-0.35	0.27	-0.03	-0.19	0.36
1B	0.69	-0.28	-0.51	-0.11	0.44	0.25	-0.35	1.00	-0.32
8A	0.96 *	-0.51	-0.42	0.85 *	-0.26	-0.35	-0.31	0.97 *	0.98 *
7B	0.28	0.84	0.71	1.00	0.98	ND	0.94	0.83	0.99 *
6B	0.98 *	-0.22	0.34	0.75	-0.31	-0.36	-0.46	0.81	0.98 *
10A	0.59	-0.92 *	-0.56	0.46	0.87 *	0.66	-0.33	0.15	-0.17
11A	0.79	0.72	-0.77	ND	0.88 *	ND	0.69	0.72	ND

Table 3.6 Linear correlation coefficients GC-MS breath VOCs vs. Measured blood glucose concentration

3.3.4.2 Blood

Blood headspace concentrations of acetone, Figure 3.39, acetaldehyde, Figure 3.40, acetic acid, Figure 3.41, 2-butanone, Figure 3.42, methanol, Figure 3.43, methanol, Figure 3.44 and methylglyoxal, Figure 3.45, were plotted against measured blood glucose concentration.

Acetone was the most abundant metabolite quantified in the samples and was greatest in volunteer 5A at 2.8 mM. This may be anomalous, as the concentration of acetone at the lowest blood glucose concentration measured for this volunteer is lower than at the 2.8 mM reading. Only one volunteer, 4A, displayed a significant correlation between blood headspace acetone concentration and blood glucose, though there are generally lower acetone concentrations at lower blood glucose concentration.

Acetaldehyde was the second most abundant VOC quantified in the samples. Again, the greatest concentration is seen in the 2.8 mM sample from volunteer 5A, again suggesting that there was some error in the way that this sample was taken or analysed.

Acetic acid concentration is elevated at low blood glucose concentration for many of the volunteers. The low concentrations would however suggest that the instrument is at the limit of detection, and that this increase at the low concentrations is due to noise.

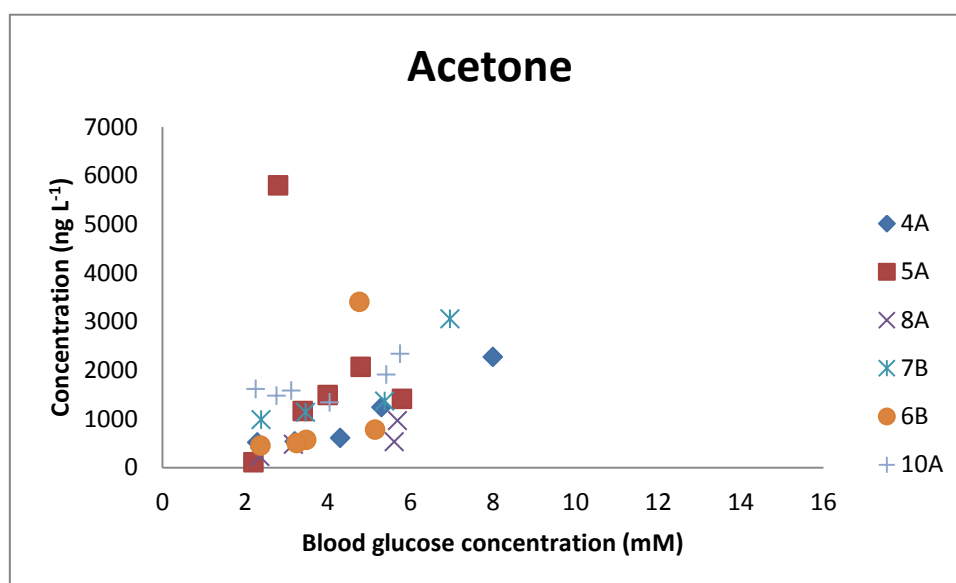


Figure 3.39 GC-MS blood headspace acetone concentration against measured blood glucose concentration for all eight volunteers during the hypoglycaemic clamp

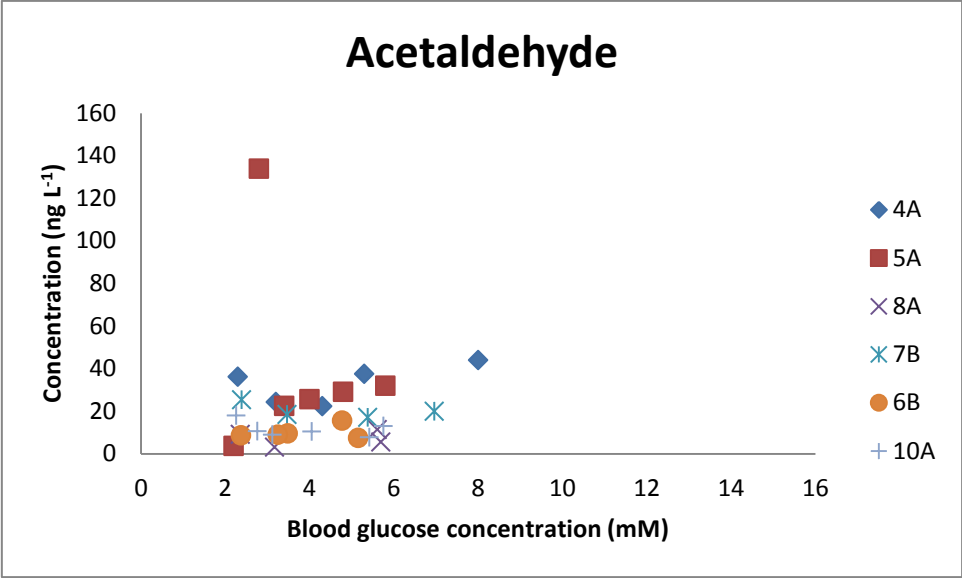


Figure 3.40 GC-MS blood headspace acetaldehyde concentration against measured blood glucose concentration for all eight volunteers during the hypoglycaemic clamp

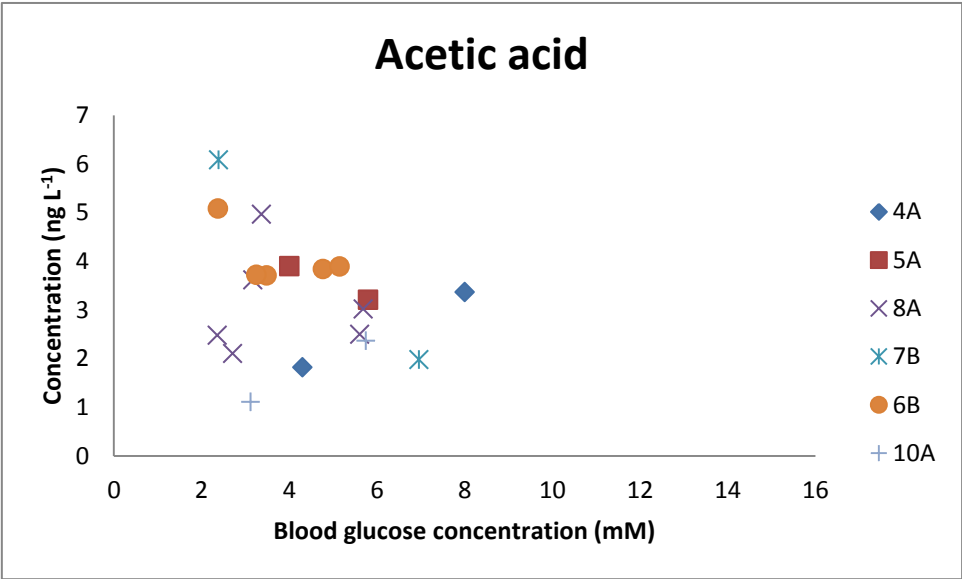


Figure 3.41 GC-MS blood headspace acetic acid concentration against measured blood glucose concentration for all eight volunteers during the hypoglycaemic clamp

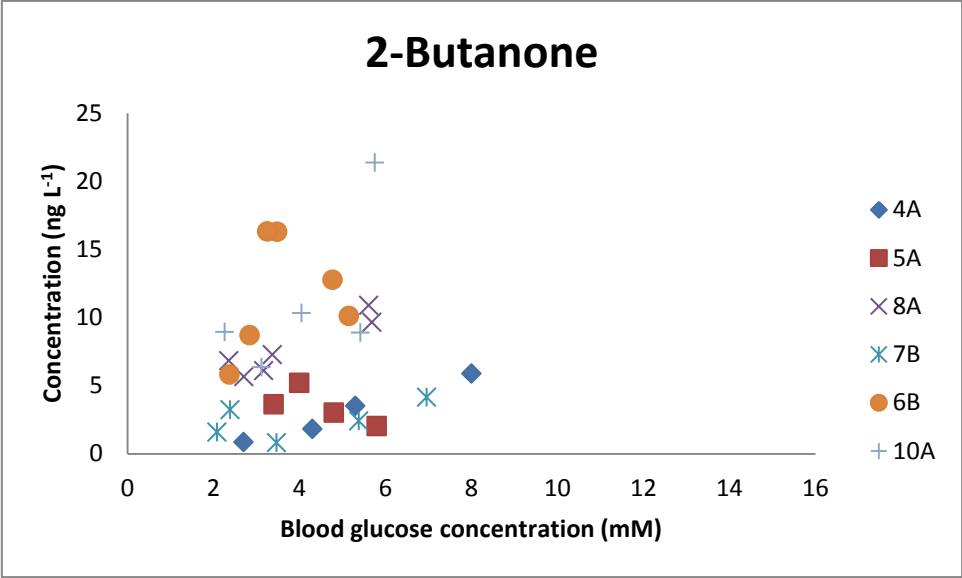


Figure 3.42 GC-MS blood headspace 2-butanone concentration against measured blood glucose concentration for all eight volunteers during the hypoglycaemic clamp

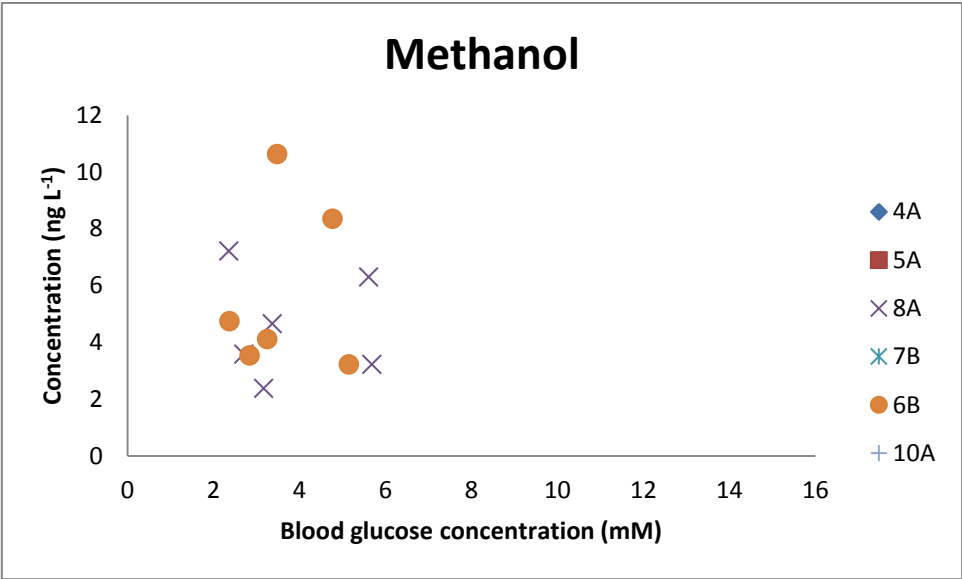


Figure 3.43 GC-MS blood headspace methanol concentration against measured blood glucose concentration for all eight volunteers during the hypoglycaemic clamp

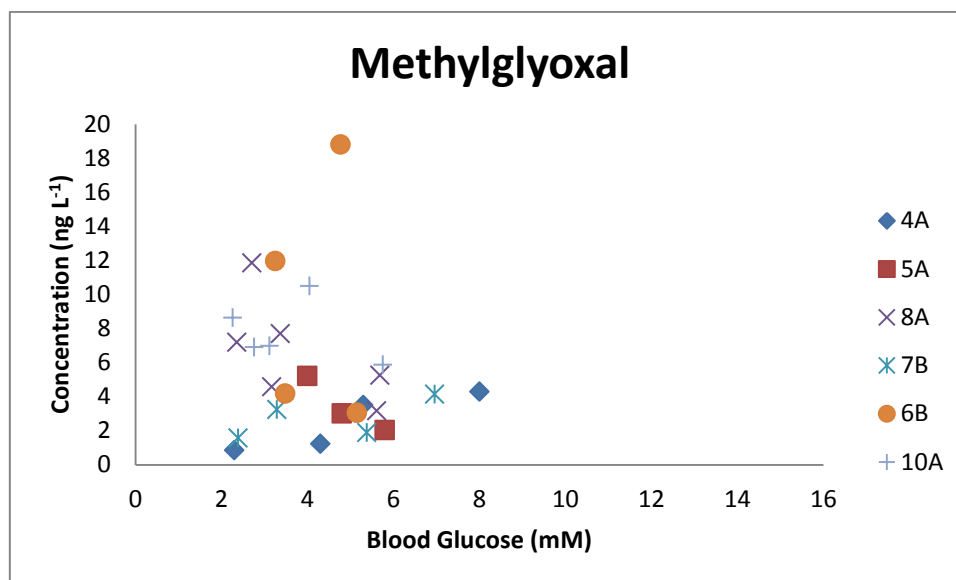


Figure 3.44 GC-MS blood headspace methylglyoxal concentration against measured blood glucose concentration for all eight volunteers during the hypoglycaemic clamp

Volunteer	Linear Correlation Coefficient (R)							
	Acetone	Acetaldehyde	Acetic acid	2-Butaone	Methanol	Methylglyoxal	Phenol	Propanol
4A	0.95 *	0.60	1.00	0.98 *	ND	0.92	0.60	ND
5A	-0.13	-0.19	-1.00	-0.74	ND	0.96	0.91 *	ND
8A	0.56	0.31	-0.05	0.93 *	-0.06	0.65	0.00	0.55
7B	0.88	-0.57	-1.00	0.57	ND	0.62	-0.13	ND
6B	0.81	0.22	-0.60	0.27	0.12	0.03	0.72	-0.40
10A	0.74	-0.40	1.00	0.65	ND	-0.29	0.10	0.98

Table 3.7 Linear correlation coefficients GC-MS blood headspace VOCs vs. Measured blood glucose concentration

3.3.5 Comparison with Breathotron sensor data

3.3.5.1 SIFT-MS

The maximum change in resistance (ΔR_{\max}) for each breath sample obtained during the experiment using the Breathotron was plotted against the equivalent exhaled breath acetone concentration quantified using SIFT-MS from each step of the hypoglycaemic clamp. The data

was plotted against both precursor ions, H_3O^+ , Figure 3.45, and NO^+ , Figure 3.46. An outlier from volunteer 10A was removed from the plots. The linear correlation coefficient was calculated for each volunteer separately; Table 3.8, and includes the outlier.

Higher acetone concentrations do not yield the greatest ΔR_{max} values using either of the precursor ions. All of the volunteers show positive correlation between ΔR_{max} and exhaled breath acetone concentration, but this is only significant in volunteers 4A and 5A. The significance is mirrored across both precursor ions. The highest acetone concentrations do not yield the greatest change in sensor resistance; this is true for both precursor ions.

All of the volunteers show positive correlation between ΔR_{max} and breath acetone quantified using the H_3O^+ precursor ion, but is only significant in volunteers 4A ($R=0.96$) and 5A ($R=0.85$). The highest acetone concentrations do not result in the greatest ΔR_{max} .

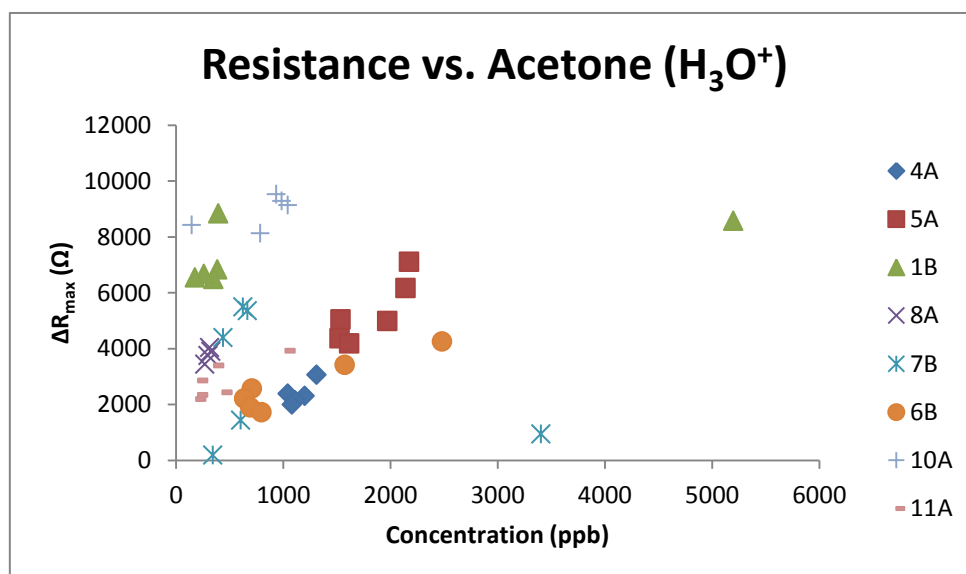


Figure 3.45 Breathatron sensor ΔR_{max} plotted against exhaled breath acetone quantified using the H_3O^+ precursor ion

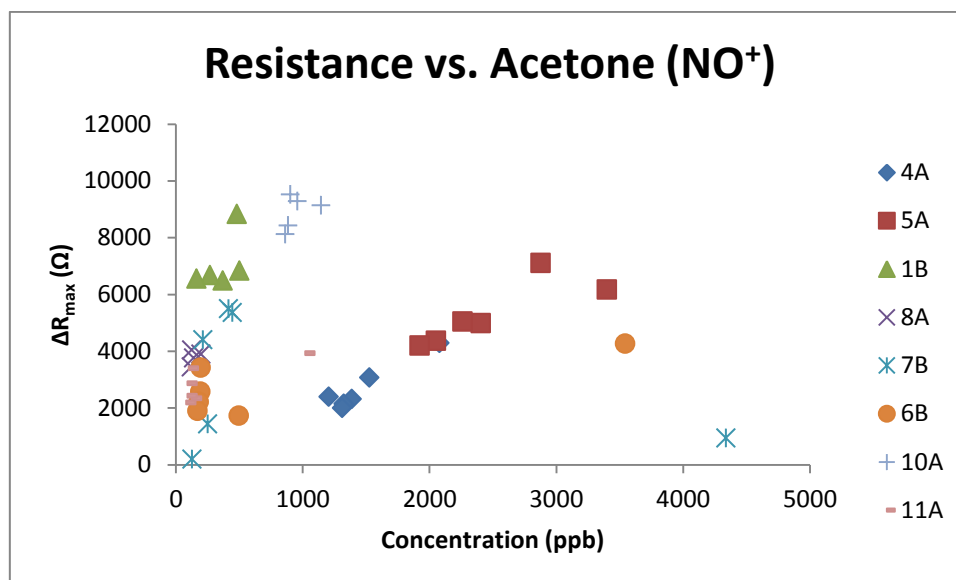


Figure 3.46 Breathotron sensor ΔR_{\max} plotted against exhaled breath acetone quantified using the NO^+ precursor ion

Volunteer	Linear Correlation Coefficient (R)	
	H_3O^+	NO^+
4A	0.96 *	0.95 *
5A	0.85 *	0.84 *
1B	0.73	0.77
8A	0.90	0.31
7B	-0.35	-0.36
6B	0.94	0.76
10A	0.63	0.61
11A	0.80	0.77

Table 3.8 Linear correlation coefficients Breathotron ΔR_{\max} vs. Acetone concentration quantified using SIFT-MS

3.3.5.2 GC-MS

As with the SIFT-MS data, the maximum change in resistance (ΔR_{\max}) for each breath sample obtained during the experiment using the Breathotron was plotted against the equivalent exhaled breath acetone concentration quantified using GC-MS from each step of the hypoglycaemic clamp, Figure 3.47. An outlier from volunteer 10A was removed from the plots. The linear correlation coefficient was calculated for each volunteer separately, Table 3.7, and includes the outlier.

All of the volunteers show positive correlation between ΔR_{\max} and blood glucose concentration though this is only significant in volunteers 6B and 11A.

As with the SIFT-MS data, the greatest ΔR_{\max} vales are not seen at higher acetone concentrations. All of the volunteers show positive correlation with blood glucose concentration, but this is only significant in volunteer 6B ($R=0.96$) and 11A (0.90).

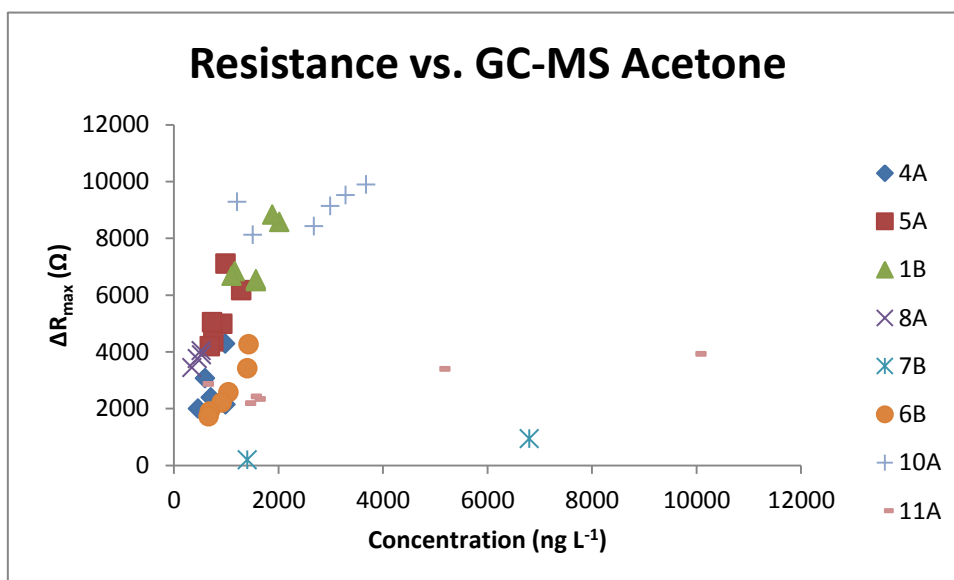


Figure 3.47 Breathotron sensor ΔR_{\max} plotted against exhaled breath acetone quantified using GC-MS

Volunteer	Linear Correlation Coefficient (R)
4A	0.45
5A	0.72
1B	0.77
8A	0.97
7B	0.92
6B	0.96 *
10A	0.58
11A	0.90 *

Table 3.9 Linear correlation coefficients Breathotron ΔR_{\max} vs. Acetone concentration quantified using GC-MS

3.3.6 Comparison of SIFT-MS data to GC-MS data

A comparison of acetone quantified using GC-MS against both H_3O^+ and NO^+ precursor ions using SIFT-MS can be seen in Figure 3.48. A sigmoidal relationship for both precursor ions can

be seen at higher concentrations. There is good agreement between the two MS methods at low concentrations.

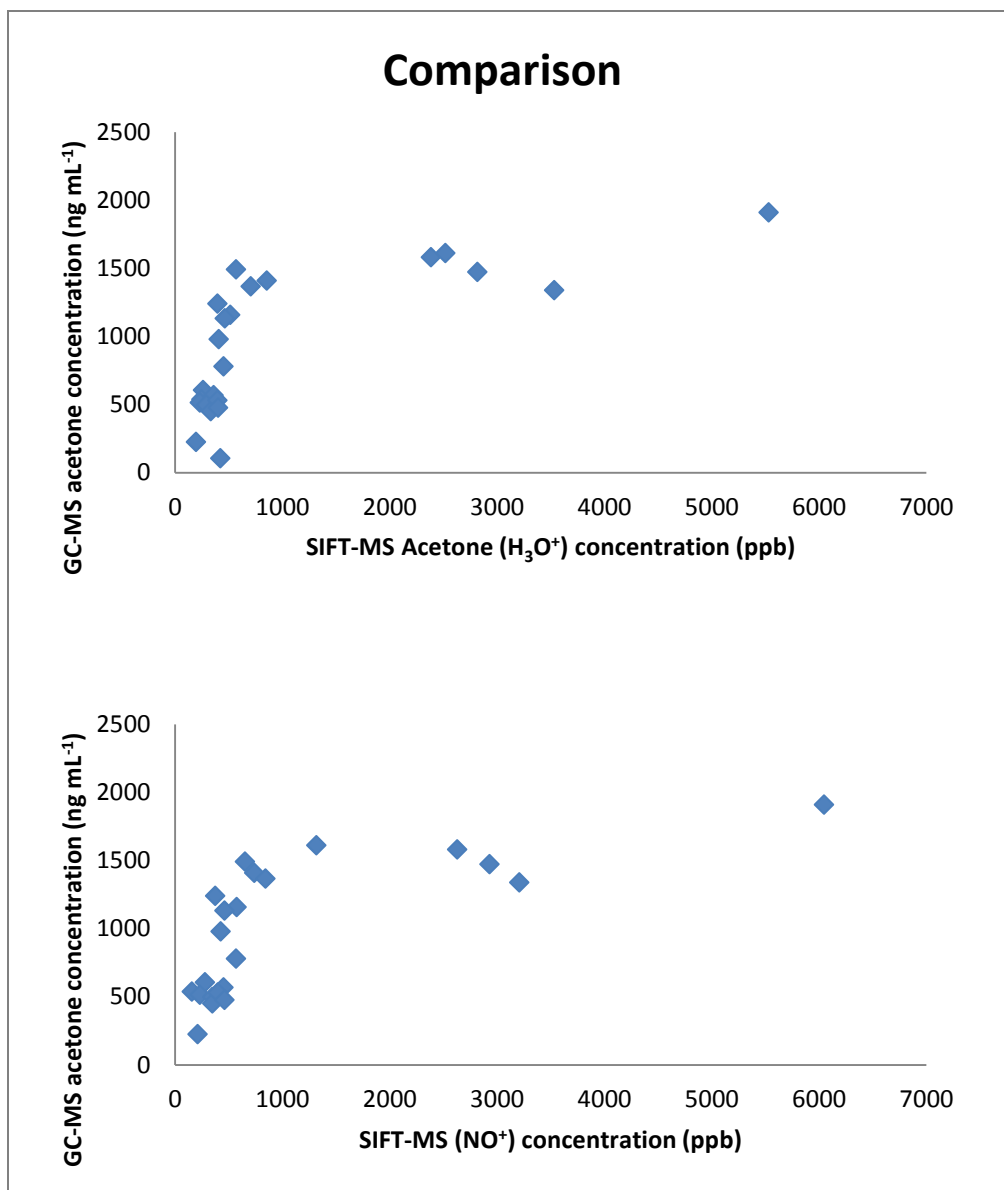


Figure 3.48 Comparison of acetone quantified using GC-MS against the concentration of acetone quantified using SIFT-MS

3.4 Discussion

No statistically significant relationship was observed between Breathotron sensor resistance and blood glucose concentration, or VOC concentration and blood glucose concentration in Type-1 diabetics during a hypoglycaemic clamp. The relationships between acetone and blood glucose concentration are however only significant in a few volunteers, and the significant relationships are inconsistent across the analytical methods.

The volunteers show large variation in ΔR , though it is similar in some volunteers at approximately the same blood glucose concentration. It was demonstrated that there was a linear decrease in peak electrical resistance with decreasing blood glucose concentration, apart from one volunteer due to instrument malfunction. There is significant correlation between ΔR_{\max} and blood glucose concentration in volunteer 10A where many of the signals in the series were clipped.

It is possible that the difference in resistance may be due in part, to catalysis of exhaled breath VOCs on the surface of the MMOS in the right conditions. This may be true in the case of propanol, which may be catalysed to acetone. In the presence of a strong oxidising agent, secondary alcohols are reduced to ketones. In the chromium titanium oxide used in the CAP25, chromium is in a high oxidation state (VI), whilst the temperature that the sensor operates at is above 400°C. Propanol would be dehydrogenated by the metal oxide to acetone. This acetone molecule would then be free to react again with the surface of the sensor increasing the resistance observed. The dehydrogenation of propanol to acetone is seen with a variety of different metal oxides. A way to prevent catalysis may be to reduce the operating temperature of the sensor, though this may have a negative impact on the performance of the sensor, the time required for the sensor to return to baseline would be extended considerably and the sensor would become less sensitive to lower concentrations of compounds (Gardner and Bartlett, 1999). There is also the possibility that the sensor response drifts over time as the sensor ages (Gardner and Bartlett, 1999), though this may be less of a problem in this study as most of the samples were collected over a short time period.

SIFT-MS analysis of exhaled breath samples from Nalophan® bags showed that the major VOC component was acetone. This was also true with skin and blood headspace samples. Acetone was also the most abundant component detected in GC-MS samples.

Though the concentration of acetone varied from person to person at the same glucose concentrations in all of the samples, the concentration of exhaled acetone decreased in exhaled breath, skin and blood headspace with decreasing blood glucose concentration in all of the volunteers using both precursor ions. A decrease in acetone concentration was also seen using GC-MS in both breath and blood headspace samples. However, this was only significant in a minority of the volunteers. Furthermore, the correlation was inconsistent between the different samples and analytical methods, where there was a good linear correlation coefficient with one volunteer and one analytical method this is not mirrored in the

others. The relationship between exhaled breath acetone and blood glucose concentration has been extensively documented in previous studies (Tassopoulos et al., 1969; Manolis, 1983; Owen et al., 1982). Acetone is very stable and considered a metabolic 'dead end'; this makes it a suitable biomarker for glycaemic status.

The concentration of acetone is similar, though a slightly lower concentration of acetone was seen when using H_3O^+ precursor ions, but the linear correlation coefficients with blood glucose concentration are greater suggesting that it is more accurate than using NO^+ ions. Although it is possible to use the NO^+ precursor ion, it is less accurate than using H_3O^+ ions because it reacts via a three-body association forming an adduct ion with a m/z of 88 which may result in greater inaccuracy in the determination of the rate co-efficient between NO^+ and acetone than between H_3O^+ and acetone (Španěl and Smith, 2001). Hence, this is a possible explanation why there greater acetone concentrations are determined using the NO^+ ion, and the linear correlation coefficient values are lower.

Though a comparison of the SIFT-MS and GC-MS acetone concentrations was made, these results have to be treated with some scepticism. The concentration of acetone is measured in different units by the different instruments; SIFT in ppb and GC-MS in ng mL^{-1} . A better way to compare the instruments would be to compare the response of both instruments to calibration gas.

Volunteers whom showed a significant correlation between exhaled acetone and blood glucose concentration with either ion showed no significant relationship using another analytical method. This was true across all three instruments.

There was no formaldehyde detectable in the breath of any of the volunteers though was detected in blood samples. Breath of healthy volunteers typically contains no more than 10 ppb (Turner et al., 2008), and most formaldehyde is absorbed from the consumption of fruit and some from the environment where it is used in glues for everyday items such as furniture (Ligor et al., 2008). It is therefore likely that the formaldehyde detected in blood samples was due to environmental contamination rather than biological process.

There was a higher concentration of acetaldehyde found in the breath of the T1DM volunteers compared to that of healthy volunteers, which contains no more than 20 ppb (Turner et al., 2006c). Acetaldehyde and ethanol concentration both increased towards the lower end of the glucose scale.

The concentration of ammonia deviated little during the course of the clamp, however the concentration of ammonia was higher than that typically found in healthy individuals (Turner et al., 2006a). The higher level of ammonia is probably attributable to damage caused by long term diabetes (Alvaro et al., 1986).

Ethanol is an end stage product of acetaldehyde that is produced during glycolysis, under anaerobic conditions. The concentration of ethanol was considerably higher in breath samples than skin or blood headspace. These high levels of ethanol in breath may be attributable to bacterial activity in the oral cavity (Smith et al., 2008), though the same increase in ethanol concentration is seen in blood headspace and to a certain extent in skin headspace. There was some correlation with the change in glucose concentration seen using SIFT-MS during the insulin infusion; this increase was coupled to an increase acetaldehyde concentration, particularly at the lower glucose concentrations. This is expected as insulin stimulates glycolysis, and would therefore increase the endogenous production of acetaldehyde and consequently ethanol would increase. However, insulin infusion was given intravenously at a constant rate; it was the glucose influx that was varied. Given that the sample size was small, this finding warrants further investigation.

Isoprene was found to increase with decreasing blood glucose concentration; this has been observed in previous studies (Turner et al. 2006b). Isoprene is a VOC that has been linked to the cholesterol degradation pathway, and is found in breath in the 40-300 ppb range (Turner et al. 2006b). The concentrations of isoprene detected using SIFT-MS were comparable for some volunteers, though it was generally elevated, particular so at low blood glucose concentration. The concentration of isoprene seen using GC-MS was higher than that seen using SIFT-MS, though this is only true for breath samples. As isoprene is a small molecule with a short retention time this is unexpected. It is likely that due to the extremely volatile nature of isoprene it was unable to be concentrated onto TD tubes from blood samples.

Virtually no isoprene was detected in skin headspace analysed in comparison to the concentrations seen in breath and blood headspace samples. However, in previous studies skin headspace was sampled directly from the volunteer's arm (Turner et al., 2008). In this study bags were removed, sealed and then transported back to the laboratory.

The compound 2-Butanone was found in blood in the majority of volunteers, and found to have a significant positive correlation with blood glucose concentration in two of the

volunteers (4A, 8A). Though 2-butanone was found in breath samples, there was no distinct relationship established. 2-Butanone is found in healthy individuals at very low concentrations, with a median concentration of 0.38 ppb (Van de Velde et al., 2008). Using GC-MS it was found that in both breath and blood 2-butanone concentration is a minimum of ten times greater – similar to that found in patients with liver disease. It has been proposed that patients with liver failure produce large amounts of the compound. This may be due to hepatic insulin resistance (Kim et al., 2004), increasing triglycerides, free fatty acids and ketones during lipolysis (Matthews et al., 1997). This insulin resistance is due to hepatic fat accumulation, this may occur in the same way as non-alcoholic fatty liver disease (NAFLD) where hepatic steatosis stimulates gluconeogenesis activating both PKC- ϵ and JNK1 interfering with the tyrosine phosphorylation of IRS-1 and IRS-2 (Samuel et al., 2004). This impairs the ability of insulin to activate glycogen synthase. Diabetes is common in patients with NAFLD, (Araya et al., 2006). It is possible that the effect of excess insulin alters liver function over time and may lead to elevated concentration of acetone in breath.

Butanoic acid was only observed in the blood headspace of one volunteer, 6A, at 2.4 mM (results not shown). The lack of butanoic acid may be explained by the fact that volunteers were held at the lowest concentrations for the least amount of time and this may not have been enough time for the compound to enter the blood stream. Another possibility is that the blood glucose concentration at which DKA occurs is different from individual to individual. It is unlikely to have been metabolised, as the blood concentration of butanoic acid has been linked to skin acetone concentrations in diabetic patients (Yamane et al., 2006).

It has been suggested that the compound methyl nitrate closely follows the glycaemic status in Type 1 diabetics (Novak et al., 2007). In this study there was no evidence to support this claim. Indeed there was no methyl nitrate present in any of the samples taken from the volunteers. As the volunteers in this study were adults it would have been more likely for them to be taking medication for cardiovascular problems, which contain nitro-compounds, which may have supported this claim. The study mentioned was focused on juveniles therefore the source of the compound is debateable. In that study the background levels of methyl nitrate were 10 ppb, whilst the highest recorded concentration was 15 ppb. It is likely that this result was due to exposure to methyl nitrate in the environment, contaminants in the column or the effects of memory in the TD tubes.

Unlike the previous experiment on non-diabetic individuals, offline (bag) sampling was used instead of online (directly into the instrument). The purpose of this was primarily due to the fact that samples needed to be collected off-site, and this also increased the number of compounds that could be analysed due to having more precursor ions available. The disadvantage of this method was that these breath samples were collected after the Breathotron and TD tube samples. This is unlikely to have significantly affected the results. The use of offline bag samples does not seem to have made a vast difference to the significance of the relationships between exhaled VOC concentration and blood glucose.

The remote skin sampling method was cast into doubt as there was little or no correlation between any of the selected ion products and blood glucose concentration. Although there was a modest increase in acetone concentration with rising blood glucose concentration, the results are statistically insignificant. There was no relationship established with blood glucose concentration for any of the other ion products. The site at which samples are taken may also be an important factor when quantifying VOCs emitted from skin and may explain the poor results, there is a difference in the VOC content and concentration from forearm and back skin, though they are similar (Gallagher et al., 2008). The surface of the skin may have also been contaminated with compounds found in cosmetic products. However Gallagher et al., (2008) found that pre-washing the surface of the skin with soap that contained no fragrance made little difference to the contaminants that were identified using GC-MS. There was also no difference in the compounds emitted from male and female volunteers suggesting that hormone breakdown products are short lived and are not excreted from the skin. Unfortunately TD GC-MS of skin headspace was not carried out in this study, but these findings warrant further investigation. Another way to collect skin headspace samples for analysis using SIFT-MS would be to transfer the headspace from the Nalophan® bag placed around the arm into another bag using an air sampling pump to avoid contamination of the sample with ambient air.

Because of the practical difficulties of removing the sampling bag from the arm, it was difficult to be certain of avoiding leakage of sample or contamination with ambient air. It is unlikely that sample degradation occurred during transportation, as it has been shown that gaseous samples in Nalophan® bags are stable for several hours (van Harreveld, 2003; Steeghs, et al., 2007).

The intensity of the internal standard (d8-toluene) peak appears to reduce over time. This may lead to incorrect quantification, and may partly explain discrepancies between SIFT-MS and GC-MS data. This is due to a headspace forming in the vials that the standard is stored in, and each time the vial is opened some of the headspace escapes. The variability in standard peak height may also be attributable to the flow rate of the Calibration Solution Loading Rig (CSLR®) (Markes International Limited, Llantrisant, UK), as the exact flow rate varies during use due to the manual operation of the device. Therefore the same amount of standard is not applied to all of the tubes. The protocol for making and storing internal standard was changed following this experiment. Standard was aliquoted into smaller disposable single use vials and placed into storage at -80°C to prevent headspace from forming. To reduce human error, a mass flow controller couple together with a microcontroller based timer could be employed to control the flow of gas through the tubes when applying standard.

In some samples there appeared to be no d8-toluene, accompanied with a considerable amount of noise. Checking the TD tube records shows that the majority of the tubes had been used previously and then reconditioned correctly, and were not used in faecal or urine sampling discounting the memory effect. Samples that were run immediately before and after these do not exhibit the same problem, ruling out problems with the instrument. It is therefore suspected that the standard used was left out on the bench, allowing the d8-toluene to evaporate, and accidentally placed back into the refrigerator.

The fact that there is some tracking of acetone concentration, the major component of all of the samples analysed, and ΔR_{\max} implies that the differences in peak electrical resistance observed using the Breathotron are linked to the acetone concentration, however the correlation between the two was only significant in two of the volunteers (4A, 5A) using SIFT-MS and two different volunteers using GC-MS (6B, 11A).

The reason as to the poor correlation between ΔR_{\max} and exhaled acetone concentration may be due to interference from other compounds within the sample. In a previous study where pure samples of acetone, ammonia and propanol together with and stimulated breath samples containing a mixture of the three compounds were introduced to the Breathotron it was observed that the peak resistance was largely determined by the most abundant VOC, but was attenuated or quenched by smaller amounts of other compounds (Patel, 2007).

Another factor to consider is that the volunteers in this experiment were hypounaware, they did not realise when their blood glucose concentration was falling dangerously low. In these situations additional hormones, such as adrenaline are used to keep the body alert (Holt et al., 2007; Pocock et al., 1999). This would lead to an increased heart rate and altered blood oxygen saturation.

3.5 Conclusion

It has been demonstrated that the Breathotron is not a suitable device for non-invasive monitoring of glycaemic status in diabetic patients. Though a relationship was established between Breathotron sensor resistance and blood glucose concentration, this was only significant in some of the volunteers. Through the analysis of exhaled breath, skin headspace and blood headspace using SIFT- and TD GC-MS, the compound found to be changing most with decreasing blood glucose concentration was acetone. Though all volunteers showed a decrease in acetone concentration with decreasing blood glucose concentration as would be expected due to the inhibition of lipolysis, this was only significant in a small number of volunteers. The significance between acetone and blood glucose concentration was inconsistent between samples and analytical methods.

There was no methyl nitrate found in any of the samples despite the fact that a relationship between breath concentrations and blood glucose concentration has been reported in the literature. It is unlikely that methyl nitrate is related to blood glucose concentration.

Furthermore, the Breathotron showed some relationship between peak sensor resistances and experimentally quantified exhaled acetone concentrations. Again however, this was not significant in the majority of the volunteers. The sensor resistance may be affected by other VOC concentration in the sample or other factors such as carbon dioxide or oxygen concentration.

The concentration of acetone quantified using SIFT-MS is similar regardless of the precursor ion used. There were however differences in significance between exhaled breath acetone concentration and blood glucose concentration with the different precursor ions. A significant relationship with one ion did not imply a significant relationship with the other.

As a result of the work in this chapter, the protocol for applying internal standard to TD tubes was altered. The change was designed to improve quantification during GC-MS analysis.

4 Monitoring the change in VOC concentration in breath under the influence of induced respiratory complication during a 6-Minute Walk Test using SIFT- and GC-MS

4.1 Introduction

Diabetes mellitus is common amongst patients suffering from chronic obstructive pulmonary disorder (COPD), affecting up to 16% of all patients with COPD (Chatila et al., 2008). The prevalence of diabetes increases in COPD patients with further lung function deterioration (Chatila et al., 2008). COPD is characterised by chronic lung inflammation and progressive irreversible airway limitation as a result of emphysematous destruction (van Berkel et al., 2010), this is typically associated with smoking tobacco (Archer and Baker, 2009). According to the WHO, COPD was the sixth highest cause of morbidity in low and middle income countries in 2001 (Mannino and Buist, 2007). The current method of COPD diagnosis is through spirometry. This is considered the gold standard method, however this does require specialist training to interpret the results. Clinical symptoms may not manifest in early stage COPD (van Berkel et al., 2010).

There is evidence to suggest that COPD may increase insulin resistance, in skeletal muscle particularly, through cytokine mediated inflammation as a result of chronic hypoxia (blood oxygen saturation <75%) and corticosteroid treatment (Archer and Baker, 2009). COPD patients with diabetes are also predisposed to developing lower respiratory tract infections (Hak et al., 2006).

Exercise is recommended in patients with diabetes by the American Diabetes Association (2004b) due to the potential therapeutic benefits, which include a better sense of wellbeing, better weight control, improved physical fitness, improved cardiovascular fitness, lower pulse and blood pressure and an improved lipid profile (Austin et al., 1993; Wasserman and Zinman, 1994). This makes analysis of breath difficult in patients that have been exercising due an increase in ventilation and blood flow which would no longer be in a steady-state, changing the rate of excretion at the alveolar-capillary membrane, therefore reducing the concentration (Risby, 2005).

These observations have implications for a non-invasive breath test for monitoring exhaled VOC concentration for medical diagnostics. It is important to find out the effects of changes in blood and ventilatory flow so that they can be compensated for. This may also be useful in the

diagnosis and treatment of respiratory disease. Ideally, breath analysis should encompass all patients. A breath test that excludes those with reduced respiratory function would reduce the appeal of non-invasively monitoring breath for medical diagnosis. Physical exercise is an important factor in preventing conditions such as cardiovascular disease, obesity and diabetes. For those suffering from diabetes, exercise is particularly encouraged as it improves glycaemic control and increases insulin sensitivity (Wasserman and Zinman, 1994; Austin et al., 1993).

Engaging in prolonged physical activity puts Type 1 diabetics at risk of their blood glucose levels falling dangerously low. Hypoglycaemia can occur during, or up to 17 hours following, exercise (Diedrich et al., 2002). It is important that diabetics monitor their blood glucose levels regularly to prevent hypoglycaemic episodes. Many diabetics fail to do this, increasing the risk of seizure, coma or, in extreme cases, death (Tuch et al., 2000).

Exercise is encouraged as part of a balanced healthy lifestyle. Individuals typically exercise to maintain or improve their level of physical fitness, but in addition to this, regular exercise helps to strengthen muscles, the cardiovascular system and boost the immune system. This may help to prevent conditions such as heart disease and obesity.

The prevalence of diabetes is ever increasing; this is mainly due to poor diet and a sedentary lifestyle, especially amongst children. For this reason exercise is especially encouraged amongst diabetic patients and those at risk of developing the illness.

The purpose of this chapter is to investigate the effect of simulating airway narrowing, associated with COPD, increased pulmonary flow and blood oxygen saturation on exhaled VOC concentration in healthy volunteers during the Australian Lung Foundation Six Minute Walk Test (6MWT) to observe, if any, changes in exhaled VOC concentration using offline SIFT-MS and TD GC-MS. The purpose of this experiment is to determine if airway narrowing or moderate physical activity has an effect on VOC concentration.

4.2 Methods and Materials

4.2.1 6-Minute walk test

With ethical approval from the University of Bedfordshire, healthy volunteers recruited from the student body were recruited and completed the 6MWT on a treadmill with a 1% gradient to simulate wind resistance (Jones and Doust, 1996). The 6MWT involves the volunteer walking as far as possible at no set pace for six minutes (Jenkins, 2007). This test is used to

assess patients with COPD. Ideally, this test is conducted in a flat, straight corridor 30-40 m long, though a treadmill can also be used. Volunteers first completed this normally and then with induced respiratory restriction, achieved by wearing a nose clip and oral breathing through a tube (drinking straw), approximately 10 mm diameter to simulate bronchoconstriction and induce a greater respiratory challenge similar to that seen in COPD patients (International COPD Patients in Action, 2007). The subjects controlled the speed of the treadmill. Heart rate (HR), blood oxygen saturation (SpO_2), rating of perceived exertion (RPE) (Borg, 1970), Table 4.1, treadmill speed and the number of rests required were recorded every minute. The total distance walked in kilometres (km) was also recorded for each volunteer. Lung function was assessed using a Vitalograph® Gold Standard spirometer (Vitalograph Ltd. Buckingham, MK18 1SW, UK). Blood glucose was determined using from a pin prick and analysed with a glucose oxidase based Yellow Springs Instrument (Yellow Springs Instruments, Palo Alto, CA, US). Heart rate and blood oxygen saturation were measured using a wireless pulse oximeter with built in display. As this was part of an undergraduate practical session these parameters were recorded by fellow colleagues of the volunteers and not by the author.

The experiment was terminated if there was an onset of angina, or angina-like symptoms, signs of poor perfusion, physical or verbal manifestations of severe fatigue, development of abnormal gait pattern, tachycardia (defined as a HR greater than 220 minus the volunteer's age) or if their SpO_2 fell below 85%. The volunteer could terminate the test at any time if they wished to do so.

Subjects were asked to breathe into a Nalophan® sampling bag with as many breaths needed to fill the bag (approximately 4.5 L) after rinsing their mouths three times with water, fingertip blood samples for glucose concentration were also collected at rest before and upon completion of the 6MWT, this was done for both walk tests without then with respiratory challenge. In total four breath samples were collected over the period of one hour. The samples were put in a black refuse bag to prevent photo-oxidative reactions and transported to Cranfield for analysis immediately after collection.

0	Nothing at all
0.5	Very, very slight (just noticeable)
1	Very slight
2	Slight
3	Moderate
4	
5	Somewhat severe
6	Severe
7	Very severe
8	
9	Very, very severe (almost maximal)
10	Maximal

Table 4.1 The Borg rating of perceived exertion (RPE) dyspnoea scale (10 point) (Borg 1970)

4.2.2 SIFT-MS

Semi-quantitative full scan (FS), and quantitative multi-ion mode (MIM) scans were performed for all of the samples. For the FS the downstream quadrupole was swept between the 10-160 m/z range 10 times using each of the three precursor ions H_3O^+ , NO^+ and O_2^+ . In the MIM ion scan the methanol, ethanol, propanol, formaldehyde, acetaldehyde, acetone, ammonia, pentene, hexane, total terpenes, hydrogen cyanide, β -hydroxybutyric acid, nitric oxide, pentane, and nitrogen dioxide product ions were selected to be quantified. Samples were introduced into the sampling port of SIFT-MS using Nalophan[®] bags incorporating following incubation for a minimum of 5 minutes at 40°C. All samples were analysed within 12 hours of collection.

4.2.3 ATD GC-MS

Breath samples were also preconcentrated onto TD tubes for analysis using GC-MS from Nalophan[®] bags using a TSI[®] Sidepak[™] SP730 (Shoreview, MN, US) at a flow rate of 100 ml min⁻¹ for 5 minutes whilst incubated at in an incubator at 40°C. The samples were then stored at 4°C. Internal standard was applied to each of the tubes as mentioned in Chapter 2 prior to analysis.

4.3 Results

4.3.1 6-Minute walk test

Eight unfasted, non-smoking, healthy volunteers were recruited and completed the experiment, 5 males (volunteers A, C, D, E and F) and 3 females (B, G and H). All of the volunteers completed the experiment without problems, though volunteer D said that they felt 'dizzy' at the end of the experiment. Height, weight, age, and respiratory function (FVC, FEV₁ and FEV_{1.0%}) in the unrestricted, control condition, and with the respiratory restriction, breathing through a tube 10 mm in diameter, were recorded for volunteers C, D, E, F, G and H, Table 4.2. Due to the nature of the experiment, where samples were taken during an undergraduate practical class, other students collected and recorded supplementary data. In some cases this data is missing for volunteers A and B. There no significant change in FVC, and FEV₁ between the control and respiratory restriction conditions. FEV_{1.0%} was over 70% for all of the volunteers, where this data was recorded, indicating that they were indeed healthy. A one tailed paired two sample means t-Test in Microsoft® Office Excel™ 2010 (Redmond, WA, US) of the data showed no significant difference in respiratory function without (Control condition) and with respiratory challenge (Respiratory restriction) (FVC $P < 0.18$, FEV₁ $P < 0.18$, FEV_{1.0%} $P < 0.18$).

Volunteer	Height (cm)	Mass (kg)	Age (years)	FVC (L)	Control			Respiratory restriction		
					FEV ₁ (L)	FEV _{1.0%}		FVC (L)	FEV ₁ (L)	FEV _{1.0%}
C	188.0	90.5	21	5.59	4.97	89		5.59	4.97	89
D	182.0	80.1	21	5.53	4.91	89		5.66	4.97	88
E	188.1	118.7	21	4.43	3.98	90		4.43	3.98	90
F	176.0	80.0	21	5.23	4.88	93		5.23	4.88	93
G	163.0	54.7	24	3.74	3.62	97		3.74	3.62	97
H	170.0	59.5	21	5.32	4.71	89		5.32	4.71	89
Mean	177.85	80.58	21.50	4.97	4.51	91		5.00	4.52	91
SD	9.23	21.08	1.12	0.67	0.52	3		0.69	0.53	3

Table 4.2 Height, weight and respiratory function data

The blood glucose concentrations were measured for volunteers C, D, E, F, G and H is shown in Figure 4.1. Due to a technical fault, blood glucose data for volunteers A and B could not be collected. An increase in glucose concentration was observed in volunteer E during the two

walk test phases, whilst there is no appreciable change in volunteer G throughout the experiment. Baseline blood glucose levels at the beginning of the experiment (R1) were a mean (\pm SD) of 4.3 mM (\pm 0.59). This fell to 3.8 mM (\pm 0.28) after the first walk test (Control). A two tailed paired two sample means t-Test in Microsoft® Office Excel™ 2010 was performed, where null hypothesis was that there was no significant difference in blood glucose concentration. The statistical test showed that there was no significant change in mean blood glucose concentration between R1 and Control ($P < 0.18$) or between R2 and Respiratory restriction ($P < 0.96$). The total distance walked by volunteers C, D, E, F, G and H during the control and with respiratory restriction walk tests can be seen in Table 4.3. There is a significant decrease in the total distance walked with respiratory restriction compared to the control 6MWT ($P < 0.001$).

The mean distance walked during the Control 6MWT was 0.83 km \pm 0.05, and during the Respiratory restriction 6MWT was 0.68 km \pm 0.10. A one tailed paired two sample means t-Test showed a significant decrease in the distance walked by the volunteers during the second 6MWT with respiratory restriction can be seen ($P < 0.001$) during the respiratory challenge.

The perceived rating of dyspnoea for both walk tests can be seen in Figure 4.2, shows that there was a range between 0, nothing at all, seen in volunteer D, to 6, severe, in volunteer G, with most of the volunteers in the 'moderate' range. During the Respiratory restriction 6MWT, the RPE was generally higher, with all of the volunteers scoring higher initial RPEs apart from volunteer G. Volunteer F said that they felt that their rating increased from 3, moderate, to 8, severe, during the second walk test with respiratory challenge.

Blood oxygen saturation deviated little during the control 6MWT, with all volunteers within the range of 92-99%, Figure 4.3. There is a greater fall in SpO₂ during the restricted 6MWT, though there was some misreading due to the pulse oximeter falling off the fingers of some of the volunteers during the experiment.

There was an increase in heart rate during the control 6MWT, which is also seen in respiratory restriction 6MWT, Figure 4.4. There are generally higher heart rates seen during the second walk test, the highest being recorded in volunteer G (187 beats per minute).

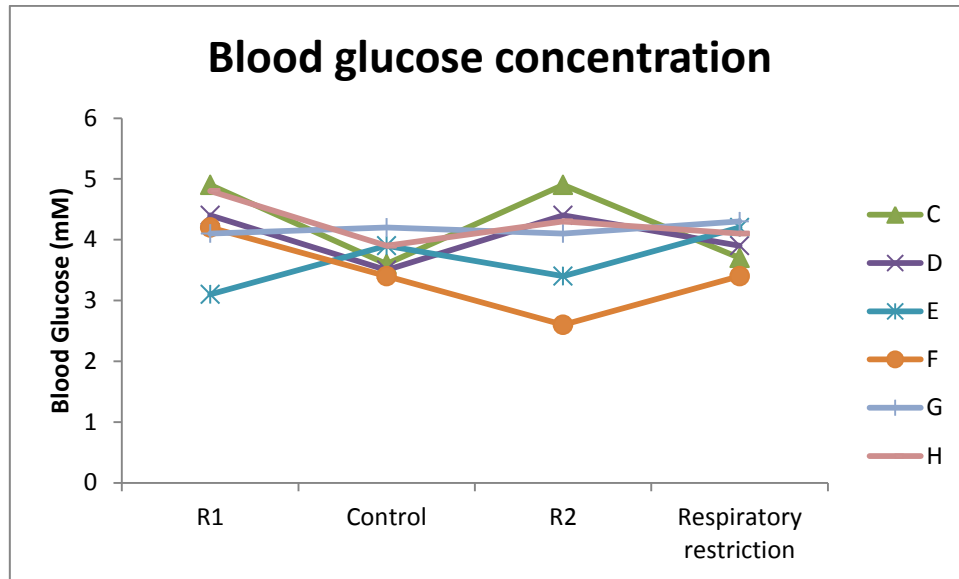


Figure 4.1 Blood glucose concentration measured at the four sampling intervals

Volunteer	Total distance (km)	
	Control	Respiratory restriction
C	0.92	0.80
D	0.78	0.59
E	0.84	0.76
F	0.83	0.72
G	0.77	0.60
H	0.84	0.58
Mean	0.83	0.68
SD	0.05	0.10

Table 4.3 Total distance walked (6MWD) during control and with respiratory restriction walk tests

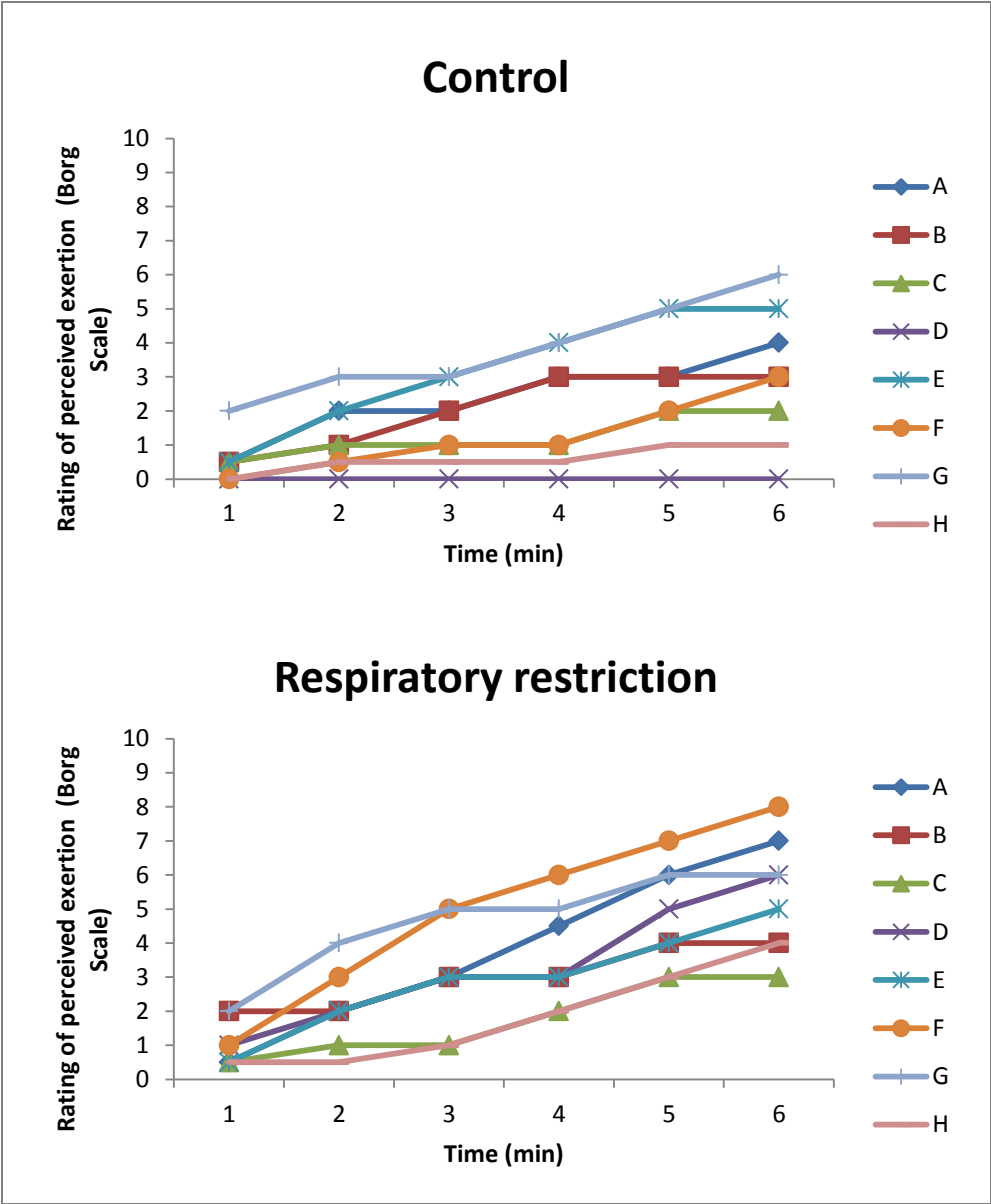


Figure 4.2 Perceived dyspnoea during the two walk tests

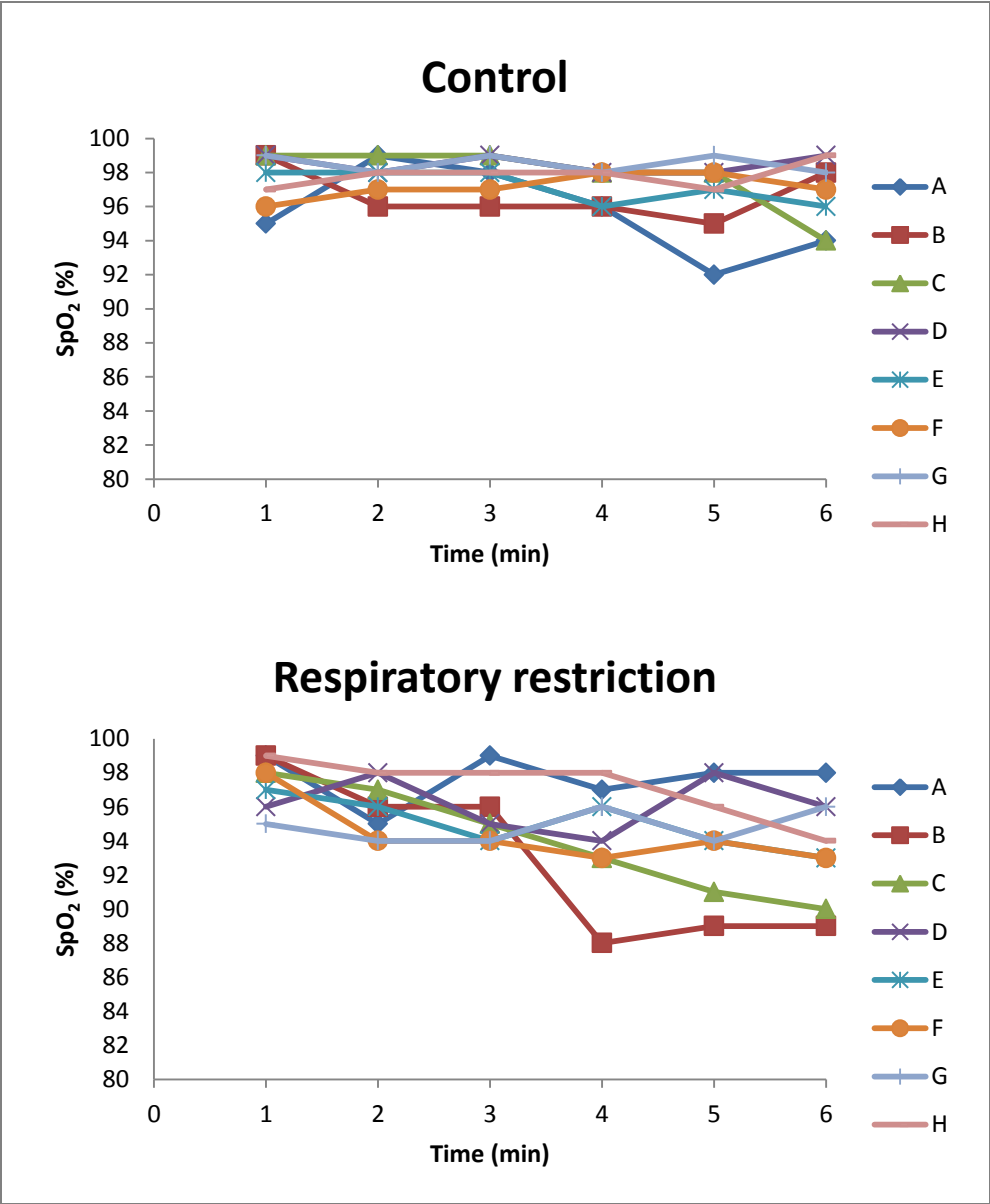


Figure 4.3 Blood oxygen saturation (SpO₂) during the two walk tests

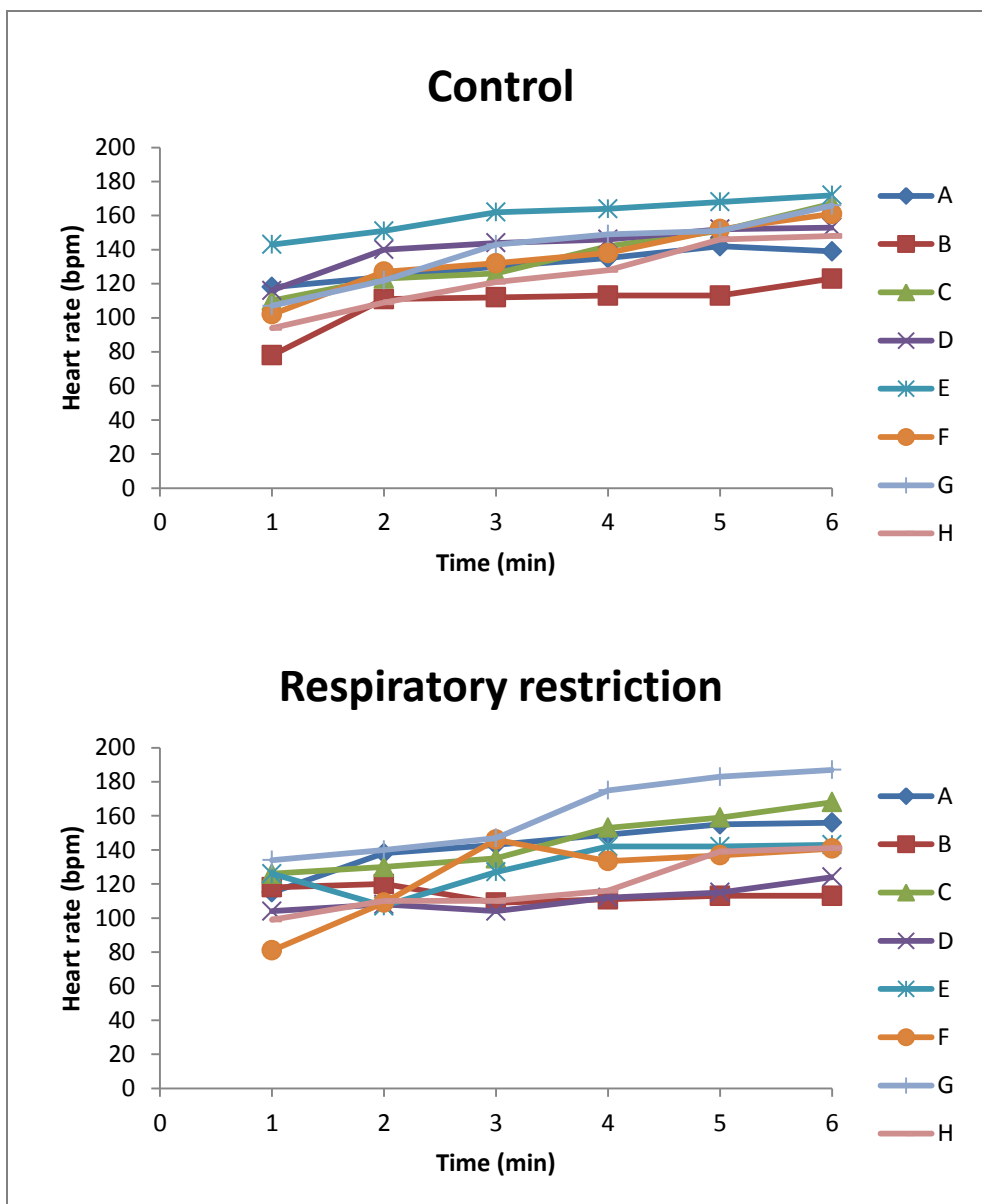


Figure 4.4 Heart rate data in beats per minute for both walk tests

4.3.2 SIFT-MS

A plot of concentration at each sampling interval for each of the VOCs quantified using the SIFT-MS was made for formaldehyde, Figure 4.5, acetaldehyde, Figure 4.6, acetone (H_3O^+), Figure 4.7, ammonia, Figure 4.8, isoprene (H_3O^+), Figure 4.9, methanol, Figure 4.10, ethanol, Figure 4.11, propanol, Figure 4.12, -hydroxybutyric acid, Figure 4.13, isoprene (NO^+), Figure 4.14, acetone (NO^+), Figure 4.15, nitric oxide, Figure 4.16, pentane, Figure 4.17, and nitrogen dioxide, Figure 4.18.

Repeated measures one-way analysis of variance (ANOVA) analysis followed by a Bonferroni post-hoc test, used to counteract the problem of multiple comparisons where the likelihood of witnessing a rare event is increased, was performed using IBM® SPSS™ Version 19 (Armonk, NY, US). This was to determine if there was a significant difference in exhaled VOC concentration between the different conditions, with the H_0 hypothesis that there was no significant difference between the samples collected at the different stages of the experiment. A table of the P values is reproduced in Table 4.4. Mauchly's Test of Sphericity (Mauchly, 1940) was used to determine if the variances of all of the combinations of groups that were being tested were equal. Where Sphericity was violated, unequal variances, ($P < 0.05$), caused by distorted variance calculations resulting in an inflated F ratio, the Greenhouse-Geisser correction (Greenhouse & Geisser, 1959) was used, which alters the degrees of freedom and results in an F ratio where the Type 1 error rate is reduced, these are indicated in the table by a superscript 1 (¹).

The highest pre-6MWT R1 concentrations of formaldehyde were seen in volunteer C (45 ppb), with the lowest in volunteer B (20 ppb). There was a mean decrease in formaldehyde during the course of the experiment.

High concentrations of acetaldehyde, Figure 4.9, are only seen in volunteers E, F, G and H that all completed the experiment on the same day. The greatest concentration is seen in volunteer H during the Control 6MWT (366 ppb). High end of experiment concentration, after the respiratory challenge 6MWT, can be seen in volunteer F (336 ppb). The mean concentration of exhaled breath acetaldehyde increases during the Control 6MWT ($147 \text{ ppb} \pm 141$) over R1 concentration ($76 \text{ ppb} \pm 90$), and is lower in the second rest period R2 ($56 \text{ ppb} \pm 41$) and subsequently increases to a similar amount seen during the Control 6MWT after the Respiratory restriction 6MWT ($143 \text{ ppb} \pm 123$).

The highest concentrations of exhaled breath acetone were observed in volunteer B, with the greatest concentration in the Control walk test sample (416 ppb). The lowest concentrations are observed in volunteer C (121 ppb). Individual volunteers show different patterns in exhaled acetone concentration. Volunteers B, D, F, G and H show no deviation in exhaled acetone concentration from R1 to the Control 6MWT, concentration decreases during R2 and increases again during the Respiratory restriction 6MWT. Acetone concentration decreases from R1 concentrations during the Control 6MWT and R2, but increases again after the Respiratory restriction 6MWT in volunteer A. For volunteer E, acetone concentration increases during the

walk test phases of the experiment, with the rest period concentrations being similar. Mean concentration of the cohort does not deviate significantly between R1 (256 ppb \pm 94), Control (252 ppb \pm 85), R2 (221 ppb \pm 67), and Respiratory restriction (239 ppb \pm 52).

Exhaled ammonia concentration was greatest in the Control sample from volunteer B (1.65 ppm), and lowest in the R1 sample from volunteer E (783 ppb). Ammonia was the most abundant VOC quantified in the breath samples. Mean concentrations between R1 (878.5 ppb \pm 169.2), Control (976.5 ppb \pm 291.4), R2 (874.8 ppb \pm 50.3) and Respiratory restriction samples (914.4 \pm 114.1) shows that there is little significant deviation in ammonia concentration during the experiment.

The greatest concentration of exhaled isoprene (H_3O^+) was seen in the R1 sample from volunteer D (345 ppb), whilst the lowest was seen in the Control sample from volunteer G (61 ppb). There is generally a decrease in exhaled isoprene between R1 and Control samples, and R2 and Respiratory restriction samples, except in volunteers C and E, where exhaled isoprene concentration decreases from R1 concentrations during the whole experiment, and volunteer D, where there is an increase in concentration in the Respiratory restriction sample.

Exhaled methanol concentration was highest in the R1 sample from volunteer H, with the lowest seen in the R1 sample from volunteer F. There is no clear pattern in methanol changes between the volunteers. Mean exhaled methanol concentration suggests that there was little change from R1 (205 ppb \pm 85), Control (191 ppb \pm 53), R2 (194 ppb \pm 39) and Respiratory restriction (187 ppb \pm 53) concentrations.

The concentration of ethanol seen in volunteer A was substantially higher than that seen in the other volunteers and was excluded from the statistical analysis. It was suspected that the volunteer either forgot to rinse their mouth with water prior to the experiment, had had consumed alcohol at some point prior to the experiment. The greatest concentration was seen in volunteer B in the R2 sample (84 ppb) and volunteer G in the R1 sample (84 ppb). There was no clear pattern seen in exhaled ethanol. Examining the mean concentrations showed that there was no significant difference between R1 (65 ppb \pm 12), Control (62 ppb \pm 13), R2 (61 ppb \pm 15), and Respiratory restriction (63 ppb \pm 13).

The greatest concentration in exhaled propanol is seen in the R2 sample from volunteer A (203 ppb), and the lowest in the R1 sample from volunteer C (63 ppb). There is an increase in mean exhaled concentration from R1 (108 ppb \pm 33.4408) to Control (139 ppb \pm 41), R2 (143 ppb \pm

48), and Respiratory restriction (151 ± 30). The post-hoc test shows that there is a significant change between R1 and Control samples ($P < 0.002$) and between R1 and Respiratory restriction samples ($P < 0.037$). All of the volunteers bar A, G and E follow this trend, there is a decrease in concentration during the walk tests for all, but there is no change in concentration between the Control and R2 samples in volunteer A.

β -hydroxybutyric acid was the least abundant VOC quantified using SIFT-MS. The greatest concentration was seen in the Respiratory restriction sample from volunteer B (3.1 ppb), and the lowest in the R2 sample from volunteer F (0.9 ppb). There was no deviation in mean β -hydroxybutyric acid concentration between R1 ($1.7 \text{ ppb} \pm 0.6$), Control ($1.6 \text{ ppb} \pm 0.4$), R2 ($1.6 \text{ ppb} \pm 0.6$) and Respiratory restriction samples ($1.7 \text{ ppb} \pm 0.6$).

Isoprene was also quantified using the NO^+ precursor ion. The greatest concentration of exhaled breath isoprene can be seen in the R1 sample from volunteer C (136 ppb) and the lowest in volunteer G in the Control sample (22 ppb). Mean exhaled concentrations for R1 ($88.1 \text{ ppb} \pm 30.0$), Control ($57.1 \text{ ppb} \pm 24.3$), R2 ($68.5 \text{ ppb} \pm 12.7$), and Respiratory restriction ($62.1 \text{ ppb} \pm 22.5$) show that there is a decrease in exhaled isoprene concentration during the Control and Respiratory restriction 6MWTs between their respective rest periods, R1 and R2. This pattern is seen in the majority of the volunteers. The post-hoc pairwise comparison shows that there is a significant difference between R1 and Control walk test samples ($P < 0.024$).

Exhaled breath acetone concentration was also quantified using the NO^+ precursor ion. The highest concentration of exhaled acetone seen using this ions was seen in the Control sample from volunteer B (519 ppb), with the lowest being observed in the Respiratory restriction sample from volunteer E (149 ppb). As with the H_3O^+ precursor ion there was a small increase in acetone concentration during the Control 6MWT, with a decrease during R2 followed again by an increase in the Respiratory restriction 6MWT. The mean concentration of acetone changed relatively little during the experiment, R1 ($269.1 \text{ ppb} \pm 95.4$), Control ($284.6 \text{ ppb} \pm 110.8$), R2 ($249.1 \text{ ppb} \pm 80.8$), and Respiratory restriction ($266.4 \text{ ppb} \pm 76.1$).

The greatest concentration of exhaled nitric oxide, Figure 4.26, was seen in the respiratory restriction sample from volunteer A (175 ppb), and the lowest in the Respiratory restriction sample from volunteer D (94 ppb). There was no real change in exhaled NO concentration, except for volunteer A, where there was a large increase in concentration in the Respiratory restriction sample. The mean concentrations reflect the lack of change in NO concentration, R1

(120.9 ppb \pm 12.8), Control (116 ppb \pm 11.9), R2 (117 ppb \pm 11.2), and Respiratory restriction (122.6 ppb \pm 24.9).

The greatest concentration of exhaled breath pentane was seen in volunteer A in the R2 sample (40 ppb), with the lowest in the Control sample from volunteer C (15.2 ppb). Pentane concentration seems to increase in the Control and R2 samples over the R1 sample, but decreases in the Respiratory restriction sample in volunteer A only, all of the other volunteers display a decrease in pentane concentration. Mean concentrations show that there is a small decrease from R1 (24.1 ppb \pm 3.0), to Control (21.7 ppb \pm 5.3), R2 (22.9 ppb \pm 7.3), and Respiratory restriction (20.9 ppb \pm 2.3) concentrations.

The greatest concentration of nitrogen dioxide, Figure 4.28, was seen in the exhaled breath of volunteer A from in the Control sample (27 ppb), and the lowest in volunteer C in the R2 sample (4.5 ppb). There is no clear trend observed in nitrogen dioxide concentration, though mean concentration between R1 (9.0 ppb \pm 3.4), Control (11.7 ppb \pm 7.6), R2 (10.5 ppb \pm 5.5), and Respiratory restriction (8.9 ppb \pm 2.3) samples shows that there is a small increase in the Control and R2 samples followed by a recovery to R1 concentration.

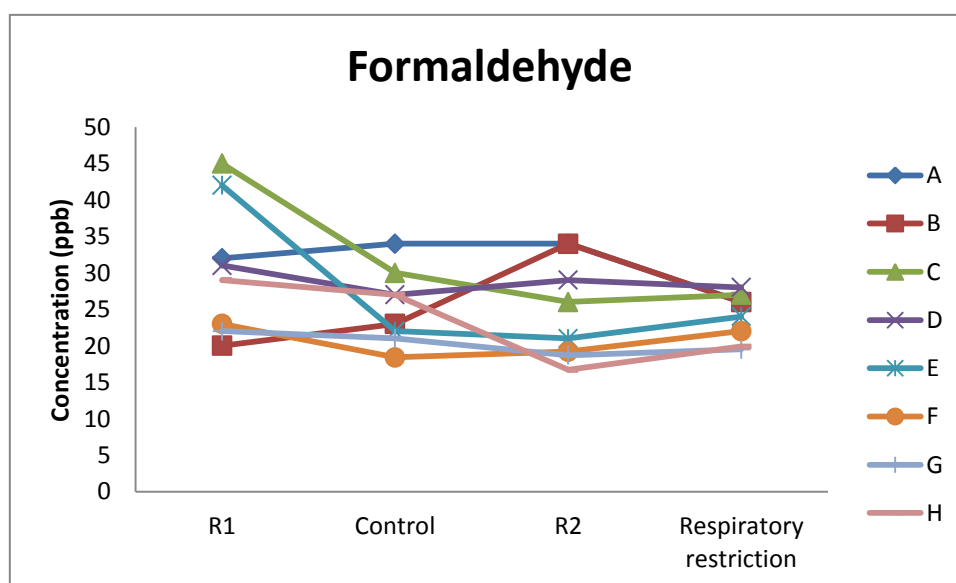


Figure 4.5 Exhaled breath formaldehyde concentration during the experiment quantified using SIFT-MS

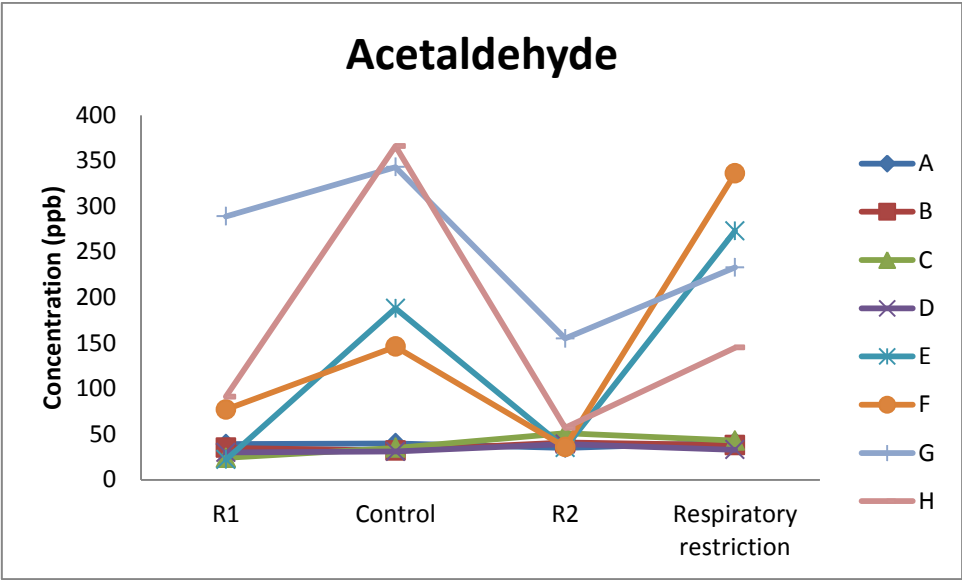


Figure 4.6 Exhaled breath acetaldehyde concentration during the experiment quantified using SIFT-MS

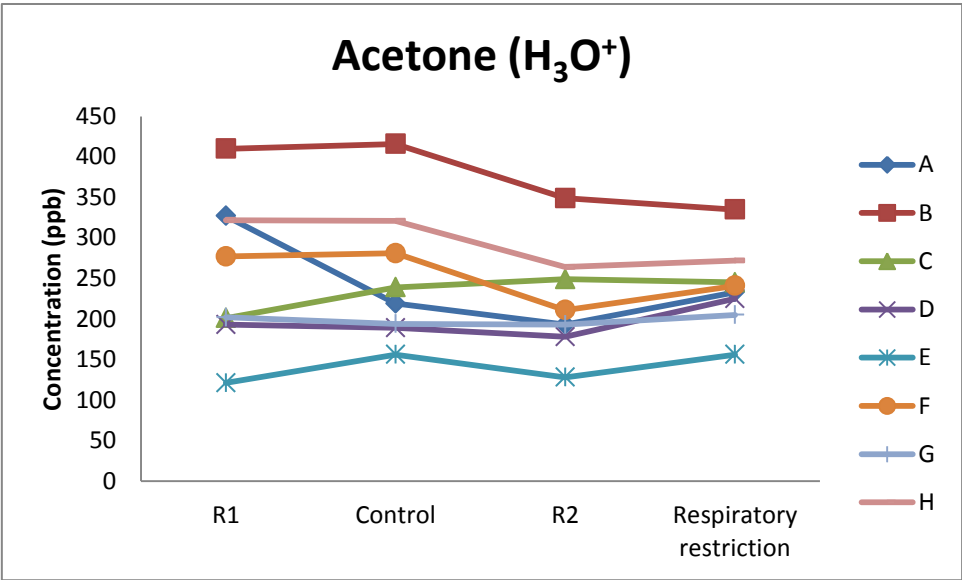


Figure 4.7 Exhaled breath acetone concentration during the experiment quantified with the H_3O^+ precursor ion using SIFT-MS

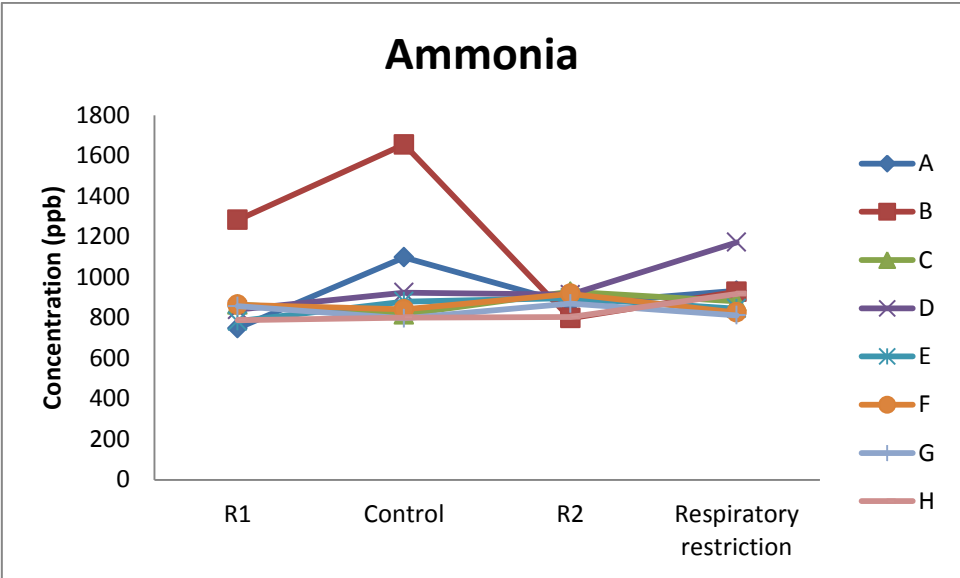


Figure 4.8 Exhaled breath ammonia concentration during the experiment quantified using SIFT-MS

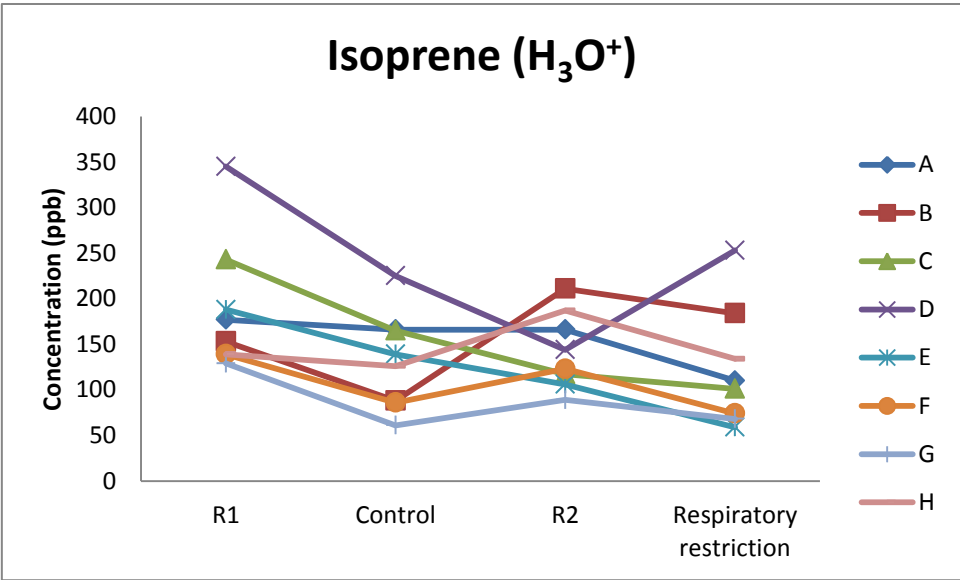


Figure 4.9 Exhaled breath isoprene concentration during the experiment quantified with the H_3O^+ precursor ion using SIFT-MS

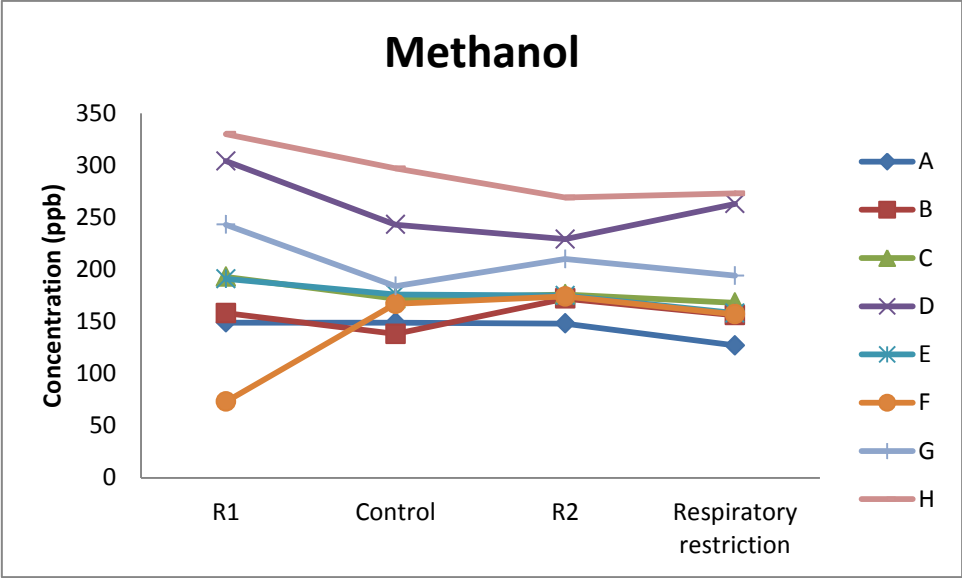


Figure 4.10 Exhaled breath methanol concentration during the experiment quantified using SIFT-MS

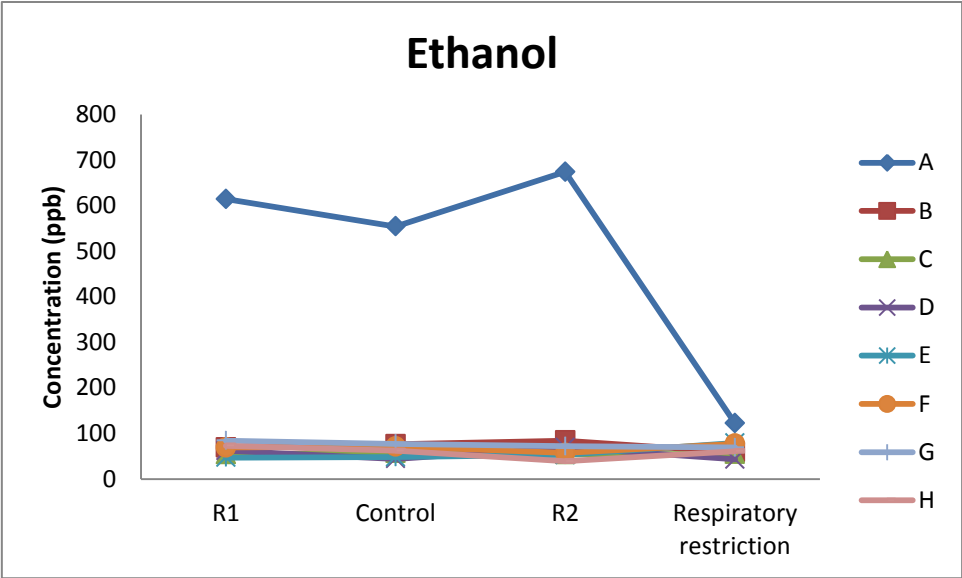


Figure 4.11 Exhaled breath ethanol concentration during the experiment quantified using SIFT-MS

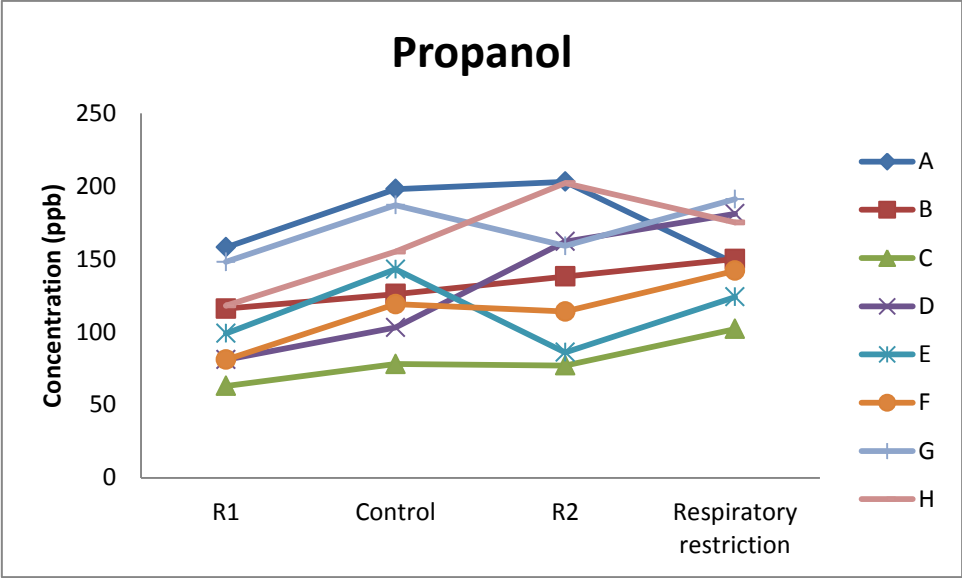


Figure 4.12 Exhaled breath propanol concentration during the experiment quantified using SIFT-MS

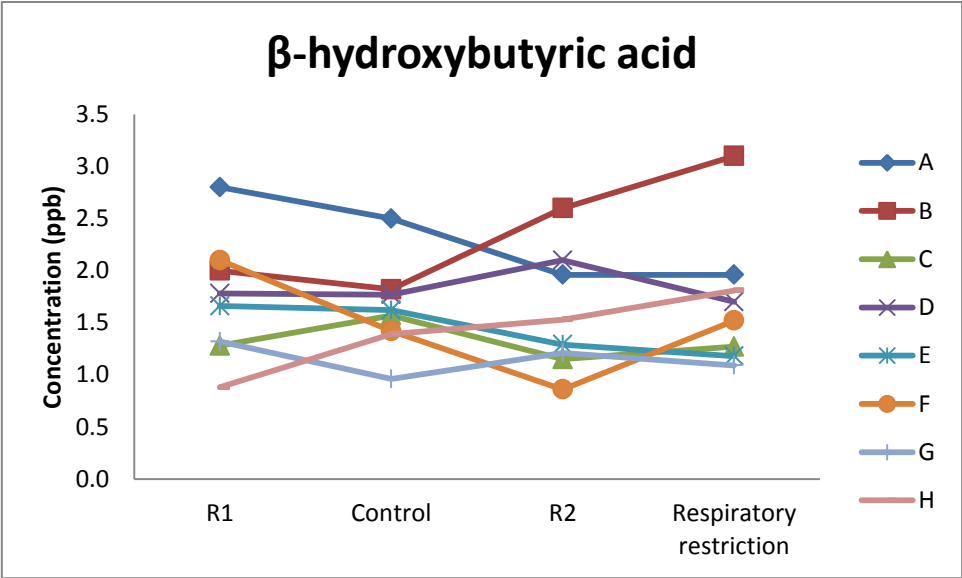


Figure 4.13 Exhaled breath β-hydroxybutyric acid concentration during the experiment quantified using SIFT-MS

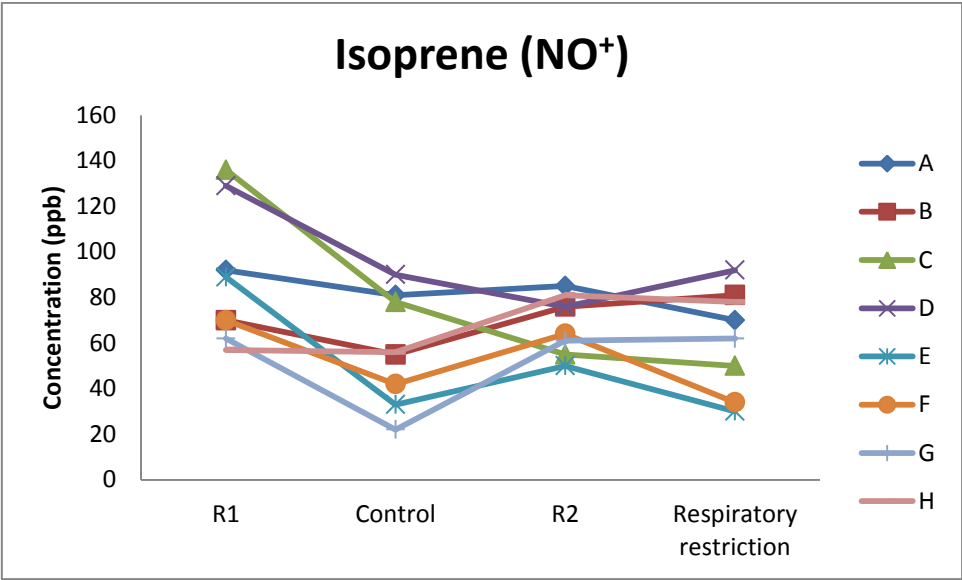


Figure 4.14 Exhaled breath isoprene concentration during the experiment quantified with the NO^+ precursor ion using SIFT-MS

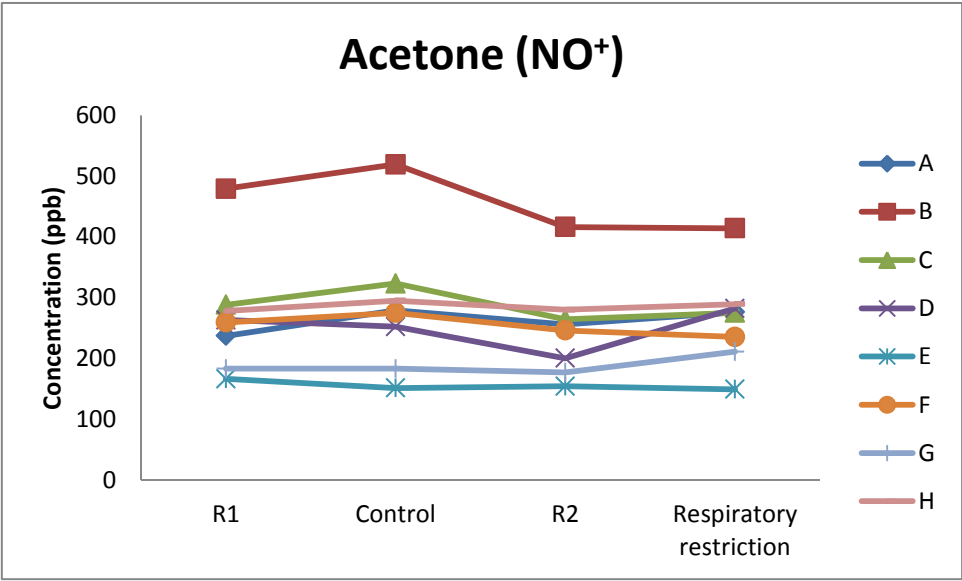


Figure 4.15 Exhaled breath acetone concentration during the experiment quantified with the NO^+ precursor ion using SIFT-MS

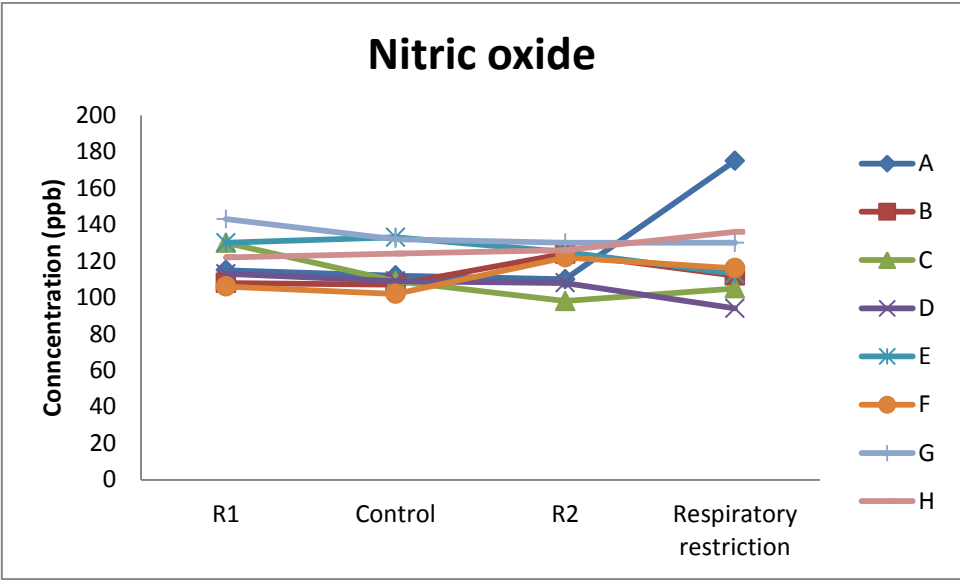


Figure 4.16 Exhaled breath nitric oxide concentration during the experiment quantified using SIFT-MS

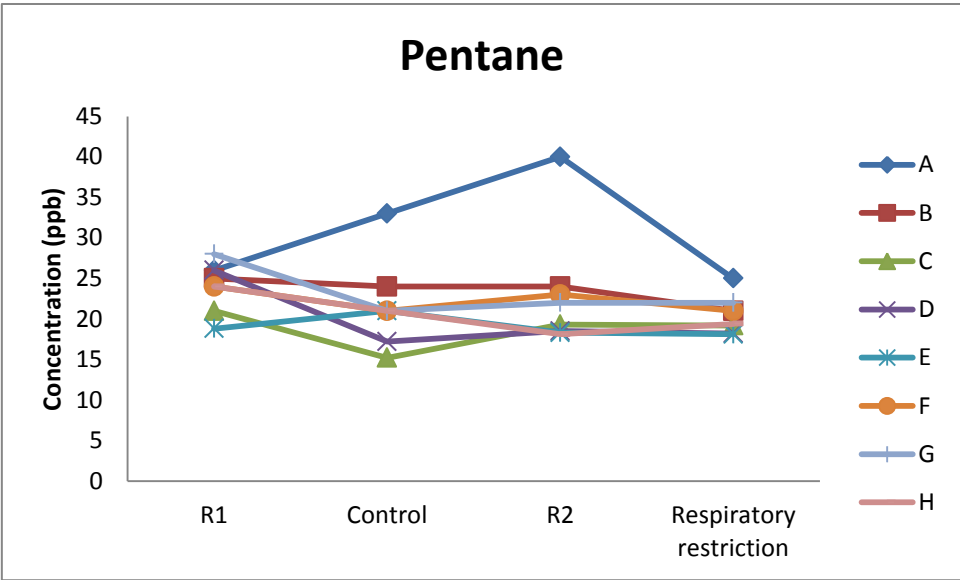


Figure 4.17 Exhaled breath pentane concentration during the experiment quantified using SIFT-MS

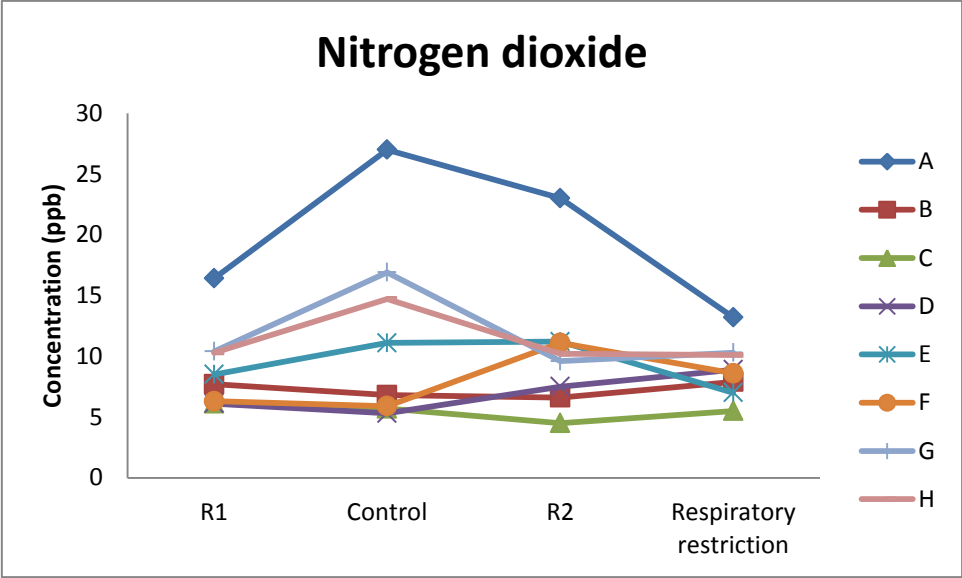


Figure 4.18 Exhaled breath nitrogen dioxide concentration during the experiment quantified using SIFT-MS

Compound	<i>P</i>
Formaldehyde	0.10
Acetaldehyde	0.06
Acetone (H ₃ O ⁺)	0.11
Ammonia	0.56
Isoprene	0.07 ¹
Methanol	0.70 ¹
Ethanol	0.91
Propanol	0.04 *
β-hydroxybutyric acid	0.88
Isoprene (NO ⁺)	0.02 *
Acetone (NO ⁺)	0.06
Nitric oxide	0.67
Pentane	0.22
Nitrogen dioxide	0.22

Table 4.4 Results of the tests within subjects ANOVA analysis on SIFT-MS data data (* = $P < 0.05$, ¹ = Greenhouse-Giessier correction applied)

4.3.3 GC-MS

Alignments were made as described previously in Chapter 2, and a list of candidate compounds generated. The compounds were acetaldehyde, Figure 4.19, isopentane, Figure 4.20, pentane, Figure 4.21, ethanol, Figure 4.22, isoprene, Figure 4.23, acetone, Figure 4.24, propanol (isopropyl alcohol), Figure 4.25, 1-propanol, Figure 4.26 and 2-butanone, Figure 4.27. Again an ANOVA analysis was performed to determine the significance of the changes in exhaled VOC concentration, Table 4.5. All of the results show an anomaly in exhaled VOC concentration in the control sample for volunteer H, most likely caused by contamination from a previous sample or a failure to seal the tube correctly. Again, one-way repeated measures ANOVA was used to statistically determine the significance of the changes in exhaled VOC concentration. There was no ethanol detected in the R2 sample for volunteer B, and no 1-propanol detected in the R2 and Respiratory restriction samples for volunteer H. For these reasons, these results were excluded from the ANAOVA analysis.

Exhaled breath acetaldehyde concentration, volunteer B (5.34 ng L⁻¹) and the lowest in the R1 sample from volunteer D (0.87 ng L⁻¹). All of the volunteers display a decrease in exhaled

acetaldehyde concentration during the Control 6MWT and R2, with recovery to R1 concentrations following the Respiratory restriction 6MWT except for volunteers A and D where concentration increases during the Control 6MWT and decreases thereafter. There is little change in mean concentration, in the first three samples taken (mean \pm SD), R1 ($3.3 \text{ ng L}^{-1} \pm 1.4$), Control ($3.1 \text{ ng L}^{-1} \pm 1.2$), R2 ($3.1 \text{ ng L}^{-1} \pm 0.9$), and Respiratory restriction ($3.6 \text{ ng L}^{-1} \pm 0.7$) concentrations but there is a small increase in concentration during the respiratory challenge.

The greatest concentration of isopentane is seen in the R1 sample from volunteer C (5.2 ng L^{-1}), with the lowest being quantified in the Respiratory restriction sample from volunteer C (1.7 ng L^{-1}). Mean concentration decreases during between R1 ($3.4 \text{ ng L}^{-1} \pm 1.3$) and Control ($2.8 \text{ ng L}^{-1} \pm 0.6$) samples and between R2 ($4.0 \text{ ng L}^{-1} \pm 0.8$) and Respiratory restriction ($2.8 \text{ ng L}^{-1} \pm 0.8$) samples.

Exhale pentane concentration was highest in the R2 sample from volunteer D (15.8 ng L^{-1}), and lowest in volunteer C (15.6 ng L^{-1}). Mean concentrations for R1 ($6.2 \text{ ng L}^{-1} \pm 5.6$), Control ($5.3 \text{ ng L}^{-1} \pm 3.0$), R2 ($9.8 \text{ ng L}^{-1} \pm 4.5$) and Respiratory restriction ($3.7 \text{ ng L}^{-1} \pm 2.1$) show that there is a decrease in concentration during the walk tests.

The greatest concentration of exhaled ethanol, can be seen in the R1 sample from volunteer C (6.8 ng L^{-1}), and the lowest in volunteer F (1.0 ng L^{-1}). There is no clear trend seen in exhaled ethanol concentration during the experiment, mean concentration between R1 ($6.2 \text{ ng L}^{-1} \pm 6.3$), Control ($5.5 \text{ ng L}^{-1} \pm 4.8$), R2 ($6.4 \text{ ng L}^{-1} \pm 4.2$) and Respiratory restriction ($3.4 \text{ ng L}^{-1} \pm 1.7$) decreases during the walk tests.

Exhaled isoprene concentration is highest in the R1 sample from volunteer D1 (323.6 ng L^{-1}), and lowest in the Respiratory restriction sample from volunteer G (101.9 ng L^{-1}). Mean concentration between R1 ($241.5 \text{ ng L}^{-1} \pm 59.7$), Control ($139.2 \text{ ng L}^{-1} \pm 27.7$), R2 ($168.9 \text{ ng L}^{-1} \pm 24.2$) and Respiratory restriction ($124.9 \text{ ng L}^{-1} \pm 45.0$) shows that isoprene concentration decreases during the experiment, the difference is significant between R1 and Control ($P < 0.019$), R1 and R2 ($P < 0.024$), and R1 and respiratory restriction ($P < 0.001$).

Exhaled acetone concentration was highest in the Respiratory restriction sample from volunteer B (346.9 ng L^{-1}), and lowest in the R1 sample from volunteer E (126.4 ng L^{-1}). Visually there is little difference in acetone concentration, except in volunteer B where acetone concentration increases during the experiment. Mean exhaled acetone concentration between

R1 ($178.7 \text{ ng L}^{-1} \pm 40.8$), Control ($197.6 \text{ ng L}^{-1} \pm 39.2$), R2 ($198.6 \text{ ng L}^{-1} \pm 63.4$) and Respiratory restriction ($210.7 \text{ ng L}^{-1} \pm 68.2$).

The highest concentration of exhaled propanol is seen in the Control sample from volunteer G (151.4 ng L^{-1}), with lowest being seen in the Control sample from volunteer E (1.1 ng L^{-1}). Mean concentration between R1 ($46.5 \text{ ng L}^{-1} \pm 31.8$), Control ($59.0 \text{ ng L}^{-1} \pm 47.1$), R2 ($28.8 \text{ ng L}^{-1} \pm 25.4$) and Respiratory restriction ($81.3 \text{ ng L}^{-1} \pm 40.0$) shows that propanol concentration increases during the walk tests, but the increase in concentration is only significant between R1 and respiratory restriction samples ($P < 0.05$).

Exhaled 1-propanol concentration was highest in the R2 sample from volunteer D (92.8 ng L^{-1}), with the lowest in the R1 sample from volunteer F (0.9 ng L^{-1}). Mean concentration between R1 ($7.9 \text{ ng L}^{-1} \pm 8.7$), Control ($11.4 \text{ ng L}^{-1} \pm 14.3$), R2 ($21.9 \text{ ng L}^{-1} \pm 32.4$) and Respiratory restriction ($16.6 \text{ ng L}^{-1} \pm 31.6$) shows that there is an increase in 1-propanol concentration during the experiments.

The highest 2-butanone concentration, is seen in the R1 sample from volunteer F (6.1 ng L^{-1}), with the lowest observed in the Respiratory restriction sample from volunteer D (2.4 ng L^{-1}). Mean concentration between R1 ($5.3 \text{ ng L}^{-1} \pm 0.7$), Control ($5.1 \text{ ng L}^{-1} \pm 0.6$), R2 ($4.9 \text{ ng L}^{-1} \pm 0.9$) and Respiratory restriction ($4.6 \text{ ng L}^{-1} \pm 1.1$) shows that there is little change in 2-butanone.

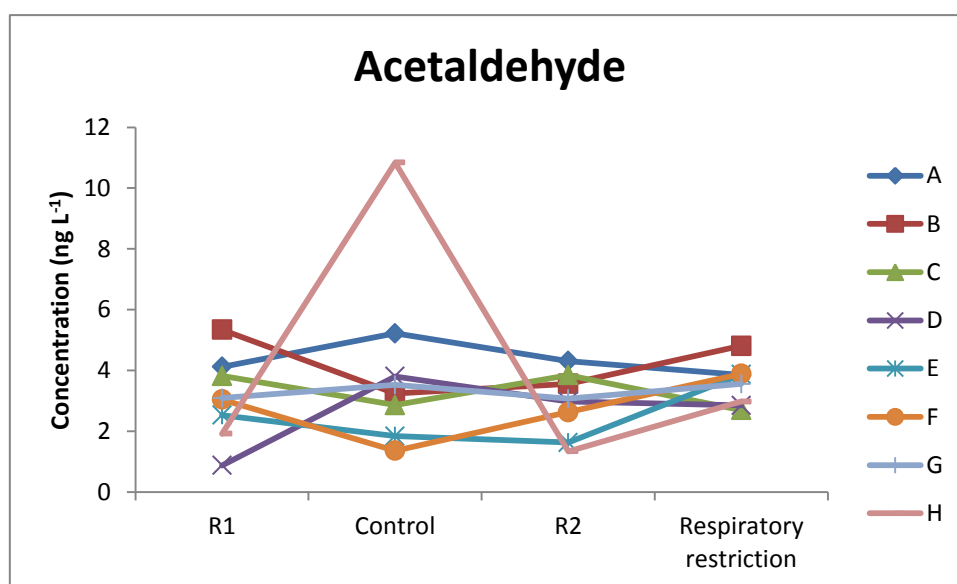


Figure 4.19 Exhaled breath acetaldehyde concentration during the experiment quantified using GC-MS

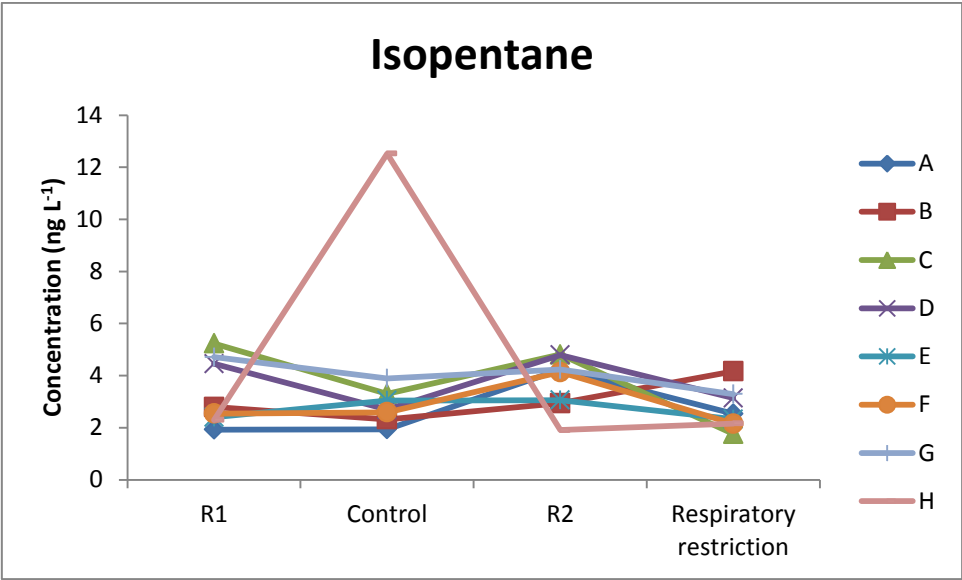


Figure 4.20 Exhaled breath isopentane concentration during the experiment quantified using GC-MS

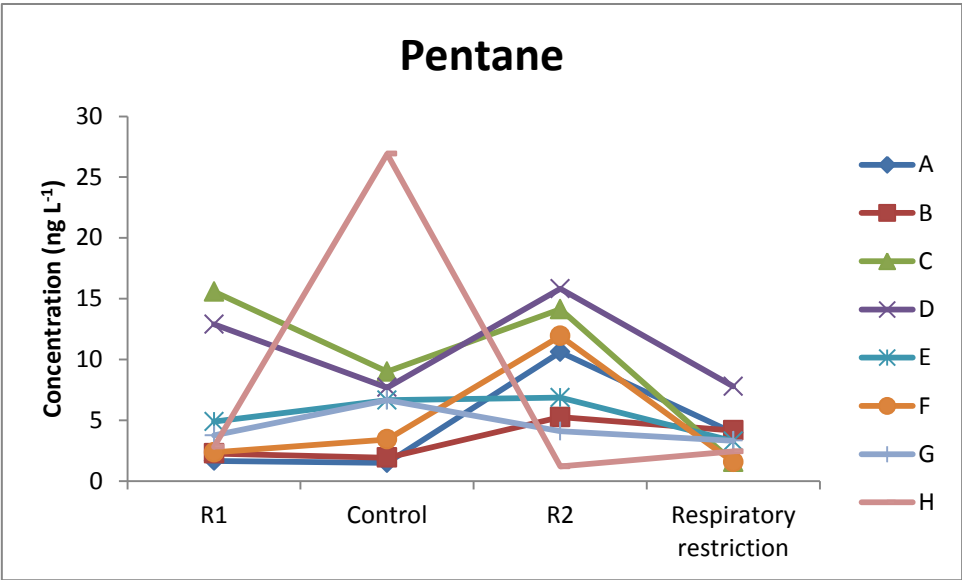


Figure 4.21 Exhaled breath pentane concentration during the experiment quantified using GC-MS

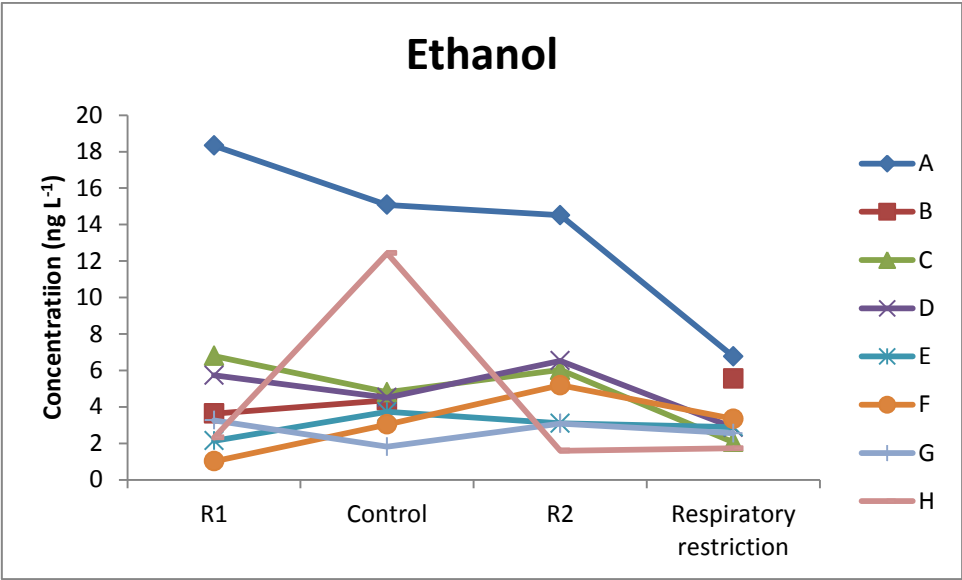


Figure 4.22 Exhaled breath ethanol concentration during the experiment quantified using GC-MS

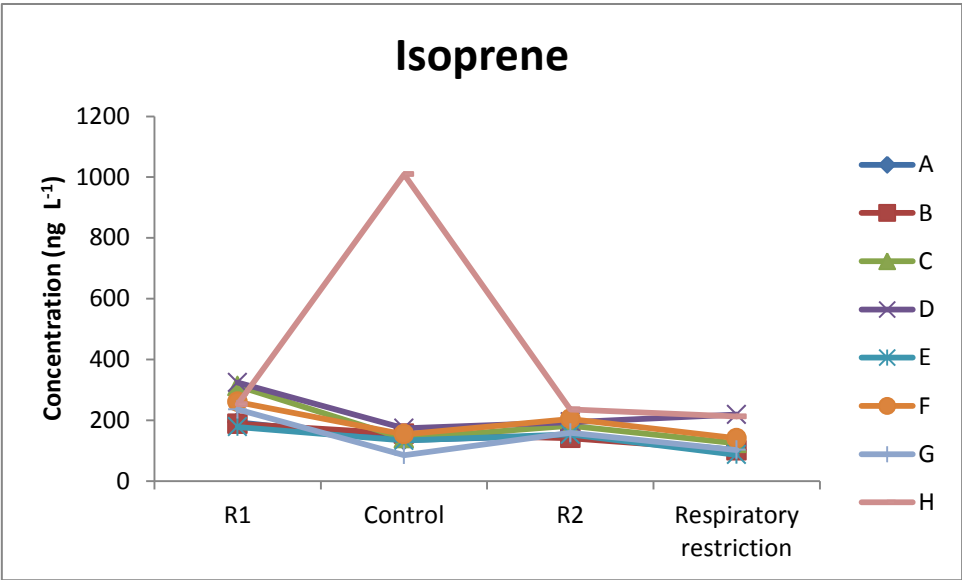


Figure 4.23 Exhaled breath isoprene concentration during the experiment quantified using GC-MS

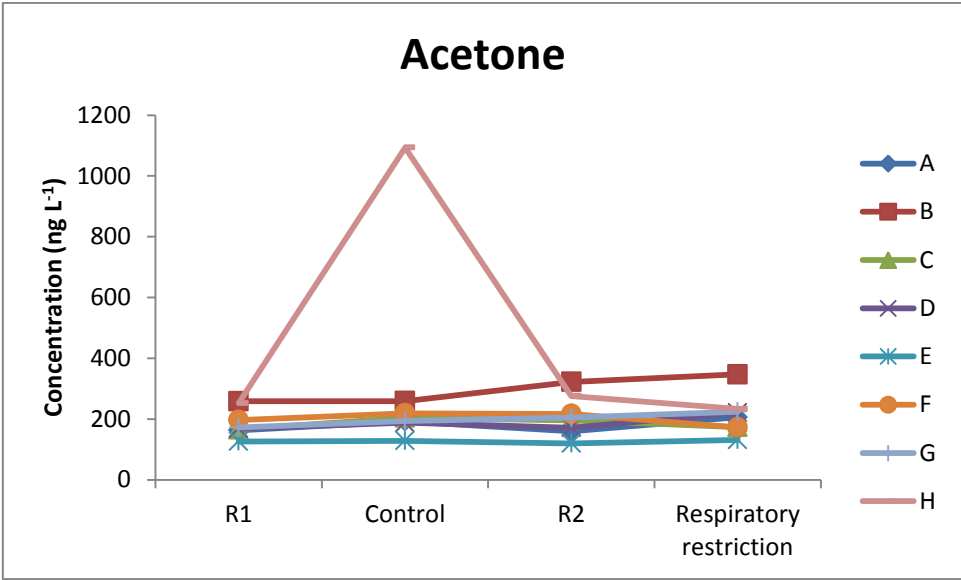


Figure 4.24 Exhaled breath acetone concentration during the experiment quantified using GC-MS

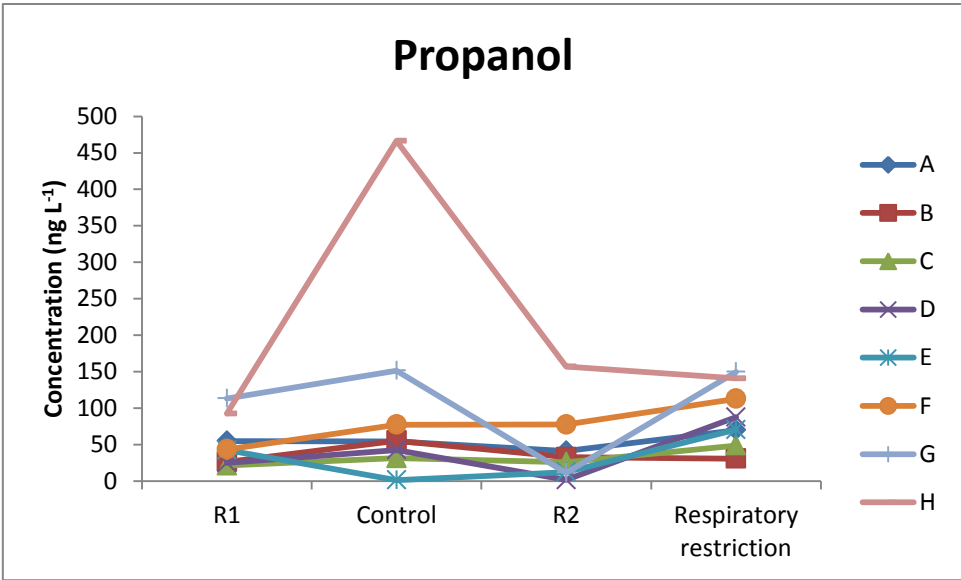


Figure 4.25 Exhaled breath propanol concentration during the experiment quantified using GC-MS

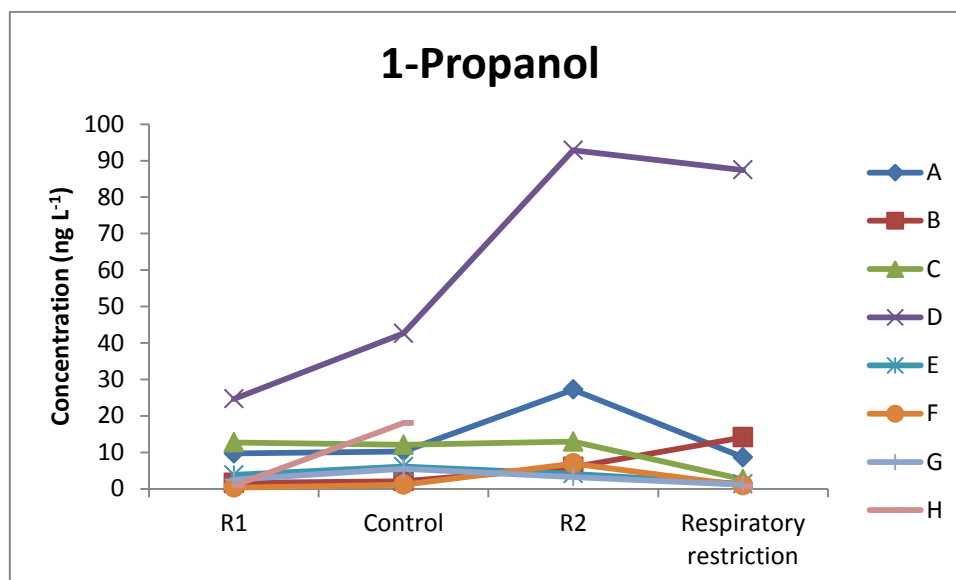


Figure 4.26 Exhaled breath 1-propanol concentration during the experiment quantified using GC-MS

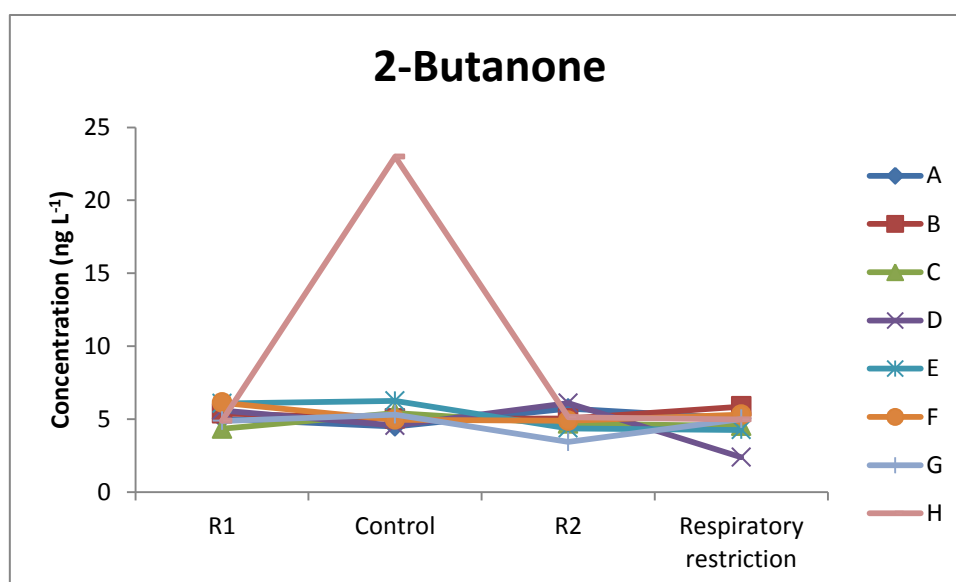


Figure 4.27 Exhaled breath 2-butanone concentration during the experiment quantified using GC-MS

Compound	<i>P</i>
Acetaldehyde	0.49
Isopentane	0.40
Pentane	0.11
Ethanol	0.11
Isoprene	0.00 *
Acetone	0.11
Propanol	0.02 *
1-propanol	0.26 ¹
2-butanone	0.49

Table 4.5 Results of the tests within subjects ANOVA analysis on GC-MS data (* = $P < 0.05$, ¹ = Greenhouse-Giessier correction applied)

4.4 Discussion

We have demonstrated using SIFT- and GC-MS there this is a significant decrease in exhaled isoprene and increase in propanol concentration in exhaled during a 6MWT with and without simulated airway narrowing, replicating symptoms of COPD in healthy volunteers. To our knowledge, this is the first time such an experiment has been performed using SIFT-MS.

There was no significant change in blood glucose concentration during the experiment between the rest periods and the two walk tests. This observation may be explained by the low intensity nature of the 6MWT. Studies have shown that blood glucose increases with the onset of exercise due to an increase in hepatic glycogen breakdown into glucose (Poortmans, 2004). Suggested regulators of hepatic glucose release are circulating hormones (insulin, glucagon, and catecholamines) and autonomic nerve impulses in liver tissue (Poortmans, 2004). It is thought that hepatic glucose glycogenolysis is stimulated by a mechanism coupled to the contraction of skeletal muscle contraction and the intensity of exercise (Poortmans, 2004). Insulin secretion decreases during exercise as muscle contractions produce an insulin-like effect, stimulating the uptake of glucose in cells (Ploug et al., 1987; Nesher et al., 1985; Hayashi et al., 1997; Holloszy et al., 2005). This enhances hepatic glucose release, when insulin levels are very low glucagon and adrenaline are more effective in stimulating glucose production (Kjaer 1998). The decrease in insulin prevents hypoglycaemia. The glucose output of 60 hour fasted volunteers was lower (0.9 mmol glucose units min⁻¹) than compared to volunteers that had fasted overnight (2.5 mmol glucose units min⁻¹) (Bjorkman and Eriksson,

1984). The greatest changes in blood glucose are seen at higher workloads, though remains constant at pre-exercise concentrations during low intensity exercise (Poortmans, 2004). The distance walked by the volunteers was reduced during the respiratory challenge and this was reflected in increased HR_{max} and a lower SpO_2 .

There was a decrease in mean exhaled isoprene concentration during the experiment, though the results were significant with only one precursor ion. Using SIFT-MS, where isoprene concentration was quantified using the H_3O^+ and NO^+ precursor ions, there was statistically no significant difference in isoprene concentration using the H_3O^+ ion, and only a significant decrease in concentration between the R1 and Control ($P < 0.024$) using the NO^+ ion. Using GC-MS there was a significant decrease in isoprene concentration between R1 and Control samples ($P < 0.019$), R1 and R2 ($P < 0.024$), and R1 and Respiratory restriction ($P < 0.001$) samples.

The reason why the decrease in exhaled isoprene concentration using the H_3O^+ precursor ion is insignificant maybe due to the fact that the protonated isoprene ($C_5H_9^+$) product ion overlaps with hydrated protonated methanol ($m/z = 69$), which is always present in breath when analysed using the H_3O^+ precursor ion (Španěl et al., 1999; Turner et al., 2006b) which may lead to overestimation of isoprene concentration. For this reason it is recommended to use the NO^+ or O_2^+ precursor ions for the quantification of isoprene in breath (Turner et al., 2006b). It therefore seems most probable that there was a reduction in exhaled isoprene concentration during this study which was not detectable by using Nalophan® bag samples, this trend may have been more visible by the use of online sampling.

Exhaled isoprene concentration was comparable to exhaled acetone concentration using SIFT-MS, and was one of the major constituents observed, this is similar to previous findings using PTR- and SIFT-MS (Taucher et al., 1997; Tuner et al. 2006b). A decrease in isoprene concentration was seen, though according to Stein and Mead, (1988) at low partial pressures of oxygen, peroxidation of squalene to isoprene is favoured, increasing the concentration in exhaled breath, though in our experiment SpO_2 did not fall below 92% in any of the volunteers and may explain why a decrease and not an increase is seen.

In our study, samples were collected in Nalophan® bags. Online sampling would have been the preferred method but was not practical in this instance. In comparison to a previous study, in one volunteer, using online PTR-MS (Karl et al., 2001), a short temporary increase in isoprene

concentration during the first 7 minutes of the experiment was reported during exercise on a bicycle ergometer followed by a decrease to below initial concentration and recovery to baseline concentration during recovery. King et al., (2009), who also performed a similar study using PTR-MS, suggested that changes in exhaled isoprene concentration are due to changes in haemodynamics or pulmonary function, and not increased clearance changes, due to the larger time constants of the endogenous biochemical pathways of isoprene production (i.e. the change in biochemical isoprene production is not within the timescale of the experiment). In a follow up study, King et al., (2010) showed during another ergometer experiment that profiles for exhaled isoprene, cardiac output and alveolar ventilation was virtually similar. According to King et al., (2010) this behaviour is attributed to the low blood:gas partition coefficient of isoprene, $\lambda_{b:air}=0.75$ at body temperature (Filser et al., 1996; Karl et al., 2001) and the fact that isoprene has a low Henry's Law constant and is not readily soluble in water (Lindinger and Jordan., 1998). In our study, there is both an increase in heart rate and decrease in SpO_2 during the individual walk tests. There is an indication that the test was more strenuous with the respiratory challenge due to the fact that the mean distance walked was considerably less. HR_{max} was greater and SpO_2 was lower, this is coupled with the lowest isoprene concentrations quantified during the entire experiment (volunteer G: H_3O^+ 22 ppb, NO^+ 68 ppb, and GC-MS 101.9 ng L⁻¹). Impaired, or poor pulmonary function may therefore explain why breath isoprene concentration was found to be lower in patients with COPD than in controls (although was statistically insignificant) (Poli et al., 2005), and significantly lower in patients with CHF than healthy controls (McGrath 2001). Isoprene production also follows circadian rhythm, similar to that seen with cholesterol biosynthesis (Stone et al. 1993), with different concentrations observed at different times of the day, so use may be limited for medically monitoring COPD in affected patients.

There was no significant change in exhaled acetone concentration during the experiment. A small increase in acetone concentration between R1 and Control 6MWTs and R2 and Respiratory restriction 6MWTs is can be seen (H_3O^+ volunteers C and E, NO^+ C and F and GC-MS C, D, E and F) which is consistent with previous findings using SIFT-MS (Senthilmohan et al., 2000; Turner et al., 2006b). In these previous studies acetone concentration was shown to increase during the exercise phase and recover to baseline concentration post-exercise. This would serve to increase lipid peroxidation, increasing the ketone bodies in exhaled breath. The lack of significant change in acetone concentration between volunteers and analytical methods may be due to several factors: The level of activity was insufficient to elicit a change in acetone

concentration, or the sample collection method was inadequate. There was no significant change in blood glucose concentration between the four samples taken; heart rate increased consistently in both 6MWTs, though greater heart rates were seen during the respiratory challenge and the blood oxygen of the volunteers did not fall below 88% (volunteer B). Short term hypoxia (SpO_2 at 75% for 30 minutes) has been shown to induce glucose intolerance in healthy individuals (Oltmanns et al., 2004). It is possible that the level of physical activity required to induce change in acetone concentration due to increased lipolysis was insufficient to induce a significant change.

Though inconsistent between the two analytical methods, increases in exhaled propanol concentration were seen with both SIFT-MS between R1 and Control ($P < 0.002$) and R1 and Respiratory restriction ($P < 0.037$), and with GC-MS between the initial, R1, and end, Respiratory restriction, samples ($P < 0.050$). The concentration of propanol was typically higher than that seen in previous studies (Turner et al., 2006a; Turner et al., 2008), and is lower than the concentration of acetone as would be expected due to enzyme mediated reduction of propanol to acetone (Marczin and Yacoub, 2002). Similar findings have been reported in ketonemic patients with elevated ratios of NADH/NAD^+ (Risby, 2002; Miekisch et al., 2004). This increase in propanol concentration may have several speculative explanations. Lactate is produced when cellular demand for energy is high, and the free concentration increases when the ability of the tissues to remove it diminishes. Propanoate metabolism is stimulated by an increase in lactate concentration and catalysed by the enzyme lactate dehydrogenase (LDH), this was possibly due to increased lactate production but, as whole blood samples were not collected and analysed for lactate there is no way to confirm this relationship.

The mean concentration of exhaled ammonia at the start of the experiment ($879.5 \text{ ppb} \pm 169.2$) was consistent with that seen in previous studies (833 ppb) (Turner et al., 2006a). The standard deviation is relatively low probably due to the fact that the volunteers were approximately of the same age; ammonia concentration has been shown to increase with age (Turner et al., 2006a). There was no significant change in exhaled ammonia concentration; though there was an increase in concentration during the two walk tests, with the higher mean concentration seen in the Control 6MWT ($976.5 \text{ ppb} \pm 291.4$). In an ergometer experiment, plasma and muscle ammonia concentration was shown to increase during exercise, and was attenuated by the consumption of carbohydrate (Snow et al., 2000). The insignificance of the increase in ammonia concentration may be due to the short duration of the experiment

limiting the breakdown of skeletal muscle for energy. During strenuous exercise, skeletal muscle ammonia production increases via the purine deamination cycle (PNC), where deamination of adenosine 5'-monophosphate (AMP) to inosine 5'-monophosphate (IMP) is catalysed by AMP deaminase (Lowenstein, 1972), and amino acid break down (Eriksson et al., 1985; Graham et al., 1993; Yuan and Chan, 2002). Unlike the liver, which can catabolise any of the twenty of the amino acids, skeletal muscle is limited to six amino acids, the branched chain amino acids (BCCA) leucine, isoleucine and valine, and glutamate, aspartate and asparagine.

There was no significant change in exhaled pentane concentration in our experiment, though the concentration of pentane has been reported to have increased in a graded aerobic exercise experiment with a decrease during recovery (Leaf et al., 1997). Inflammation and oxidative stress increases the concentration of lipid peroxidation products such as ethane and pentane (Miekisch et al., 2004). There was however no ethane detected in the chromatograms generated using GC-MS (our SIFT-MS instrument was not able to quantify ethane as kinetic information on that compound was not available). Gorham et al., (2009) argued that exhaled concentrations of ethane and pentane are biomarkers of environmental exposure and are not biomarkers of airway inflammation or oxidative stress.

NO concentration decreased during the exercise phases and returned to baseline concentration during the rest phases. This is intriguing as NO is a vasodilator, helping to open up the airways and increase blood flow. Persson et al., (1993) also observed a decrease in NO concentration during physical activity, but they state that when the increased ventilatory minute volume is taken into account the concentration of NO in exhaled breath increases. This may also be true for other compounds found within exhaled breath. This suggests that NO concentration increases during exercise and during hyperventilation at rest. An increase in exhaled breath NO during exercise was also observed by Mantione et al., (2007) using a Kiernan NO breath analyser. With Nalophan® bag samples that were collected in this experiment, the volunteers were instructed to breathe directly into the bag with as many out breaths needed until the bag was full. This method of sample collection does not take into account the minute volume; though it may be possible in the future to collect this information even with bagged samples using a Breathotron facemask with an incorporated flow sensor.

4.5 Conclusion

The concentration of isoprene and propanol changed significantly during the 6MWT. Two VOCs were shown to change significantly in concentration during a 6MWT in eight healthy adults with induced respiratory restriction.

There was little or no change in exhaled VOC concentration, with the majority of it being statistically insignificant. There was no statistically significant change in blood glucose concentration during the short exercise period. This suggests that it is unlikely that a short duration of physical activity or simulated respiratory narrowing will adversely affect exhaled VOC concentration and that this is linked to blood glucose concentration.

The decrease in exhaled isoprene concentration is more likely to be due to changes in blood flow and ventilatory rate, which was affected by the simulated airway narrowing, than biochemical changes. It is reported in the literature that isoprene concentration increases temporarily when using online fast flow tube methods. This phenomenon was probably not observed due to the use of Nalophan® sampling bags. This would suggest that this would also be true in patients with COPD. The decrease in propanol concentration may be a by-product of lactate breakdown.

NO concentration falls during the experiment, and this has also been seen to fall in previous studies. If the flow rate is measured, NO is shown to increase. It may be beneficial for the flow rate to be measured during exercise physiology experiments. Previous studies of this type that have used mass spectrometry tend to favour online sampling. Nalophan® bags may not be suitable for measuring isoprene in exercise physiology experiments due to the extremely volatile nature and rate of decay of the sample in air.

Whilst other studies have reported changes in concentration of the other VOCs quantified, this was not the case in this experiment. This may be due to several factors, such as the relatively short intensity of the exercise regime and dietary intake prior to the experiment.

As the volunteers were unfasted, the effects of not eating on VOC quantification are not really understood. One way to investigate this would be to include a positive and negative control, where one individual who has eaten but does not exercise, and another fasts before completing the experiment. The effects of repeating the experiment with the same volunteer are also not understood.

5 Monitoring the effect of exercise on exhaled metabolite concentration in real time using SIFT-, GC-MS and Breathotron

5.1 Introduction

In the previous chapters it was found that acetone concentration was not linked to blood glucose during an OGTT in healthy volunteers, a hypoglycaemic clamp in Type-1 diabetic patients and in healthy volunteers exercising under the influence of simulated airway narrowing (COPD). There were however, changes in exhaled VOC concentration that were unrelated to glycaemic status. In the previous chapter the effect of physical exercise and airway narrowing was investigated and found to have an effect on some exhaled VOC concentration during a 6 minute walk test with simulated respiratory narrowing. This experiment used offline SIFT-MS analysis, and Breathotron samples were not taken.

There have been several studies that have investigated the changes in VOC concentration during exercise (Senthilmohan et al., 2001; Turner et al., 2006b; King et al., 2009; King et al., 2010). It has been reported that there is a temporary increase in isoprene and acetone concentration during physical exercise attributed to increased blood flow rather than changes in biochemical production (clearance) (King et al., 2009; King et al., 2010). In the previous chapter this increase in isoprene concentration was not observed possibly due to the use of Nalophan® bags samples. In this chapter we shall investigate this phenomenon using online SIFT-MS and TD GC-MS to investigate if this temporary increase adversely affects Breathotron sensor performance.

5.2 Materials and methods

5.2.1 Modifications to the Breathotron Face Mask

In order to determine VOC clearance, breath flow rate must be measured. Though the Breathotron incorporates a flow sensor the maximum flow rate which can be recorded is 52 L min⁻¹. Whilst this is adequate for sedentary subjects, it is unsuitable for monitoring flow rates in exercising subjects, where flow rates are considerably greater. The solution to this problem was to employ a secondary flow sensor. A second flow sensor was placed in series with the first, Figure 5.1. This allowed flow rates up to 200 L min⁻¹ to be recorded. The second flow sensor was connected to an external 5 V power supply which shared a common ground with an Arduino Duemilanove microcontroller, the script that was uploaded to the microcontroller is included in Appendix B.2.1. The Arduino was connected to a personal computer (PC) running

a terminal listener, DevSys32 (Cranfield Health, Cranfield University, MK43 0AL), to provide data logging during the experiment. The data was saved in csv format.

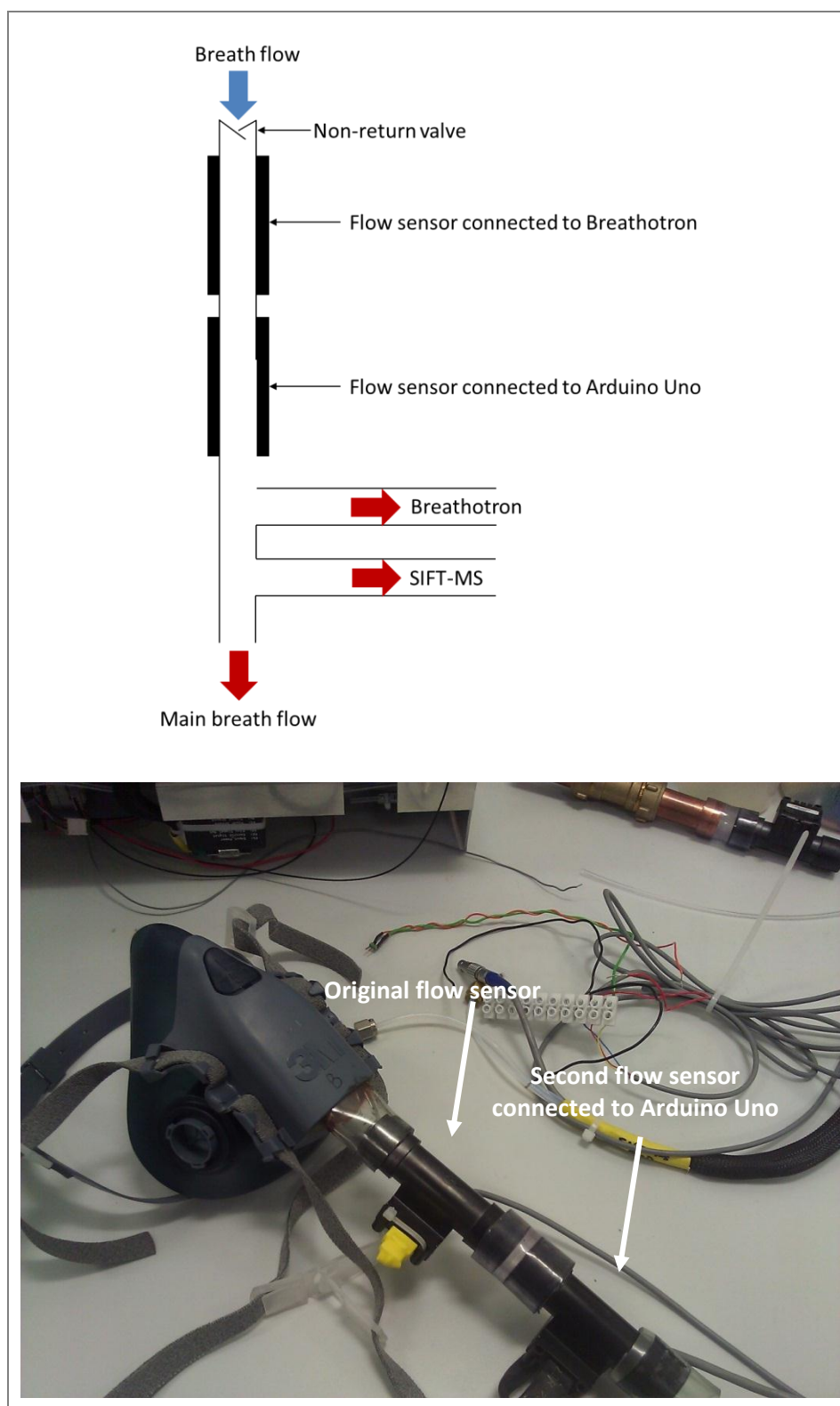


Figure 5.1 Line diagram (top) photograph (bottom) of the modified Breathotron face mask with secondary flow sensor in series and two sample outlets

5.2.2 Calibration of the bicycle ergometer

A bicycle ergometer can be used to measure the work performed by an individual. There is a distinction between work and power during exercise, individuals may be able to complete the same amount of work, but the time required to complete that work can vary between individuals. Conversely, given a set amount of time, not all individuals may be able to complete a similar quantity of work. The principles of how a bicycle ergometer works can be seen in Figure 5.2.

This description of cycle ergometry is derived from Roberts et al., (1997). The flywheel is driven a belt connected to the pedals. The force applied to the pedals drives the flywheel which in turn moves a pendulum attached to the belt. The distance moved by the pendulum is calibrated, and often includes a scale which increment in 0.5 kg units. The distance traversed by the circumference of the flywheel multiplied by the frictional force is equal to work.

The circumference of the flywheel was measured, 0.74 m, and the number of turns per 1 pedal revolution calculated, this equated to a distance of 6.105 m per pedal revolution. The cadence (revolutions per minute) was calculated by converting 22 km h⁻¹ to m min⁻¹ and then dividing circumference of the flywheel. Equation 5.1 was then used to calculate the work done during 1 minute with a cadence of 60.06 rpm and a (pendulum) load of 2 kg, this equates to approximately 120 watts (W).

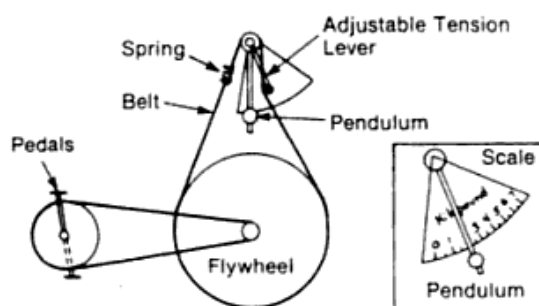


Figure 5.2 Principle of cycle ergometry (Reproduced from Roberts et al., 1997)

$$\text{Work} = \text{Cadence (rpm)} \times \text{load (kg)} \times 6.105 \text{ (m)} \times \text{duration (min)}$$

(5.1)

5.2.3 Bicycle ergometer challenge

With ethical approval from the CUHREC, the relevant paperwork is reproduced in Appendix D.2; volunteers from within the school (Health) were recruited by mass email. The volunteers

were asked to fast for a period of 8-14 hours before the experiment. During the fasting period they were permitted to drink water and prohibited from brushing their teeth with toothpaste (permitted using water only), showering, shaving or using any other cosmetic products.

Because there was a small but finite chance that the fasting blood glucose measurement would have an abnormal value indicative of a stage of diabetes or insulin resistance, a research nurse was present at each bicycle ergometer challenge to interpret and discuss the implications of this with the affected volunteer, and to assist volunteers in taking blood samples if they are unable to do so themselves.

Prior to the experiment each volunteer was assigned a random letter drawn by the volunteer 'from a hat'. The random letter assigned was known only to the volunteer and the researcher, no other identifying data was collected. Two of these letters were assigned as positive (did not fast and underwent the ergometer challenge) and negative controls (fasted but did not take part in the ergometer challenge). Upon arrival in the SIFT-MS laboratory their weight (kg) and height (m) then measured and recorded using a set of bathroom scales and a tape measure. These were then used to calculate body mass index (BMI) using Equation 2.1. Any volunteer that had a BMI less than 18 (medically considered to be underweight) or greater than 25 (overweight) was not permitted to enter the study as per the recruitment criteria. Lung function was evaluated using a hand held spirometer (MicroMedical, MicroPlus, Basingstoke, RG22 4BS) three times, averaged and recorded.

A face mask connected to both the SIFT-MS and the Breathotron was placed around the volunteer's face. The bicycle ergometer (BodyGuard, Ergometer 990, Jonas Øglænd, Aksjeslskap, Norway) was then adjusted to the volunteer's comfort, and the volunteer then then to ask to mount the ergometer. The volunteer was then instructed to breathe into the face mask at a steady normal rate (no special breathing techniques were required), simultaneously, the SIFT-MS, Breathotron and flow rate logging PC were started. A TD tube was also inserted into the Breathotron prior to starting the experiment to collect a sample for analysis using GC-MS.

Once a representative sample was obtained, the volunteer was asked to maintain a speed of approximately 22 km h⁻¹ (13.67 mph) for 5 minutes on a bicycle ergometer set at 120 Watts. Immediately after the 5 minute cycling period another sample of breath was analysed using the Breathotron, with a new TD tube inserted into the Breathotron before this sample was

analysed, whilst a final sample was analysed following a 15 minute rest period after finishing the exercise portion of the experiment.

Pulse rate and blood oxygen saturation was recorded every minute for the duration of the experiment via a pulse oximeter (Smiths Medical International Ltd, BCI® 3301, Watford, WD24 4LG) attached to the volunteer's finger. Core body temperature was measured at each interval that a Breathotron sample was analysed using a Braun® Thermoscan™ ear thermometer (Proctor & Gamble, Cincinnati, Ohio, US), as was blood glucose concentration (Abbot, Therasense, Illinois, IL, US).

The experiment was stopped in the event that the volunteer felt uncomfortable, or became exhausted whilst cycling. They were also free to withdraw at any time without providing a reason. In the event that the volunteer's heart rate exceeded approximately 80% of their calculated maximum heart rate ($220 - \text{volunteer's age in years}$) (HR_{\max}), they were asked by the researcher to stop immediately and rest on a medical crash trolley. Figure 5.4 shows the experimental set up, with Breathotron, ergometer, crash cart and Arduino data logger all within the vicinity of the SFIT-MS.

Each volunteer completed the experiment twice, with the second experiment being conducted 7 days after the first.



Figure 5.3 Ergometer challenge experimental set up showing the proximity of the ergometer to the Breathotron and SIFT-MS

5.2.4 SIFT-MS

Online sampling of breath directly into the SIFT-MS was used in this experiment through the Breathotron face mask as previously described in 2.2.5. In the MIM ion scan the isoprene, acetone, nitric oxide, ammonia and pentane product ions were selected to be quantified using the O_2^+ precursor ion. SIFT-MS sampling commenced with the start of Breathotron sampling and did not finish until the last Breathotron sample had been collected.

5.2.5 Breathotron

Breathotron 001 was selected at random to be used in this study. The Breathotron was switched on and the baseline resistance of the sensor was left to stabilise for a minimum period of fifteen minutes before any samples were taken. Prior to starting the experiment, the ambient laboratory air was analysed.

Three breath samples were analysed at different stages during the experiment. The first of these was the Rest sample, taken at the beginning of the experiment. Once this sample had been collected the volunteer commenced the ergometer challenge, described in the previous section. At the end of the Cycling phase another sample was taken. A further sample was recorded 15 minutes after the end of the Cycling phase; this was known as the Recovery phase sample.

5.2.6 GC-MS

Breath samples were also preconcentrated onto TD tubes using the Breathotron. These samples mirrored the Breathotron sensor samples. Following the experiment the samples were then stored at 4°C before analysis. Internal standard was applied to each of the tubes as mentioned in Chapter 2 prior to analysis. The GC-MS method used was the same as in Chapter 2.

5.3 Results

5.3.1 Bicycle ergometer challenge

Initially eight volunteers, 4 male and 4 female, were recruited from within the school to take part in the experiment. One volunteer, E withdrew on medical grounds between the first and second experiment. The data from volunteer E is not presented in the results. Volunteer H was the positive control, had eaten less than 8 hours prior to the experiment, and volunteer N was the negative control, fasted but did not participate in the ergometer challenge. All of the volunteers that completed the experiment displayed no diabetic characteristics following the overnight fast, and all fell within the BMI criteria. None of the volunteers exhibited abnormal lung function.

Spirometry, pin prick blood glucose concentration and BMI data is reproduced in Table 5.1. There is considerable difference in the age between the youngest and oldest volunteers, 32 years, though there is less deviation in lung function and BMI.

Volunteer	Age (years)	Gender	FEV ₁ (L)	FVC (L)	FER (L)	PEF (L min ⁻¹)	BMI (kg m ⁻²)
B	28	M	4.94	5.18	95	675	23.7
K	39	F	2.35	2.80	84	322	18.4
D	22	M	4.87	5.37	87	540	22.9
H (Positive control)	26	M	3.69	4.72	77	453	25.4
M	30	F	3.33	3.86	86	497	22.0
L	32	M	3.19	3.83	83	451	24.8
N (Negative control)	54	F	2.52	2.81	89	261	25.6
Mean	33	-	3.56	4.08	86.0	457	23.2
Standard deviation	10.7	-	1.00	1.10	5.6	137.2	2.5
Median	30	-	3.33	3.86	86	453.3	23.7
Range	32	-	2.59	2.57	18	414.67	7.19

Table 5.1 Lung function and BMI of the seven volunteers

The various physiological parameters, heart rate, blood oxygen saturation, body temperature and blood glucose concentration are shown aligned to the continuous online SIFT-MS data and the clearance rate, in mg min⁻¹, derived from the additional flow sensor, with the experiment number appended to the volunteer identifier.

Clearance in mg L⁻¹ was derived by dividing concentration by 24.4, the volume occupied by 1 mole of gas in a litre, and multiplying by the weight of the compound being converted. This was then multiplied by the volume exhaled each minute.

Vertical dashed lines indicate the various stages of the experiment: rest, cycling and recovery. As the initial rest phase was dependant on Breathotron sampling times they vary in length from volunteer to volunteer and sample to sample.

Data from the first and second experiments seen for volunteer B in Figure 5.4 and Figure 5.5, K Figure 5.6 and Figure 5.7, D Figure 5.8 and Figure 5.9, H, the positive control, in Figure 5.10 and Figure 5.11, M Figure 5.12 and Figure 5.13, L in Figure 5.14 and Figure 5.15 and N, the negative control, in Figure 5.16 and Figure 5.17. There is a small offset noticeable in some of the continuous SIFT-MS data which is believed to be due to the dead space of the sampling head.

Repeated measures ANOVA analysis was performed in IBM SPSS version 19, with the null hypothesis that there was no change in physiological parameters or VOC concentration during the experiment. The null hypothesis was rejected if $P < 0.05$.

The continuous change in heart rate is shown in the top graphs for all volunteers. The data is incomplete in some cases due to the fact that heart rate was recorded by hand by the researcher, and in some cases the pulse oximeter fell off the volunteer's finger. The instances where this has occurred are recorded on the graphs.

The bicycle ergometer challenge caused an increase in BPM in all of the volunteers that were asked to exercise. There is little change in BPM of the negative control volunteer, N. This is true for both experiments, though higher BPMs are seen in the second experiment for volunteers B, K and L.

Blood oxygen saturation was also recorded manually, and like the heart rate data is incomplete, again the instances of where the sensor became detached from the volunteer are shown in the graphs. There generally a small decrease in SpO_2 during the cycling phase of the experiment which returns to pre-exercise levels during recovery. SpO_2 does not fall below 90% in either ergometer challenge experiment except in the case of volunteers D and H in the first experiment and volunteer K during the second.

All of the volunteers, bar volunteer D, display a small decrease in core body temperature during the first ergometer challenge, except for volunteer L where there is a small increase in temperature at the end of the experiment. Mean temperature (\pm SD) during the Rest phase during the first ergometer challenge changes little, Rest 36.5 °C (± 0.3), Cycling 36.4 °C (± 0.1) and Recovery 36.3 °C (± 0.2). The decrease in temperature is seen again in the second experiment, where mean temperature during the Rest phase is 36.7 °C (± 0.3), Cycling 36.6 °C (± 0.1) and Recovery 36.6 °C (± 0.2), though there is an increase in body temperature during the recovery phase in volunteers K and L. There is no significant change in core body temperature $P < 0.85$.

There is no change in blood glucose concentration in either of the ergometer challenges, during the first ergometer challenge mean (\pm SD) Rest blood glucose concentration is 5.3 mM (± 0.7), Cycling 5.1 mM (± 0.8) and during the Recovery phase 5.2 mM (± 0.8). In the second ergometer challenge mean Rest blood glucose concentration is 5.2 mM (± 0.3), immediately

after Cycling 5.1 mM (\pm 0.6) and during Recovery 5.2 mM (\pm 0.6). Statistical analysis confirms that there was no significant change in blood glucose concentration $P < 0.05$.

There is an increase in acetone and isoprene concentration with the onset of the Cycling phase in volunteer B, Figure 5.26, during the first experiment (B1) which decreases during the recovery phase. Acetone is the highest concentration component, whilst isoprene and pentane are equally lowest. There is also an increase in water vapour during the cycling phase. There is negligible change in the other VOCs quantified during the Rest and Recovery phases. The increase in all selected ion products towards the end of the experiment is due to electrical interference, as seen in previous experiments. The VOC clearance for experiment B1, Figure 5.27, shows that all selected ion products increase in concentration during the Cycling phase from Rest concentrations and decrease during the Recovery phase.

In experiment B2, isoprene, acetone and pentane concentration is lower than in the previous experiment, whilst ammonia is similar to that seen in experiment B1. The increase in isoprene and acetone concentration is lower than was seen in the previous experiment with this volunteer. The concentration of nitric oxide in B2 is higher than B1. As in experiment B1, the rate of VOC production increases in experiment B2 with the onset of the Cycling phase. There is a greater increase in nitric oxide than in experiment B1. The rate of isoprene, acetone ammonia and pentane increase is less than seen in experiment B1.

Volunteer K found the cycling phase to be too difficult during the first experiment, and hence the phase lasts for approximately 2 minutes and this may have contributed to the lack of change in VOC concentration. Of the VOCs, the concentration of ammonia is greatest whilst pentane is the least abundant. There is little change in nitric oxide concentration during the experiment. In the second experiment, K2, again the concentration of all VOCs is similar to the previous experiment with this volunteer. The VOC production graphs for K1, show a greater increase in pentane production in comparison to the other VOCs, this is not true in the second experiment, K2, where nitric oxide production is greater than all other VOCs.

In experiment D1 of acetone is the greatest in concentration, whilst pentane is the least abundant. There is an increase in isoprene and acetone concentration with the onset of the Cycling phase and a decrease in nitric oxide. The clearance graph for experiment D1 shows an increase in nitric oxide and all other VOCs during the Cycling phase. The concentration of nitric oxide is lower in the second experiment, D2; in comparison to D1 the concentration of nitric

oxide is lower, whilst the concentration of the VOCs is similar to the previous experiment. There is a smaller increase in nitric oxide and VOC clearance in D2, in comparison to experiment D1.

Volunteer H was the positive control. The VOC profile from H1 can be seen. Ammonia is the most abundant VOC, whilst pentane concentration is the lowest. There is a decrease in ammonia during the Rest and Cycling phases, with an increase towards the end of the experiment. There is a temporary increase in acetone and isoprene concentration with the onset of the Cycling phase, which decreases during the Recovery phase. There is little change in nitric oxide concentration during the experiment. There is an increase in all selected ion concentration towards the end of the experiment due to suspected electrical interference. The greatest increase in clearance during the Cycling phase was seen in nitric oxide in experiment H1. The increase in acetone concentration was greater than the change in ammonia, despite the fact that ammonia concentration was greater in the raw time profile. In the second experiment, H2 Figure 5.40, again the concentration of ammonia was greater than the other VOCs, but lower than the first experiment. Again pentane concentration is lowest of all of the VOCs quantified. The concentration of nitric oxide remains largely constant, though there is an increase towards the end of the experiment. The concentration of acetone and isoprene increases during the Cycling phase, which decreases during the Recovery phase.

There is an increase in nitric oxide concentration during the experiment in M1. Ammonia is the most abundant VOC throughout the experiment, with little change in concentration. The acetone and isoprene concentration increase temporarily during the Cycling phase and decrease during the Recovery phase. There is no change in pentane, the least abundant VOC, concentration. The VOC clearance time profile for M1 shows the greatest change in rate for nitric oxide. There is an increase in acetone and isoprene, ammonia and pentane concentration before the start of the Cycling phase this may have been caused by the volunteer talking during sampling. There is a decrease in nitric oxide and acetone concentration during the second experiment in M2 in comparison to M1. The concentration of ammonia, isoprene and pentane are similar to M1. There is an increase in acetone and isoprene concentration with the start of the Cycling phase. The change in clearance during M2 is comparable to M1, though there is a greater change in nitric oxide in the previous experiment.

The greatest exhaled breath acetone concentration was seen in volunteer L. The concentration of acetone does not change in experiment L1 even with the onset of the Cycling phase. This is also true for isoprene, ammonia and pentane. There is a small decrease in nitric oxide during the Cycling phase, but there is a small increase during the recovery phase. The clearance time profile for L1, shows an increase in nitric oxide and all VOCs during the Cycling phase, there is a temporary increase in acetone and nitric oxide concentration during the Recovery phase. This may have been caused by the volunteer moving from the bike to the crash cart. In experiment L2, the concentration of acetone and nitric oxide are similar, there is a small decrease in both during the Cycling phase, and a small, temporary increase in exhaled isoprene concentration. Ammonia and pentane, least abundant, concentration remains constant throughout the experiment. There is an increase in clearance in M2 in all selected ion products apart from isoprene during the Cycling phase, with a decrease during the Recovery phase. The increase in acetone, ammonia and pentane is greater than in the first experiment, L1.

Volunteer N was the negative control. In the first experiment, N1 there is no change in nitric oxide or VOC concentration for the duration of the experiment. Ammonia concentration is greatest of the VOCs, whilst pentane is the least abundant. The clearance time profile for N1, Figure 5.50, shows that there is no change in the rate of production of any of the selected ion products. The raw time profile from N2, Figure 5.51, again displayed no change in nitric oxide or VOC concentration during the experiment, though the concentration of acetone was greater than seen in N1. The clearance time profile for N2 shows the same pattern as seen in N1, no change in the rate of production of selected ion products.

Repeated measures ANOVA of both the raw and VOC clearance time profiles was performed by taking the concentrations from the time points that the Breathotron samples were collected, in the case of VOC clearance where the flow data was truncated the final point was used, Table 5.2. The concentrations from each of the time points were treated as variables in the statistical analysis to determine if there was a significant change within and between experiments and sampling time points. The statistical analysis did not include the positive and negative controls. Significant correlations are marked in the table with an asterisk (*). There was only a significant change in acetone clearance between the Rest and Cycling phases ($P < 0.05$) and the Rest and Recovery phases ($P < 0.05$).

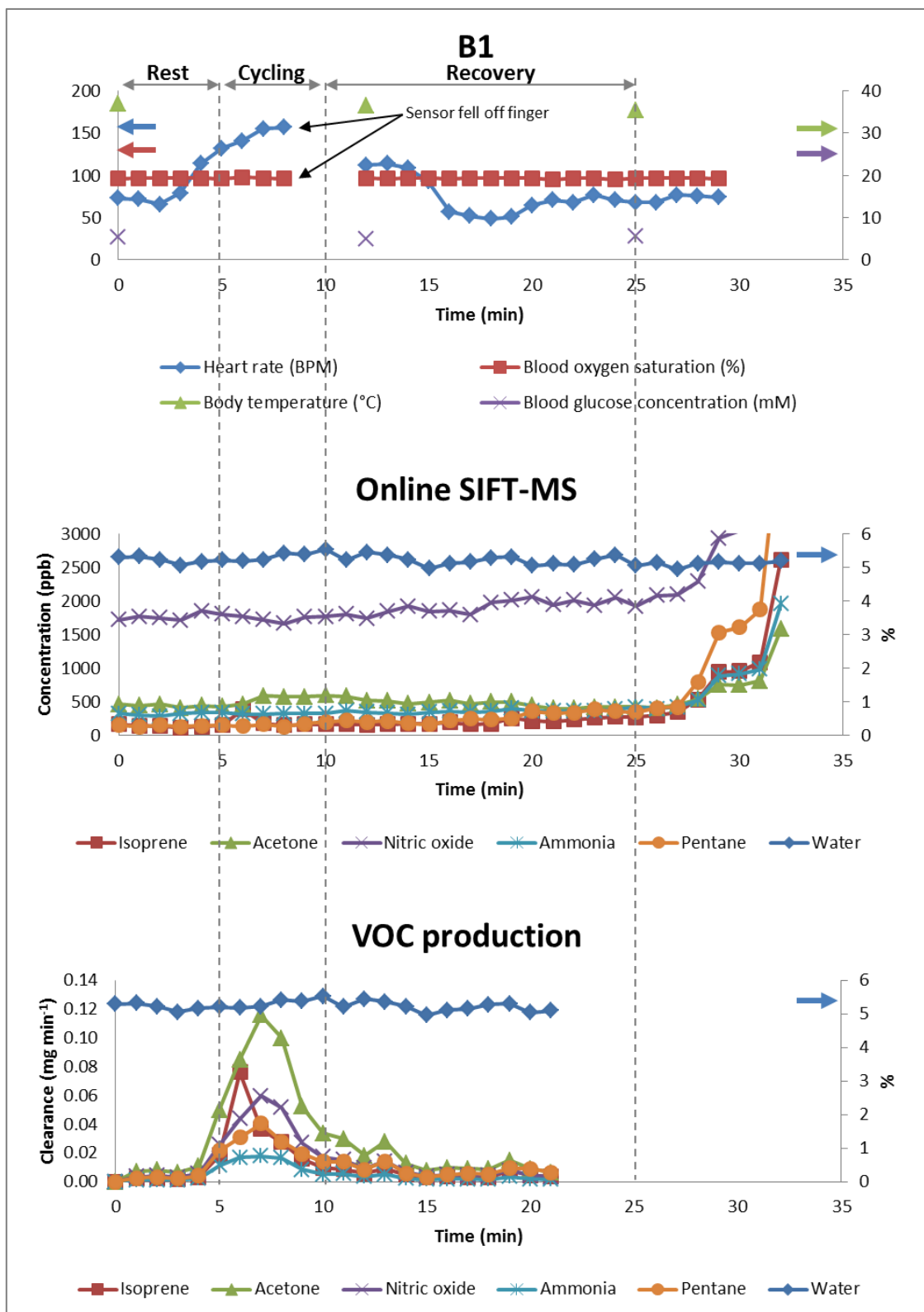


Figure 5.4 Physiological parameters and continuous online sampling of exhaled breath from volunteer B during the first ergometer challenge

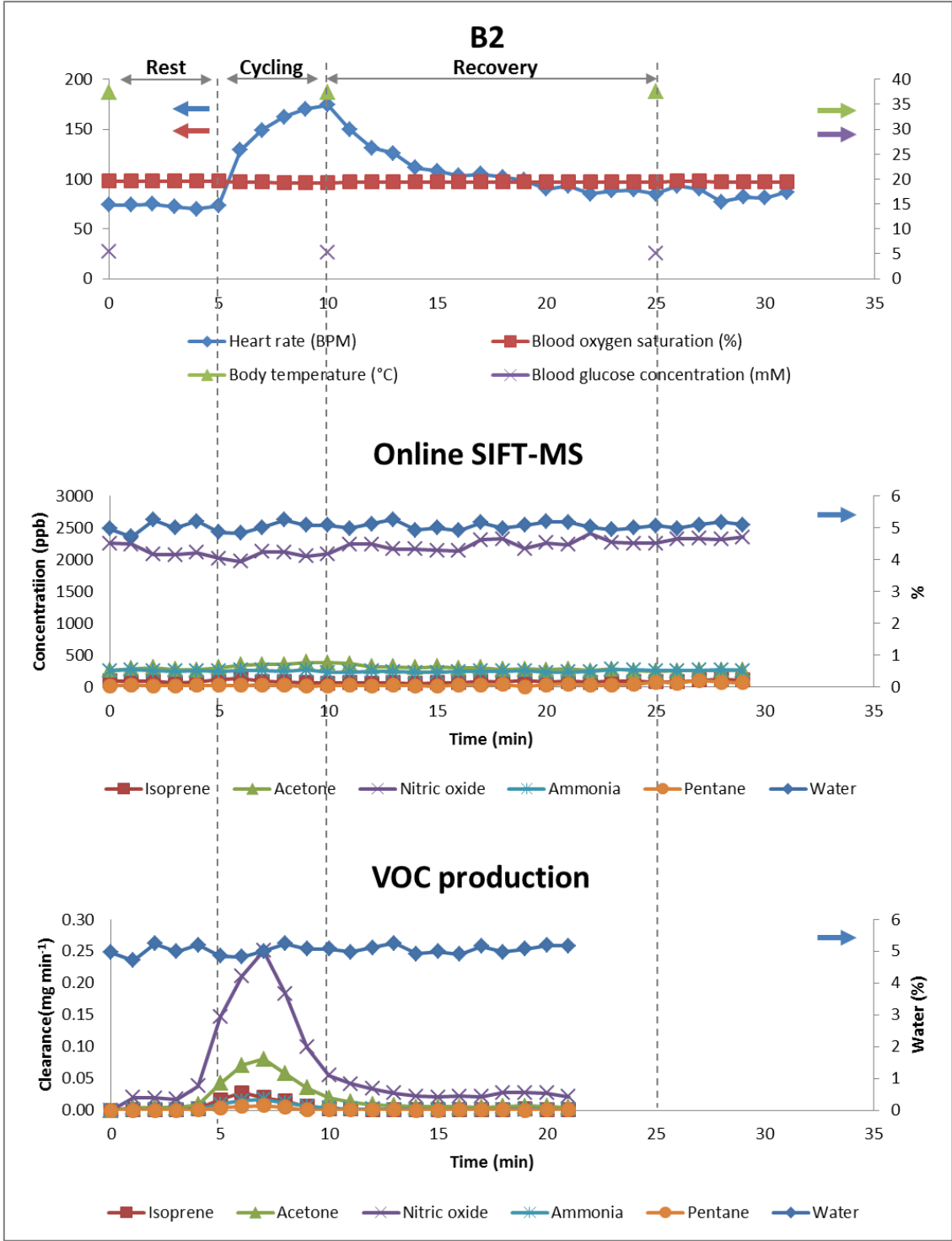


Figure 5.5 Physiological parameters and continuous online sampling of exhaled breath from volunteer B during the second ergometer challenge

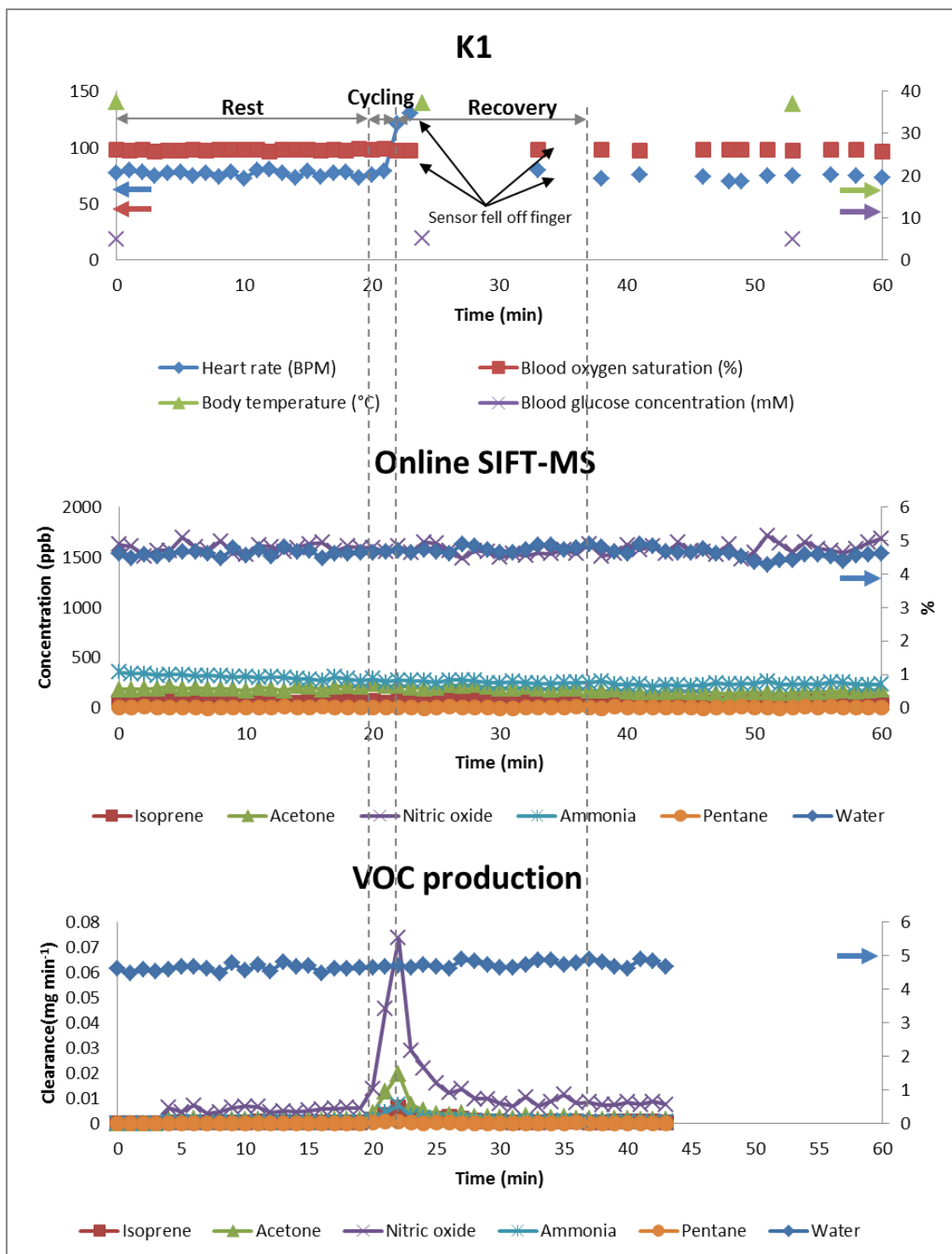


Figure 5.6 Physiological parameters and continuous online sampling of exhaled breath from volunteer K during the first ergometer challenge

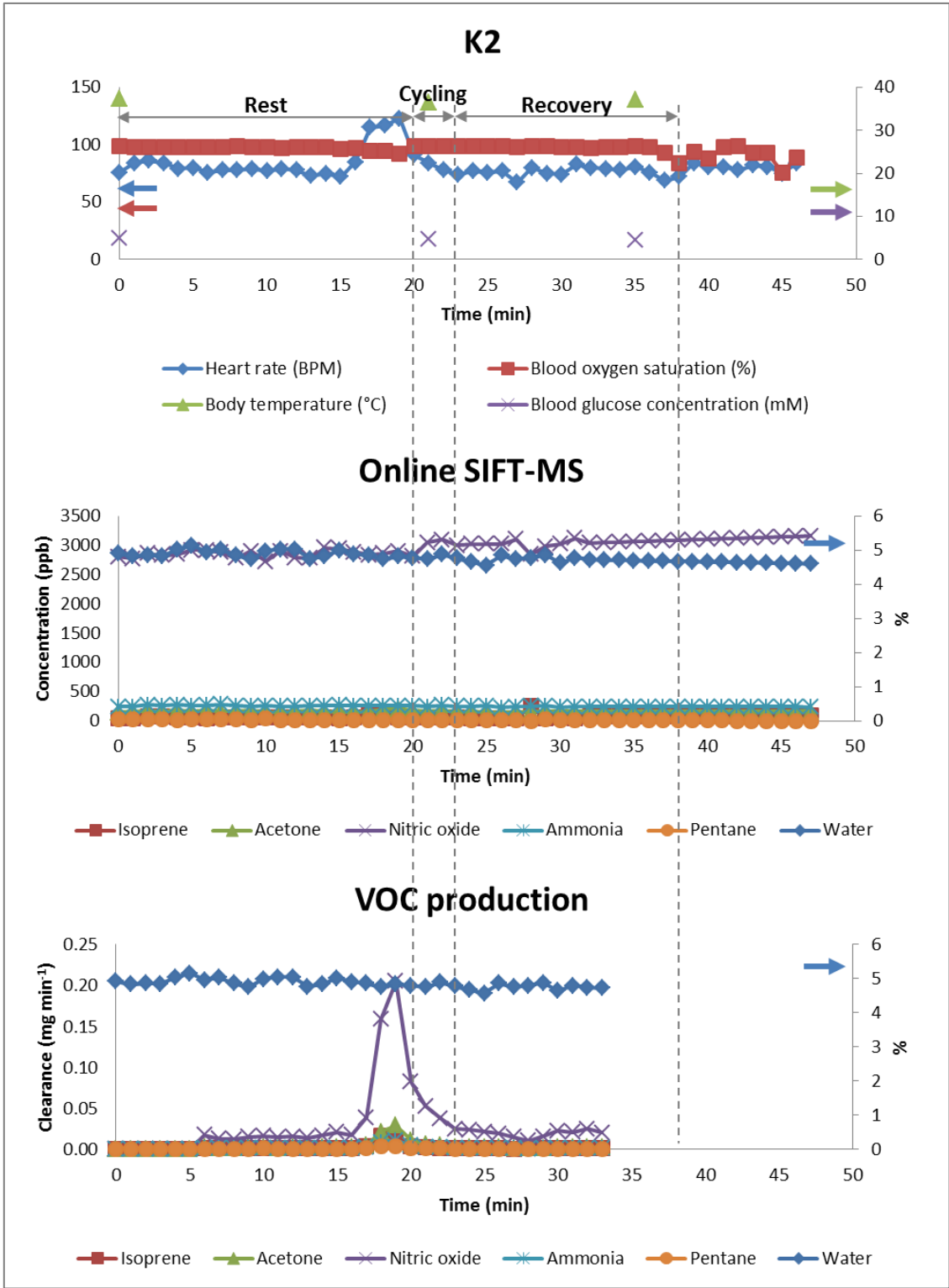


Figure 5.7 Physiological parameters and continuous online sampling of exhaled breath from volunteer K during the second ergometer challenge

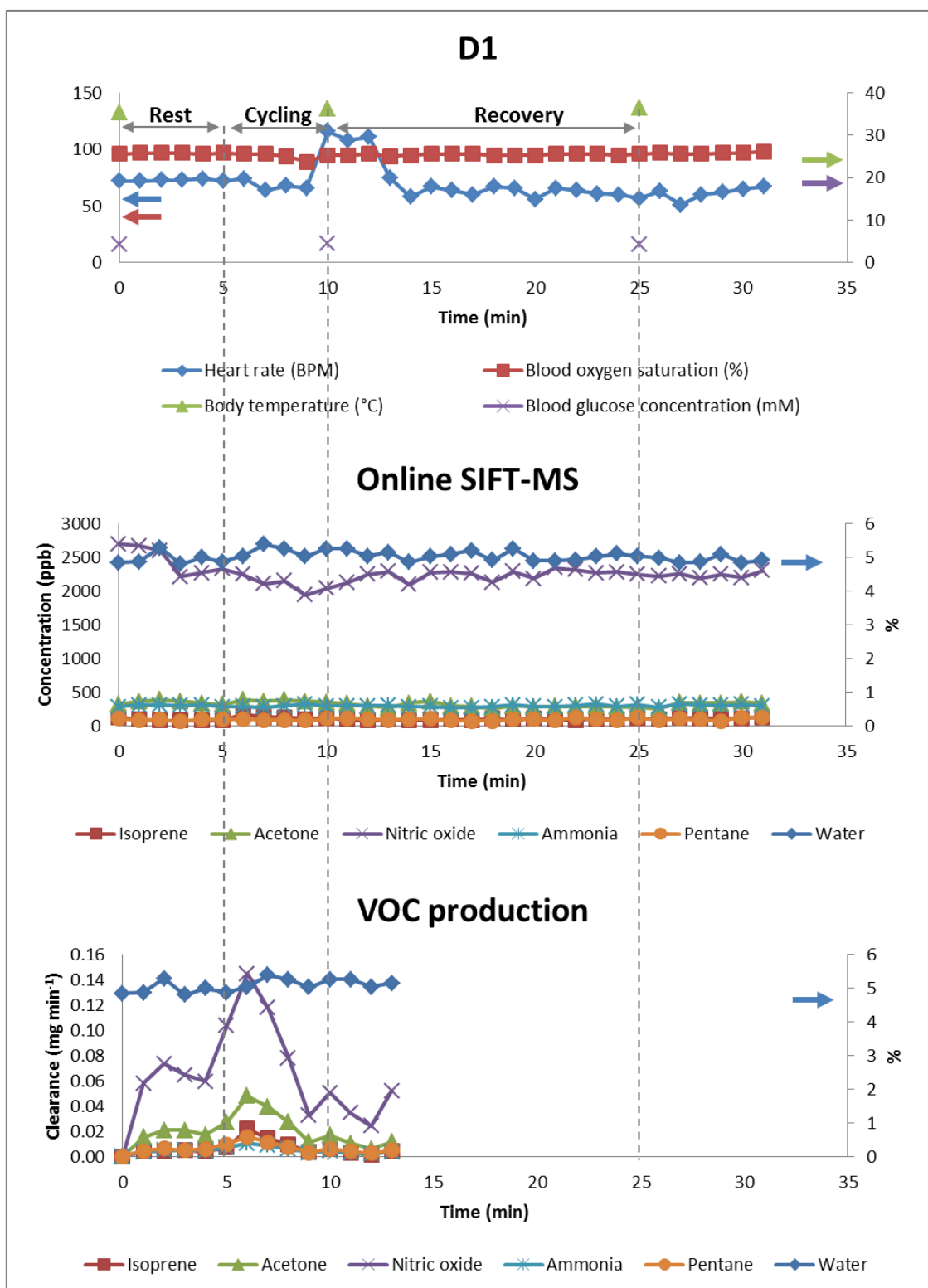


Figure 5.8 Physiological parameters and continuous online sampling of exhaled breath from volunteer D during the first ergometer challenge

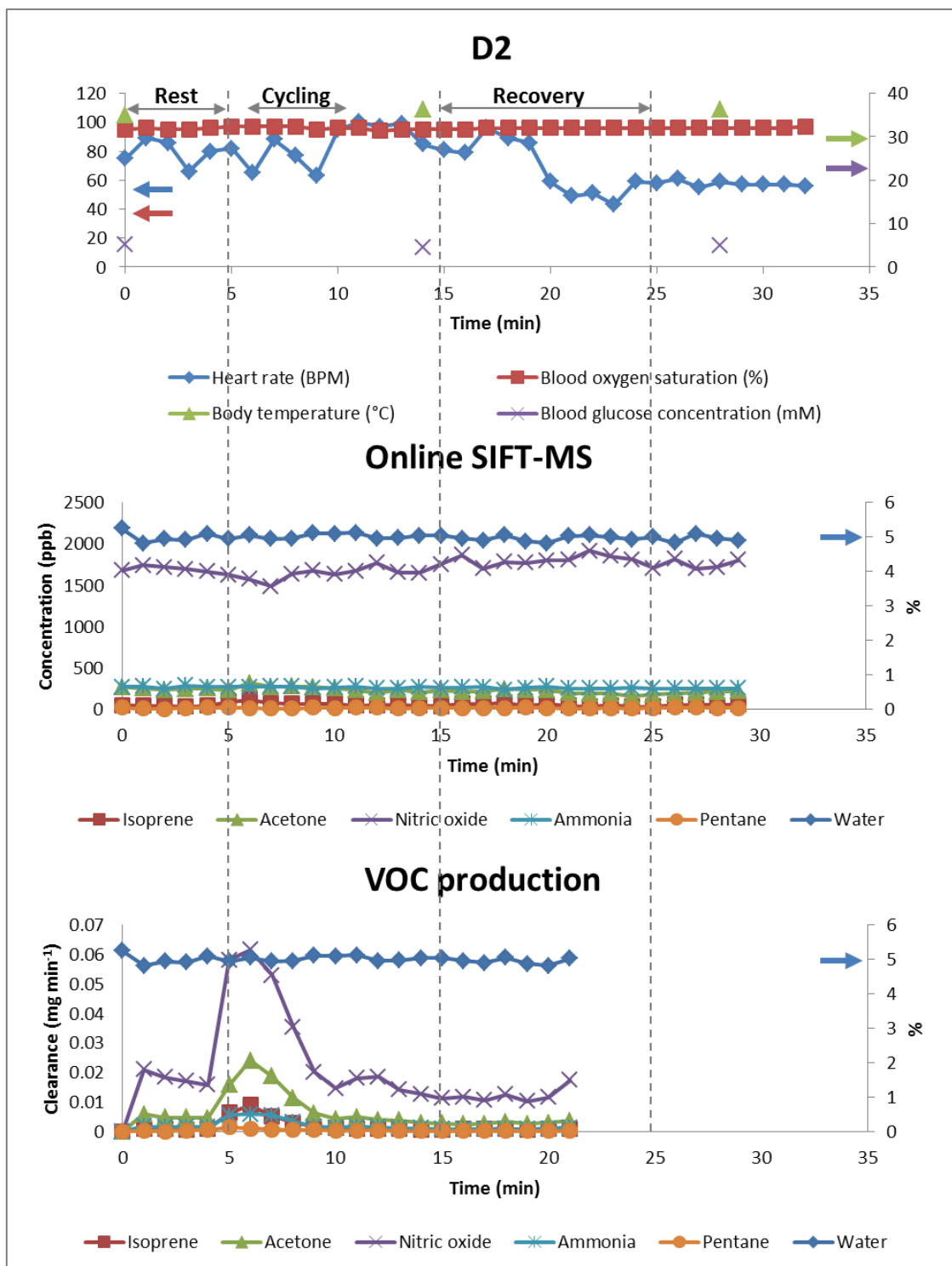


Figure 5.9 Physiological parameters and continuous online sampling of exhaled breath from volunteer K during the second ergometer challenge

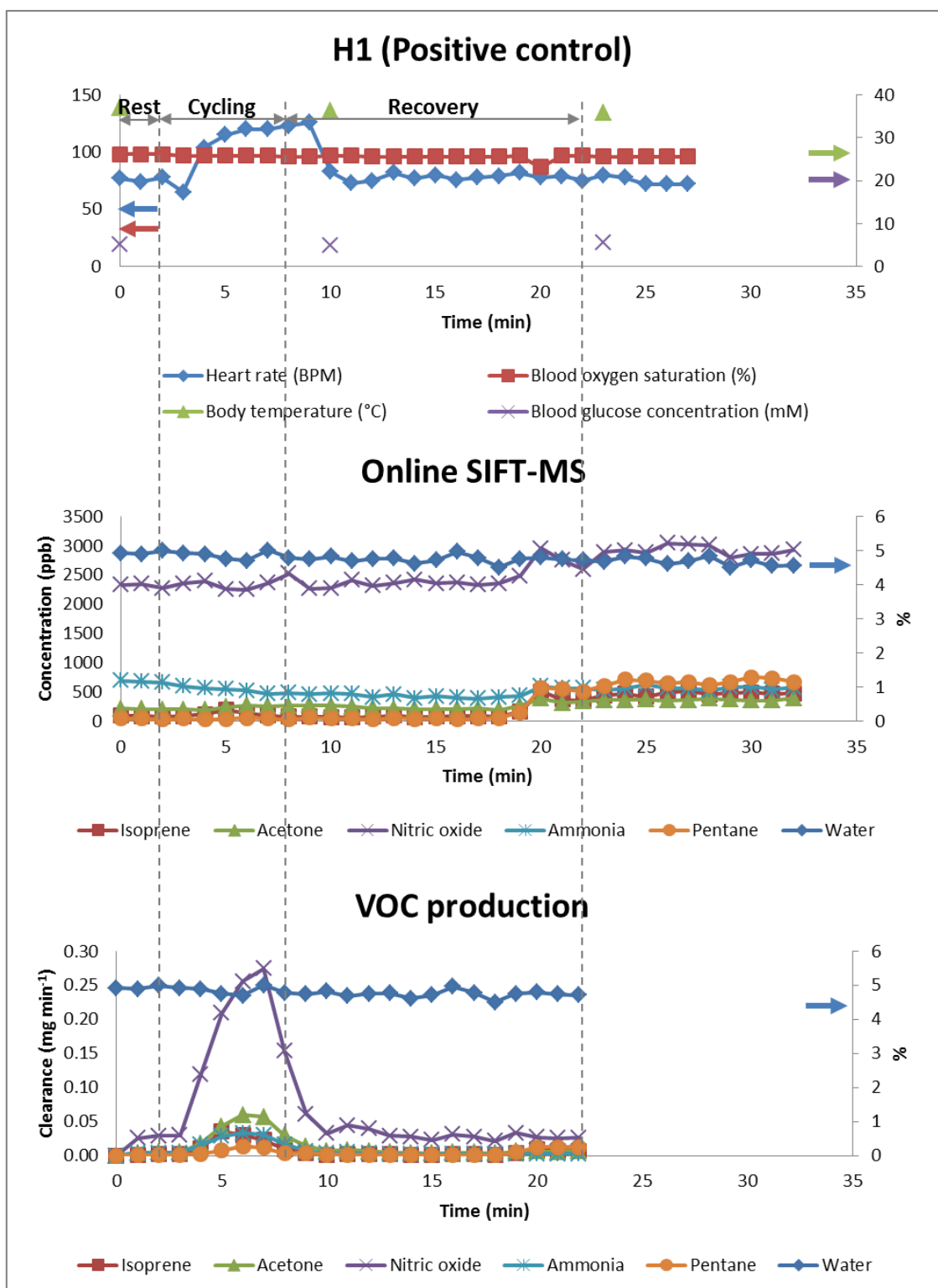


Figure 5.10 Physiological parameters and continuous online sampling of exhaled breath from volunteer H, the positive control, during the first ergometer challenge

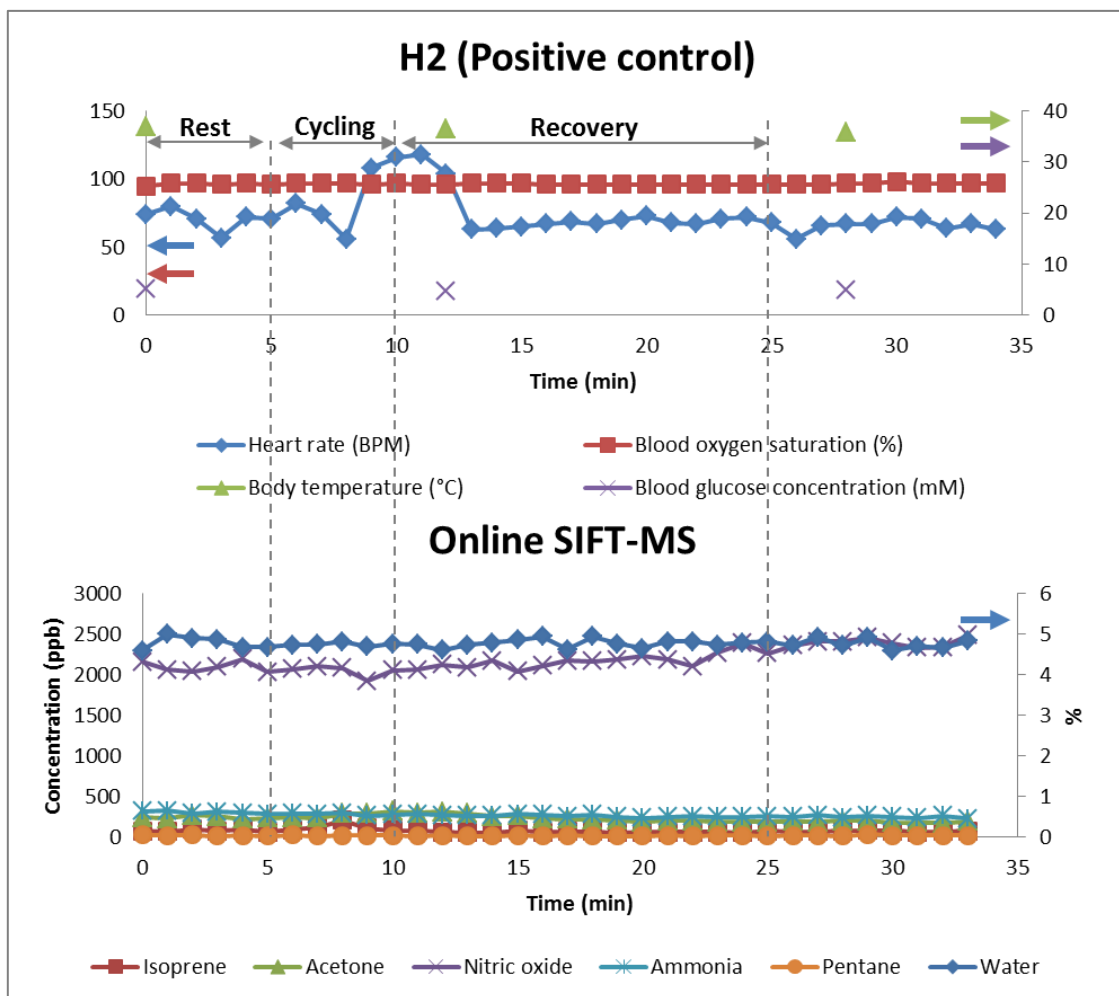


Figure 5.11 Physiological parameters and continuous online sampling of exhaled breath from volunteer H, the positive control, during the second ergometer challenge, VOC production could not be calculated due to a problem with the flow sensor

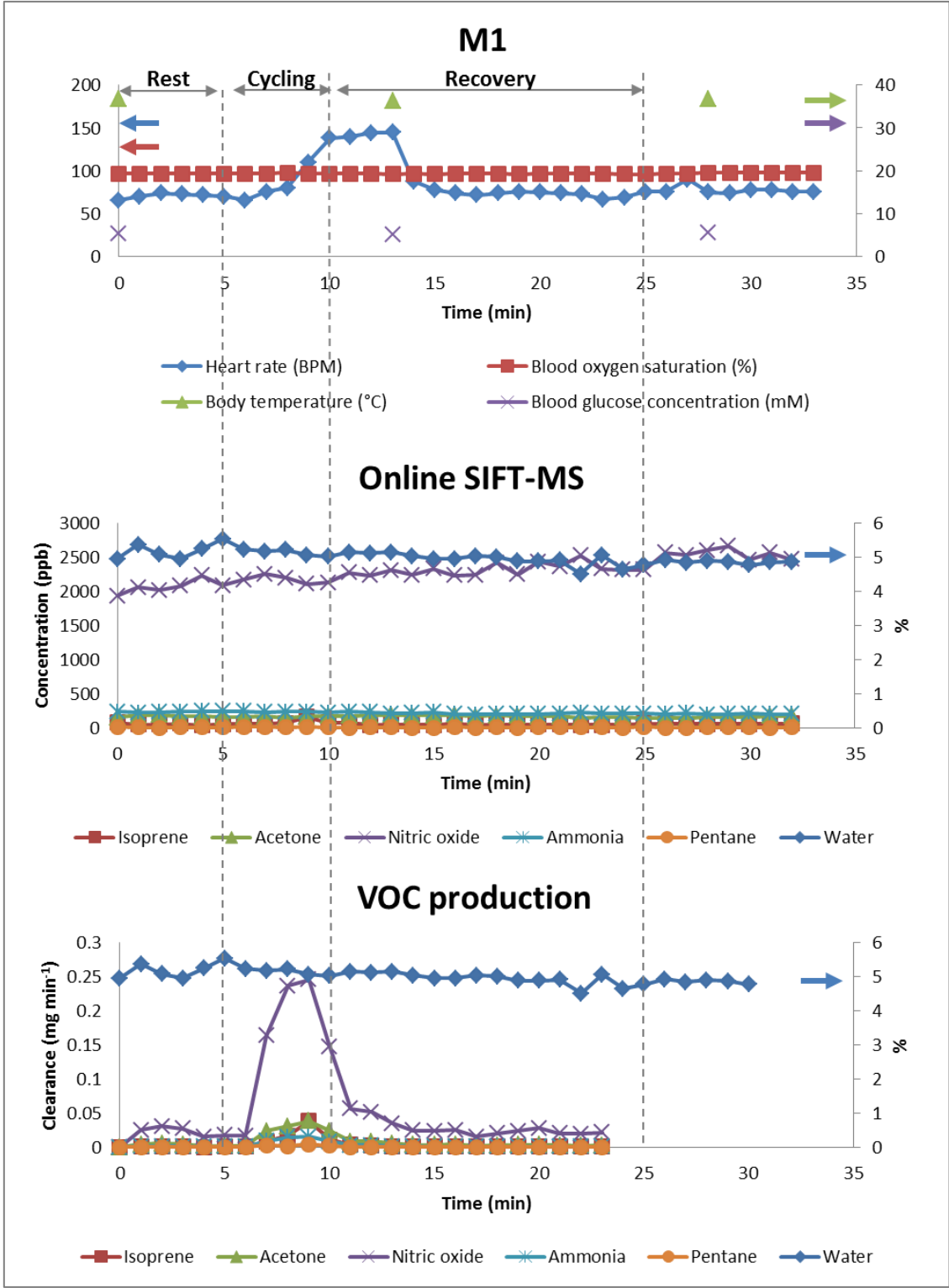


Figure 5.12 Physiological parameters and continuous online sampling of exhaled breath from volunteer M during the first ergometer challenge

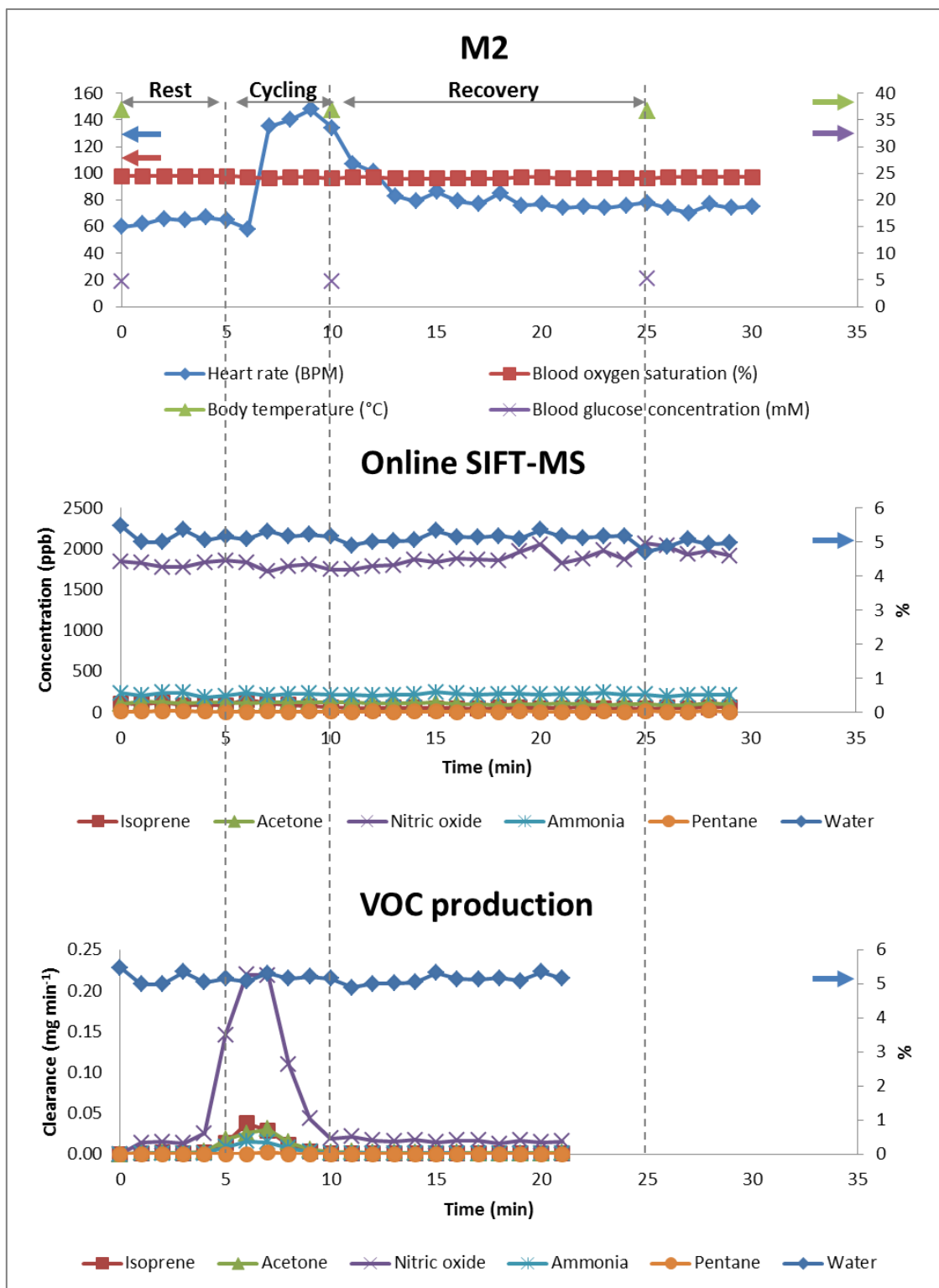


Figure 5.13 Physiological parameters and continuous online sampling of exhaled breath from volunteer M during the second ergometer challenge

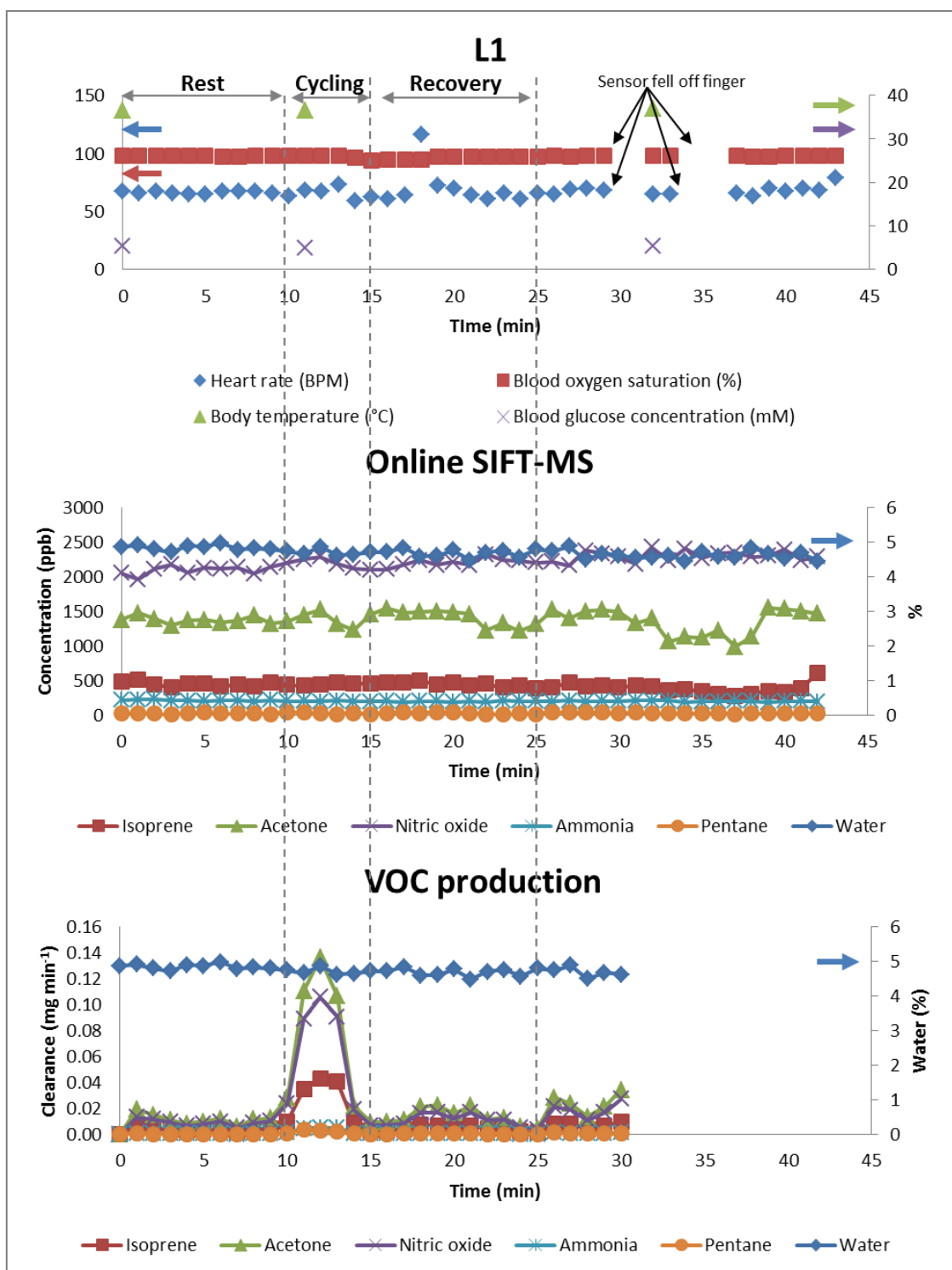


Figure 5.14 Physiological parameters and continuous online sampling of exhaled breath from volunteer L during the first ergometer challenge

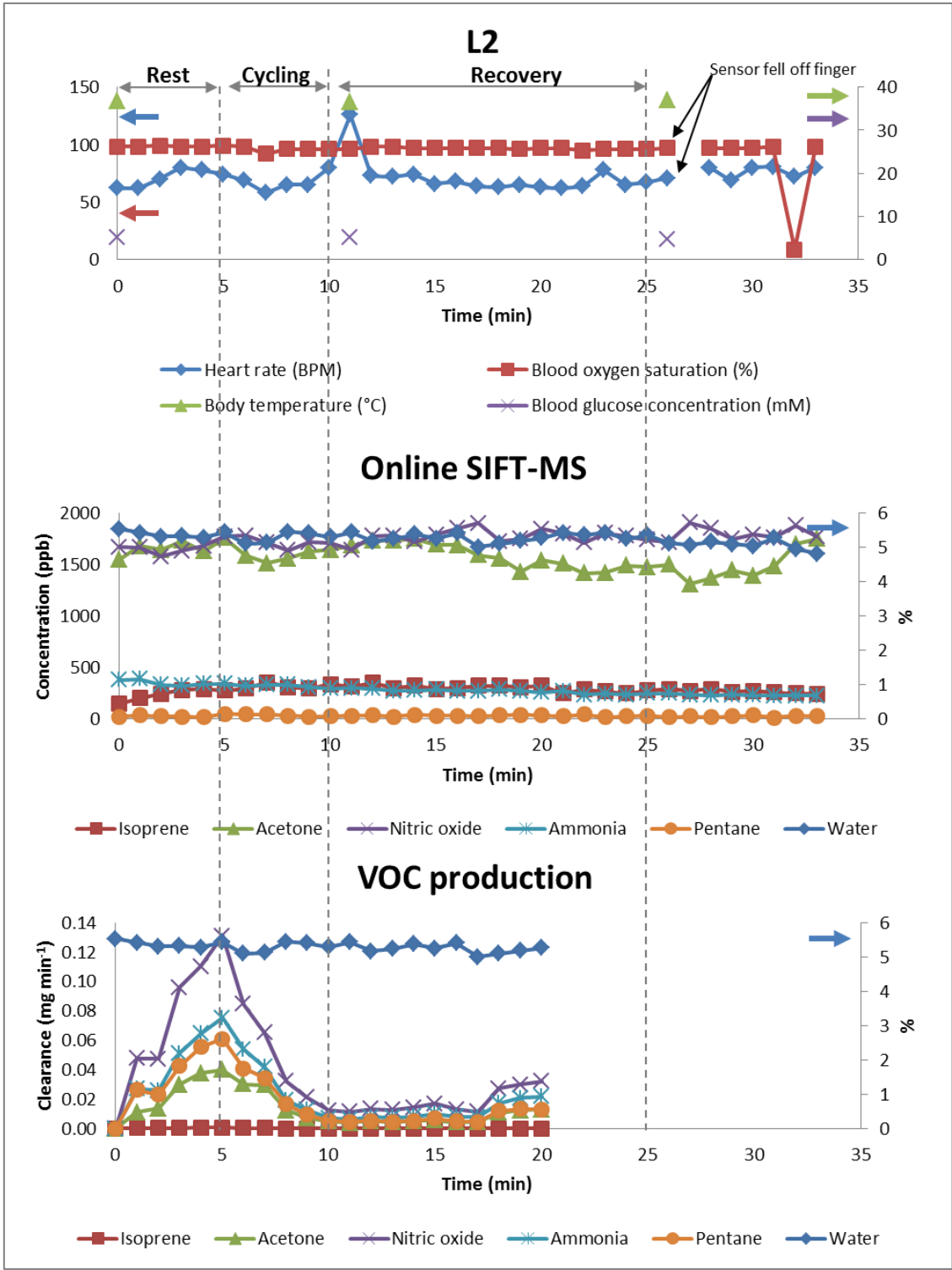


Figure 5.15 Physiological parameters and continuous online sampling of exhaled breath from volunteer M during the second ergometer challenge

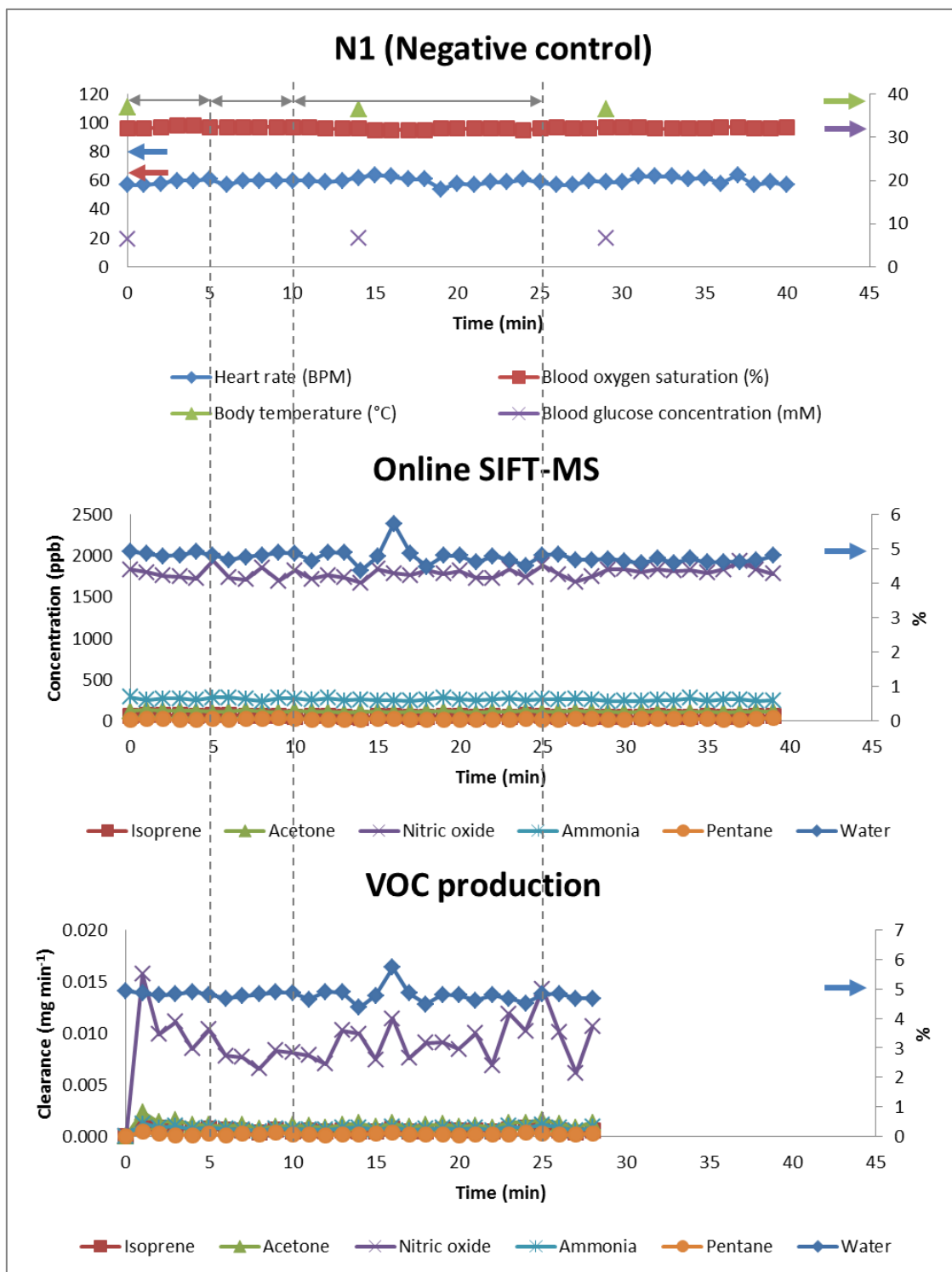


Figure 5.16 Physiological parameters and continuous online sampling of exhaled breath from volunteer N during the first negative control experiment (did not exercise)

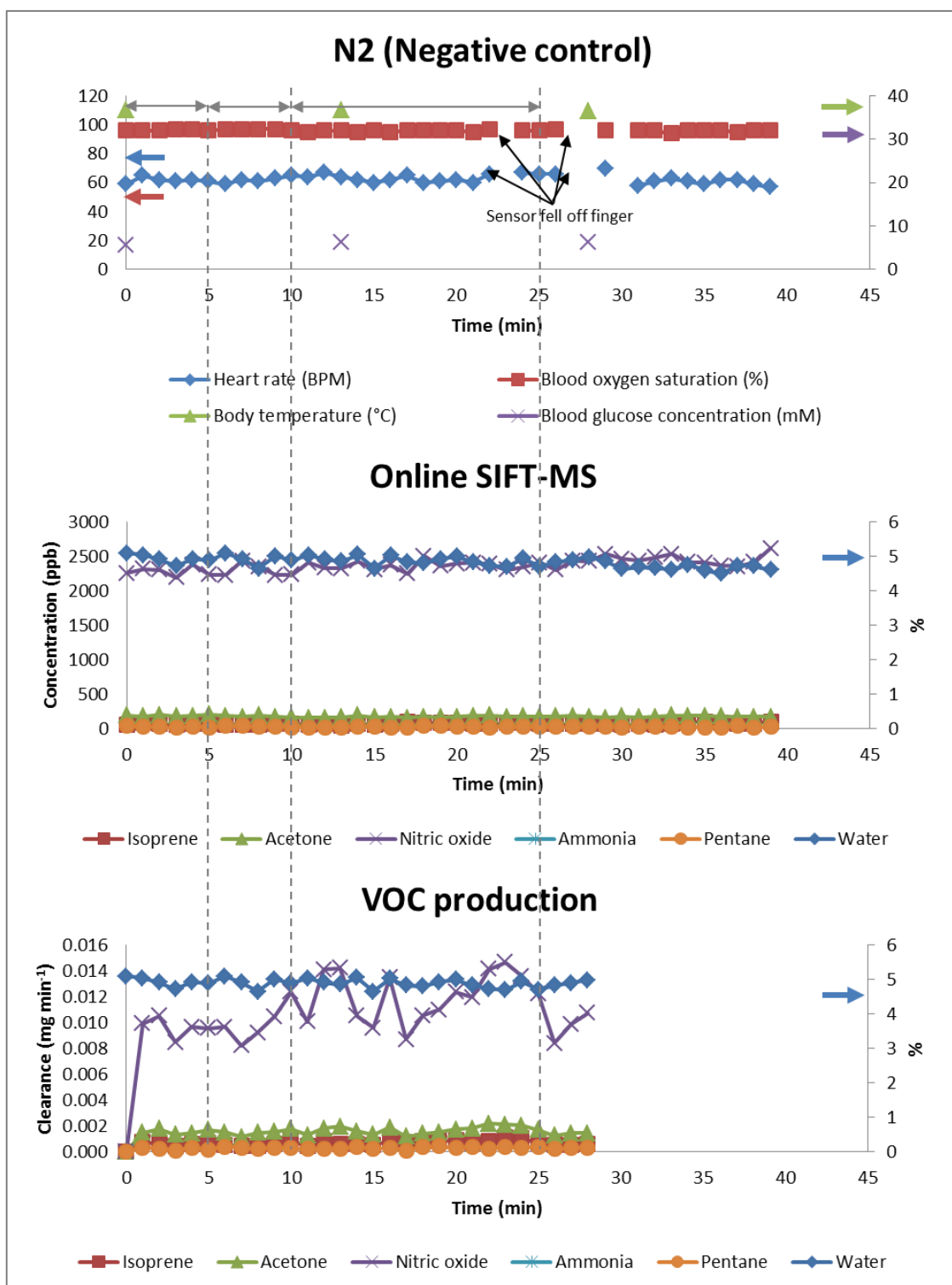


Figure 5.17 Physiological parameters and continuous online sampling of exhaled breath from volunteer N during the second negative control experiment (did not exercise)

Compound	Online SIFT-MS (<i>P</i>)	Clearance (<i>P</i>)
Isoprene	0.11	0.06
Acetone	0.44	0.01 *
Nitric oxide	0.91	0.06
Ammonia	0.87	0.30
Pentane	0.17	0.65

Table 5.2 ANOVA analysis of online SIFT-MS and clearance data

5.3.2 Breathotron

A decrease in sensor resistance between Rest and Cycling phases of experiment K1 was seen with an increase in sensor resistance during the Recovery phase. There is a negligible difference in sensor resistance between Rest and Cycling phases in experiment K2 though sensor resistance increases during the Recovery phase. The signals in K2 also contain an unexplained artefact, though these do not appear to have influenced the baseline or maximum resistance. The Cycling signal is missing from D1, Figure 5.13, due to user error, though there is negligible difference sensor resistance between the Rest and Recovery phases. There is an artefact in the recovery signal from D2, Figure 5.14, due to a lack of a stable sensor baseline resistance being achieved prior to sampling. There is an unexplained artefact in the Rest signal in experiment H1, Figure 5.15. There is negligible difference in resistance between the Cycling and Recovery phases. There is an unexplained artefact in the Cycling and Recovery phase signals during the sampling phase. In experiment H2, Figure 5.16, the same artefact during the sampling phase can be seen in all three signals. There is negligible difference in maximum resistance between the Rest and Cycling phases, but there is an increase in maximum resistance during the Recovery phase. The Rest signal in experiment M1, Figure 5.17, is clipped, whilst all signals show an unstable baseline resistance. These signals also have artefacts during the sampling phases similar that seen in volunteer H. There is an increase in maximum sensor resistance during the Recovery phase. Again in experiment M2, Figure 5.18, all of the signals have an unstable baseline resistance whilst the maximum sensor resistance seen in the Rest signal is considerably greater than the signals from the other two phases. This is thought to be an erroneous reading, and may be been influence by solvent contamination in the laboratory. There is an increase in resistance during the Recovery phase. None of the signals from experiments L1, Figure 5.19, or L2, Figure 5.20, are analysable due to clipping. The Rest signal from experiment N1, Figure 5.21, is not analysable due to a suspected problem

with the sensor heater temperature, there is negligible difference in maximum sensor resistance between Cycling and Recovery signals. In experiment N2, Figure 5.22, there is no difference in maximum sensor resistance between the Rest and Cycling signals, whilst there is an increase in maximum resistance during the Recovery phase. For clarity, the maximum change in resistance (ΔR_{\max}) for the first and second ergometer challenges are plotted in Figures 5.16 and 5.17 respectively. Due to a lack of useable data, one way repeated measures ANOVA could not be performed on ΔR_{\max} .

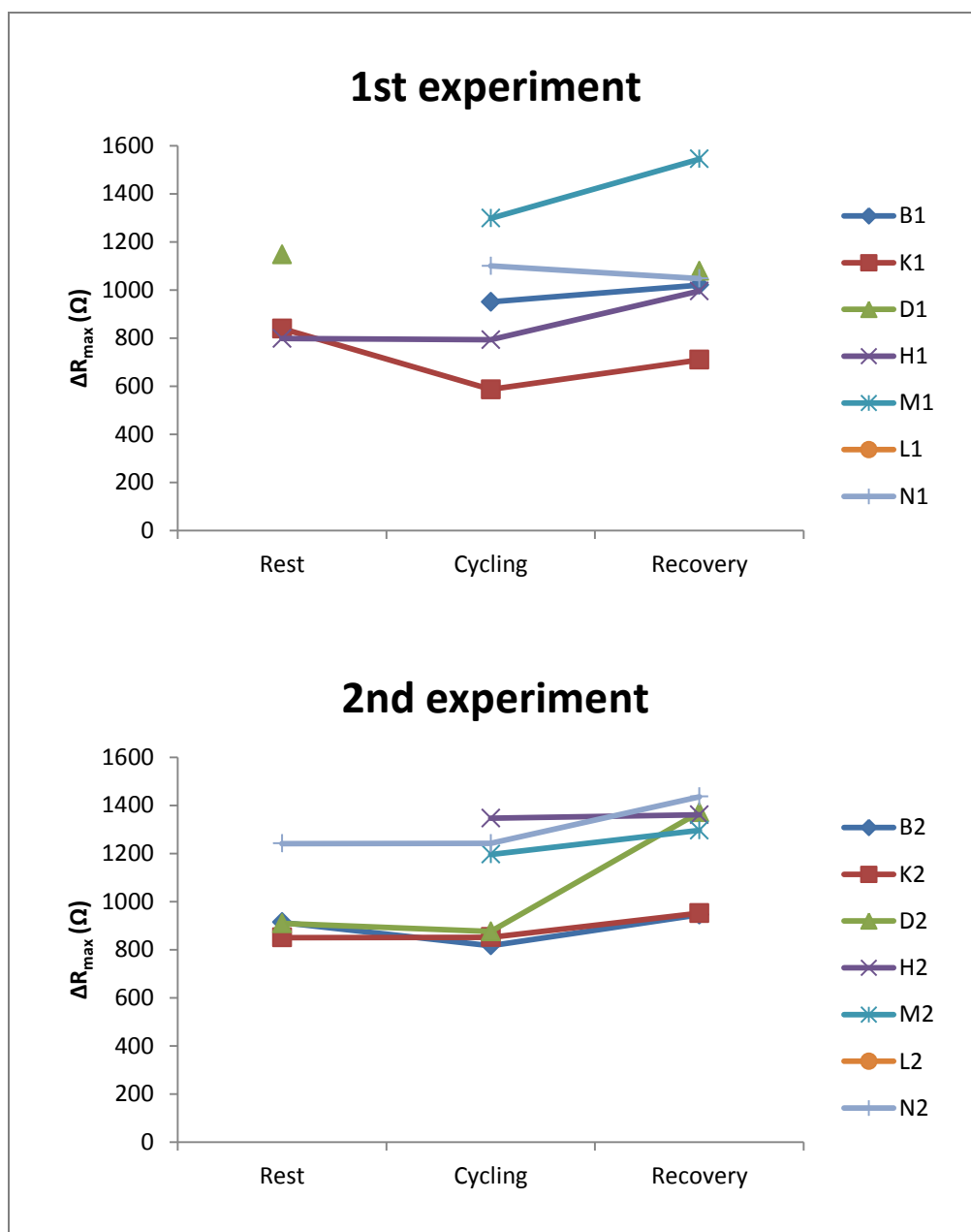


Figure 5.18 Change in maximum Breathotron sensor resistance ΔR_{\max} during the first experiment

5.3.3 Principal components analysis

Variables for principal components analysis (PCA) were generated using the same method described in 2.3.4.2. Only 30 signals were suitable for PCA. The scores plot for the PCA can be seen in Figure 5.19. The individual volunteers are distinguished by colour, whilst the shape of the point dictates the phase (Rest, Cycling and Recovery) and whether the sample was from the first or second ergometer challenge (1 or 2). The variance captured by PC1 is 78.51 % and

for PC2 19.52 %, to give a cumulative variance of 98.03 %. There is no pattern to the clustering; samples from individuals tend to cluster together, but not the samples from both experiments.

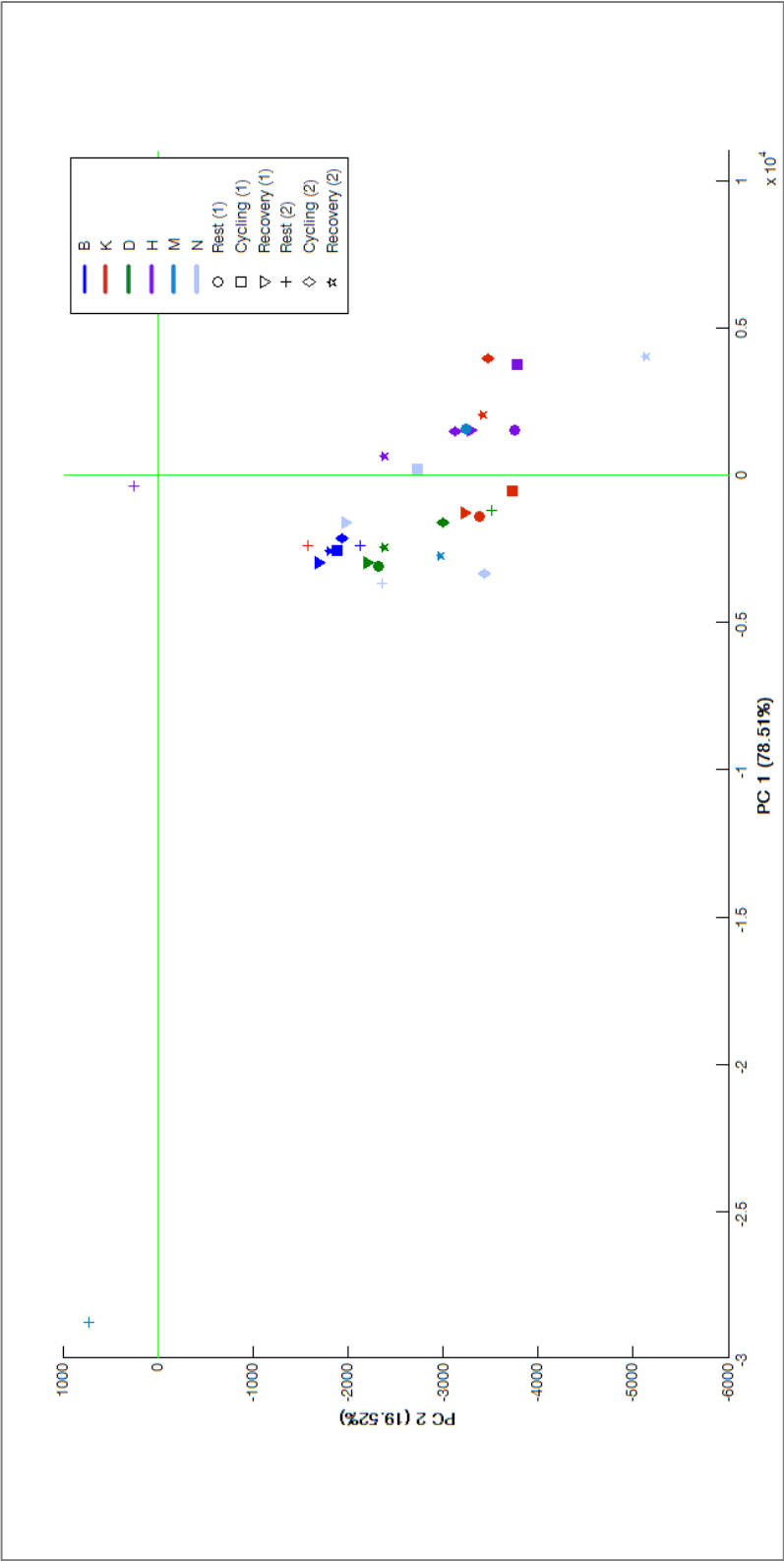


Figure 5.19 Scores plot from both ergometer challenges shows that samples from individual volunteers cluster together, but not by phases of the experiment with no repeatability between the first and second experiment

5.3.4 GC-MS

The compounds were quantified using the method described in 2.6.3.2, and plotted against the phase of the experiment. The acetone, isoprene, acetaldehyde and propanol concentration from the first experiment and second experiments for volunteers B, K, D, H, M, L and N can be seen in Figure 5.20, Figure 5.21, Figure 5.23 and Figure 5.24 respectively.

An increase in mean acetone concentration can be seen in the first experiment between the Rest and Cycling phases of the experiment, with a decrease in concentration during the Recovery phase. The greatest change in exhaled acetone concentration was observed in volunteer B. The lowest concentration of acetone was observed in volunteer N, the negative control, where there was no change in acetone concentration during the experiment. In the second experiment, the greatest concentration of exhaled acetone was quantified from volunteer L, though the lowest was seen in the exhaled breath of volunteer B. A decrease in acetone concentration is seen in volunteers B and K between the Rest and Cycling phases, whilst there is no change in acetone concentration between the Rest and Cycling phases in volunteers H and L. There is an increase in acetone concentration between Rest and Cycling phases in volunteers D, M and N.

There is no clear trend seen in isoprene concentration during the first set of experiments, The greatest concentration of exhaled breath isoprene is observed in volunteer B, with the lowest in volunteer K. whilst volunteers B, H and N show a decrease in exhaled isoprene concentration during the experiment, volunteers K, D and M display an increase. There is a decrease in exhaled breath isoprene concentration in volunteer K only during the second experiment. There is an increase in concentration in volunteers D, M, L and N during the Cycling phase.

There is negligible change in acetaldehyde concentration between the phases during the first set of experiments. This is also true during the second set of experiments except in the case of volunteer L, where acetaldehyde concentration is considerably higher. This could be dismissed as contamination, but it is possible that this is due to natural variation given that higher concentrations of acetone were observed in this volunteer's breath samples.

There are varying patterns in exhaled propanol concentration between volunteers, phases and experiments. In the first ergometer challenge, propanol concentration increases after the Cycling phase in volunteers K, D and N, but only falls during the Recovery phase in volunteer K.

There is a decrease in concentration in volunteer M between the Rest and Cycling phases with a further decrease in concentration after the Recovery phase. The Cycling sample for volunteer B is missing, though there is no difference in propanol concentration between the Rest and Recovery phases. There is no data for volunteer L. Propanol concentration is lower in the second set of experiments for all of the volunteers. There is again an increase in concentration between the Rest and Cycling phases in volunteers B, K, L and N, there is a decrease in concentration in volunteers D and H.

Due to the lack of data through missing samples, further statistical analysis could not be performed on the dataset.

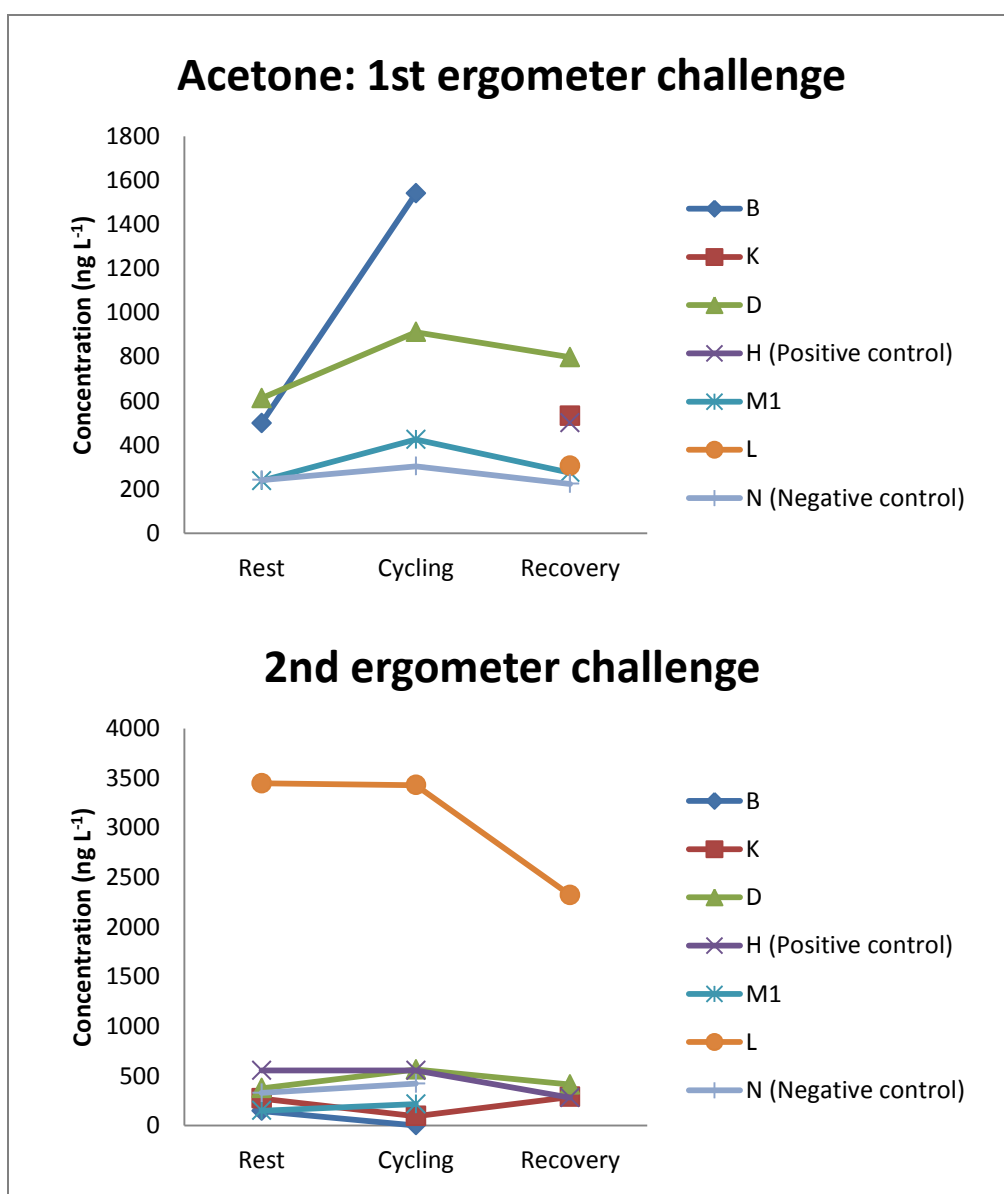


Figure 5.20 Change in exhaled breath acetone concentration quantified using GC-MS during both ergometer challenges

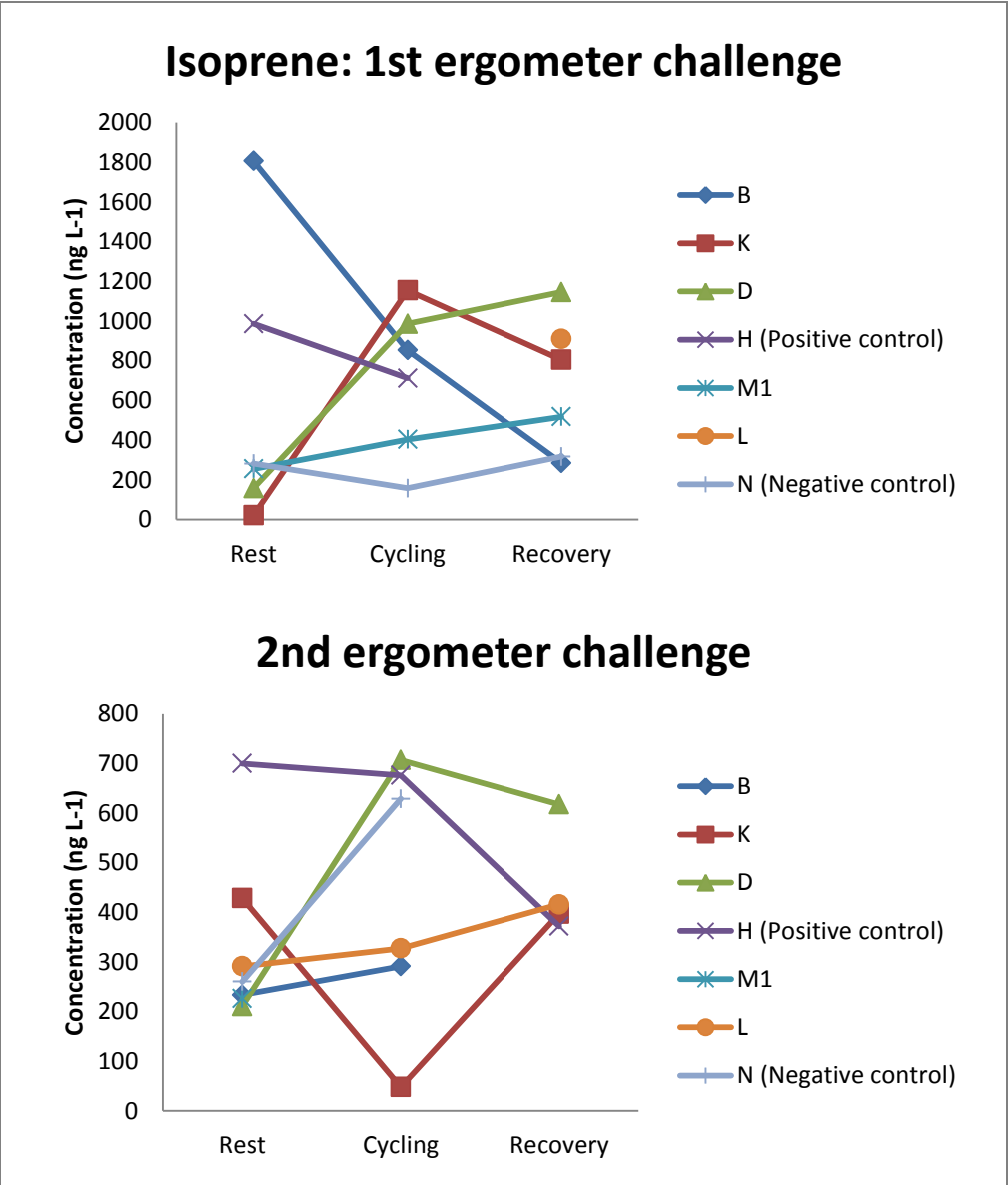


Figure 5.21 Change in exhaled breath isoprene concentration quantified using GC-MS during both ergometer challenges

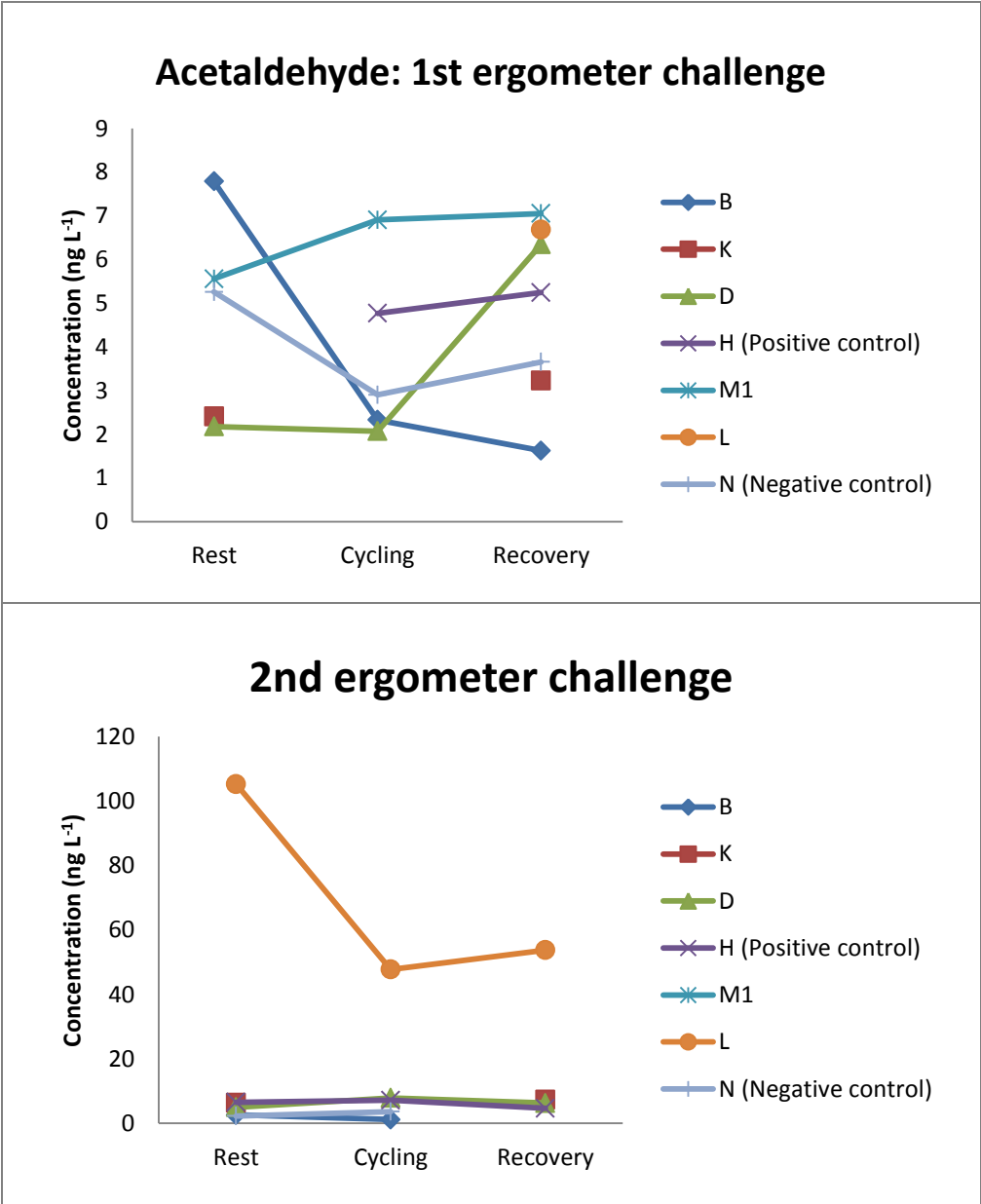


Figure 5.22 Change in exhaled breath acetaldehyde concentration quantified using GC-MS during both ergometer challenges

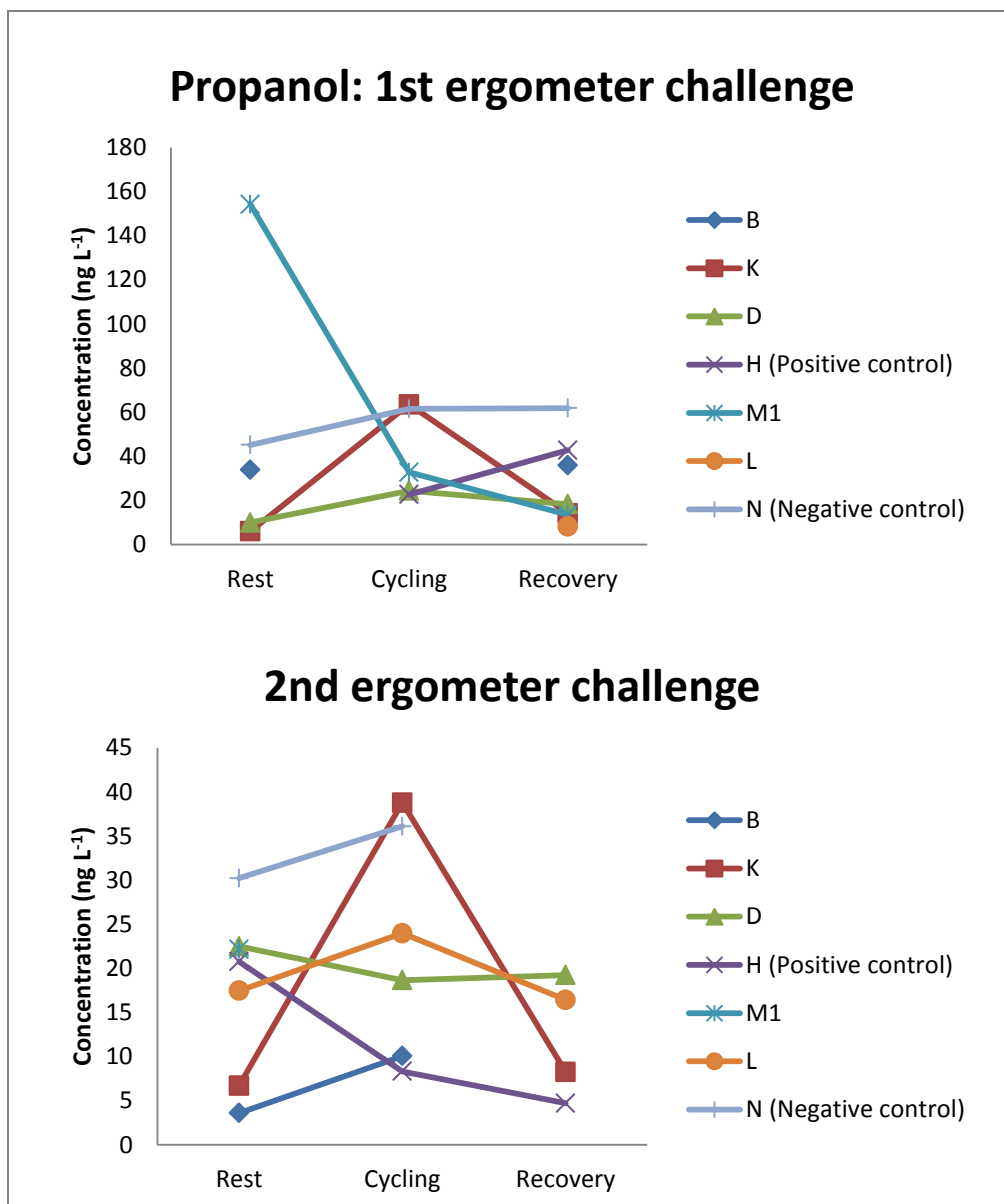


Figure 5.23 Change in exhaled breath propanol concentration quantified using GC-MS during both ergometer challenges

5.4 Discussion

In this experiment we have investigated the concentration of endogenously produced VOCs and their clearance during a bicycle ergometer challenge following an overnight fast using Breathotron, online SIFT-MS and TD GC-MS. To the best of our knowledge, there have only been two previous of breath VOCs during exercise using online sampling with PTR-MS (King et al., 2009; King et al. 2010). The results show that there is no significant change in Breathotron sensor response between the three phases of the experiment, nor was there a significant change in exhaled VOC concentration, though there is a significant change in acetone

clearance during the ergometer challenge with a decrease during recovery. It is unlikely that the Breathotron sensor is affected by short term increases in ventilation (increased breath flow and volume).

Due to ethical restrictions imposed by CUHREC, the intensity and duration of the ergometer challenge was kept to as low intensity and duration as short as possible, unlike in other similar studies, where the duration was either longer, more intensive or incremental in nature (Senthilmohan et al., 2000; King et al., 2009). This may have contributed to the lack of change in blood glucose concentration, blood oxygen saturation and body temperature.

Minor fluctuations in body temperature were within error of the device, and may have been influenced slightly by ambient temperature but not significantly. Anomalies in measuring blood oxygen saturation were caused by the pulse oximeter falling off the volunteers' fingers rather than any physiological change.

There was no increase in core body temperature and this is unlikely to have influenced VOC concentration. Temperature was measured using an ear thermometer. The temperature reading was always recorded from the same ear (typically the right ear for most volunteers) on each occasion that core temperature was taken to eliminate discrepancies between the ears (Childs et al., 1999). The increase in core body temperature typically associated with prolonged exercise is due to dehydration, which leads to reduced sweat production and the reduced ability to dissipate heat (Ehrman, 2009). Dehydration also affects the cardiovascular system, resulting in reduced stroke volume, blood pressure and maximal oxygen consumption, as well as altering muscle metabolism and reducing the anaerobic threshold, the point where metabolism switches from aerobic to anaerobic metabolism (Ehrman, 2009). As the intensity of exercise was not particularly strenuous, and the shortness in the duration of the ergometer challenge, it is unlikely that the volunteers would have become dehydrated during the ergometer challenge especially as they had been permitted to drink water during the fasting phase.

Blood glucose concentration did not change significantly during the experiment. A significant change in blood glucose concentration was not seen in the previous Chapter (6-minute walk test), suggesting that this is not dependant on fasting state as these volunteers were not fasted. Various exercise physiology studies have shown that plasma glucose concentration increases during intense exercise due to an increase in hepatic glucose output from the liver

exceeding the utilization by tissues (Kjaer et al., 1986; Kjaer et al., 1987; Kjaer et al. 1991). Again, this lack of significant change is probably due to the short duration and relatively low intensity of the ergometer challenge, and is unlikely to have influenced VOC concentration.

An increase in heart rate is seen in all of the volunteers that completed the ergometer challenge. This is to meet the blood flow demands of active muscles and it remains elevated for some time before returning to the resting rate (Wilmore et al. Physiology of sport and exercise). Differences in resting heart rate and HR_{max} between individuals can be explained by the difference in age and levels of fitness.

Evaluation of lung function shows that for all parameters, FEV_1 , FVC, FER and PEF, all volunteers were within 1 standard deviation of the mean. It is therefore unlikely that resting lung function contributed to the concentration of VOCs observed in exhaled breath. Similarly, there is no deviation in BMI, as all volunteers bar one (K) fall within 1 standard deviation of each other, but the volunteers show a large difference in exhaled VOC concentration.

There was a small decrease in the change in (ΔR) Breathotron sensor resistance between the resting and post-exercise samples, with recovery to pre-exercise resistance upon completion of the experiment. A greater sensor resistance is seen the volunteer (L) with the greatest acetone in their exhaled breath using SIFT-MS. Indeed, with this volunteer the sensor signal is clipped, most likely due to the higher acetone content in their breath than seen in the other volunteers. In previous experiments, the maximum sensor resistance has been shown to be influenced by the greatest concentration VOC component of exhaled breath (Patel, 2007). Due to a lack of useable data, statistical analysis could not be performed and it cannot be determined if the change in sensor resistance is statistically significant. It is likely that the decrease is not due to biochemical change, especially when there is an increase in the major VOC component of breath acetone as determined using SIFT-MS.

The decrease may possibly have been caused by changes in nitric oxide concentration, a known reducing gas. But, as there was no significant increase in nitric oxide concentration or clearance, it is unlikely to be the cause. This decrease is more likely to have been caused by the return to baseline and sensor drift. The return to baseline problem is caused as a result of the relatively short, 5 minute, sampling interval between the initial Rest and Cycling samples, this means that the sensor has failed to reach the original baseline resistance before the next sample is analysed. When the next sample is analysed, the response is smaller due to the

higher baseline resistance, thus when the ΔR is plotted it appears to be smaller than the change in the initial sample. As the final sample is recorded 15 minutes later, it is more likely that the baseline resistance is the same as the initial sample. Sensor drift is a problem caused by the tendency of the baseline resistance to change over time. This is not so much a problem between sequentially analysed samples, but may be a potential problem during the second set of ergometer challenges. There is evidence of this in the PCA analysis where one would expect samples from the different phases to cluster by volunteer, so that the Rest, Cycling and Recovery samples from a particular volunteer cluster together regardless of whether the sample was from the first or second ergometer challenge. The time to return to baseline and sensor drift are some of the disadvantages of using MMOS sensors (Gardner and Bartlett, 1999), though this may be overcome by using a different sensor (See Chapter 6 for more information).

There was a decrease in isoprene clearance during the experiment, though it was statistically insignificant. The decrease in isoprene clearance was also seen by King et al., (2009) using PTR-MS. Though Senthilmohan et al., (2001) reports an initial decrease in isoprene concentration an increase was seen after approximately 30 minutes of continuous exercise. The range of isoprene concentration from our study is greater than that seen by Senthilmohan et al., (2001), though this may be due to a variety of factors, the fact that they used trained athletes and single breath samples whereas in our experiment we used fasted individuals of varying ability for a relatively short ergometer challenge. Karl et al., (2001) showed that breath isoprene concentration increased significantly in eight subjects during a bicycle ergometer challenge using PTR-MS. Our results may differ as the isoprene concentration and clearance rates from the end of the cycling phase from both sets of experiments were used in repeated measures ANOVA whereas Karl et al., (2001) used the peak isoprene concentration and compared it to resting isoprene concentration in their analysis.

A temporary increase in isoprene concentration is seen in the time profile, this is a common phenomenon also seen in other studies which used either SIFT or PTR-MS during an ergometer challenge (Karl et al., 2001; Turner et al., 2006b; King et al., 2009). Though this was not observed by Senthilmohan et al., (2001), and this may be due to the fact that single exhaled breaths were analysed rather than a continuous sample. The rapid increase is probably due to the increase in heart rate during exercise or an increase in the depth of the breath, due to drawing more VOC molecules from the alveoli and should probably be treated as an artefact of

SIFT-MS sampling. This increase is probably due to the increased ventilation rate rather than changes in biochemical production, the change in synthesis rate is known to have a larger rate constant (Stein and Mead., 1988; Stone et al., 1993; Kuzma et al., 1995). This view is also supported by King et al., (2009).

There was no significant increase in acetone concentration, though there was a significant increase in acetone clearance. An increase in acetone concentration during the exercise phase was seen in previous studies using both SIFT- and PTR-MS (Senthilmohan et al., 2001; Turner et al., 2006a-b; King et al., 2009). The increase in acetone clearance is probably due to the increased ventilation rather than an increase in fatty acid metabolism. Fatty acid availability increases during prolonged exercise in order to reduce dependence on glycogen stores within muscle and liver (Kang Bioenergetics primer for exercise). The increase in fat metabolism decreases intracellular concentrations of AMP and Pi which reduces carbohydrate breakdown (Dyck et al. 1993; Dyck et al., 1996). Fatty acid oxidation increases from rest to exercise and peaks at 65% of maximal oxygen uptake (Krogh and Lindhard, 1920). Fatty acid oxidation is higher at 65% than at 25, or 85% of maximal oxygen uptake (Romjin et al., 1993). The variation in exhaled acetone may be explained by the individual volunteers' diet. Galbo et al., (1979) report a significant reduction in fatty acid oxidation following exercise on a bicycle ergometer on a carbohydrate rich diet than on a fat rich diet. King et al., 2009 states that they could not determine a relationship between BMI and breath acetone concentration. Our results neither proves, nor disproves this observation.

Unlike Senthilmohan et al., (2001), who reported an initial increase ammonia concentration followed by a fall, we do not see a significant change in ammonia concentration. One would be led to believe that this observation is due to the longer duration of exercise in the Senthilmohan et al., (2001) experiment, though as the ammonia time profile is not provided, the time point at which the concentration rises and falls is unknown. The concentration ranges reported (50-500 ppb) by Senthilmohan et al., (2001) are consistent with our data. Higher concentrations of ammonia in exhaled breath are possibly due to the oxidation of protein from dietary sources (Španěl and Smith, 1998). As the fasting period of the experiment was limited to 8 hours, it is unlikely that carbohydrate stores were sufficiently depleted for protein breakdown to be required to generate energy.

There was no significant change in nitric oxide concentration, or even the nitric oxide clearance. Persson et al., (2003) reports an increase in concentration when the increased

minute ventilation is taken into account (which the clearance rate does). It is likely that the intensity and duration of the exercise was not sufficient to significantly affect nitric oxide concentration. Exhaled concentrations of nitric oxide were however greater than those reported in other studies, though these did not use SIFT-MS (Shin and George, 2002) but a dedicated NO analyser.

The results collected in this experiment are from mixed breath, both upper respiratory tract and alveolar breath and may not represent true physiological concentrations. Though there have been numerous methods for the offline collection of alveolar breath, which use exhalation gas temperature, flow or partial pressure of carbon dioxide to determine alveolar portion of exhaled breath (Miekisch et al., 2004; Miekisch et al., 2008; Basanta et al., 2007; Larstad et al., 2007; Lindstrom et al., 1996; Ma et al., 2010) there is no consistent method for collecting this data for online sampling.

Currently, the Breathotron has a fixed deadspace volume of 150 mL programed in software, and is not user changeable, which is an estimate of the dead space volume of the upper respiratory tract (Marczin, 2000). This is not analysed by the device. It may be possible in future developments of the Breathotron to use either the change in exhaled breath temperature using a thermistor, placed inside the face mask, to monitor changes in breath temperature or a software algorithm, similar to that used by Schwoebel et al., (2011), instead of an flow sensor to accurately measure and eliminate the upper respiratory tract portion of exhaled breath.

5.5 Conclusion

We have demonstrated that Breathotron sensor performance is not negatively affected by changes in endogenous VOC concentration during brief periods of exercise, but may instead be affected by the time period required to return to baseline resistance when samples are taken in quick succession (5 minutes apart). There was no repeatability between the first and second ergometer challenges, and this is reflected in the PCA where there is no pattern observable in the clustering, which may be due to sensor drift over time but is more likely to be influenced by VOC concentration.

Endogenous VOC concentration was not affected by blood glucose concentration, blood oxygen saturation or a change in core body temperature. Though there is a detectable increase in acetone and decrease in isoprene concentration measured using SIFT-MS in all volunteers

that took part in the ergometer challenge and not the negative control, this increase in concentration is likely to be an artefact caused by a sudden increase in heart rate and the rate and depth of breathing rather than through a biochemical change.

A significant increase in acetone clearance was seen during the ergometer challenge. This observation is more likely to be due to the increase in ventilation rather than any biochemical effect, though the clearance may increase with an increased intensity and duration of exercise. There was no change in nitric oxide, ammonia or pentane concentration, this may be due to the relatively low intensity of the ergometer challenge as these compounds have been reported to change in other experiments.

However, this conclusion may have possibly differed if the intensity and duration of the ergometer challenge was greater, as seen in other studies which used SIFT- or PTR-MS.

6 Investigating and improving the reliability and reproducibility of the Breathotron

6.1 Introduction

The Breathalyser is a well-established method for measuring exogenous ethanol in exhaled breath. Currently, there are no devices available for the analysis of VOCs in exhaled breath to aid in clinical monitoring and diagnosis. For breath analysis to become commonplace for medical diagnostics a smaller, lighter, cheaper and easy to use device must be developed.

The Breathotron is based around a single mixed metal oxide semiconductor (MMOS) gas sensor, and is a development of the eNostril device (Lee-Davey, 2004). This provides the ability for semi-quantitative and qualitative chemical information from a single sensor, unlike other similar devices such as the electronic nose (eNose) which typically rely on an array of electrochemical sensors (Patel, 2007). Previous in vitro studies have investigated the linearity of sensor response and the ability to distinguish between mixtures of several volatile compounds (Bishop, 2006; Patel, 2007). In all of these studies, the Breathotron used a City Technology® CAP25 mixed metal oxide semiconductor (MMOS) gas sensor, which has since been discontinued by the manufacturer.

In Chapter 3 a relationship between exhaled breath acetone concentration and blood glucose concentration was established for a minority of the volunteers. The lack of consistent data may have been due to sensor performance of the CAP25 sensor used. In Chapter 5, it was found that samples could not be taken between relatively short sampling intervals due to the poor return to baseline of the CAP25.

In this chapter, three Breathotron systems using CAP25 sensors were evaluated. This was to determine sources of variation between the instruments and, if there were any, whether they were from the electronics, or the sensor itself. The response of the systems to dry and humid samples was also investigated. Following these initial experiments on the original CAP25 based systems, two of these systems were then modified to accept Figaro® sensors, and calibration curves for acetone, ammonia and propanol were generated for the unmodified and modified systems.

6.2 Materials and methods

6.2.1 Breathotron maintenance

Prior to any experiments being performed, all three systems were serviced. This involved removing and refilling the hydrocarbon traps, and the removal of the MMOS sensor from the sensor block. This was to ensure that the instruments were the same for experimental purposes. There are two Breathotron Mk IIb systems in existence, and a version which is technically the same but lacks thermal desorption (TD) tube capability known as the VapourGuard.

6.2.1.1 Removal and refitting of hydrocarbon trap

The hydrocarbon trap is required by the Breathotron as a hydrocarbon free air supply. The typical lifecycle of the hydrocarbon trap is typically 6 months. It is more efficient and practical to use a hydrocarbon trap than a pressurised cylinder containing zero grade air.

The hydrocarbon trap was removed from the instrument and refilled with new Supelcarb® adsorbent (Sigma-Aldrich, Gillingham, Dorset, SP8 4XT). The refilled hydrocarbon trap was then refitted to the instrument.

6.2.1.2 Sensor block cleaning procedure

The sensor block was removed from the instrument. Wearing powder free nitrile gloves, the block was dismantled. The block was then sonicated in reverse osmosis (RO) water (Millipore, Billerica, MA, US) for 10 minutes, then acetone (Fisher Scientific, Loughborough, LE11 5RG) for 10 minutes and finally methanol for a further 10 minutes. The block was then dried in an oven at 60 °C for approximately 2 hours. This procedure is the same for newly built sensor blocks that have not been fitted previously.

6.2.1.3 PCB fitting

The inner (sensor mounting) surface of the sensor 'piggyback' printed circuit board (PCB) was swabbed with acetone on a Kim wipe. A piggyback board, shown the sensor mounting side, can be seen in Figure 6.1. The outer plastic cover from the CAP25, datasheet in Appendix C.1.1, sensors were removed using a scalpel and fitted to the PCB, aligning Pin 1 with the square pad on the PCB. The PCB was then swabbed again with acetone and dried using a heat gun on a low heat setting. A small quantity of heat sink compound was applied to the recess of the chamber temperature sensor. The sensor block was then rebuilt with new gaskets and bolts.

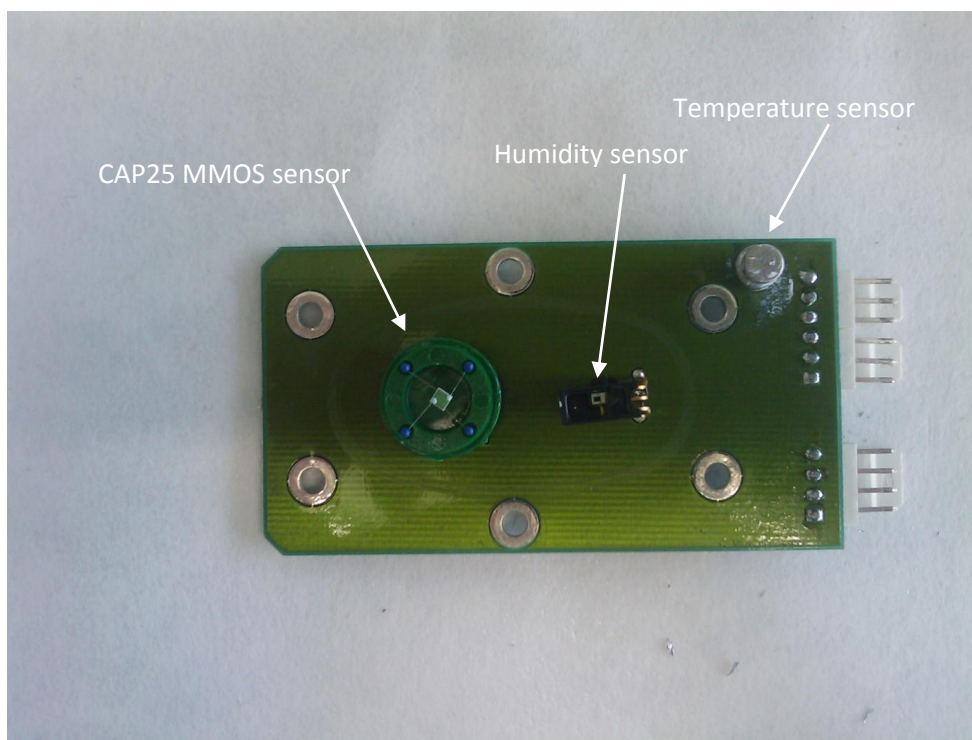


Figure 6.1 CAP25 'piggyback' board shown with sensors in place

6.2.1.4 Leak testing

The block was then immersion leak tested in a beaker of water. A $\frac{1}{4}$ "-28 PTFE plugs into the downstream fitting and a $\frac{1}{4}$ " -28 barb fitting was used to connect the upstream port to the regulator of a cylinder containing zero-grade air. The block was then carefully immersed into a beaker of water and inspected for visible bubbles. If bubbles were seen, the block was removed and the bolts each tightened another quarter of a turn and the leak test was performed again.

6.2.1.5 Refitting the sensor block

Heat sink compound was applied to both sides of the peltier device before reattaching the heat sink and cooling fan. Refitting the sensor block back into the instrument was the reverse of removal. A fully reassembled and refitted sensor block can be seen in Figure 6.2.



Figure 6.2 A fully assembled sensor block on a Breathotron

6.2.2 Breathotron system tests

The purpose of the system tests was to identify sources of variation between the three different instruments, whether they came from the construction of the electronics or from the sensor itself. The electronics were tested by injecting a signal generated from a signal generator. The difference between the instruments in response to reference gas, both dry and humidified was then investigated.

6.2.3 Sine wave

A generated signal was injected into each of the instruments to determine if the electronic components were a potential source of variation. The Molex connector connecting the piggyback PCB to the signal conditioning board was disconnected and a 1Hz, 500 mV peak to peak sine wave with a 2.5 mV offset generated using a Black Star Jupiter 2000 function generator (Cambridge). The signal was monitored using a Tektronix TDS210 oscilloscope (Beaverton, Oregon, US). All of the instruments were set to an offset of 3.37 V and a unity gain (1) using the VapourGuard software on a PC. A sample was then recorded in the usual manner

for the two Breathotron and VapourGuard instruments. The software programmable gain was then increased to 2, and finally 4, recording a sample on each of the instruments at each stage the software gain were increased.

6.2.3.1 Response of Breathotron to dry and humid acetone gas samples

The two Breathotron and VapourGuard instruments were connected to a personal computer (PC) running Microsoft® Windows XP™ SP2 (Redmond, US) for then analysis of samples were analysed using PC based VapourGuard software (Cranfield Health, Bedfordshire, MK43 0AL). All three instruments were connected to the same computer, the two Breathotrons by serial (COM) port and the VapourGuard by universal serial bus (USB). The Breathotrons were then switched on for a minimum period of 15 minutes to allow the sensor to achieve a stable baseline resistance (the same procedure used in previous experiments).

The three Breathotron systems were connected to a 40 L cylinder of (nominal) 10.8 ppm acetone in synthetic air (BOC Gases, Guilford, Surrey, GU2 7XY) via a cross piece to ensure that flow was consistent to each of the devices. 30 samples of acetone gas were analysed consecutively on each of the instruments to give a total of 90 dry gas samples in total. Sampling was simultaneous on each of the instruments, to ensure that the same sample was being analysed by the instruments at the same time. Each instrument was allowed to reach its respective baseline resistance, established prior to the start of the experiments, before the next sample was analysed.

Following the analysis of dry gaseous acetone, humidified 'wet' samples of 10 ppm acetone in water were made by application of Henry's Law and pipetted into 4.5 L Nalophan® bags (see Chapter 3 for details on how Nalophan® bags were made). Each system had a separate sample bag of acetone attached to it. Prior to analysis, the actual concentration of the sample was confirmed using SIFT-MS in the MIM mode using the H_3O^+ precursor ion. Again, 30 samples were analysed consecutively by each of the instruments to give 90 wet gas samples in total.

The response to hydrocarbon free CP grade zero air (BOC Gases, Guilford, Surrey, GU2 7XY) in Nalophan® bags was also investigated. Each instrument had a separate bag. And again, 30 samples were analysed to give 90 samples of zero grade air in total.

This yielded a sufficient amount of data for principal components analysis (PCA), 270 samples in total over three instruments. Samples of a certain type (e.g. dry acetone gas) were collected

on the same day to minimise effects of sensor drift and variation between separately prepared samples.

6.2.4 Breathotron modifications

6.2.4.1 Sensor selection

Many different sensors were looked at during the selection procedure. Ultimately Figaro TGS 2600 series gas sensors were chosen for development work because of their relatively low cost and availability from RS Components. A photograph of the three different sensors can be seen in Figure 6.3, left to right: City Technology CAP25 general air quality sensor; Figaro® TGS 2602; Figaro® 2620. Size is shown relative to CAP25.

The Figaro® TGS 2600 series (Figaro Engineering Inc., Osaka, Japan) gas sensors are thick film screen printed metal oxide semiconductors. The main advantage of the 2600 series is the small footprint; they are housed in standard TO-5 metal can enclosures, and low power consumption, 250mW for the TGS2602, datasheet in Appendix C.2.1, and 210 mW for the TGS2620, datasheet in Appendix C.2.2, in comparison to 350mW for the CAP25. Two different TGS 2600 series sensors were chosen to be evaluated, the TGS 2602 and the TGS 2620 as they are sensitive to components typically found in exhaled human breath. The TGS 2602 has high sensitivity to contaminants in air and is also sensitive to low concentrations of ammonia and hydrogen sulphide, whilst the 2620 displays high selectivity to VOC vapours.



Figure 6.3 A comparison of the three different MMOS sensors that were selected to be evaluated

6.2.4.2 Prototyping

Due to the smaller physical size and power consumption requirements of the Figaro® TGS 2600 series sensors, these sensors could not be 'plugged' straight into the pre-existing 'piggyback' PCB. Several modifications needed to be made to the sensor board in order to accommodate them. Electrically, the 2602 and 2620 are the same though the construction of the TO5 can housing is different.

The first stage was to examine sensor behaviour by prototyping a 'piggyback' board. This prototype was based on an example by Rosie Daniel (Interactive Mud Hut, www.rosiedaniel.com accessed 11th June 2010). The circuit diagram for this prototype is reproduced in Figure 6.4 where R_s is the resistance across the sensor, R_L is the load resistance, R_H is the resistance across the heater, V_S is the voltage across the sensor and V_H is the heater voltage. One of the sensors was soldered onto VeroBoard®, Figure 6.5. The negative heater pin, 1, was connected to the ground of the Arduino, the positive heater pin, 4, was connected to the external power supply running at 5.0 V, in theory the Arduino can power the gas sensor. The signal output pin, 2, was connected to a resistor box (RS Components) and in turn was connected to analogue input pin 2 on the Arduino a digital volt meter (DVM) was connected in series to confirm voltage. The code for reading back the resistance values can be seen in Appendix B.2.2. The principle is the same for the TGS 2602. The working prototype connected to an Arduino, which was in turn connected to a laptop PC that logged ADC values from the Arduino at 100 hertz (Hz).

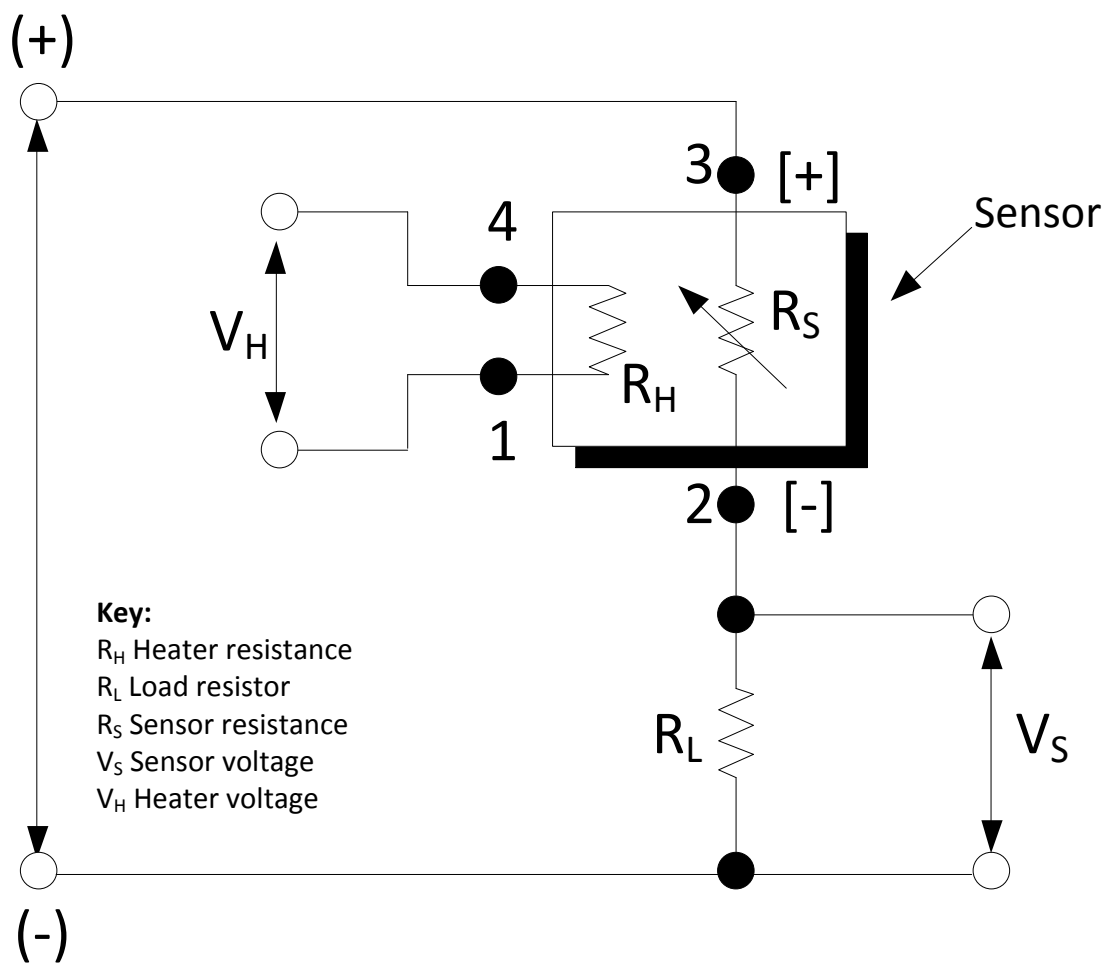


Figure 6.4 Circuit diagram for Figaro® 'piggyback' board prototype

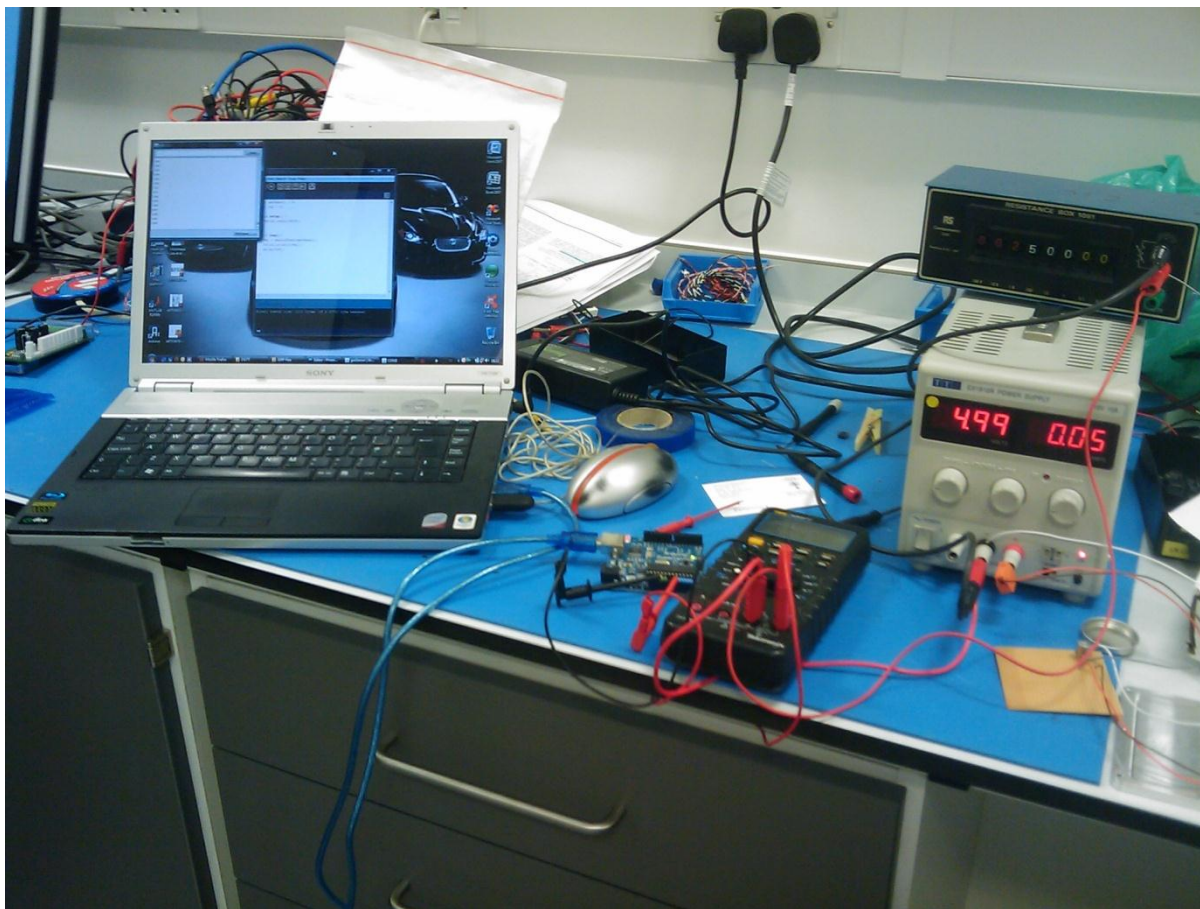


Figure 6.5 Prototype Figaro® MMOS sensor 'piggyback' board connected to an Arduino

6.2.4.3 Modifications to the Breathotron piggyback board

The existing sensor 'piggyback' boards were then modified to accommodate the new sensors. An existing 'piggyback' board can be seen in Figure 6.6 with a CAP25 MMOS sensor in place. The first modification was to remove the signal amplifier which was not required for the Figaro sensors, and was originally intended for the CAP25. The 2600 sensors were soldered in by bending their pins rather than using sockets due to the physical size of the original CAP25 sensor that the board was designed for. A modified sensor 'piggyback' board can be seen in Figure 6.6. The VapourGuard, that lacks thermal desorption capability, was refitted with a TGS2620 sensor, whilst Breathotron 001 was fitted with a TGS2602 sensor. This selection was chosen at random. The sensors were fitted into new, rather than existing blocks. Modified Molex connectors were needed, as the sensor heaters had to be powered from an external power supply supplying 5 V instead of the 12 V required by the CAP25. The block temperature read back did not function due to the modifications required to accommodate the Figaro® sensors.

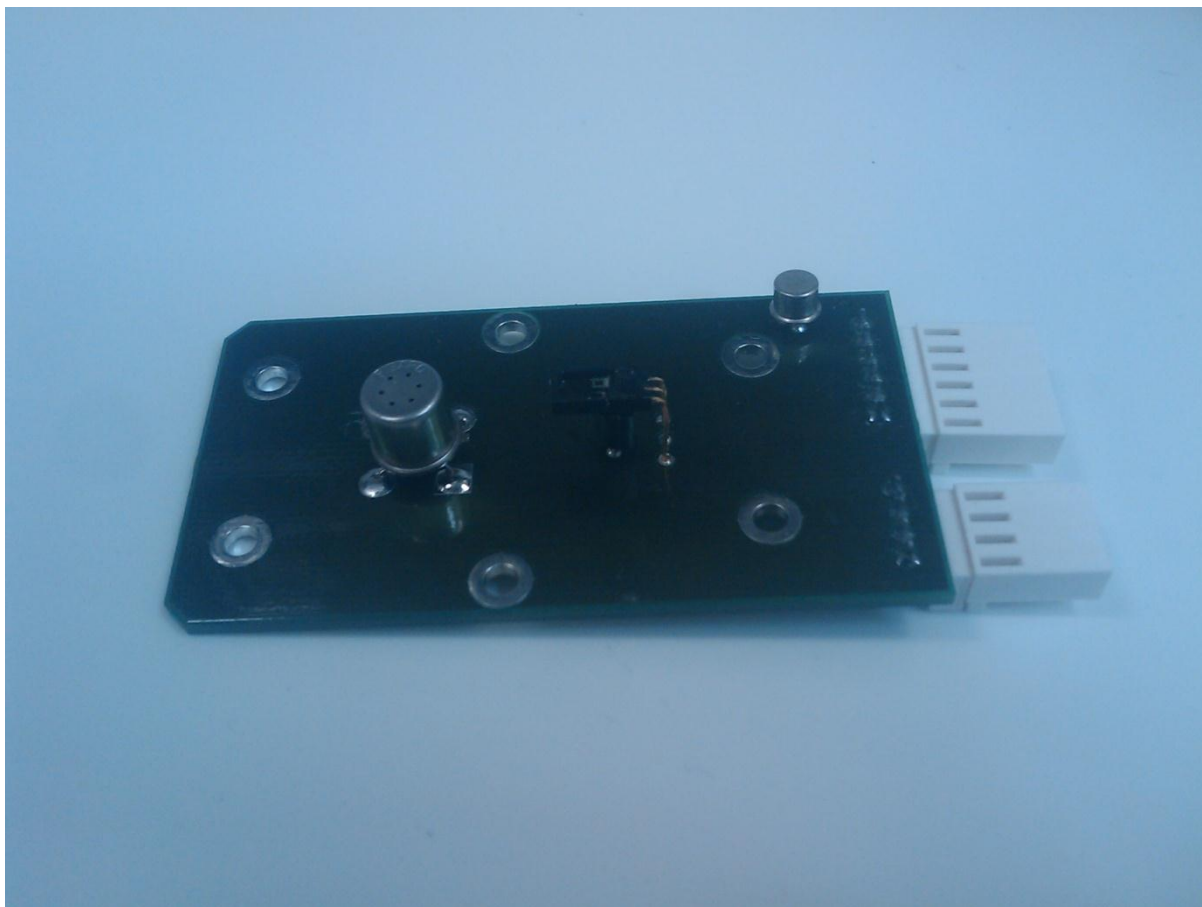


Figure 6.6 Modified 'piggyback' board shown with Figaro® TGS2602

The top of the board is shown there are further modifications on the other side of the board that include the removal of the amplifier.

6.2.5 Response of the modified systems to dry and humid gas samples

The modified systems were rebuilt and leak tested using the same method described previously in this chapter for the unmodified systems. This part of the experiment is the same as 6.2.3.1, except that only the response from the modified systems was investigated.

6.2.6 Acetone, ammonia and propanol calibration curves

Calibration curves were produced for acetone, ammonia and propanol between 0 and 100 ppm. These were produced by making a stock solution of nominally 100 ppm in RO water using Henry's Law for each of the compounds. A serial dilution of the stock solution provided nominal concentrations of 0.0, 0.1, 0.2, 0.5, 1.0, 2.0, 5.0, 10.0, 20.0, 50.0 and 100 ppm. The serial dilutions were pipetted into Nalophan® bags and filled with zero grade air. Prior to sampling, the bags were analysed using SIFT-MS to determine the actual concentration. Each

bag was analysed 5 times, which resulted in a 50 point calibration curve for acetone, ammonia and propanol for each of the instruments.

6.3 Results

6.3.1 Breathotron system tests

6.3.1.1 Sine wave

The responses recorded at unity, 2 and 4 software programmable gain were analysed. An example of the overlaid sine waves at unity gain for each of the three systems can be seen in Figure 6.7. It was observed that there was negligible difference in signal peak to peak, with no detectable time or phase shift between the signals at each of the gain settings suggesting that variation in signal response between the different systems is not due to the electronic components of the system.

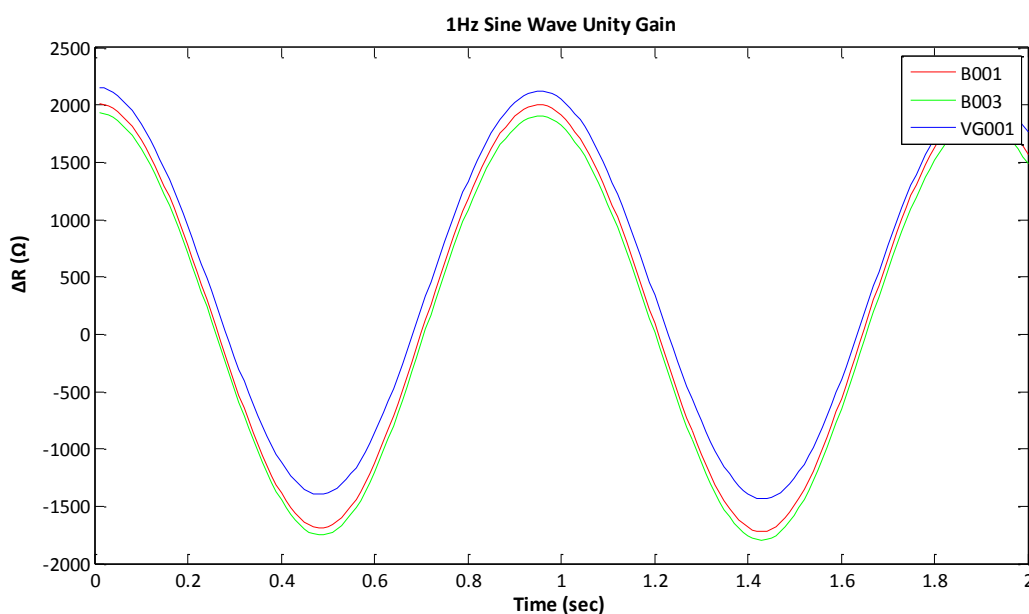


Figure 6.7 Overlay of 1Hz injected sine waves at unity gain for each of the three systems

6.3.2 Response of Breathotron to dry and humid acetone gas samples

Data collected from the three instruments, each with CAP25 sensors, was analysed using the method described in Chapter 2. The unsmoothed sensor response to dry acetone, Figure 6.8, shows there is a considerable difference in the baseline resistance of the three sensors. Each of the sensor signals has its own distinct shape, with each sensor returning to baseline at a different rate. This is despite the fact that all three sensors were new and fitted to the

instruments at the same time, and had similar operation times. There is also a difference in response to reference gas, with the greatest resistance being seen in the sensor fitted to Breathotron 001. Though the sensor fitted to Breathotron 003 has a lower baseline resistance than the sensor fitted to VapourGuard 001, the change in resistance is much greater.

A difference between the sensors is also seen in response to wet acetone, Figure 6.9. It can be seen that Breathotron 001 has a higher baseline resistance, with Breathotron 003 having the lowest. The ΔR_{\max} for wet acetone, Figure 6.13, shows a different relationship to that seen with dry acetone, there is a greater increase in sensor resistance in Breathotron 003 and VapourGuard 001 in response to wet acetone than Breathotron 001. The ΔR_{\max} for all of the sensors is lower with wet acetone than that seen with dry acetone.

There was little difference in sensor response to zero grade air, Figure 6.10, though the difference between the baseline resistances can still be seen. There was a greater increase in ΔR_{\max} seen with Breathotron 001 than the other two instruments which may have been due to contamination or electrical interference in this particular sample. The signal response is much lower than that seen with either dry or wet acetone.

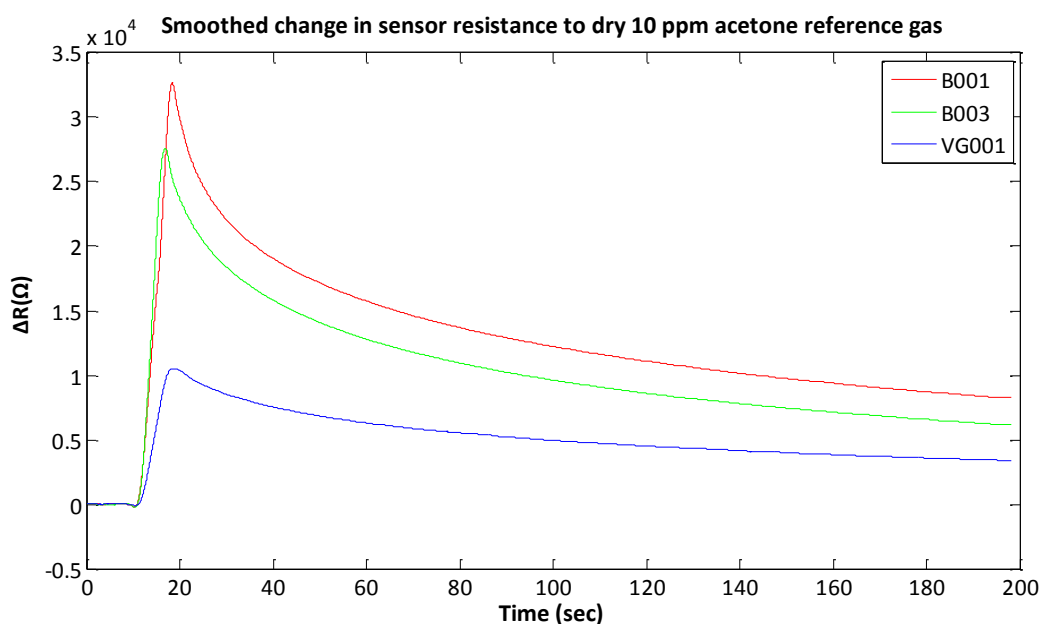


Figure 6.8 Difference in typical smoothed change in sensor resistance in response to dry 10 ppm acetone reference gas

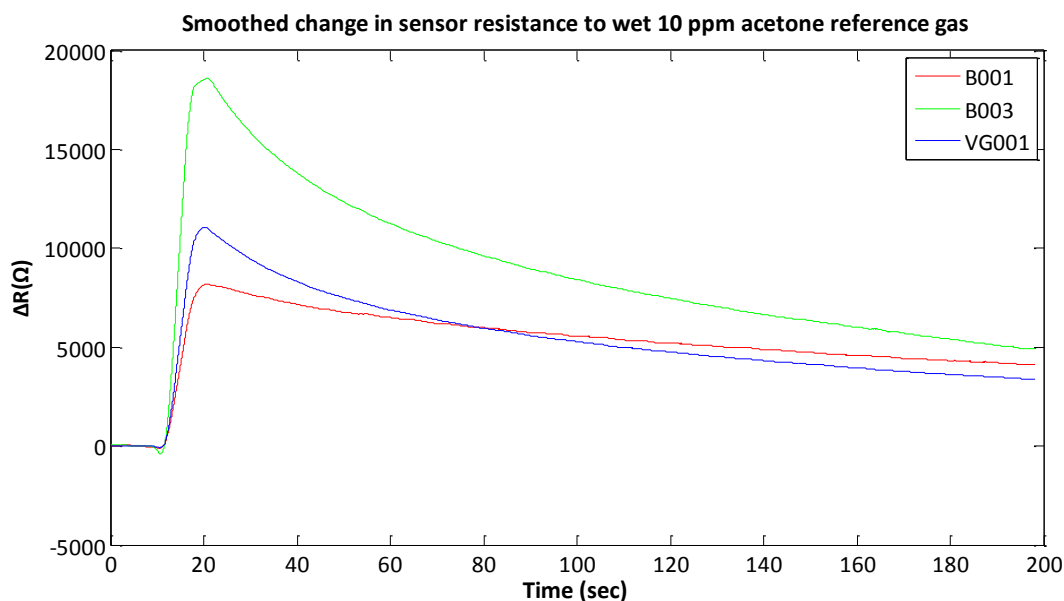


Figure 6.9 Difference in typical smoothed change in sensor resistance in response to wet 10 ppm acetone reference gas

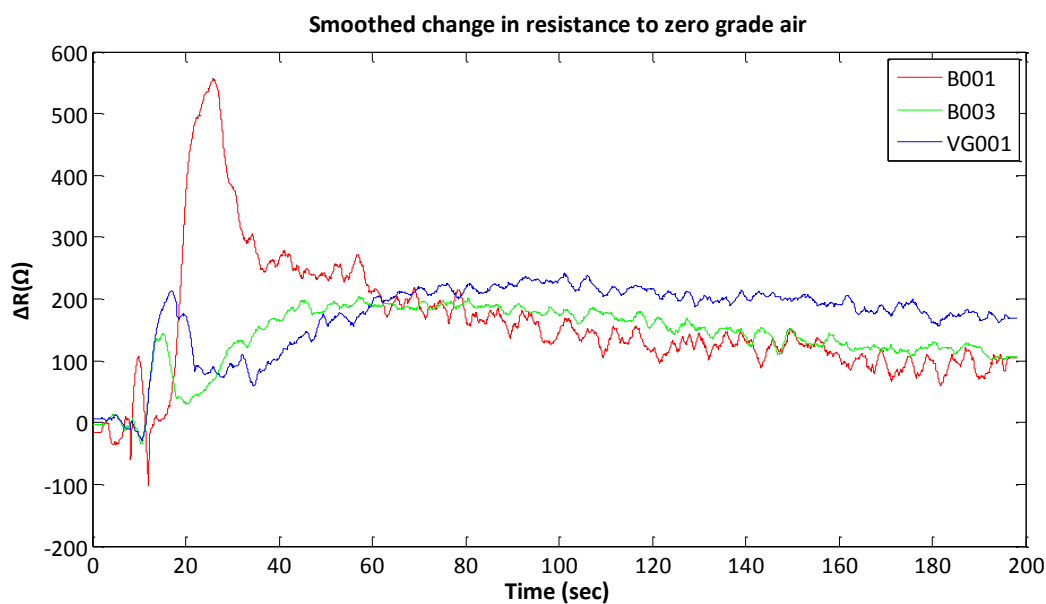


Figure 6.10 Difference in typical smoothed change in sensor resistance in response to zero grade air

6.3.3 Principal components analysis

The dry and wet 10 ppm acetone and zero air data was imported into Matlab® R2009b (Mathworks, Natick, MA, US) for PCA using the same method as mentioned in Chapter 2, except the data was autoscaled unlike in previous chapters as this yielded the greatest cumulative variance and most distinctive clustering pattern. The scores plot for the analysis of

dry and wet 10 ppm acetone and zero grade air can be seen in Figure 6.11. Samples from Breahtotron 001 (B001) are shown in blue, Breathotron 003 (B003) in green and VapourGuard 001(VG001) in red, whilst the shapes of the points represent the type of sample where circles are dry (Dry) acetone samples, squares wet (Wet) acetone samples and triangles are zero grade air (Air) samples. From the figure, it can be seen that there is large variation in sensor response to zero grade air within and between the different instruments. The acetone clusters are tighter, though there is better clustering amongst the wet samples despite the fact that dry acetone was delivered to the instruments directly from the cylinder. The clustering pattern for the wet replicate samples from each instrument may have been influenced by a combination of effusion of acetone from the Nalophan® bags, the long nature of the return to baseline and sensor drift given the time for the sensor resistance to return to baseline and the number of samples that were analysed. The analysis suggests that there is little differentiation between dry and wet gas in the VapourGuard.

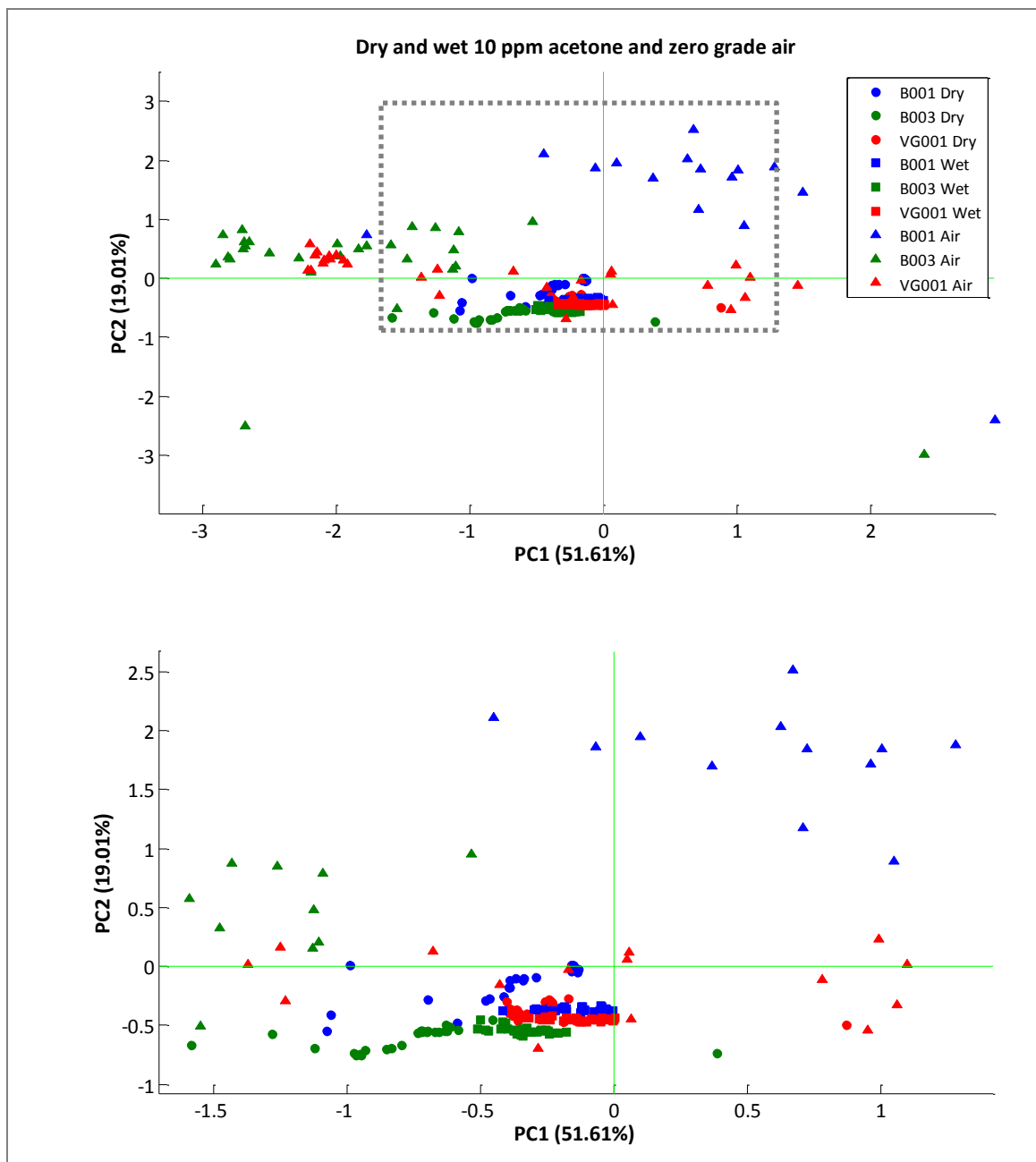


Figure 6.11 PCA scores plot of dry and wet 10 ppm acetone reference gas and zero grade air

6.3.4 Breathotron modifications

6.3.4.1 Prototyping

The Veroboard® prototype was tested by passing a clean laboratory tissue soaked in acetone near the sensor. Initially the response was too large, so the resistance was changed from 100 kΩ to 2 kΩ. This leads to a considerably smaller signal, the raw unsmoothed change in voltage across the sensor can be seen in Figure 6.12. These initial tests showed that there was a

greater change in response without the need for an amplifier in comparison to the CAP25 sensor. From this data it was determined that there was no need for a signal amplifier on the modified sensor board. There is also a better signal to noise (S2N) ratio than that seen with the CAP25 for the 2602 (the 2620 was not prototyped).

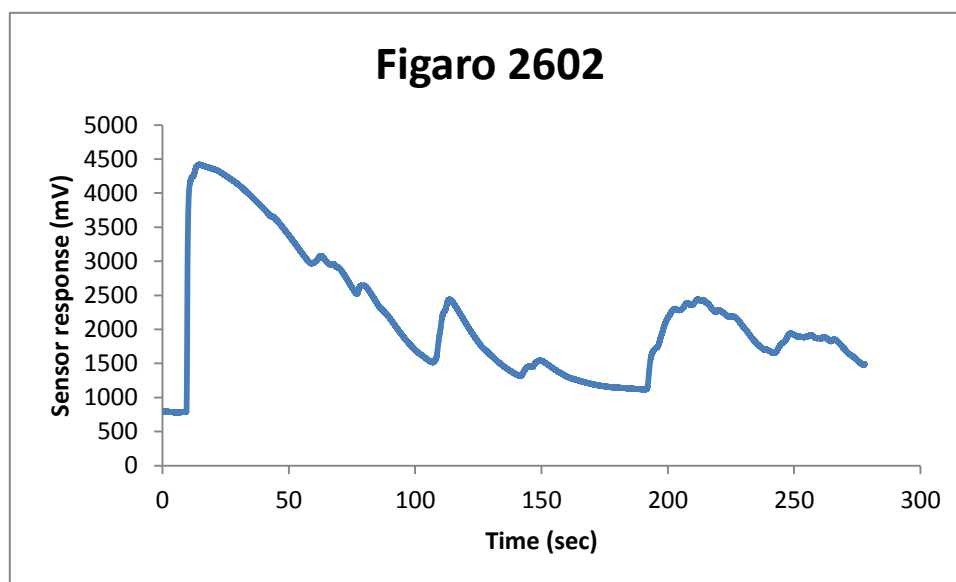


Figure 6.12 Raw unsmoothed Figaro® TGS 2602 sensor response to acetone in lab air

6.3.4.2 Response of the modified Breathotron systems to dry and humid gas samples

Once the modified systems were rebuilt and leak tested they were switched on. It was noted that the baseline resistance was achieved within a minute of switching on the instrument, though the instruments were left for 15 minutes before samples were analysed to ensure consistency with the unmodified systems and to allow the sensor block to achieve a constant temperature.

Dry and wet acetone reference gas and zero grade air was then analysed on each of the modified systems in the same way as the unmodified systems. Though the principal for reading the data from the text files into Matlab® is the same as 1.3.2, a modified version of MMOSOhms100.m was created for data from the Figaro® based systems, FigaroOhms100.m Appendix B.1.3. Dry and wet 10 ppm acetone and zero grade air samples were analysed in the same way as in the unmodified Breathotron, these can be seen in Figure 6.13, Figure 6.14 and Figure 6.15 respectively. Data from the Figaro® sensors is shown in comparison to the CAP25.

The response to dry acetone is much greater in the CAP25, Figure 6.13, but this is amplified in comparison to the signals from the Figaro® sensors which are unamplified. There is little

change in resistance in the TGS2620 in response to dry acetone in comparison to the other Figaro® sensor, where there is initially an increase followed by a decrease in sensor resistance. The return to baseline is considerably shorter for the Figaro® sensors than the CAP25.

The response to wet acetone is greater in the CAP25 sensor than the Figaro® sensors. The change in resistance in response to wet acetone is much lower than the change seen with dry gas for all of the sensors, again the 2620 does not respond as well as the other sensors.

The raw signal from the CAP25 is considerably noisier in response to zero grade air than the Figaro® sensors, whilst the baseline resistance is greater. The noise is still present in comparison to the Figaro® sensors when looking at the ΔR_{\max} . Though there is an increase in resistance in the TGS2602, a decrease in resistance can be seen for the TGS2620.

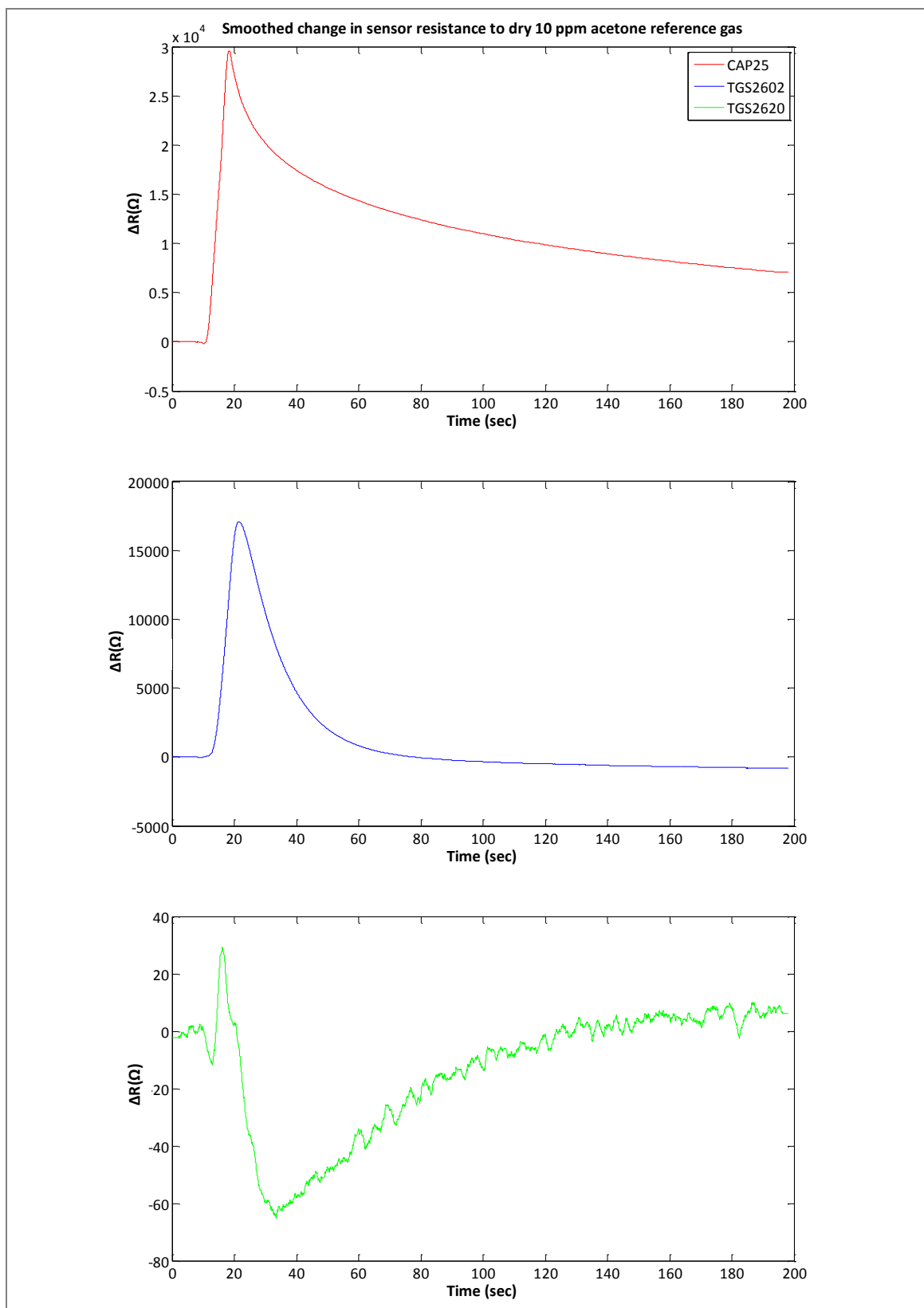


Figure 6.13 Comparison of CAP25, Figaro® TGS2602 and 2620 gas sensors to dry 10 ppm acetone gas from a cylinder

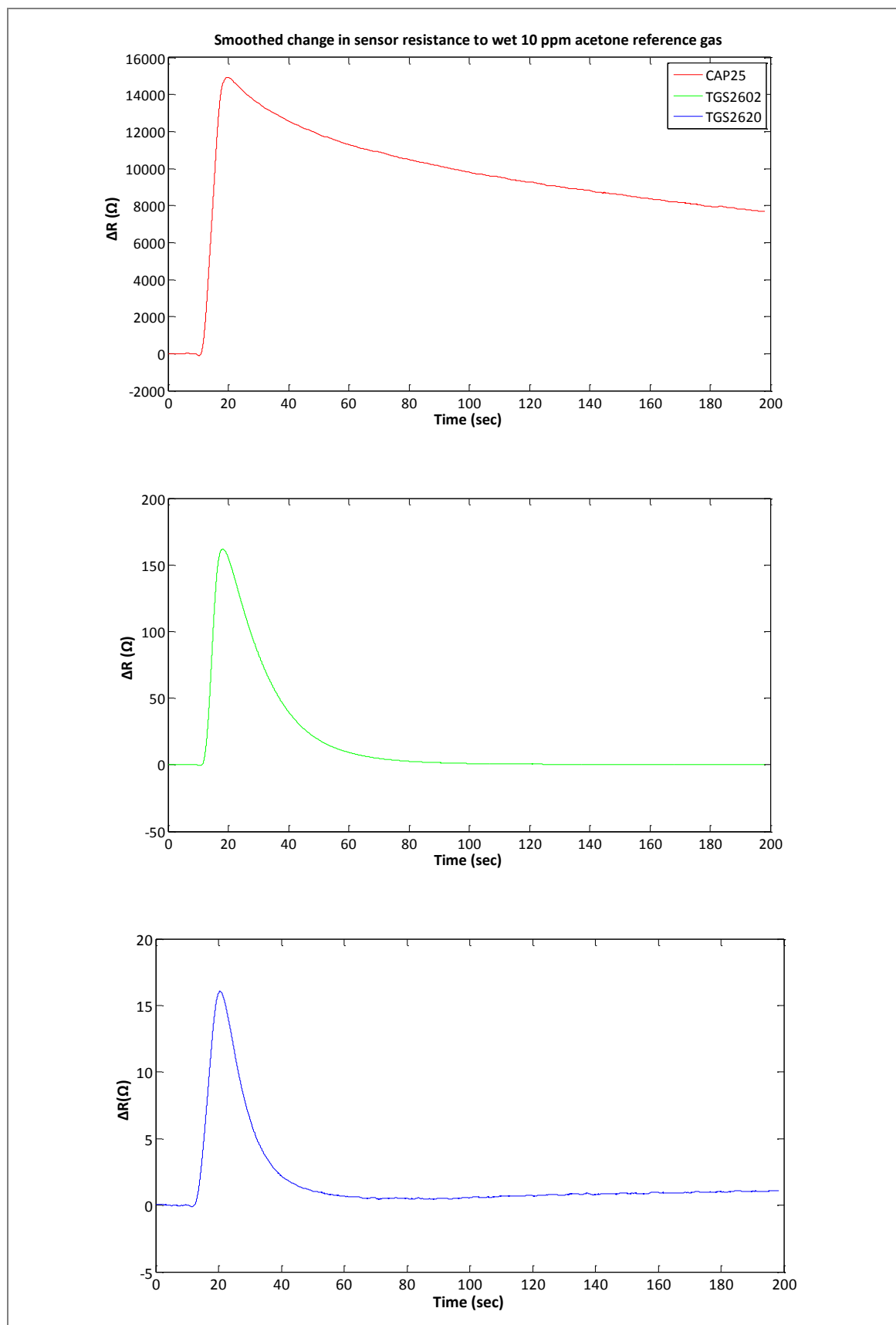


Figure 6.14 Comparison of CAP25, Figaro® TGS2602 and 2620 gas sensors to humid 10 ppm acetone gas

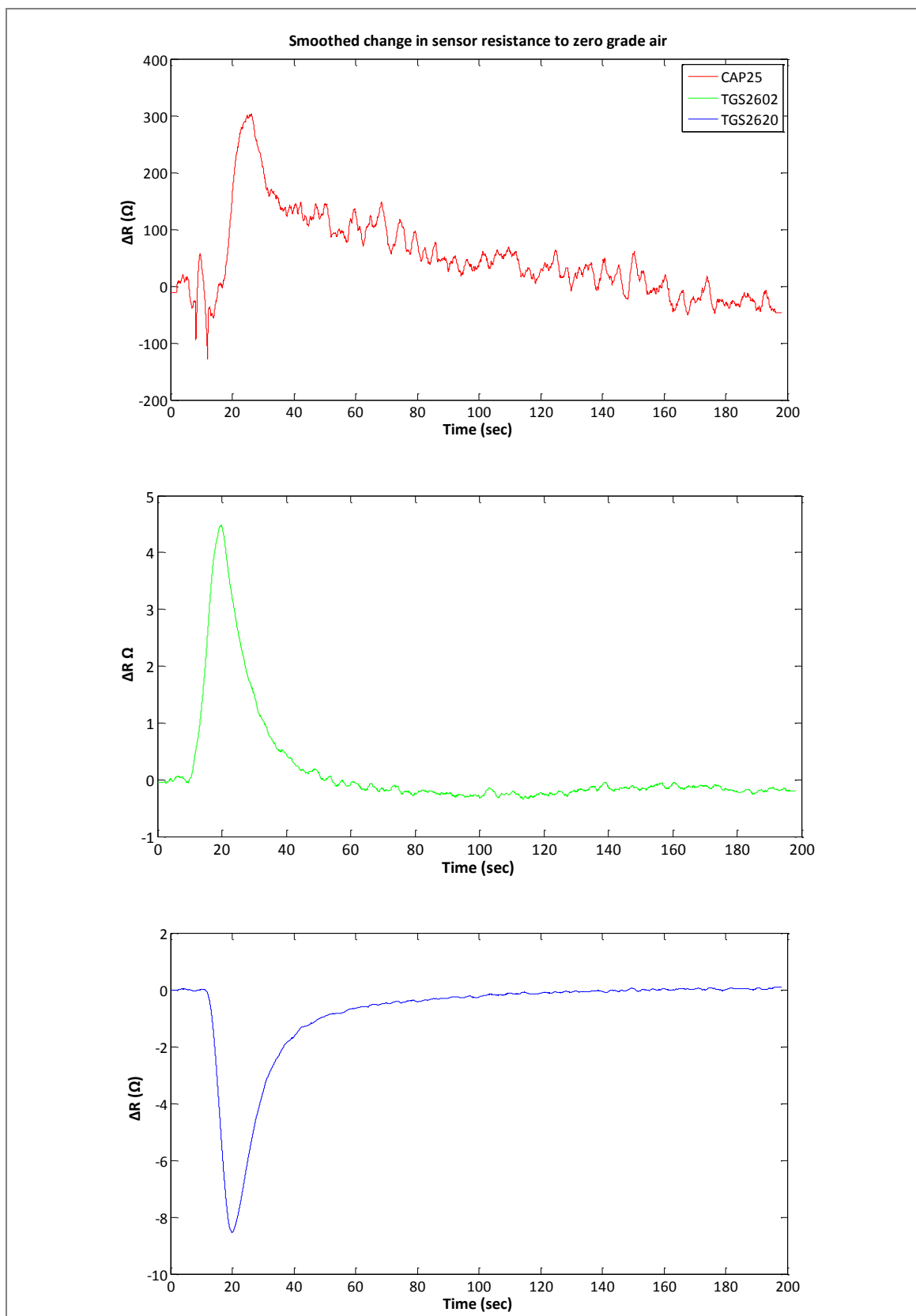


Figure 6.15 Comparison of CAP25, Figaro® TGS2602 and 2620 gas sensors to zero grade air

6.3.4.2.1 Principal components analysis

PCA was performed in the same way on autoscaled data as mentioned in 6.4.3.1, Figure 6.17. Data from the two Figaro® sensors was compared to the CAP25 data collected and analysed in 6.4.3.1. The scores plot for the analysis can be seen in Figure 6.25. Samples with a greater ΔR_{\max} tend to lie towards the right hand side of the plot, as in the case of the amplified signal from the CAP25, which is greatest in response to dry acetone reference gas. Wet and dry acetone and zero grade air samples from the CAP25, are considerably more scattered in comparison to the samples analysed using the Figaro® gas sensors suggesting that the Figaro® sensors have greater reproducibility than the CAP25. Intriguingly, as with the previous PCA in 6.4.3.1, there is better clustering of the wet acetone samples than the dry acetone samples. This is due to the small response of the sensors rather than greater reproducibility.

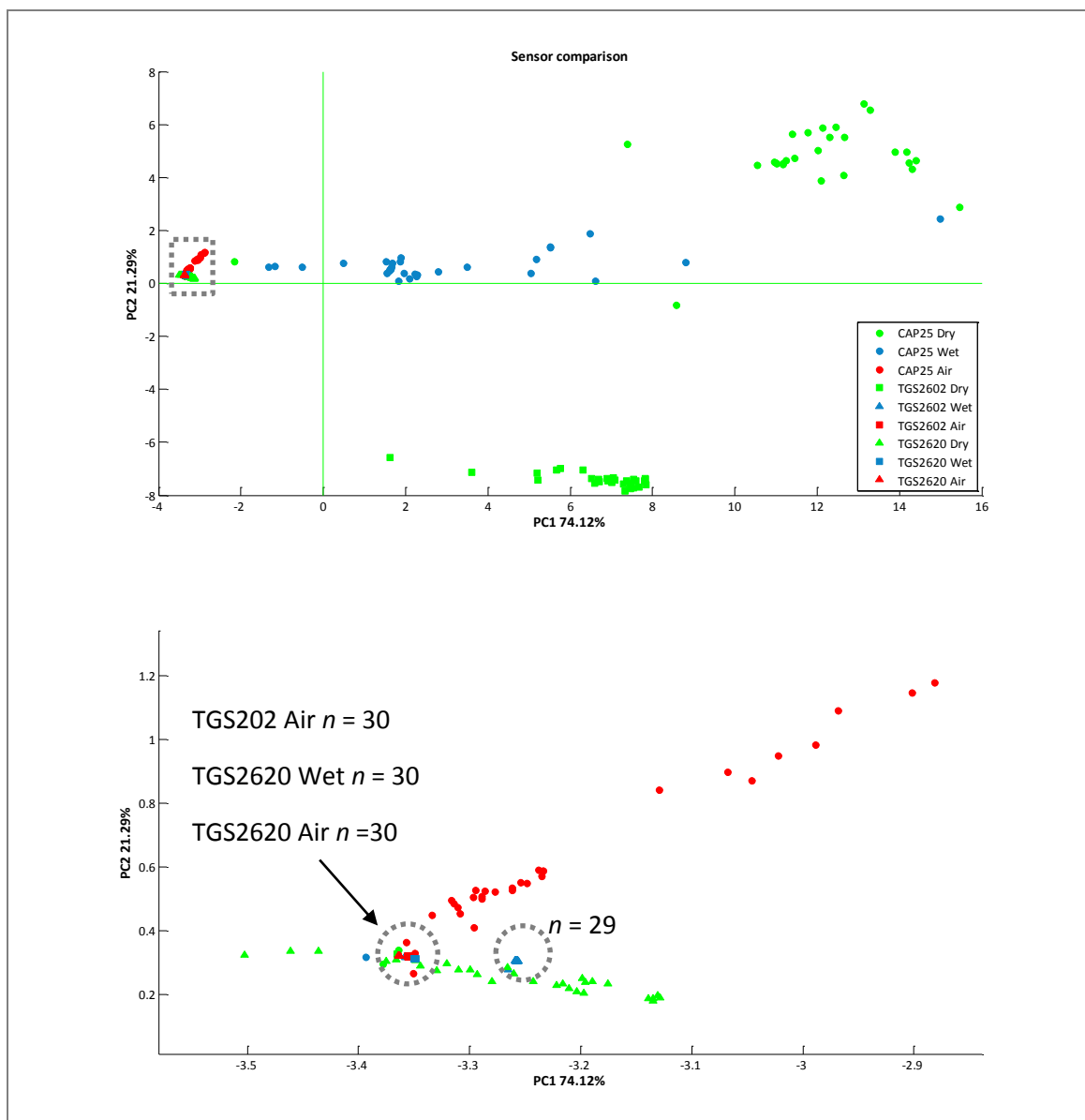


Figure 6.16 Scores plot for dry and wet 10 ppm acetone and zero grade air comparing CAP25, Figaro® TGS2602 and 2620 gas sensors, with zoomed inset

6.3.5 Acetone, ammonia and propanol calibration curves

Calibration curves were produced on the unmodified and modified systems for humid samples of acetone, ammonia and propanol using Henry's Law. Nominal concentrations of 0.0, 0.1, 0.2, 0.5, 1.0, 2.0, 5.0, 10.0, 20.0 and 100 ppm were made, but the actual concentration was determined prior to sampling using SIFT-MS. The maximum resistance (ΔR_{\max}) is plotted against actual concentration determined using. Each calibration curve has 50 points, except where software errors prevented the processing of the data file.

Acetone log-log plots for measured concentrations of acetone between 0 to 100 ppm for the CAP25, TGS2602 and TGS2620 can be seen in Figures 6.18 respectively. The advantage of using log-log plots is the ability to see the linear relationship at the lower concentrations. The ammonia log-log plots for measured concentrations between 0 and 300 ppm for the CAP25, TGS2602 and TGS2620 can be seen in Figures 6.19 respectively. The propanol calibration curves for measured concentrations between 0 and ppm for the CAP25, TGS2602 and TGS2620 can be seen in Figures 6.20 respectively. The linear correlation coefficient (R) was calculated in Microsoft® Office Excel 2010™ using the Regression function in the Data Analysis Toolpak, and can be seen in Table 6.1.

There is good positive correlation between acetone concentration and ΔR_{\max} for the CAP25 sensor ($R = 0.96$), Figure 6.27. At higher concentrations however, ΔR_{\max} is less consistent. There is stronger positive correlation between acetone concentration and ΔR_{\max} for both the TGS2602 ($R = 0.99$) and TGS2620 ($R = 0.99$). A greater increase in ΔR_{\max} in response to acetone is seen in the TGS2602 than the TGS2620 at the same concentrations.

Though the nominal concentrations were set at between 0 and 100 ppm, when the ammonia samples were quantified on the SIFT-MS the greatest concentration measured was 300 ppm. There is strong positive correlation between ammonia concentration and ΔR_{\max} for the CAP25 ($R = 0.98$), Figure 6.28. Though there is good positive correlation for the TGS2602, Figure 6.29, between concentration and ΔR_{\max} ($R = 0.98$), not all of the samples above 10 ppm fall onto the calculated line. There is stronger positive linear correlation between concentration and ΔR_{\max} than the TGS2602 ($R = 0.99$). The ΔR_{\max} is greater, but similar to, that seen with the TGS2602.

There is good positive correlation between propanol concentration and ΔR_{\max} with all three sensors right through the concentration range. The correlation coefficient for the CAP25 ($R = 0.98$) is however the lowest, with the two Figaro® sensors sharing the greatest (TGS2602 $R = 0.99$, TGS2620 $R = 0.99$). The ΔR_{\max} for the CAP25 in response to propanol is greater than that for acetone and ammonia, Figure 6.33, though this is not true for the two Figaro® sensors. The TGS202 has the greatest ΔR_{\max} in comparison to the TGS2620, though the difference is not as great as seen with acetone samples.

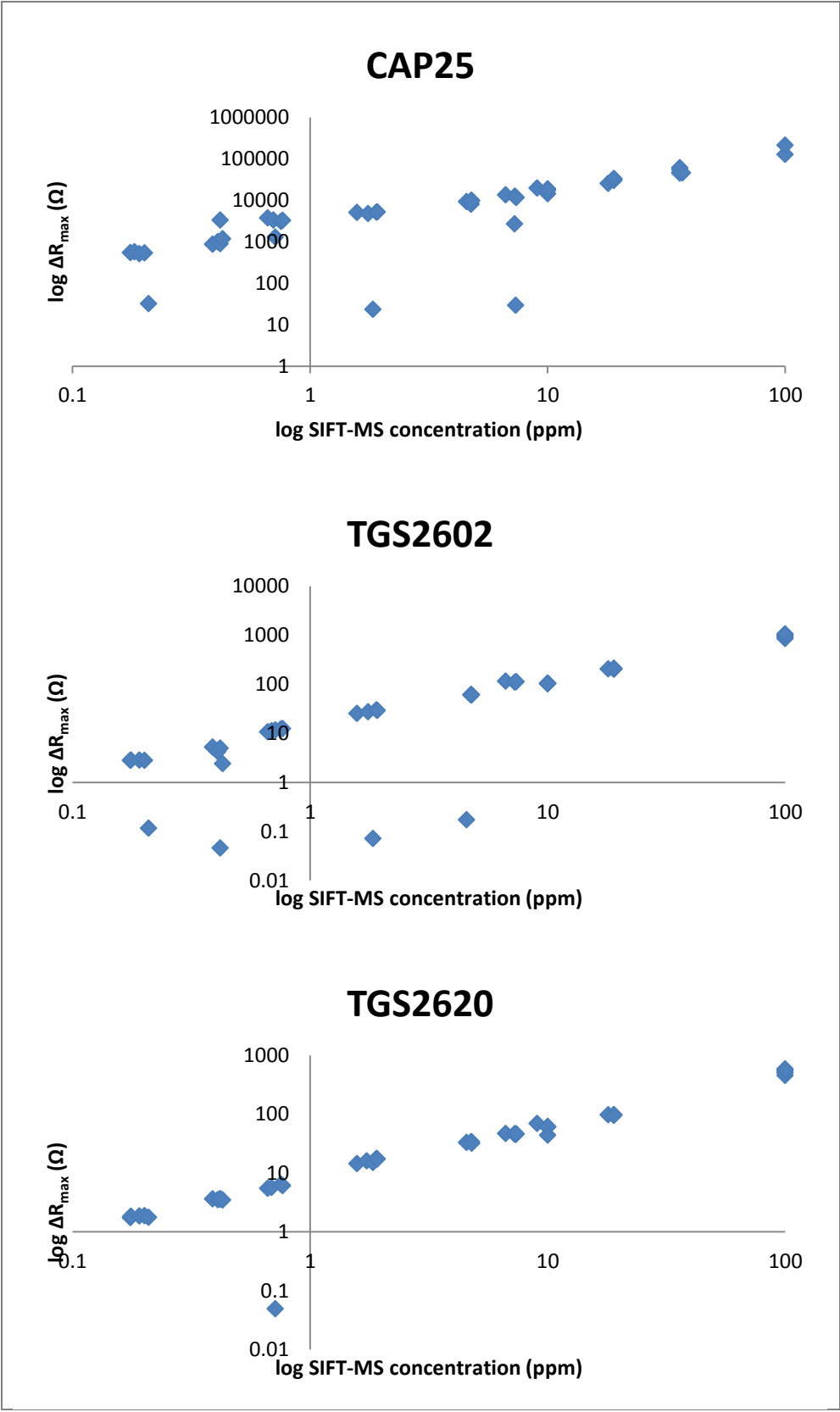


Figure 6.17 Log-log plots for the CAP25, TGS2602 and 2620 in response to acetone

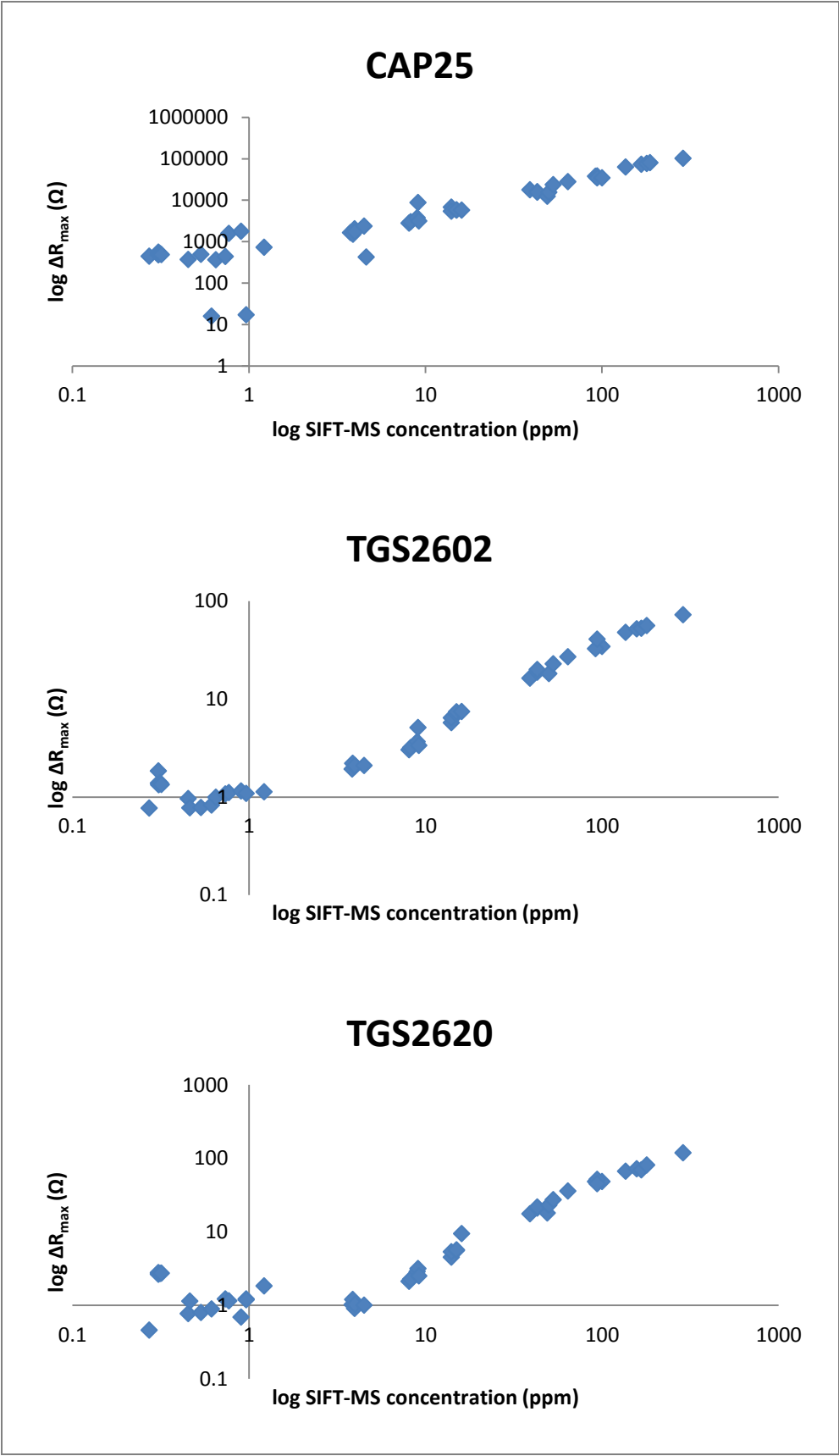


Figure 6.18 Log-log plots for the CAP25, TGS2602 and 2620 in response to ammonia

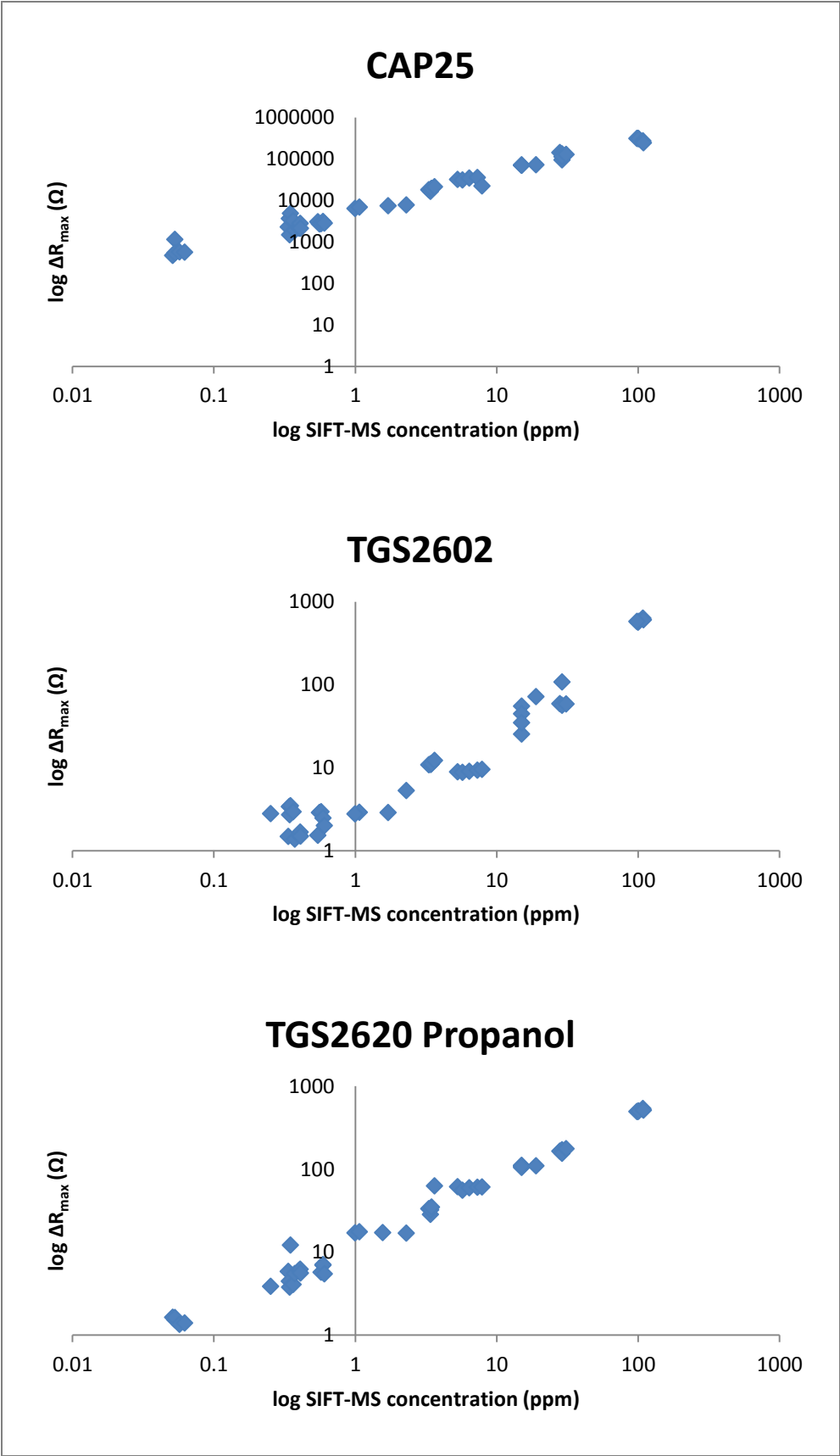


Figure 6.19 Log-log plots for the CAP25, TGS2602 and 2620 in response to propanol

Sensor	Acetone	Ammonia	Propanol
CAP25	0.96	0.98	0.98
TGS2602	0.99	0.98	0.99
TGS2620	0.99	0.99	0.99

Table 6.1 Linear correlation coefficients for the CAP25, TGS2602 and TGS2620 calibration curves

6.4 Discussion

In this experiment we took three identical Breathotron instruments and subjected them to various tests to determine if there was any variation between the systems – whether this was due to the construction of the electronics or the sensor itself. An important aspect of this study was the verification of the instruments themselves, this aspect was tested by injected signal. All of the instruments behaved similarly with only minor differences found.

It was found that there is poor intra- and inter-system repeatability in response to dry and humid acetone reference gas and zero grade air for the CAP25 gas sensor. There was greater repeatability with the modified systems that used the Figaro® TGS2602 and TGS2620 gas sensors. All of the sensors displayed positive linear correlation in the change in resistance (ΔR_{\max}) of the sensor against concentration of acetone, ammonia and propanol within physiological concentrations.

The CAP25 is a general air quality sensor designed for aeronautical and automotive applications (McGeehin, 2000), and was used originally used in the predecessor to the eNostril developed by Lee-Davey, (2004) (Department of Analytical Science and Instrumentation, Cranfield University, Silsoe, MK45 4DT) for the analysis of headspace over transformer oil. The CAP25 has been used in an eNose studies examining the spoilage of meat, and the growth of mould species (Panigrahi et al., 2006; Kuske et al., 2006). In these applications, the CAP25 was used alongside other MOS sensors unlike our single sensor application. Previous studies have attempted to determine features that best classify the signals and determining the limits of detection and analysis of complex mixtures (Panigrahi et al., 2006; Bishop, 2006; Patel, 2007)

Figaro® gas sensors, specifically the TGS822, have been used in previous studies to investigate compounds in exhaled breath such as ethanol and acetaldehyde (Paulsson et al., 2000; Mitsubayashi et al., 2005). Though the later generations of the sensors used here (TGS2600

and TGS2602) have been used in sensing robots (Purnamadjaja and Russell, 2007), to our knowledge, this is the first time that they have been used in a breath gas sampling device.

The short warm up time and quicker return to baseline for the Figaro® sensors in comparison to the CAP25 has several practical benefits. Higher throughput sampling can be achieved, as seen in the dry and humidified 10 ppm acetone reference gas repeatability trial, where the shorter sampling interval results in more consistent signals between samples. This would also be of benefit in a clinical setting, where samples may need to be analysed rapidly, or in quick succession. More frequent samples would result in more analysable and representative breaths. This could also conceivably allow the device to be switched off in between sampling, which would preserve sensor life and possibly would allow the device to be battery powered.

There was considerable difference in the baseline resistance and the change in resistance (ΔR_{\max}) of the three CAP25 gas sensors in response to dry and humid acetone reference gas and zero grade air. Signals from the different instruments had a different shape and amplitude, despite the fact that all of the sensors were installed from new and the devices serviced prior to the experiments. In comparison, there is greater consistency between samples with the modified Figaro® systems. The response to dry 10 ppm acetone for the VapourGuard was lower than in a previous experiment where the gas sensor was not changed, or the hydrocarbon trap changed prior to analysing gaseous samples (Patel, 2007). This may be due to differences between the sensors that were installed into the devices at each given time. All of the sensors, CAP25 and Figaro®, were allowed to return to approximately 1k Ω of the starting baseline resistance before the next sample was analysed. This variation in sensor response cannot be due to the fabrication of the electronics which was confirmed by the injection of a sine wave into each of the systems, but is more likely to be due to differences in the manufacture of the individual CAP25 sensors.

The Figaro® sensors gave a sufficiently large signal at unity gain without the need for signal amplification, unlike the CAP25 where a large offset (2.5 V) is needed. The CAP25 also introduces a large offset (tens of millivolts at the sensor terminals) which must be counteracted in order for adequate signal gain to be applied. This is not required with the Figaro® gas sensors.

The clustering patterns seen with dry acetone reference gas samples could not have been caused by thermal spots within the block due to its machined aluminium construction. This

ensures that heat is spread uniformly throughout the sensor block. As this spread is mostly seen with the dry samples that were fed into the systems directly from the cylinder and not into Nalophan® bags, it is probably due to perturbation in the flow to the instruments or stratification of gas in the cylinder. This could be avoided in future by possibly using a heated jacket around the cylinder to prevent stratification, or by using smaller cylinders of gas that are easier to roll.

In a previous study that investigated the effect of ambient humidity on CAP25 sensor performance in ambient laboratory air found that an increase in humidity led to a lower response (Bishop, 2006). The tighter clustering, seen with all sensor types, of the zero grade air and wet samples may be due to reduced error as the signal intensity is not as large as dry acetone samples.

There was a linear relationship between concentration and ΔR_{\max} for all of the sensors with all three analytes, though the linear correlation coefficients are marginally better for the two Figaro® sensors. The detection of ammonia and propanol was better using the TGS2620, which did not produce as great a response as the TGS2602 in the presence of acetone. This result with ammonia is unusual, as the manufacturer claims that the TGS2602 is better suited to detecting ammonia than the TGS2620.

The limit of detection (LOD) for all of the sensors was below 100 ppb, this was confirmed using SIFT-MS. In a previous study with dry gaseous samples of acetone, ammonia and propanol nominally between 0 and 10 ppm (Patel, 2007), there was strong positive correlation between acetone ($R = 0.99$) and propanol and ΔR_{\max} ($R = 0.99$), but weak positive correlation between ammonia and ΔR_{\max} ($R = 0.46$). The poor correlation in the previous experiment may be due to several factors: Firstly, samples were diluted from stock concentrations of nominally 10 ppm gas using zero grade air with a crude gas mixer comprised of two mass flow controllers with manual controls. Secondly, each of these samples was tested on the VapourGuard without verification of the actual concentration of gas in the sample using an analytical method such as GC-MS or SIFT-MS, a PID may have also been sufficient.

The effect of varying the sensor heater temperature on the Figaro® sensors was not investigated. The behaviour of MOS sensors is highly dependent on temperature (Seiyama et al., 1962), and can be exploited to modify sensor selectivity (Morrison, 1987; Sears et al., 1989; Lee and Reedy, 1999). Indeed, this is exactly what has been done to the existing CAP25 gas

sensor used in the Breathotron. The manufacturer states that the CAP25 has an operating temperature of approximately 300°C, but adjusting the heater voltage we have demonstrated (unpublished data) that increasing the temperature to 420°C results in an increase in signal response to the same analyte. The disadvantage of increasing the heater temperature with the CAP25 increases the return to baseline time. In the same way, the heater temperature of the Figaro® sensors can be modified to increase selectivity (Purnamadjaja and Russell, 2007). A calibration curve for the TGS2602 heater temperature is given by Purnamadjaja and Russell, (2000) where a potential divider is used to calculate the heater resistance, though the relationship between heater resistance and heater temperature is unclear. Purnamadjaja and Russell, (2007) found that decreasing the heater voltage decreased sensitivity to eucalyptus oil (a complex mixture). Decreasing the heater voltage also increases the time required to return to baseline.

The sample delivery flow rate from the sampling loop to the sensor chamber was the same for both CAP25 and Figaro sensors. Anecdotal evidence suggests that reducing the flow rate to the sensor increases the signal response for the CAP25. As the effect of flow rate on Figaro® signal response was not investigated, it is not known if the existing flow rate used by the device is the optimal for these sensors. However, decreasing the flow rate would increase the time required to sample.

The resistance of a gas sensor is dependent on the partial pressure of oxygen in the atmosphere (Figaro 2005, datasheet in Appendix ?). As oxygen content varies in exhaled human breath, this may influence the signal. To monitor this, the system could be adapted to accept an oxygen sensor (O_2), and possibly a carbon dioxide (CO_2). From the data from the experiments collected in the other chapters it is unlikely that this would be important in sedentary subjects as CO_2 concentration remained stable.

The original experimental plan called for the analysis of mixtures of the selected analytes, acetone, ammonia and propanol. These were selected as they were used in a previous study which involved the use of dry gaseous samples of these analytes between 0 and 10 ppm. This was prevented by the sudden catastrophic failure of the sensors which was probably the result of an electrical spike in the power supply (both sensors were connected to the same supply).

An important aspect of this experiment was the use of individual sensors installed from new. Completing the original plan would have meant repeating the whole experiment from the beginning with fresh examples – this was therefore not pursued because of time limitations.

The Figaro® sensors have characteristics that would allow the Breathotron design to be improved. One such improvement would be feasible to use a commercially available Arduino Uno (Atmel® 328P) or Netduino Plus (ARM 7) (or a custom built board with an Arduino bootloader due to the open source nature of the platform) rather than the multiple custom built boards, as the signal post processing is not required by the Figaro® sensors. This could potentially reduce system complexity, size, power consumption and cost. The sensitivity of the device could be improved by using a specially designed sensor rather than one available commercially. de Lacy Costello et al., (2002) produced custom made tin dioxide (25%) and zinc oxide (75%) gas sensors and found that they were 60 times more sensitive than the commercially available Figaro® TGS822. Though fabricating a custom designed sensor would potentially increase the cost of the instrument significantly. There would also be a question of reproducibility with custom made sensors in comparison to those that can be bought commercially. Though sensitivity of sensors can be improved, this often amplifies their problems.

Due to the smaller footprint of the Figaro® gas sensors the physical size of the block could be reduced on future developments of the Breathotron. This would reduce the thermal mass of the block. A smaller heater could be employed, with a lower power requirement, which would translate to a shorter warm up time for the sensor block. Insulating the block would also ensure that more heat is retained saving further power.

One way of introducing selectivity into the device without the need for a specific sensor would be to, in effect, make a miniature GC-MS using a low powered gas sensor as the detector. This could be achieved by micromachining a column in silicone.

6.5 Conclusion

We have demonstrated that there is considerable variation between identical Breathotron instruments using the Capteur® CAP25 general air quality sensor. The source of this variation is not due to the electronics, but due to inherent differences between individual CAP25 sensors. This resulted in poor reproducibility in response to dry and humid samples of acetone

reference gas and zero grade air. This level of reproducibility would be unacceptable for a medical diagnostic device.

Modification of the systems to accept Figaro® gas sensors showed that there was a better signal to noise ratio in comparison to the CAP25 sensor. The unamplified signal for acetone vapour was almost as great as an amplified signal from the CAP25 in response to 10 ppm acetone gas from a cylinder for the TGS2602 but not the 2620. This demonstrated that an amplifier would not be needed for a Breathotron based on the Figaro® range of sensors. The Figaro® gas sensor also display a shorter return to baseline and warm up time than the CAP25.

Better clustering was seen with the Figaro® sensors than the CAP25 in PCA. The broad clustering pattern seen with the CAP25 is most likely due to the poor return to baseline of the CAP25 sensor. Poor clustering was also seen with dry acetone samples using the Figaro®, and this was suspected to be influenced by the method of sample delivery than being a characteristic of the Figaro® sensors.

There was strong positive correlation between concentration and the change in sensor resistance for the CAP25, TGS2602 and the TGS2620 in response to a range of concentrations ranging from 0 to 100 ppm for acetone and propanol and 0 to 300 ppm for ammonia samples. The performance of the Figaro® sensors was marginally better than the CAP25. Due to sensor failure mixtures of the three different analytes could not be analysed. It would have been useful to create a classification model using this data.

The Figaro® TGS2602 gas sensor provides a comparable unamplified signal to the CAP25 in response to dry 10 ppm acetone gas. Other advantages include the short warm up time, faster return to baseline and a reduced footprint in comparison to the CAP25 which would lead to other improvements in the Breathotron, such as improved S2N, lower power consumption, reduced system complexity, size and cost. The next stage would be to modify the Breathotron to accept the TGS2602 and repeat the experiments described in chapters 2, 3 and 5 using the modified system for comparison.

7 Conclusions and future work

7.1 Conclusions

Breath gas analysis is commonplace in medical diagnosis and sports science, for the detection of bacterial infections, monitoring of asthma, quantification of ethanol in breath and blood gases but none of these involve the analysis of endogenously produced metabolites.

Anecdotal evidence and previous studies investigating monitoring of exhaled breath metabolites in diabetic and non-diabetic individuals have reported a link between exhaled VOC concentration, principally acetone, and blood glucose concentration.

The Breathotron breath gas sampling device, originally known as the eNostril, was conceived for monitoring the headspace of transformer oil and was subsequently adapted for analysis of exhaled breath gas. Previous studies in vitro studies determined the lower limits of detection for several common components of exhaled breath and the effects of humidity and heater temperature on the operation of the device.

Described within this thesis is the development of a non-invasive exhaled breath gas analysis device for monitoring chronic metabolic and respiratory diseases, with particular emphasis on monitoring glycaemic status in diabetic patients as an alternative to the 'pin prick' blood glucose test. The aim was to experimentally determine suitable biomarkers using two mass spectrometry techniques, SIFT- and TD GC-MS, and develop a mixed metal oxide gas sensor based device for monitoring the identified biomarkers by evaluating the current systems performance and identifying potential improvements.

In Chapter 2, non-diabetic individuals took part in an oral glucose tolerance test where exhaled breath was analysed using online SIFT-MS and the Breathotron. TD samples were also collected for offline analysis using GC-MS. VOC concentration, and Breathotron sensor resistance was expected to fall in response to drinking the glucose solution. There was little or no change in VOC concentration or Breathotron sensor resistance during the experiment, with none of the volunteers displaying a significant correlation between sensor resistance and blood glucose concentration. Principal components analysis of the Breathotron data showed that samples collected from each individual volunteer clustered together rather than by the measured blood glucose concentration. The use of online SIFT-MS sampling meant that only one precursor ion could be used for analysis, limiting the number of compounds which could be quantified. GC-MS analysis identified the same potential candidates that were quantified

using SIFT-MS. A large variation in exhaled VOC concentration at similar blood glucose concentrations was observed in the individuals prior to the start and during the experiment. There was no significant deviation in exhaled VOC concentration and no statistically significant relationship between any of the exhaled VOCs quantified using SIFT- or GC-MS and blood glucose concentration was observed.

The hypoglycaemic clamp experiment was designed to monitor exhaled VOC concentrations in three different matrices: exhaled breath, and skin and blood headspace. This was to determine if Type-1 diabetic individuals behaved differently to non-diabetic individuals. This experiment required offline sampling, where samples were collected in Nalophan® bags, and was not performed in vicinity of the SIFT-MS. As with the OGTT experiment, there was considerable variation between the volunteers at similar blood glucose concentrations. A positive correlation between sensor resistance and blood glucose concentration was seen in the majority of the volunteers. However, these correlations were only significant in a minority of the volunteers. For these volunteers, significant relationships between exhaled VOC concentration and blood glucose were not replicated using either mass spectrometry technique. The pattern of significant correlations between blood headspace VOC concentration and blood glucose were not replicated in the other matrices, and varied between SIFT- and GC-MS. No relationship was established between skin headspace VOCs and blood glucose concentration; this is thought to be due to a limitation in the remote skin headspace sampling protocol.

Two experiments were designed to measure the potential effects exercise on VOC quantification. In the first of these experiments, the effects simulated airway narrowing during a six minute walk test on VOC quantification was investigated. In addition, heart rate and blood oxygen saturation data was collected to complement the mass spectrometry data. There was no significant change in blood glucose concentration in any of the volunteers in response to the walk test, with or without the simulated airway narrowing, but there was a decrease in exhaled isoprene and propanol concentration as a result of airway narrowing. Though there was still variation between the individuals, this was less than that seen in the other experiments. This is probably to the fact that there were the same number of male and female volunteers, and they were of similar age. The literature suggested that an increase in isoprene would be observed, and that the decrease in isoprene concentration was thought to be due to the use of remote, offline sampling. Nalophan® bags were also believed to be inappropriate for

the analysis of nitric oxide due to the rapid dissociation of the molecule in air. There was no evidence of oxidative stress products in exhaled breath, and this was most likely due to the short intensity and duration of the walk test phases of the experiment. The volunteers that took part in this experiment were also not fasted, and the effects of this on VOC concentration were not known.

In the second of the exercise experiments volunteers were fasted before a bicycle ergometer challenge. Breath was analysed using the NO^+ precursor ion only during online SIFT-MS. An increase in exhaled isoprene, nitric oxide and acetone concentrations was seen during the onset of a bicycle ergometer challenge, with a decrease to pre-exercise levels during the recovery phase. This temporary increase in isoprene concentration was not observed when breath samples were collected during a six minute walk test. This increase was independent of blood glucose concentration, and is thought to be an artefact of fast flow tube analysis, as a similar phenomenon is seen when using both SIFT- and PTR-MS. Not only was inter- volunteer variation observed, but also intra- volunteer variation during the repeat experiments. There was no relationship between Breathotron sensor resistance and blood glucose concentration, with little deviation in sensor response at the three time points that breath samples were collected. It was not possible to take samples within quick succession due to the prolonged time to return to baseline resistance of the Breathotron. It is likely that further changes in exhaled VOC concentration were not seen due to the short duration and low intensity of the ergometer challenge.

There was significant variation in sensor response between three identical CAP25 gas sensors when exposed to dry and humidified acetone and zero grade air samples. This level of variation between sensors would be unacceptable for a medical diagnostic device. Two of the systems were subsequently modified to accept Figaro® TGS2602 and TGS2620 gas sensors. The response of the Figaro® and CAP25 systems to three common breath metabolites, acetone, ammonia and propanol demonstrated that all had good correlation and linearity between 0-100 ppm, though the unamplified signal from the TGS2602 was just as good as the CAP25. The main advantage of the Figaro® sensors was the lower power consumption in comparison to the CAP25 (5 V vs. 12 V). The Figaro® sensors also returned to baseline resistance quicker than the CAP25. The sensors also have a smaller footprint to the CAP25 which would reduce the sensor chamber size, lowering the thermal mass, further reducing the power consumption and progressing to a less complex, handheld device.

As a result of the *in vivo* studies no relationship was established between VOC concentrations and blood glucose concentration in any of the three different matrices, exhaled breath, and skin or blood headspace. This was true in both diabetic and non-diabetic individuals, both whilst sedentary and during short duration and low intensity physical activity. Where relationships were observed between VOC concentration and blood glucose in specific individuals, these were not observed using all of the analytical methods and therefore were not sufficiently statically robust. The issues of breath analysis are not methodological, if there are changes in VOC concentration they would be detected. Age, gender, diet and physiology or a combination of these factors has an influence on endogenous VOC concentration which limits the use of breath analysis for medical diagnostics and monitoring.

7.2 Future work

In the author's opinion, the future potential of the Breathotron device would be in environmental exposure monitoring of exogenous VOCs in exhaled breath. For this several improvements could be made to the Breathotron. The first of these improvements would be to reengineer the device around the Figaro® TGS2602 MOS gas sensor. This would mean that a potential MkIII Breathotron would have lower power consumption due to the reduced power requirement of the TGS2602 in comparison to the CAP25. The sensor chamber could also be reduced in size to lower the thermal mass and reduce the power consumption further as less power would be required to heat it. This would also reduce the warm up time of the instrument. The experiments described in Chapters 2, 3 and 5 should then be repeated for comparison to the modified system. Any potential MkIII could be based around the Arduino/Netduino platform to reduce the number of software development environments required. The added advantage of this would be the ability to easily port the code into C if and when required. This would also allow pre-existing and commercially available break out boards to be easily incorporated, adding Bluetooth or Wi-Fi communications, allowing a tablet computer or smartphone to control, view and save data collected.

Though breath analysis for medical diagnosis and monitoring may not be possible, there is a potential use in sports science. The bicycle ergometer experiment should be repeated using online SIFT-MS, but with incremental intensity and duration to measure the effects on VOC concentration. The effect of a controlled diet could also be potentially investigated. The inlet of the SIFT-MS should be reengineered to shorten the sample path length, to reduce the dead space, and should also be heated. This would enable breath-by-breath analysis of samples, and

may provide better quantification due to reduced condensation of compounds within the sample transfer line.

REFERENCES

- (2003) Report of the expert committee on the diagnosis and classification of diabetes mellitus. *Diabetes Care*, 26 Suppl 1, S5-20.
- (2004a) Gestational diabetes mellitus. *Diabetes Care*, 27 Suppl 1, S88-90.
- (2004b) Physical activity/exercise and diabetes. *Diabetes Care*, 27 Suppl 1, S58-62.
- ABBOTT, S. M., ELDER, J. B., ŠPANĚL, P. & SMITH, D. (2003) Quantification of acetonitrile in exhaled breath and urinary headspace using selected ion flow tube mass spectrometry. *International Journal of Mass Spectrometry*, 228, 655-665.
- ADAMS, N. G. & SMITH, D. (1976) The selected ion flow tube (SIFT); A technique for studying ion-neutral reactions. *International Journal of Mass Spectrometry and Ion Physics*, 21, 349-359.
- ALLERHEILIGEN, S. R., LUDDEN, T. M. & BURK, R. F. (1987) The pharmacokinetics of pentane, a by-product of lipid peroxidation. *Drug Metab Dispos*, 15, 794-800.
- ALVARO, D., ANGELICO, M., CANTAFORA, A., DI BIASE, A., DE SANTIS, A., BRACCI, F., MINERVINI, G., GINANNI CORRADINI, S., ATTILI, A. F. & CAPOCACCIA, L. (1986) Biliary secretion of phosphatidylcholine and its molecular species in cholecystectomized T-tube patients: effects of bile acid hydrophilicity. *Biochem Med Metab Biol*, 36, 125-35.
- ALVING, K., WEITZBERG, E. & LUNDBERG, J. M. (1993) Increased amount of nitric oxide in exhaled air of asthmatics. *Eur Respir J*, 6, 1368-1370.
- AMANN, A. & SMITH, D. (2005) *Breath analysis for clinical diagnosis and therapeutic monitoring*, Singapore ; London, World Scientific.
- ARAYA, Q. A., VALERA, M. J., CONTRERAS, B. J., CSENDES, J. A., DIAZ, J. J., BURDILES, P. P., ROJAS, C. J., MALUENDA, G. F., SMOK, S. G. & PONIACHIK, T. J. (2006) [Glucose tolerance alterations and frequency of metabolic syndrome among patients with non alcoholic fatty liver disease]. *Rev Med Chil*, 134, 1092-8.
- ARCHER, J. R. H. & BAKER, E. H. (2009) Diabetes and metabolic dysfunction in COPD. *Respiratory Medicine: COPD Update*, 5, 67-74.

- ATKINSON, M. A., BOWMAN, M. A., KAO, K. J., CAMPBELL, L., DUSH, P. J., SHAH, S. C., SIMELL, O. & MACLAREN, N. K. (1993) Lack of immune responsiveness to bovine serum albumin in insulin-dependent diabetes. *N Engl J Med*, 329, 1853-8.
- AUSTIN, A., WARTY, V., JANOSKY, J. & ARSLANIAN, S. (1993) The relationship of physical fitness to lipid and lipoprotein(a) levels in adolescents with IDDM. *Diabetes Care*, 16, 421-5.
- BANTLE, J. P. & THOMAS, W. (1997) Glucose measurement in patients with diabetes mellitus with dermal interstitial fluid. *J Lab Clin Med*, 130, 436-41.
- BARATON, #160, MARIE-ISABELLE, MERHARI & LHADI (2001) *Influence of the particle size on the surface reactivity and gas sensing properties of SnO₂ nanopowders*, Sendai, JAPON, Japan Institute of Metals.
- BASANTA, M., KOIMTZIS, T., SINGH, D., WILSON, I. & THOMAS, C. L. (2007) An adaptive breath sampler for use with human subjects with an impaired respiratory function. *Analyst*, 132, 153-63.
- BELLAR, T. A., LICHTENBERG, J. J. & LONNEMAN, S. C. (1979) RECOVERY OF ORGANIC COMPOUNDS FROM ENVIRONMENTALLY CONTAMINATED BOTTOM SAMPLES. *ACS Division of Environmental Chemistry, Preprints*, 19, 17-11.
- BEST, C. H., TAYLOR, N. B. & WEST, J. B. (1990) *Best and Taylor's physiological basis of medical practice*, Baltimore, Williams & Wilkins.
- BISHOP, L. (2006) Application of Chemometric methods applied to breath analysis. Cranfield University: Cranfield Health. MSc Thesis.
- BJORKMAN, O., FELIG, P. & WAHREN, J. (1984) Role of basal glucagon levels in the regulation of splanchnic glucose output and ketogenesis in insulin-deficient humans. *Clin Physiol*, 4, 227-41.
- BORG, G. (1970) Perceived exertion as an indicator of somatic stress. *Scand J Rehabil Med*, 2, 92-8.
- BOSHIER, P. R., PRIEST, O. H., HANNA, G. B. & MARCZIN, N. Influence of respiratory variables on the on-line detection of exhaled trace gases by PTR-MS. *Thorax*, 66, 919-20.

- BRECHNER, V. L. & BETHUNE, R. W. (1965) Determination of acetone concentration in arterial blood by vapor phase chromatography of alveolar gas. *Diabetes*, 14, 663-5.
- BRIGGS, A. P. & SHAFFER, P. A. (1921) THE EXCRETION OF ACETONE FROM THE LUNGS. *J. Biol. Chem.*, 48, 413-428.
- BROZEK, R., ROGALEWICZ, R., KOCZOROWSKI, R. & VOELKEL, A. (2008) The influence of denture cleansers on the release of organic compounds from soft lining materials. *J Environ Monit*, 10, 770-4.
- BUCKLEY, T. J., PLEIL, J. D., BOWYER, J. R. & DAVIS, J. M. (2001) Evaluation of methyl tert-butyl ether (MTBE) as an interference on commercial breath-alcohol analyzers. *Forensic Sci Int*, 123, 111-8.
- CAPODICASA, E., TROVARELLI, G., DE MEDIO, G. E., PELLI, M. A., LIPPI, G., VERDURA, C. & TIMIO, M. (1999) Volatile alkanes and increased concentrations of isoprene in exhaled air during hemodialysis. *Nephron*, 82, 331-7.
- CASTEELS, K. & MATHIEU, C. (2003) Diabetic ketoacidosis. *Rev Endocr Metab Disord*, 4, 159-66.
- CHANCE, J. J., LI, D. J., JONES, K. A., DYER, K. L. & NICHOLS, J. H. (1999) Technical evaluation of five glucose meters with data management capabilities. *Am J Clin Pathol*, 111, 547-56.
- CHATILA, W. M., THOMASHOW, B. M., MINAI, O. A., CRINER, G. J. & MAKE, B. J. (2008) Comorbidities in chronic obstructive pulmonary disease. *Proc Am Thorac Soc*, 5, 549-55.
- CHEN, E. T., NICHOLS, J. H., DUH, S. H. & HORTIN, G. (2003) Performance evaluation of blood glucose monitoring devices. *Diabetes Technol Ther*, 5, 749-68.
- CHILDS, C., HARRISON, R. & HODKINSON, C. (1999) Tympanic membrane temperature as a measure of core temperature. *Arch Dis Child*, 80, 262-6.
- CHOI, K. M., LEE, K. W., KIM, S. G., KIM, N. H., PARK, C. G., SEO, H. S., OH, D. J., CHOI, D. S. & BAIK, S. H. (2005) Inflammation, insulin resistance, and glucose intolerance in acute myocardial infarction patients without a previous diagnosis of diabetes mellitus. *J Clin Endocrinol Metab*, 90, 175-80.

- CHOU, S., TEOH, L., LAI, W., SU, Y. & HON, M. (2006) ZnO:Al Thin Film Gas Sensor for Detection of Ethanol Vapor. *Sensors*, 6, 1420-1427.
- CLARK, L. C., JR., KAPLAN, S., MATTHEWS, E. C. & SCHWAB, L. (1956) Oxygen availability to the brain during inflow occlusion of the heart in normothermia and hypothermia. *J Thorac Surg*, 32, 576-82.
- CLARK, L. C., JR. & LYONS, C. (1962) Electrode systems for continuous monitoring in cardiovascular surgery. *Ann N Y Acad Sci*, 102, 29-45.
- COUNCIL DIRECTIVE (EC) 1999/13/EC of March 1999 on the limitation of emissions of volatile organic compounds due to the use of organic solvents in certain activities and installations
- CRUMP, D., HARRISON, P., & WALTON, C. (2011) *Aircraft cabin air sampling study: Part 1 of the final report*. Cranfield: Department of Transport
- CRYER, P., E. (1997) *Hypoglycemia: Pathophysiology, Diagnosis, and Treatment*, Oxford, Oxford University Press
- DASGUPTA, A. (2011) *The Science of Drinking: How Alcohol Affects Your Body and Mind*, Plymouth, Rowman & Littlefield Publishers, Inc.
- DAVIES, S., ŠPANĚL, P. & SMITH, D. (1997) Quantitative analysis of ammonia on the breath of patients in end-stage renal failure. *Kidney Int*, 52, 223-8.
- DE LACY COSTELLO, B. P. J., EWEN, R. J., GUERNION, N. & RATCLIFFE, N. M. (2002) Highly sensitive mixed oxide sensors for the detection of ethanol. *Sensors and Actuators B: Chemical*, 87, 207-210.
- DEFRONZO, R. A., TOBIN, J. D. & ANDRES, R. (1979) Glucose clamp technique: a method for quantifying insulin secretion and resistance. *Am J Physiol*, 237, E214-23.
- DENG, C., ZHANG, J., YU, X., ZHANG, W. & ZHANG, X. (2004) Determination of acetone in human breath by gas chromatography-mass spectrometry and solid-phase microextraction with on-fiber derivatization. *J Chromatogr B Analyt Technol Biomed Life Sci*, 810, 269-75.

- DI FRANCESCO, F., FUOCO, R., TRIVELLA, M. G. & CECCARINI, A. (2005) Breath analysis: trends in techniques and clinical applications. *Microchemical Journal*, 79, 405-410.
- DIEDRICH, L., SANDOVAL, D. & DAVIS, S. N. (2002) Hypoglycemia associated autonomic failure. *Clin Auton Res*, 12, 358-65.
- DYCK, D. J., PETERS, S. J., WENDLING, P. S., CHESLEY, A., HULTMAN, E. & SPRIET, L. L. (1996) Regulation of muscle glycogen phosphorylase activity during intense aerobic cycling with elevated FFA. *Am J Physiol*, 270, E116-25.
- DYCK, D. J., PUTMAN, C. T., HEIGENHAUSER, G. J., HULTMAN, E. & SPRIET, L. L. (1993) Regulation of fat-carbohydrate interaction in skeletal muscle during intense aerobic cycling. *Am J Physiol*, 265, E852-9.
- EBERHART, M. S., OGDEN, C. & ENGELGAU, M. (2005) Prevalence of Overweight and Obesity Among Adults With Diagnosed Diabetes--United States, 1988-1994 and 1999-2002. *JAMA*, 293, 546-547.
- EHRMAN, J. K. (2009) *Clinical exercise physiology*, Leeds, Human Kinetics.
- EKNOYAN, G. (2008) Adolphe Quetelet (1796-1874)--the average man and indices of obesity. *Nephrol Dial Transplant*, 23, 47-51.
- ERIKSEN, S. P. & KULKARNI, A. B. (1963) Methanol in normal human breath. *Science*, 141, 639-640.
- ERIKSSON, L. S., BROBERG, S., BJÖRKMAN, O. & WAHREN, J. (1985) Ammonia metabolism during exercise in man. *Clinical Physiology*, 5, 325-336.
- FERRANTE DO AMARAL, C. E. & WOLF, B. (2008) Current development in non-invasive glucose monitoring. *Med Eng Phys*, 30, 541-9.
- FILSER, J. G., CSANADY, G. A., DENK, B., HARTMANN, M., KAUFFMANN, A., KESSLER, W., KREUZER, P. E., PUTZ, C., SHEN, J. H. & STEI, P. (1996) Toxicokinetics of isoprene in rodents and humans. *Toxicology*, 113, 278-87.
- FOGH-ANDERSEN, N. & D'ORAZIO, P. (1998) Proposal for standardizing direct-reading biosensors for blood glucose. *Clin Chem*, 44, 655-9.

- FOWLER, D., P. (2010) Analysis of volatile marker compounds in body fluid samples from patients with gastrointestinal disease. Cranfield University: Cranfield Health MSc by Research Thesis
- FRAGKOU, V., TURNER, A.P.F. (2008) Commercial Biosensors for Diabetes. In: Tuchin, V. V. ed. *Handbook of optical sensing of glucose in biological fluids and tissues*, Boca Raton, Fla. ; London, Chapman & Hall.
- FRASER-REID, B. O., TATSUTA, K. & THIEM, J. (2001) *Glycoscience : chemistry and chemical biology I-III*, Berlin ; London, Springer.
- GALASSETTI, P. R., NOVAK, B., NEMET, D., ROSE-GOTTRON, C., COOPER, D. M., MEINARDI, S., NEWCOMB, R., ZALDIVAR, F. & BLAKE, D. R. (2005) Breath ethanol and acetone as indicators of serum glucose levels: an initial report. *Diabetes Technol Ther*, 7, 115-23.
- GALBO, H., HOLST, J. J. & CHRISTENSEN, N. J. (1979) The effect of different diets and of insulin on the hormonal response to prolonged exercise. *Acta Physiol Scand*, 107, 19-32.
- GALLAGHER, M., WYSOCKI, C. J., LEYDEN, J. J., SPIELMAN, A. I., SUN, X. & PRETI, G. (2008) Analyses of volatile organic compounds from human skin. *Br J Dermatol*, 159, 780-91.
- GARDNER, J. W. & BARTLETT, P. N. (1994) A brief history of electronic noses. *Sensors and Actuators B: Chemical*, 18, 210-211.
- GARDNER, J. W. & BARTLETT, P. N. (1999) *Electronic noses : principles and applications*, Oxford, Oxford University Press.
- GARDNER, J. W., SHIN, H. W. & HINES, E. L. (2000) An electronic nose system to diagnose illness. *Sensors and Actuators B: Chemical*, 70, 19-24.
- GORDON, B. L. M. D. F. C. I. S. (1960) *Medieval and Renaissance Medicine*, pp. xii. 843. Peter Owen: London.
- GORHAM, K. A., SULBAEK ANDERSEN, M. P., MEINARDI, S., DELFINO, R. J., STAIMER, N., TJOA, T., ROWLAND, F. S. & BLAKE, D. R. (2009) Ethane and n-pentane in exhaled breath are biomarkers of exposure not effect. *Biomarkers*, 14, 17-25.
- GRAHAM, T., BANGSBO, J. & SALTIN, B. (1993) Skeletal muscle ammonia production and repeated, intense exercise in humans. *Can J Physiol Pharmacol*, 71, 484-90.

- GREENHOUSE, S. & GIESSER, S. (1959) On methods in the analysis of profile data. *Psychometrika*, 24, 95-112
- GROTE, C. & PAWLISZYN, J. (1997) Solid-Phase Microextraction for the Analysis of Human Breath. *Analytical Chemistry*, 69, 587-596.
- GUSTAFSSON, L. E., LEONE, A. M., PERSSON, M. G., WIKLUND, N. P. & MONCADA, S. (1991) Endogenous nitric oxide is present in the exhaled air of rabbits, guinea pigs and humans. *Biochem Biophys Res Commun*, 181, 852-7.
- HAK, E., ROVERS, M. M., KUYVENHOVEN, M. M., SCHELLEVIS, F. G. & VERHEIJ, T. J. (2006) Incidence of GP-diagnosed respiratory tract infections according to age, gender and high-risk co-morbidity: the Second Dutch National Survey of General Practice. *Fam Pract*, 23, 291-4.
- HALLIKAINEN, M., TOPPINEN, L., MYKKANEN, H., AGREN, J. J., LAAKSONEN, D. E., MIETTINEN, T. A., NISKANEN, L., POUTANEN, K. S. & GYLLING, H. (2006) Interaction between cholesterol and glucose metabolism during dietary carbohydrate modification in subjects with the metabolic syndrome. *Am J Clin Nutr*, 84, 1385-92.
- HANADA, M., KODA, H., ONAGA, K., TANAKA, K., OKABAYASHI, T., ITOH, T. & MIYAZAKI, H. (2003) Portable oral malodor analyzer using highly sensitive In₂O₃ gas sensor combined with a simple gas chromatography system. *Analytica Chimica Acta*, 475, 27-35.
- HANSEL, A., JORDAN, A., HOLZINGER, R., PRAZELLER, P., VOGEL, W. & LINDINGER, W. (1995) Proton transfer reaction mass spectrometry: on-line trace gas analysis at the ppb level. *International Journal of Mass Spectrometry and Ion Processes*, 149, 609-619.
- HAYASHI, T., WOJTASZEWSKI, J. F. & GOODYEAR, L. J. (1997) Exercise regulation of glucose transport in skeletal muscle. *Am J Physiol*, 273, E1039-51.
- HILGER, C., GRIGIONI, F., DE BEAUFORT, C., MICHEL, G., FREILINGER, J. & HENTGES, F. (2001) Differential binding of IgG and IgA antibodies to antigenic determinants of bovine serum albumin. *Clin Exp Immunol*, 123, 387-94.
- HOFFMANN, E. D. & STROOBANT, V. (2007) *Mass spectrometry : principles and applications*, Hoboken, N.J., Wiley ; Chichester : John Wiley [distributor].

- HOLLOSZY, J. O. (2005) Exercise-induced increase in muscle insulin sensitivity. *J Appl Physiol*, 99, 338-43.
- HOLT, R. I. G., HANLEY, N. A. & BROOK, C. G. D. E. E. (2007) *Essential endocrinology and diabetes*, Oxford, Blackwell.
- HÜBSCHMANN, H.-J. (2009) *Handbook of GC/MS : fundamentals and applications*, Weinheim, Wiley-VCH ; [Chichester : John Wiley, distributor].
- IKEGAMI, A., KANEYASI, M., (1985) Olfactory detection using integrated sensors, *Proc. 3rd Int. Conf. Solid-State Sensors and Actuators (Transducers '85)*, Philadelphia, PA, USA, June 7-11: 136-139
- ISO (2003) 15197:2003. *In vitro diagnostic test systems -- Requirements for blood-glucose monitoring systems for self-testing in managing diabetes mellitus*. Geneva: Switzerland
- ISRAELI, E., ILAN, Y., MEIR, S. B., BUENAVIDA, C. & GOLDIN, E. (2003) A novel ¹³C-urea breath test device for the diagnosis of *Helicobacter pylori* infection: continuous online measurements allow for faster test results with high accuracy. *J Clin Gastroenterol*, 37, 139-41.
- JENKINS, S. C. (2007) 6-Minute walk test in patients with COPD: clinical applications in pulmonary rehabilitation. *Physiotherapy*, 93, 175-182.
- JENSEN, B. M., BJERRING, P., CHRISTIANSEN, J. S. & ORSKOV, H. (1995) Glucose content in human skin: relationship with blood glucose levels. *Scand J Clin Lab Invest*, 55, 427-32.
- JONES, A. M. & DOUST, J. H. (1996) A 1% treadmill grade most accurately reflects the energetic cost of outdoor running. *J Sports Sci*, 14, 321-7.
- KALAPOUS, M. P. (2003) On the mammalian acetone metabolism: from chemistry to clinical implications. *Biochim Biophys Acta*, 1621, 122-39.
- KANEYASU, M., IKEGAMI, A., ARIMA, H. & IWANAGA, S. (1987) Smell Identification Using a Thick-Film Hybrid Gas Sensor. *Components, Hybrids, and Manufacturing Technology, IEEE Transactions on*, 10, 267-273.

- KARJALAINEN, J., MARTIN, J. M., KNIP, M., ILONEN, J., ROBINSON, B. H., SAVILAHTI, E., AKERBLUM, H. K. & DOSCH, H. M. (1992) A bovine albumin peptide as a possible trigger of insulin-dependent diabetes mellitus. *N Engl J Med*, 327, 302-7.
- KARL, T., PRAZELLER, P., MAYR, D., JORDAN, A., RIEDER, J., FALL, R. & LINDINGER, W. (2001) Human breath isoprene and its relation to blood cholesterol levels: new measurements and modeling. *J Appl Physiol*, 91, 762-70.
- KAYASHIMA, S., ARAI, T., KIKUCHI, M., NAGATA, N., ITO, N., KURIYAMA, T. & KIMURA, J. (1992) Suction effusion fluid from skin and constituent analysis: new candidate for interstitial fluid. *Am J Physiol*, 263, H1623-7.
- KEMBALL, M. & BLOOM, A. (1966) Clinical application of "Dextrostix" in estimating blood glucose levels. *Diabetologia*, 1, 245-247.
- KHALIL, O. S. (2004) Noninvasive photonic-crystal material for sensing glucose in tears. *Clin Chem*, 50, 2236-7.
- KHARITONOV, S. A., YATES, D., ROBBINS, R. A., LOGAN-SINCLAIR, R., SHINEBOURNE, E. A. & BARNES, P. J. (1994) Increased nitric oxide in exhaled air of asthmatic patients. *Lancet*, 343, 133-5.
- KIM, C., NEWTON, K. M. & KNOPP, R. H. (2002) Gestational diabetes and the incidence of type 2 diabetes: a systematic review. *Diabetes Care*, 25, 1862-8.
- KIM, H. J., KIM, H. J., LEE, K. E., KIM, D. J., KIM, S. K., AHN, C. W., LIM, S.-K., KIM, K. R., LEE, H. C., HUH, K. B. & CHA, B. S. (2004) Metabolic Significance of Nonalcoholic Fatty Liver Disease in Nonobese, Nondiabetic Adults. *Arch Intern Med*, 164, 2169-2175.
- KING, J., KUPFERTHALER, A., UNTERKOFER, K., KOC, H., TESCHL, S., TESCHL, G., MIEKISCH, W., SCHUBERT, J., HINTERHUBER, H. & AMANN, A. (2009) Isoprene and acetone concentration profiles during exercise on an ergometer. *J Breath Res*, 3, 027006.
- KING, J., MOCHALSKI, P., KUPFERTHALER, A., UNTERKOFER, K., KOC, H., FILIPIAK, W., TESCHL, S., HINTERHUBER, H. & AMANN, A. (2010) Dynamic profiles of volatile organic compounds in exhaled breath as determined by a coupled PTR-MS/GC-MS study. *Physiol Meas*, 31, 1169-84.

- KJAER, M., FARRELL, P. A., CHRISTENSEN, N. J. & GALBO, H. (1986) Increased epinephrine response and inaccurate glucoregulation in exercising athletes. *J Appl Physiol*, 61, 1693-700.
- KJAER, M., KIENS, B., HARGREAVES, M. & RICHTER, E. A. (1991) Influence of active muscle mass on glucose homeostasis during exercise in humans. *J Appl Physiol*, 71, 552-7.
- KJAER, M., SECHER, N. H., BACH, F. W. & GALBO, H. (1987) Role of motor center activity for hormonal changes and substrate mobilization in humans. *Am J Physiol*, 253, R687-95.
- KNEEPKENS, C. M., LEPAGE, G. & ROY, C. C. (1994) The potential of the hydrocarbon breath test as a measure of lipid peroxidation. *Free Radic Biol Med*, 17, 127-60.
- KNUTSON, M. D. & VITERI, F. E. (1996) Concentrating breath samples using liquid nitrogen: a reliable method for the simultaneous determination of ethane and pentane. *Anal Biochem*, 242, 129-35.
- KOLB, H., KOLB-BACHOFEN, V. & ROEP, B. O. (1995) Autoimmune versus inflammatory type I diabetes: a controversy? *Immunol Today*, 16, 170-2.
- KROGH, A. & LINDHARD, J. (1920) The Relative Value of Fat and Carbohydrate as Sources of Muscular Energy: With Appendices on the Correlation between Standard Metabolism and the Respiratory Quotient during Rest and Work. *Biochem. J.*, 14, 290-363.
- KRYNSKI, I. A. & LOGAN, J. E. (1967) Dextrostix as a quantitative test for glucose in whole blood. *Can Med Assoc J*, 97, 1006-11.
- KUSKE, M., PADILLA, M., ROMAIN, A. C., NICOLAS, J., RUBIO, R. & MARCO, S. (2006) Detection of diverse mould species growing on building materials by gas sensor arrays and pattern recognition. *Sensors and Actuators B: Chemical*, 119, 33-40.
- KUZMA, J., NEMECEK-MARSHALL, M., POLLOCK, W. H. & FALL, R. (1995) Bacteria produce the volatile hydrocarbon isoprene. *Curr Microbiol*, 30, 97-103.
- LAFFEL, L. (1999) Ketone bodies: a review of physiology, pathophysiology and application of monitoring to diabetes. *Diabetes Metab Res Rev*, 15, 412-26.
- LAFFEL, L. (2000) Sick-day management in type 1 diabetes. *Endocrinol Metab Clin North Am*, 29, 707-23.

- LARSSON-COHN, U. (1976) Differences between capillary and venous blood glucose during oral glucose tolerance tests. *Scand J Clin Lab Invest*, 36, 805-8.
- LARSTAD, M. A., TOREN, K., BAKE, B. & OLIN, A. C. (2007) Determination of ethane, pentane and isoprene in exhaled air--effects of breath-holding, flow rate and purified air. *Acta Physiol (Oxf)*, 189, 87-98.
- LAWRENCE, J. M., CONTRERAS, R., CHEN, W. & SACKS, D. A. (2008) Trends in the prevalence of preexisting diabetes and gestational diabetes mellitus among a racially/ethnically diverse population of pregnant women, 1999-2005. *Diabetes Care*, 31, 899-904.
- LEAF, D. A., KLEINMAN, M. T., HAMILTON, M. & BARSTOW, T. J. (1997) The effect of exercise intensity on lipid peroxidation. *Med Sci Sports Exerc*, 29, 1036-9.
- LEBOVITZ, H. E. (1995) Diabetic ketoacidosis. *Lancet*, 345, 767-72.
- LEE, A. P. & REEDY, B. J. (1999) Temperature modulation in semiconductor gas sensing. *Sensors and Actuators B: Chemical*, 60, 35-42.
- LEE, J., NGO, J., BLAKE, D., MEINARDI, S., PONTELLO, A. M., NEWCOMB, R. & GALASSETTI, P. R. (2009) Improved predictive models for plasma glucose estimation from multi-linear regression analysis of exhaled volatile organic compounds. *J Appl Physiol*, 107, 155-60.
- LEE-DAVEY, J. (2004) Application of Machine Olfaction principles for the detection of high voltage transformer oil degradation. Cranfield University: Institute of Bioscience and Technology. EngD Thesis
- LIGOR, T., LIGOR, M., AMANN, A., AGER, C., BACHLER, M., DZIEN, A. & BUSZEWSKI, B. (2008) The analysis of healthy volunteers' exhaled breath by the use of solid-phase microextraction and. *Journal of Breath Research*, 2, 046006.
- LINDINGER, W. & JORDAN, A. (1998) Proton-transfer-reaction mass spectrometry (PTR-MS): on-line monitoring of volatile organic compounds at pptv levels. *Chemical Society Reviews*, 27, 347-375.
- LINDSTROM, A. B. & PLEIL, J. D. (1996) Alveolar breath sampling and analysis to assess exposures to methyl tertiary butyl ether (MTBE) during motor vehicle refueling. *J Air Waste Manag Assoc*, 46, 676-82.

- LINDSTROM, A. B. & PLEIL, J. D. (2002) A review of the USEPA's single breath canister (SBC) method for exhaled volatile organic biomarkers. *Biomarkers*, 7, 189-208.
- LUDVIGSSON, J. (1984) Determination of glucosuria, an obsolete form of self-monitoring in diabetes? *Diabetes Res*, 1, 213-7.
- MA, V., LORD, H., MORLEY, M. & PAWLISZYN, J. (2010) Application of membrane extraction with sorbent interface for breath analysis. *Methods Mol Biol*, 610, 451-68.
- MAKISIMOVICH, N., VOROTYNTSEV, V., NIKITINA, N., KASKEVICH, O., KARABUN, P. & MARTYNIENKO, F. (1996) Adsorption semiconductor sensor for diabetic ketoacidosis diagnosis. *Sensors and Actuators B: Chemical*, 36, 419-421.
- MALFERTHEINER, P., MEGRAUD, F., O'MORAIN, C., BAZZOLI, F., EL-OMAR, E., GRAHAM, D., HUNT, R., ROKKAS, T., VAKIL, N. & KUIPERS, E. J. (2007) Current concepts in the management of *Helicobacter pylori* infection: the Maastricht III Consensus Report. *Gut*, 56, 772-81.
- MANNINO, D. M. & BUIST, A. S. (2007) Global burden of COPD: risk factors, prevalence, and future trends. *Lancet*, 370, 765-73.
- MANOLIS, A. (1983) The diagnostic potential of breath analysis. *Clin Chem*, 29, 5-15.
- MANTIONE, K. J., ESCH, T. & STEFANO, G. B. (2007) Detection of nitric oxide in exhaled human breath: exercise and resting determinations. *Med Sci Monit*, 13, MT1-5.
- MARCH, W., LAZZARO, D. & RASTOGI, S. (2006) Fluorescent measurement in the non-invasive contact lens glucose sensor. *Diabetes Technol Ther*, 8, 312-7.
- MARCZIN, N. E. & YACOUB, M. H. E. (2002) *Disease markers in exhaled breath : basic mechanisms and clinical applications*, IOS Press.
- MATHEWS, J. M., RAYMER, J. H., ETHERIDGE, A. S., VELEZ, G. R. & BUCHER, J. R. (1997) Do Endogenous Volatile Organic Chemicals Measured in Breath Reflect and Maintain CYP2E1 Levels in Vivo? *Toxicology and Applied Pharmacology*, 146, 255-260.
- MAUCHLY, J.W. (1940). Significance Test for Sphericity of a Normal n-Variate Distribution. *The Annals of Mathematical Statistics*, 11, 204–209

- MCGEEHIN, P. (2000) Gas sensors for improved air quality in transportation. *Sesnsor Review*, 20, 106-112.
- MCGRATH, L. T., PATRICK, R. & SILKE, B. (2001) Breath isoprene in patients with heart failure. *Eur J Heart Fail*, 3, 423-7.
- MCMASTER, M. C. (2008) *GC/MS : a practical user's guide*, Hoboken, N.J., Wiley ; Chichester : John Wiley [distributor].
- MIEKISCH, W., KISCHKEL, S., SAWACKI, A., LIEBAU, T., MIETH, M. & SCHUBERT, J. K. (2008) Impact of sampling procedures on the results of breath analysis. *J Breath Res*, 2, 026007.
- MIEKISCH, W., SCHUBERT, J. K. & NOELDGE-SCHOMBURG, G. F. E. (2004) Diagnostic potential of breath analysis--focus on volatile organic compounds. *Clinica Chimica Acta*, 347, 25-39.
- MIEKISCH, W., SCHUBERT, J. K., VAGTS, D. A. & GEIGER, K. (2001) Analysis of volatile disease markers in blood. *Clin Chem*, 47, 1053-60.
- MITSUBAYASHI, K., MATSUNAGA, H., NISHIO, G., TODA, S. & NAKANISHI, Y. (2005) Bioelectronic sniffers for ethanol and acetaldehyde in breath air after drinking. *Biosensors and Bioelectronics*, 20, 1573-1579.
- MOCHALSKI, P., WZOREK, B., SLIWKA, I. & AMANN, A. (2009) Suitability of different polymer bags for storage of volatile sulphur compounds relevant to breath analysis. *Journal of Chromatography B*, 877, 189-196.
- MORRISON, S. R. (1987) Mechanism of semiconductor gas sensor operation. *Sensors and Actuators*, 11, 283-287.
- MUELLER, W., SCHUBERT, J., BENZING, A. & GEIGER, K. (1998) Method for analysis of exhaled air by microwave energy desorption coupled with gas chromatography-flame ionization detection-mass spectrometry. *Journal of Chromatography B: Biomedical Sciences and Applications*, 716, 27-38.
- MUSA-VELOSO, K., LIKHODII, S. S. & CUNNANE, S. C. (2002) Breath acetone is a reliable indicator of ketosis in adults consuming ketogenic meals. *Am J Clin Nutr*, 76, 65-70.

- NAITOH, K., INAI, Y., HIRABAYASHI, T. & TSUDA, T. (2002) Exhalation behavior of four organic substrates and water absorbed by human skin. *Biol Pharm Bull*, 25, 867-71.
- NEGI CHANDRA, S. (2010) *Introduction to Endocrinology*, New Dehli, Prentice-Hall of India Pvt.
- NESHER, R., KARL, I. E. & KIPNIS, D. M. (1985) Dissociation of effects of insulin and contraction on glucose transport in rat epitrochlearis muscle. *Am J Physiol*, 249, C226-32.
- NEWMAN, J. D. & TURNER, A. P. (2005) Home blood glucose biosensors: a commercial perspective. *Biosens Bioelectron*, 20, 2435-53.
- NEWMAN, J., TURNER, A.P.F. (2007) Historical Perspective of Biosensor and Biochip Development. In: Marks, R. ed. *Handbook of biosensors and biochips*, Chichester, John Wiley.
- NOVAK, B. J., BLAKE, D. R., MEINARDI, S., ROWLAND, F. S., PONTELLO, A., COOPER, D. M. & GALASSETTI, P. R. (2007) Exhaled methyl nitrate as a noninvasive marker of hyperglycemia in type 1 diabetes. *Proc Natl Acad Sci U S A*, 104, 15613-8.
- NYLABDER C.; ARMGRATH M. & LUNDSTROM I. (1983) An ammonia detector based on a conducting polymer. *Proceedings of the International Meeting on Chemical Sensors*, Fukuoka, Japan, , 203-207.
- O'BRIEN, R. M. & GRANNER, D. K. (1990) PEPCK gene as model of inhibitory effects of insulin on gene transcription. *Diabetes Care*, 13, 327-39.
- OLTMANN, K. M., GEHRING, H., RUDOLF, S., SCHULTES, B., ROOK, S., SCHWEIGER, U., BORN, J., FEHM, H. L. & PETERS, A. (2004) Hypoxia causes glucose intolerance in humans. *Am J Respir Crit Care Med*, 169, 1231-7.
- OWEN, O. E., TRAPP, V. E., SKUTCHES, C. L., MOZZOLI, M. A., HOELDTKE, R. D., BODEN, G. & REICHARD, G. A., JR. (1982) Acetone metabolism during diabetic ketoacidosis. *Diabetes*, 31, 242-8.
- PANIGRAHI, S., BALASUBRAMANIAN, S., GU, H., LOGUE, C. & MARCHELLO, M. (2006) Neural-network-integrated electronic nose system for identification of spoiled beef. *LWT - Food Science and Technology*, 39, 135-145.

- PATEL, M., (2007) Breath analysis for medical diagnosis. Cranfield University: Cranfield Health MSc Thesis.
- PARKER, D., (2006) Application of artificial neural networks to the tandem breath analyser. Cranfield University: Cranfield Health MSc Thesis.
- PAULSSON, N., LARSSON, E. & WINQUIST, F. (2000) Extraction and selection of parameters for evaluation of breath alcohol measurement with an electronic nose. *Sensors and Actuators A: Physical*, 84, 187-197.
- PEARCE, R. H. & GRIMMER, B. J. (1972) Age and the chemical constitution of normal human dermis. *J Invest Dermatol*, 58, 347-61.
- PERSAUD, D. R. & BARRANCO-MENDOZA, A. (2004) Bovine serum albumin and insulin-dependent diabetes mellitus; is cow's milk still a possible toxicological causative agent of diabetes? *Food Chem Toxicol*, 42, 707-14.
- PERSAUD, K. & DODD, G. (1982) Analysis of discrimination mechanisms in the mammalian olfactory system using a model nose. *Nature*, 299, 352-355.
- PERSSON, M. G., WIKLUND, N. P. & GUSTAFSSON, L. E. (1993) Endogenous nitric oxide in single exhalations and the change during exercise. *Am Rev Respir Dis*, 148, 1210-4.
- PERSSON, M. G., ZETTERSTROM, O., AGRENIUS, V., IHRE, E. & GUSTAFSSON, L. E. (1994) Single-breath nitric oxide measurements in asthmatic patients and smokers. *Lancet*, 343, 146-7.
- PETERSEN, A. M. & KROGFELT, K. A. (2003) Helicobacter pylori: an invading microorganism? A review. *FEMS Immunol Med Microbiol*, 36, 117-26.
- PHILLIPS, M. (1992) Breath tests in medicine. *Sci Am*, 267, 74-9.
- PHILLIPS, M. (1997) Method for the collection and assay of volatile organic compounds in breath. *Anal Biochem*, 247, 272-8.
- PHILLIPS, M. & GREENBERG, J. (1992) Ion-trap detection of volatile organic compounds in alveolar breath. *Clin Chem*, 38, 60-5.
- PICKUP, J. C., HUSSAIN, F., EVANS, N. D., ROLINSKI, O. J. & BIRCH, D. J. (2005) Fluorescence-based glucose sensors. *Biosens Bioelectron*, 20, 2555-65.

- PLEIL, J. D. & LINDSTROM, A. B. (1997) Exhaled human breath measurement method for assessing exposure to halogenated volatile organic compounds. *Clin Chem*, 43, 723-30.
- PLOUG, T., GALBO, H., VINTEN, J., JORGENSEN, M. & RICHTER, E. A. (1987) Kinetics of glucose transport in rat muscle: effects of insulin and contractions. *Am J Physiol*, 253, E12-20.
- POCOCK, G. & RICHARDS, C. D. (1999) *Human physiology : the basis of medicine*, Oxford, Oxford University Press.
- POIRIER, J. Y., LE PRIEUR, N., CAMPION, L., GUILHEM, I., ALLANNIC, H. & MAUGENDRE, D. (1998) Clinical and statistical evaluation of self-monitoring blood glucose meters. *Diabetes Care*, 21, 1919-24.
- POLI, D., CARBOGNANI, P., CORRADI, M., GOLDONI, M., ACAMPA, O., BALBI, B., BIANCHI, L., RUSCA, M. & MUTTI, A. (2005) Exhaled volatile organic compounds in patients with non-small cell lung cancer: cross sectional and nested short-term follow-up study. *Respir Res*, 6, 71.
- POORTMANS, J. (2004) *Principles of exercise biochemistry*, Basel ; London, Karger.
- POTTS, R. O., TAMADA, J. A. & TIERNEY, M. J. (2002) Glucose monitoring by reverse iontophoresis. *Diabetes Metab Res Rev*, 18 Suppl 1, S49-53.
- PURNAMADJAJA, A. H., & RUSSELL, R. A. (2000). A sense of smell for a humanoid robot. In *Proceedings of the international conference on artificial intelligence in science and technology* (pp. 312–316), Hobart, Australia.
- PURNAMADJAJA, A. & RUSSELL, R. (2007) Guiding robots' behaviors using pheromone communication. *Autonomous Robots*, 23, 113-130.
- RAMSAY, G. & TURNER, A. P. F. (1988) Development of an electrochemical method for the rapid determination of microbial concentration and evidence for the reaction mechanism. *Analytica Chimica Acta*, 215, 61-69.
- REICHARD, G. A., JR., HAFF, A. C., SKUTCHES, C. L., PAUL, P., HOLROYDE, C. P. & OWEN, O. E. (1979) Plasma acetone metabolism in the fasting human. *J Clin Invest*, 63, 619-26.

- RISBY, T. (2005) Trace Gas Analysis in Exhaled Human Breath for Disease Diagnosis. *Conference on Lasers and Electro-Optics/Quantum Electronics and Laser Science and Photonic Applications Systems Technologies*. Optical Society of America.
- RISBY, T. H. & SEHNERT, S. S. (1999) Clinical application of breath biomarkers of oxidative stress status. *Free Radical Biology and Medicine*, 27, 1182-1192.
- ROAD TRAFFIC ACT 1988 (c.52) London: The Stationary Office
- ROBERTS, S. (2006) Turning the corner: Improving diabetes care. London: Department of Health
- ROBERTS, S., ROBERGS, R. A. & HANSON, P. (1997) *Clinical exercise testing and prescription : theory and application*, Boca Raton ; London, CRC Press.
- ROBINSON, A. B. & PAULING, L. (1974) Techniques of orthomolecular diagnosis. *Clin Chem*, 20, 961-5.
- ROHRSCHEIB, M., ROBINSON, R. & EATON, R. P. (2003) Non-invasive glucose sensors and improved informatics--the future of diabetes management. *Diabetes Obes Metab*, 5, 280-4.
- RISBY, T., H. (2005) In: Amann, A. & Smith, D. ed *Breath analysis for clinical diagnosis and therapeutic monitoring*, Singapore ; London, World Scientific.
- ROMIJN, J. A., COYLE, E. F., SIDOSSIS, L. S., GASTALDELLI, A., HOROWITZ, J. F., ENDERT, E. & WOLFE, R. R. (1993) Regulation of endogenous fat and carbohydrate metabolism in relation to exercise intensity and duration. *Am J Physiol*, 265, E380-91.
- ROTHER, K. I. (2007) Diabetes treatment--bridging the divide. *N Engl J Med*, 356, 1499-501.
- RUZSANYI, V., BAUMBACH, J. I., SIELEMANN, S., LITTERST, P., WESTHOFF, M. & FREITAG, L. (2005) Detection of human metabolites using multi-capillary columns coupled to ion mobility spectrometers. *J Chromatogr A*, 1084, 145-51.
- SAAD, R. J. & CHEY, W. D. (2007) Breath tests for gastrointestinal disease: the real deal or just a lot of hot air? *Gastroenterology*, 133, 1763-6.

- SAMUEL, V. T., LIU, Z. X., QU, X., ELDER, B. D., BILZ, S., BEFROY, D., ROMANELLI, A. J. & SHULMAN, G. I. (2004) Mechanism of hepatic insulin resistance in non-alcoholic fatty liver disease. *J Biol Chem*, 279, 32345-53.
- SCHADE, D. S. & EATON, R. P. (1982) Metabolic and clinical significance of ketosis. *Spec Top Endocrinol Metab*, 4, 1-27.
- SCHMIDTKE, D. W., FREELAND, A. C., HELLER, A. & BONNECAZE, R. T. (1998) Measurement and modeling of the transient difference between blood and subcutaneous glucose concentrations in the rat after injection of insulin. *Proc Natl Acad Sci U S A*, 95, 294-9.
- SCHOLPP, J., SCHUBERT, J. K., MIEKISCH, W. & GEIGER, K. (2002) Breath markers and soluble lipid peroxidation markers in critically ill patients. *Clin Chem Lab Med*, 40, 587-94.
- SCHUBERT, J. K., ESTEBAN-LOOS, I., GEIGER, K. & GUTTMANN, J. (1999) In vivo evaluation of a new method for chemical analysis of volatile components in the respiratory gas of mechanically ventilated patients. *Technology and Health Care*, 7, 29-37.
- SCHUBERT, J. K., SPITTLER, K.-H., BRAUN, G., GEIGER, K. & GUTTMANN, J. (2001) CO₂-controlled sampling of alveolar gas in mechanically ventilated patients. *J Appl Physiol*, 90, 486-492.
- SCHWAB, T. M., HENDEY, G. W. & SOLIZ, T. C. (1999) Screening for Ketonemia in Patients With Diabetes. *Annals of Emergency Medicine*, 34, 342-346.
- SCHWOEBEL, H., SCHUBERT, R., SKLORZ, M., KISCHKE, S., ZIMMERMANN, R., SCHUBERT, J. K. & MIEKISCH, W. (2010) Phase-resolved real-time breath analysis during exercise by means of smart processing of PTR-MS data. *Anal Bioanal Chem*, 401, 2079-91.
- SEARS, W. M., COLBOW, K. & CONSADORI, F. (1989) General characteristics of thermally cycled tin oxide gas sensors. *Semiconductor Science and Technology*, 4, 351.
- SEIYAMA, T., KATO, A., FUJISHI, K. & NAGATANI, M. (1962) A New Detector for Gaseous Components Using Semiconductive Thin Films. *Analytical Chemistry*, 34, 1502-1503.
- SENTHILMOHAN, S. T., MILLIGAN, D. B., MCEWAN, M. J., FREEMAN, C. G. & WILSON, P. F. (2000) Quantitative analysis of trace gases of breath during exercise using the new SIFT-MS technique. *Redox Rep*, 5, 151-3.

- SERVICE, F. J., O'BRIEN, P. C., WISE, S. D., NESS, S. & LEBLANC, S. M. (1997) Dermal interstitial glucose as an indicator of ambient glycemia. *Diabetes Care*, 20, 1426-9.
- SHIN, H. W. & GEORGE, S. C. (2002) Impact of axial diffusion on nitric oxide exchange in the lungs. *J Appl Physiol*, 93, 2070-80.
- SHIRIN, H., WEINSTEIN, I. B. & MOSS, S. F. (2001) Effects of *H. pylori* infection of gastric epithelial cells on cell cycle control. *Front Biosci*, 6, E104-18.
- SIEG, A., GUY, R. H. & DELGADO-CHARRO, M. B. (2004) Noninvasive glucose monitoring by reverse iontophoresis in vivo: application of the internal standard concept. *Clin Chem*, 50, 1383-90.
- SILKOFF, P. E., CARLSON, M., BOURKE, T., KATIAL, R., OGREN, E. & SZEFLER, S. J. (2004) The Aerocrine exhaled nitric oxide monitoring system NIOX is cleared by the US Food and Drug Administration for monitoring therapy in asthma. *J Allergy Clin Immunol*, 114, 1241-56.
- SILKOFF, P. E., CHATKIN, J., QIAN, W., CHAKRAVORTY, S., GUTIERREZ, C., FURLOTT, H., MCCLEAN, P., RAI, S., ZAMEL, N. & HAIGHT, J. (1999) Nasal nitric oxide: a comparison of measurement techniques. *Am J Rhinol*, 13, 169-78.
- SILKOFF, P. E., ROBBINS, R. A., GASTON, B., LUNDBERG, J. O. & TOWNLEY, R. G. (2000) Endogenous nitric oxide in allergic airway disease. *J Allergy Clin Immunol*, 105, 438-48.
- SILVERSTEIN, J. H. & ROSENBLOOM, A. L. (2003) The journey to metabolic control in diabetes: many more miles to go. *J Pediatr*, 143, 704-6.
- SINGH, M. (2010) *Introduction to Biomedical Instrumentation*, New Dehli, Prentice-Hall of India Pvt.Ltd.
- SMITH, D. & ŠPANĚL, P. (2005) Selected ion flow tube mass spectrometry (SIFT-MS) for on-line trace gas analysis. *Mass Spectrom Rev*, 24, 661-700.
- SMITH, D., WANG, T., PYSANENKO, A. & ŠPANĚL, P. (2008) A selected ion flow tube mass spectrometry study of ammonia in mouth- and nose-exhaled breath and in the oral cavity. *Rapid Commun Mass Spectrom*, 22, 783-9.

- SMITH, P. A., LEPAGE, C. J., HARRER, K. L. & BROCHU, P. J. (2007) Hand-Held Photoionization Instruments for Quantitative Detection of Sarin Vapor and for Rapid Qualitative Screening of Contaminated Objects. *Journal of Occupational and Environmental Hygiene*, 4, 729-738.
- SMOOT, D. T. (1997) How does *Helicobacter pylori* cause mucosal damage? Direct mechanisms. *Gastroenterology*, 113, S31-4; discussion S50.
- SNOW, R. J., CAREY, M. F., STATHIS, C. G., FEBBRAIO, M. A. & HARGREAVES, M. (2000) Effect of carbohydrate ingestion on ammonia metabolism during exercise in humans. *J Appl Physiol*, 88, 1576-80.
- ŠPANĚL, P., DAVIES, S. & SMITH, D. (1998) Quantification of ammonia in human breath by the selected ion flow tube analytical method using H₃₀⁺ and O₂⁺ precursor ions. *Rapid Commun Mass Spectrom*, 12, 763-66.
- ŠPANĚL, P., DAVIES, S. & SMITH, D. (1999) Quantification of breath isoprene using the selected ion flow tube mass spectrometric analytical method. *Rapid Commun Mass Spectrom*, 13, 1733-8.
- ŠPANĚL, P., TURNER, C., WANG, T., BLOOR, R. & SMITH, D. (2006) Generation of volatile compounds on mouth exposure to urea and sucrose: implications for exhaled breath analysis. *Physiological Measurement*, N7.
- SPANGLER, G., CARRICO, J. & CAMPBELL, D. (1985) Recent advances in ion mobility spectrometry for explosives vapor detection. *J Test Eval*, 13: 234-240.
- SRINIVASAN V., PAMULA V., POLLACK M. & FAIR B. (2003) Clinical diagnostics on human whole blood, plasma, serum, urine, saliva, sweat, and tears on a digital microfluidic platform. *7th International Conference on Miniaturized Chemical and Biochemical Analysis Systems*
- STEEGHS, M. M., CRISTESCU, S. M. & HARREN, F. J. (2007) The suitability of Tedlar bags for breath sampling in medical diagnostic research. *Physiol Meas*, 28, 73-84.
- STEIL, G. M., REBRIN, K., HARIRI, F., JINAGONDA, S., TADROS, S., DARWIN, C. & SAAD, M. F. (2005) Interstitial fluid glucose dynamics during insulin-induced hypoglycaemia. *Diabetologia*, 48, 1833-40.

- STEIN, R. A. & MEAD, J. F. (1988) Small hydrocarbons formed by the peroxidation of squalene. *Chem Phys Lipids*, 46, 117-20.
- STEWART, R. D. & BOETTNER, E. A. (1964) EXPIRED-AIR ACETONE IN DIABETES MELLITUS. *N Engl J Med*, 270, 1035-1038.
- STONE, B., BESSE, T., DUANE, W., DEAN EVANS, C. & DEMASTER, E. (1993) Effect of regulating cholesterol biosynthesis on breath isoprene excretion in men. *Lipids*, 28, 705-708.
- TAMADA, J. A., BOHANNON, N. J. & POTTS, R. O. (1995) Measurement of glucose in diabetic subjects using noninvasive transdermal extraction. *Nat Med*, 1, 1198-201.
- TAMADA, J. A., GARG, S., JOVANOVIĆ, L., PITZER, K. R., FERMI, S. & POTTS, R. O. (1999) Noninvasive glucose monitoring: comprehensive clinical results. Cygnus Research Team. *Jama*, 282, 1839-44.
- TANG, Z., LEE, J. H., LOUIE, R. F. & KOST, G. J. (2000) Effects of different hematocrit levels on glucose measurements with handheld meters for point-of-care testing. *Arch Pathol Lab Med*, 124, 1135-40.
- TASSOPOULOS, C. N., BARNETT, D. & FRASER, T. R. (1969) Breath-acetone and blood-sugar measurements in diabetes. *Lancet*, 1, 1282-6.
- TAUCHER, J., HANSEL, A., JORDAN, A., FALL, R., FUTRELL, J. H. & LINDINGER, W. (1997) Detection of isoprene in expired air from human subjects using proton-transfer-reaction mass spectrometry. *Rapid Commun Mass Spectrom*, 11, 1230-4.
- TUCH, B., DUNLOP, M. & PROIETTO, J. (2000) *Diabetes research : a guide for postgraduates*, Amsterdam, Harwood Academic.
- TUCHIN, V. V. (2008) *Handbook of optical sensing of glucose in biological fluids and tissues*, Boca Raton, Fla. ; London, Chapman & Hall.
- TURNER, A. P., RAMSAY, G. & HIGGINS, I. J. (1983) Applications of electron transfer between biological systems and electrodes. *Biochem Soc Trans*, 11, 445-8.
- TURNER, C., PAREKH, B., WALTON, C., ŠPANĚL, P., SMITH, D. & EVANS, M. (2008) An exploratory comparative study of volatile compounds in exhaled breath and emitted

- by skin using selected ion flow tube mass spectrometry. *Rapid Commun Mass Spectrom*, 22, 526-32.
- TURNER, C., ŠPANĚL, P. & SMITH, D. (2006a) A longitudinal study of ammonia, acetone and propanol in the exhaled breath of 30 subjects using selected ion flow tube mass spectrometry, SIFT-MS. *Physiol Meas*, 27, 321-37.
- TURNER, C., ŠPANĚL, P. & SMITH, D. (2006b) A longitudinal study of breath isoprene in healthy volunteers using selected ion flow tube mass spectrometry (SIFT-MS). *Physiological Measurement*, 13.
- TURNER, C., ŠPANĚL, P. & SMITH, D. (2006c) A longitudinal study of ethanol and acetaldehyde in the exhaled breath of healthy volunteers using selected-ion flow-tube mass spectrometry. *Rapid Communications in Mass Spectrometry*, 20, 61-68.
- TURNER, C., ŠPANĚL, P. & SMITH, D. (2006d) A longitudinal study of methanol in the exhaled breath of 30 healthy volunteers using selected ion flow tube mass spectrometry, SIFT-MS. *Physiological Measurement*, 637.
- VAN BERKEL, V., KUO, E. & MEYERS, B. F. Pneumothorax, bullous disease, and emphysema. *Surg Clin North Am*, 90, 935-53.
- VAN DEN VELDE, S., NEVENS, F., VAN HEE, P., VAN STEENBERGHE, D. & QUIRYNEN, M. (2008) GC-MS analysis of breath odor compounds in liver patients. *Journal of Chromatography B*, 875, 344-348.
- VAN HARREVELD, A. P. (2003) Odor concentration decay and stability in gas sampling bags. *J Air Waste Manag Assoc*, 53, 51-60.
- VENN, R. F. (2008) *Principles and practice of bioanalysis*, Boca Raton, Fla., CRC ; London : Taylor & Francis [distributor].
- VON ZGLINICKI, T., LINDBERG, M., ROOMANS, G. M. & FORSLIND, B. (1993) Water and ion distribution profiles in human skin. *Acta Derm Venereol*, 73, 340-3.
- WANLESS, D. (2002), *Securing Our Future Health: Taking a Long-Term View*. London: HM Treasury

- WASSERMAN, D. H. & ZINMAN, B. (1994) Exercise in individuals with IDDM. *Diabetes Care*, 17, 924-37.
- WEBER, C. (2009) Sniffing out cancer - an evaluation of GC-MS and eNose for early bladder cancer detection. Cranfield University: Cranfield Health MSc Thesis.
- WEBER, C. M., CAUCHI, M., PATEL, M., BESSANT, C., TURNER, C., BRITTON, L. E. & WILLIS, C. M. (2010) Evaluation of a gas sensor array and pattern recognition for the identification of bladder cancer from urine headspace. *Analyst*, 136, 359-64.
- WEITGASSER, R., GAPPMEYER, B. & PICHLER, M. (1999) Newer portable glucose meters-- analytical improvement compared with previous generation devices? *Clin Chem*, 45, 1821-5.
- WENTHOLT, I. M., VOLLEBREGT, M. A., HART, A. A., HOEKSTRA, J. B. & DEVRIES, J. H. (2005) Comparison of a needle-type and a microdialysis continuous glucose monitor in type 1 diabetic patients. *Diabetes Care*, 28, 2871-6.
- WEST, J. B. (2008) *Respiratory physiology : the essentials*, Philadelphia ; London, Lippincott Williams & Wilkins.
- WHELAN, J. (2007) When diabetes strikes twice. *The New Scientist*, 196, 48-51.
- WIDMARK, E. M. (1920) Studies in the Acetone Concentration in Blood, Urine, and Alveolar Air. II: The Passage of Acetone and Aceto-Acetic Acid into the Urine. *Biochem J*, 14, 364-78.
- WILD, S., ROGLIC, G., GREEN, A., SICREE, R. & KING, H. (2004) Global prevalence of diabetes: estimates for the year 2000 and projections for 2030. *Diabetes Care*, 27, 1047-53.
- WILHELM, B., FORST, S., WEBER, M. M., LARBIG, M., PFUTZNER, A. & FORST, T. (2006) Evaluation of CGMS during rapid blood glucose changes in patients with type 1 diabetes. *Diabetes Technol Ther*, 8, 146-55.
- WILLIAMS, G. & S. V. COLES, G. (1998) Gas sensing properties of nanocrystalline metal oxide powders produced by a laser evaporation technique. *Journal of Materials Chemistry*, 8, 1657-1664.
- YAMADA, K. & KAKEHI, K. (2011) Recent advances in the analysis of carbohydrates for biomedical use. *J Pharm Biomed Anal*, 55, 702-27.

- YAMANE, N., TSUDA, T., NOSE, K., YAMAMOTO, A., ISHIGURO, H. & KONDO, T. (2006) Relationship between skin acetone and blood beta-hydroxybutyrate concentrations in diabetes. *Clin Chim Acta*, 365, 325-9.
- YATES, D. H., KHARITONOV, S. A., ROBBINS, R. A., THOMAS, P. S. & BARNES, P. J. (1995) Effect of a nitric oxide synthase inhibitor and a glucocorticosteroid on exhaled nitric oxide. *Am. J. Respir. Crit. Care Med.*, 152, 892-896.
- YU, J.-B., LIM, J.-O., BYUN, H.-G. & HUH, J.-S. Exhaled Breath Analysis of Lung Cancer Patients Using Metal Oxide Sensor. *Proceedings of the 2011 First ACIS/JNU International Conference on Computers, Networks, Systems and Industrial Engineering*. IEEE Computer Society.
- YUAN, Y., SO, R., WONG, S. & CHAN, K. M. (2002) Ammonia threshold—comparison to lactate threshold, correlation to other physiological parameters and response to training. *Scandinavian Journal of Medicine & Science in Sports*, 12, 358-364.
- ZLATKIS, A., ANDERSON, J. W. & HOLZER, G. (1977) Concentration and analysis of trace impurities in styrene monomer. *Journal of Chromatography A*, 142, 127-129.
- ZOLOTOV, Y. (2005) Breath Analysis. *Journal of Analytical Chemistry*, 60, 497.
- ZWAARDEMAKER, H., HOEGWIND, F. (1920) On spray-electricity and waterfall-electricity. *Proc. Acad. Sci. Amst.*, 22, 429-437

Websites:

<http://www.rosiedaniel.com/2007/04/gas-sensors.htm> (Rosie Daniel) accessed 11/06/2010

APPENDICES (ON CD)